Investigation of novel receptor tyrosine kinase mediated non-canonical signalling in breast cancer

Eleanor Jane Cawthorne

Submitted in accordance with the requirements for the degree of Doctor of Philosophy

The University of Leeds

School of Molecular and Cellular Biology

The Astbury Centre for Structural Molecular Biology

July 2021

The candidate confirms that the work submitted is her own and that appropriate credit has been given where reference has been made to the work of others.

This copy has been supplied on the understanding that it is copyright material and that no quotation from the thesis may be published without proper acknowledgement.

The right of Eleanor Jane Cawthorne to be identified as author of this work has been asserted by her in accordance with the Copyright, Designs and Patents Act 1988.

© 2021 The University of Leeds and Eleanor Jane Cawthorne

Acknowledgements

I would like to thank my supervisor Professor John Ladbury for his guidance throughout my PhD project and the time within his laboratory group. I would also like to thank all current and former members of the Ladbury Laboratory for all their help and advice. In particular the advice and mentorship from Dr. Chris Jones and Dr. Natalie Stephenson (even though this was only for a very brief time), your help was invaluable.

I would like to thank my fellow PhD lab members for their support and helping during my PhD project. In particular, to Dovilė Milonaitytė for the endless supplies of bubble teas, hot chocolates and chocolate. Thank you to Dr. Sophie Ketchen, Dr. Caroline Seiler, Dr. Janne Darell and Amy Stainthorpe for your friendship and encouragement throughout my PhD.

My PhD project has been funded through the Leeds Alumni Scholarship scheme and has been kindly donated by Mr. Mark and Mrs. Marian Deere. I will be forever grateful for your generosity and support to study a PhD in the field of cancer research at the University of Leeds. Thank you so much for the opportunity.

A massive thank you to the LIGHT building crew including Julie, Courtney, Pooja, Liz, for keeping my spirits up and thoroughly enjoying dinner times with you all. And thank you to all my friends outside of Leeds for your continued support and encouragement.

Finally I would like to thank my family for all their love and support during my PhD. I would not have got through it without my mum, my sister Fran, and the continued support of my gran through gifts of food and treats. Also, my dog Ralph has been my work-buddy throughout writing my thesis and has kept me going when times have been tough.

Abstract

Introduction: It has been discovered by our laboratory group that a novel cell signalling mechanism (Tier 2 signalling) can occur via receptor tyrosine kinases and SH3 domain-containing proteins when cellular environmental conditions are perturbed. Aberrant Tier 2 signalling in response to stress-induced changes to protein expression is implicated in tumorigenesis and is physiologically relevant to tumour cells under microenvironmental stress. The role of aberrant receptor tyrosine kinases expression in breast cancer pathogenesis and the high levels of anti-receptor tyrosine kinase resistance, suggest that aberrant Tier 2 signalling may play a role in breast cancer progression and drug-resistance.

Objectives: To investigate whether overexpression or upregulated expression of receptor tyrosine kinases and SH3 domain-containing proteins in response to GF-deprivation leads to the non-canonical activation of SH3 domain-containing proteins in breast cancer cells. The possible aberrant downstream Tier 2 signalling mechanisms which could lead to an oncogenic outcome in breast cancer cells, was also examined.

Methods: Relative cell protein levels were determined via immunoblotting. Various protein-protein interaction methods were utilised, including the use of Co-IP, pull-downs and FRET, to validate candidate non-canonical protein-protein interactions. Phenotypic cellular assays were performed to determine the phenotypic consequence of non-canonical activation of SH3 domain-containing proteins.

Results: The work presented here demonstrates that breast cancer cells change their proteome in response to growth under serum-deprivation stress. A particular non-canonical protein-protein interaction was established to occur between the second proline-rich motif of the receptor tyrosine kinase VEGFR2 and the SH3-domain of Src-kinase in breast cancer cells, under serum-deprived conditions. The VEGFR2-mediated non-canonical activation of Src was observed to play a role in breast cancer cell migration.

Conclusions: The data within this thesis supports a novel Tier 2 signalling pathway in breast cancer cells, which is upregulated in response to growth

under serum-deprived stress and may be implicated in breast cancer cell migration. This aberrant Tier 2 mechanism may play an important role in breast cancer progression and resistance mechanisms, when under serum-deprived microenvironmental stress.

Table of Contents

List of Tables

List of Figures

List of Abbreviations

A - Alanine

Akt/PKB– Protein kinase B

Arp – Actin-related protein

ATF2 - Cyclic AMP-dependent transcription factor

ATP – Adenosine triphosphate

BAD - B-cell lymphoma-1 associated death promoter

BBB – Blood brain barrier

BC – Breast cancer

BCA – Bicinchoninic acid assay

BCBM – Breast cancer brain metastasis

BM - Brain metastasis

BrdU - Bromodeoxyuridine

BSA – Bovine serum albumin

Ca^{2+} - Calcium

Cdc42 - Cell division cycle 42

CFP – Cerulean fluorescent protein

Chk-2 – Checkpoint kinase-2

CI – Confidence interval

CNS – Central nervous system

CO_2 – Carbon dioxide

Co-IP – Co-immunoprecipitation

CREB - cAMP-response element binding protein

C-SH2 – Carboxy-terminal SH2 domain

Csk – Src-specific kinase

C-terminal – Carboxy terminal

CTT – C-terminal tail

DAG – Diglyceride

DMEM – Dulbecco’s modified eagle’s medium

DMSO – Dimethyl sulfoxide

DNA – Deoxyribonucleic acid

dNTPs – deoxyribose nucleotide triphosphate

dPBS – Dulbecco’s phosphate buffered saline

EB – Elution buffer

ECL- Enhanced chemilluminescence

EGFR – Epidermal growth factor receptor

ELISA – Enzyme-linked immunosorbent assay

Elk1 - ETS domain-containing protein

EMT – Epithelial to mesenchymal transition

eNOS - Nitric-oxide synthase-3

ER – Estrogen receptor

Erk - Extracellular signal-regulated kinase

FAK – Focal adhesion kinase

FBS – Foetal bovine serum

FGF – Fibroblast growth factor

FGFR – Fibroblast growth factor receptor

FGFR2 – Fibroblast growth factor receptor-2

FL – Full length

FOXO - Forkhead box O

FRET – Förster resonance energy transfer

FRS2 – Fibroblast growth factor receptor substrate 2

Gab1 – Grb2 associated binder

GF – Growth factor

GFP – Green fluorescent protein

Grb2 – Growth factor receptor-bound protein-2

HCL – Hydrochloric acid

HER1 - Human epidermal growth factor receptor-1

HER2 - Human epidermal growth factor receptor-2

HER3 - Human epidermal growth factor receptor-3

HER4 - Human epidermal growth factor receptor-4

HGFR/C-Met – Hepatocyte growth factor receptor

HIF-1 - Hypoxia inducible factor-1

HR – Hazard ratio

HRP – Horseradishperoxidase

HSP60 – Heat shock protein 60

HSPG – Heparan sulphate proteoglycan

IF – Immunoflourescence

Ig – Immunoglobulin

IGF-1R – Insulin-like growth factor receptor-1

ILK - Integrin-linked kinase

IP – Immunoprecipitation

IP_3 – Inositol triphosphate

IPTG - Isopropyl β-D-1-thiogalactopyranoside

IQGAP1 - IQ-motif-containing GTPase-activating protein-1

IR – Insulin receptor

JMD – Juxta-membrane domain

K – Lysine

KD – Kinase dead

kDa – Kilo-Dalton

KDR - Kinase domain region

KI – Kinase insert

LB – Lysogeny broth

M - Methionine

mAb – Monoclonal antibody

MAPK – Mitogen-activated protein kinase

MBP – Maltose binding protein

MMP – Metalloproteinase

mRNA – Messenger RNA

mTOR - Mammalian target of rapamycin

MTT - 3-(4,5-dimethylthiazol-2-yl)-2,5-diphenyl tetrazolium bromide

Nck - Non-catalytic region of tyrosine kinase adaptor protein

NEB – New England Biolabs

NGFR – Neuregulin growth factor receptor

N-SH2 – Amino-terminal SH2 domain

N-terminal – Amino terminal

O_2 – Oxygen

OS – Overall survival

P – Proline

p70 S6 kinase - 70kDa ribosomal protein S6 kinase

PAK - p21-activated protein kinase

PCR – Polymerase chain reaction

PDK1 - Phosphoinositide-dependent kinase 1

PD-L1 – Programmed death-ligand-1

Pen-strep – Penicillin-streptomycin

PFA – Paraformaldehyde

PH – Pleckstrin homology

PI3K – Phosphoinositide-3-kinase

PIP_2 - Phosphatidylinositol 4,5,-bisphosphate

PIP_3 - Phosphatidylinositol 3,4,5-triphosphate

PKC – Protein kinase C

PLC – Phospholipase C

Plcg1 – Phospholipase C gamma-1

PLGF – Placenta growth factor

PPI – Protein-protein interaction

PPII – Proline-rich type II

PR – Progesterone receptor

PRAS40 - Proline-rich Akt substrate

PTB – Phosphotyrosine binding

PTEN - Phosphatase and tensin homologue deleted on chromosome 10

PVDF – Polyvinylidene fluoride

pY – Phosphorylated Tyrosine

PYK2 – Proline-rich tyrosine kinase-2

R - Arginine

RFP – Red fluorescent protein

RTK – Receptor tyrosine kinase

S – Serine

SCK - SHC-transforming protein B

SDM – Site directed mutagenesis

SDS-PAGE - Sodium Dodecyl Sulphate-Polyacrylamide Gel Electrophoresis

SFK – Src family of kinases

SH2 – Src homology-2

SH3 – Src homology-3

SH4 – Src homology-4

SHB - SH2-domain containing adaptor protein B

Shc - Shc-transforming protein-1

Shp2 - Src homology region 2 (SH2)-containing protein tyrosine phosphatase-2

SOC – Super optimal broth

SOS - Son of sevenless

STAT3 – Signal transducers and activators of transcription-3

T – Threonine

TBS- Tris-buffered saline

TBST – Tris-buffered saline-Tween

TCGA-RPPA - The Cancer Genome Atlas-reverse phase protein array

TK – Tyrosine kinase

TKD – Tyrosine kinase domain

TKI – Tyrosine kinase inhibitor

TMB - 3,3’,5,5’-tetramethylbenzidine

TNBC – Triple negative breast cancer

TNM - Tumour Node Metastasis

Tor – Target of rapamycin

TSAd - T-cell-specific adaptor molecule

VEGF – Vascular endothelial growth factor

VEGF-A – Vascular endothelial growth factor-A

VEGF-B - Vascular endothelial growth factor-B

VEGF-C - Vascular endothelial growth factor-C

VEGF-D - Vascular endothelial growth factor-D

VEGF-E - Vascular endothelial growth factor-E

VEGFR – Vascular endothelial growth factor receptor

VEGFR1 – Vascular endothelial growth factor receptor-1

VEGFR2– Vascular endothelial growth factor receptor-2

VEGFR3 – Vascular endothelial growth factor receptor-3

WASp – Wiskott - Aldrich syndrome protein

WAVE – WASp-family verprolin-homologous protein

WT – Wildtype

Y – Tyrosine

YFP – Yellow fluorescent protein

Chapter 1 Introduction

1.1 Receptor Tyrosine Kinases (RTKs)

RTKs are a large family of cell surface receptors that play a crucial role in many fundamental cell processes. These include cellular proliferation, cell metabolism, cell migration, the cell cycle and cell survival (Blume-Jensen and Hunter, 2001; Ullrich and Schlessinger, 1990). RTK membrane receptors all have a similar molecular architecture. They all contain an extracellular ligand binding domain, to which particular growth factors (GFs) and ligands can bind. The ligand binding domain is connected to the intracellular domain via a single transmembrane helix. The intracellular cytoplasmic domain contains a conserved tyrosine kinase domain (TKD), carboxy (C-) terminal and juxtamembrane regulatory sequences, which determines autophosphorylation and phosphorylation by protein kinases. Activated RTK's catalyse the transfer of the γ phosphate of ATP to hydroxyl groups exposed on specific tyrosine (Y) residues on downstream target proteins (Schlessinger, 2000). RTKs can therefore be thought of as a single node that activates various signalling networks, to transmit information from outside to the inside of the cell.

RTKs and the intracellular signalling pathways that they activate are evolutionary conserved, emphasising the important roles they play in a diversity of cellular processes (Lemmon and Schlessinger, 2010). Humans have 58 known RTKs, which fall into 20 subfamilies (Manning et al., 2002; Lemmon and Schlessinger, 2010; Robinson et al., 2000). All RTKs, except for the insulin receptor (IR) family, are monomer receptor proteins within the cell membrane, under basal conditions (Schlessinger, 2000).

Aberrant activation of RTKs, such as through mutation or the overexpression of the RTK or its ligand, results in pathogenesis of many diseases. These include cancer, diabetes, inflammation, severe-bone disorders, arteriosclerosis, and angiogenesis. There are four main principle mechanisms found in human cancers that utilise aberrant RTK signalling. These include RTK overexpression, chromosomal translocations, autocrine activation and

gain of function mutations (Lemmon and Schlessinger, 2010). A large number of mutations have been found in a range of different cancer types, in numerous RTKs and collected in the Catalogue of Somatic Mutations in Cancer (COSMIC) database (Forbes et al., 2010).

1.1.1 RTK activation and autoinhibitory mechanisms

In general, ligand binding to the extracellular region of RTKs induces receptor dimerisation, which results in the activation of the TKD via transphosphorylation and subsequent autophosphorylation of their cytoplasmic domains (**Figure 1.1**) (Ullrich and Schlessinger, 1990; Du and Lovly, 2018). All TKDs have an N-lobe and a C-lobe. Key regulatory domains including the activation loop and the αC helix in the kinase N-lobe adopt a specific configuration in all activated TKDs, which is required for catalysis of phosphotransfer to downstream effector proteins (Nolen et al., 2004). Inactive TKDs differ between RTKs, which reflects the diversity of mechanisms that they regulate. Each TKD is *cis*-autoinhibited by intramolecular interactions that are specific for each receptor. The release of this inhibition is the key event that elicits RTK activation (Lemmon and Schlessinger, 2010; Huse and Kuriyan, 2002). Receptor dimerisation increases the local concentration of the tyrosine kinase (TK) and leads to more efficient *trans*-phosphorylation of Y residues in the activation loop of the catalytic domain (Weiss and Schlessinger, 1998; Hubbard et al., 1998). Upon phosphorylation, the activation loop adopts an ‘open’ configuration which permits access to ATP and other substrates, and enables the phosphotransfer from ATP to a Y on the receptor itself and to cellular proteins involved in signal transmission (Schlessinger, 2000). Autophosphorylation of the receptor occurs in a precise order of events which destabilises *cis*-autoinhibition interactions. The first phase of autophosphorylation events enhance the catalytic activity of the RTK once the receptor binds to its activating ligand. The second phase requires first phase activation of the kinase and leads to the phosphorylation of specific phosphorylated-Y (pY) sites which recruits cytoplasmic signalling proteins to bind via their Src homology-2 (SH2) and phosphotyrosine-binding (PTB) domains (Lemmon and Schlessinger, 2010).

In the absence of ligand binding, some RTKs exhibit ligand-independent or basal autophosphorylation of Y residues (Hubbard et al., 1998). Basal phosphorylation does not produce a signal of sufficient amplitude to elicit a cellular response and therefore, basal phosphorylation was thought to not have any biological function (Belov and Mohammadi, 2012). Our laboratory group however challenged this theory and revealed that basal phosphorylation of RTKs is a physiologically relevant event which is inhibited by the binding of intracellular effector proteins and serves to 'prime' receptors for a rapid response to ligand stimulation (Lin, C.C. et al., 2012). It is also thought that receptor overexpression can utilise auto-phosphorylation to activate downstream pathways in the absence of ligand binding leading to uncontrolled RTK signalling in many human diseases (Du and Lovly, 2018).

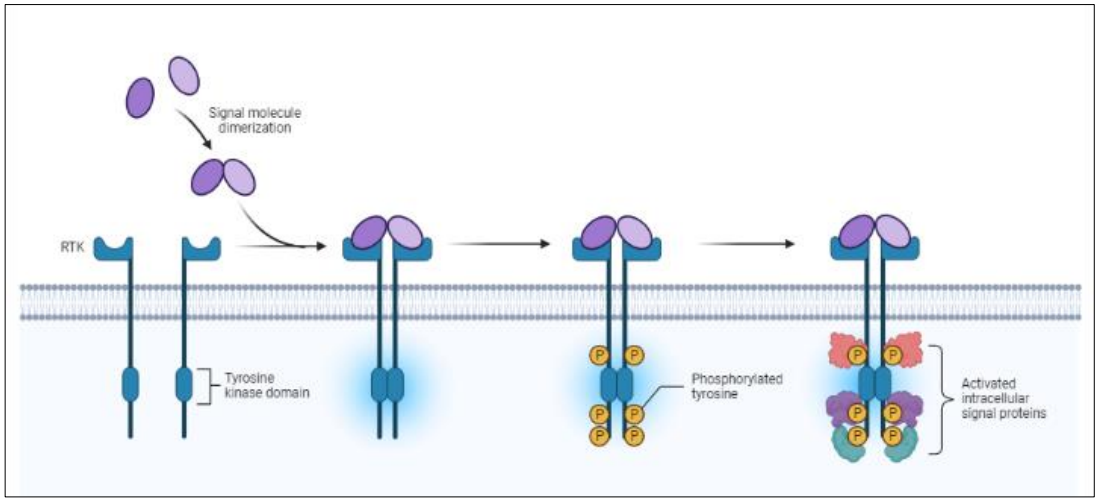

Figure 1.1 Canonical RTK activation.

Inactive RTK monomers are maintained in an autoinhibited state until ligand-binding. In the presence of a specific ligand, particular RTKs are brought into close proximity and co-dimerise which stimulates TKD activity. The activation of the RTK induces autophosphorylation of specific residues in the C-terminal tail. The resulting phosphorylation activates effector proteins which bind to these sites and relays a signalling cascade within the cell. Adapted from BioRender.com.

1.1.2 Tier 1 signalling

The cell signalling response through ligand-induced RTK activation is termed within this thesis as Tier 1 cell signalling. The activation and consequent autophosphorylation of ligand-activated RTKs, initiates the recruitment of downstream signalling proteins. These molecules are recruited via their SH2 or PTB domains and bind to pY sites within the intracellular domain of the RTK (Pawson, 2004; Schlessinger and Lemmon, 2003). Here, the binding of docking proteins to the particular phospho-site on the phosphorylated RTK, activates the docking proteins themselves. This occurs via the activated RTK catalysing the phosphorylation of the docking protein. Docking proteins which bind to the receptor itself usually contain a membrane-targeting site at their amino (N) terminus, followed by several pY sites. These pY sites serve as binding sites for other downstream signalling proteins (Lemmon and Schlessinger, 2010). Downstream cytoplasmic signalling molecules are then recruited indirectly by interacting with docking proteins that are phosphorylated by activated RTKs (Schlessinger, 2000). This elicits a Tier 1 cell signalling cascade within the cell, which results in many different proteins to become activated.

There are many different interaction domains of proteins which are responsible for the activation of signalling cascades stimulated by activated RTKs. Some proteins bind via receptor proximal interactions (e.g. SH2, PTB) and others bind through more spatial and distal interactions including Src Homology 3 (SH3), WW, and PDZ domains to the activated signalling protein (Pawson, 2004; Schlessinger and Lemmon, 2003). These domains are typically seen alongside the SH2 domain in typical multi-domain proteins that signal downstream from RTKs (Lemmon and Schlessinger, 2010). These multi-domains allow for many different protein-protein interactions (PPIs) to occur with both receptors and other downstream signalling molecules.

With multiple pY sites and other binding sites embedded within the cytoplasmic domain of RTKs, their activation via ligand-binding can elicit many different signalling proteins and Tier 1 signalling pathways to become activated (Schlessinger, 2000). This canonical way of cell signalling will

therefore provide a cellular response depending on the particular Tier 1 signalling pathway activated.

1.2 SH3 domains

SH3 domains are peptide-recognition modules which mediate PPIs in many eukaryotic cell signalling mechanisms. The SH3 domain family is one of the largest and best characterised peptide-recognition module families. There are over 300 domains in over 200 human proteins, which are together involved in cell signalling pathways which include cell growth regulation, endocytosis, and cytoskeletal control (Mayer, B.J. and Gupta, 1998). Mutations in SH3 domains can also be oncogenic. Mutations in the SH3 domains of oncoproteins Src and Abl are known to be activating mutations (Kay et al., 2000).

SH3 domains consist of a defined, homologous structure of approximately 60 amino acids. This provides a hydrophobic binding surface that recognises proline-rich sequences containing the core PxxP (where P is a proline residue and x denotes any amino acid) which folds to a left-handed proline-rich type II (PPII) helix (Cicchetti et al., 1992; Ren et al., 1993). The PPII helix is pseudo-symmetrical, meaning that the SH3 domain can recognise peptides in both orientations by using two different binding modes. Adjacent to the PxxP-binding site, SH3 domains contain another binding region called an RT loop between strands β1 and β2 and the n-Src loop between strands β2 and β3, called the specificity site (Yu et al., 1994; Lim et al., 1994). In canonical SH3 domains, the site is negatively charged and recognises a positively charged R/K residue located at either side of the PxxP motif (Teyra et al., 2017). Based on SH3 domain binding preferences, two classes of canonical PxxP motifs have been defined (Lim et al., 1994; Yu et al., 1994). Class I SH3 domains bind to peptides that conform to the consensus motif $R^{-3}xx\underline{P^{0}xxP}^{3}$ (**Figure 1.2, left**) in a plus orientation. Here, the P residues pack against two external hydrophobic sites in the area of the RT loop. Class II domains recognise peptides that have the sequence $^{0}PxxPxR^{+5}$ (**Figure 1.2, right**), in a minus orientation (Feng et al., 1994; Lim et al., 1994). Here, the P residues pack against two internal hydrophobic sites located near the n-Src loop.

Some SH3 domains have been found to exhibit non-canonical specificities and bind to a wide variety of peptide motifs (Saksela and Permi, 2012; Teyra et al., 2017). The wide variety of binding specificities gives rise to the diversity of SH3-domains to recognise protein ligands. Therefore, SH3 domains could play a far more varied role in cell signalling than has been previously known. Further investigation into the non-canonical binding motifs is required to fully understand SH3 domain function (Teyra et al., 2017).

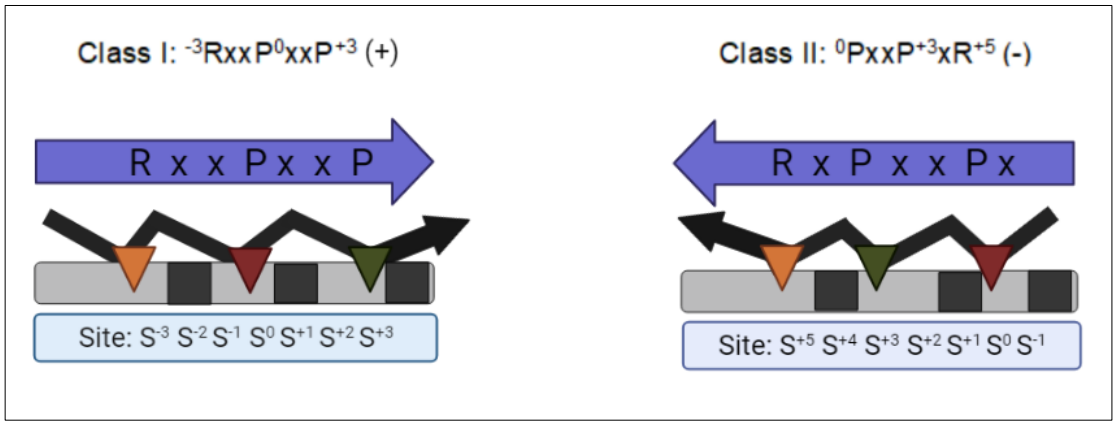

Figure 1.2 Canonical SH3:PxxP domain interactions.

Representative schematic of the binding orientations of class I and class II PxxP peptides interacting with SH3 domains. The PxxP peptide backbone is shown via the black arrow with the C terminus of the protein shown by the arrowhead. The important binding residues are shown as triangles, coloured to show residues P^{0} (red), P^{+3} or P^{-3} (green) and R^{-3} or R^{+5} (yellow). The SH3 domain backbone is shown in grey and the SH3 domain binding sites represented by black boxes. Site S^{0} is the site of P^{0}. Adapted from (Teyra et al., 2017). Made using BioRender.com.

1.2.1 The prevalence of PxxP sequences in RTKs

Of the 58 known RTKs in humans (Lemmon and Schlessinger, 2010), the majority have many proline-rich sequences within their C-termini. Around 70% of human RTKs express varying numbers of PxxP sites (**Figure 1.3**). These sequences have the propensity to bind to over 200 proteins that have over 300 SH3 domains embedded within their structures (Mayer, B.J. and Gupta, 1998). Interactions occur between RTKs and SH3 domain-containing proteins

without the need for external stimulation (e.g. via ligands and GFs) and occur depending on the relative concentration of these proteins within the cell (Timsah et al., 2014).

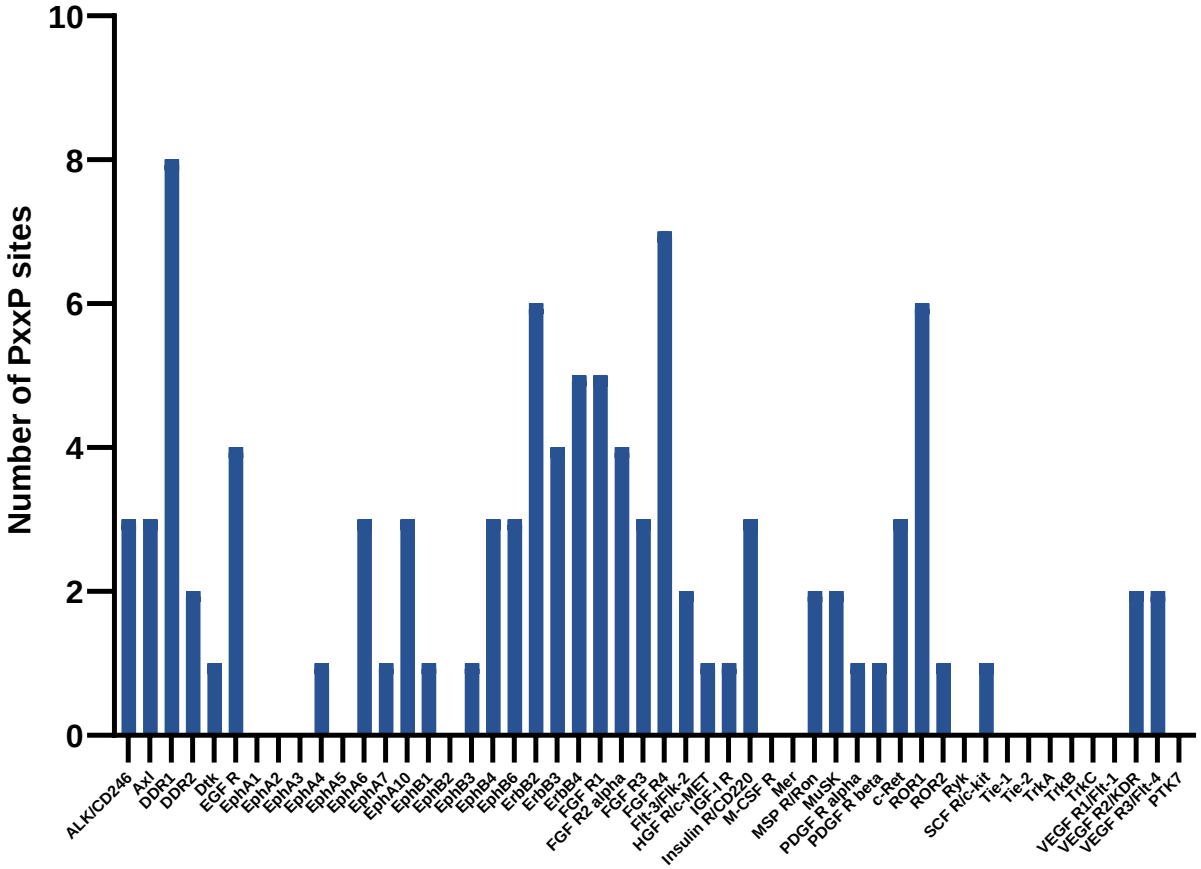

Figure 1.3 The prevalence of PxxP sites in RTK C-terminal tails.

The number of PxxP sites within the cytoplasmic C-terminal domains of RTKs expressed by human cells. C-terminal domains were obtained via (UniProt, 2021).

1.3 Tier 2 signalling

Homeostatic signals within the cell have been found to occur in cells grown under GF-deprived or basal conditions, these can occur through RTKs and through RTK-associated cytoplasmic proteins (Timsah et al., 2014; Suen et al., 2013; Lin et al., 2012; Lin et al., 2021). This has been termed ‘Tier 2 signalling’ (Lin et al., 2021).

Tier 2 signalling is defined by the cell signalling response and functional activation of proteins associated with RTK-mediated signalling pathways, under periods where there is no cellular external stimulation (nutrients and ligands) to elicit a cell signalling response. It is hypothesised that Tier 2 signalling is important to maintain cell viability and homeostasis in periods where there is no cellular external stimulation and thus, under cellular stress. One example of a Tier 2 cell signalling response can be through intracellular SH3 domain-containing proteins interacting with non-active RTKs, whereby the SH3 domains of the intracellular proteins bind to proline-rich motifs within the C-terminal tail of non-activated RTKs. This binding event can activate the intracellular SH3 domain-containing protein, which in turn can activate downstream cell signalling cascades of the intracellular protein. Proteomic imbalances of the proteins involved in these interactions can elicit a non-homeostatic response however, and contribute to activating oncogenic signalling pathways in cancer cells (Timsah et al., 2014; Timsah et al., 2016; Timsah et al., 2015; Lin et al., 2021). Proteomic imbalances of these proteins can be due to environmental change-related stress conditions,

Non-stimulatory conditions show many features of tumorigenesis and progression in cells, as well as prevailing in resistant cells treated with kinase inhibitors. Therefore, understanding how cells adapt to growth under these conditions is necessary to develop more efficient therapeutic strategies.

1.3.1 Grb2 and FGFR2

Growth factor receptor-bound protein-2 (Grb2) is an intracellular adaptor protein consisting of an SH2 domain sandwiched between two SH3 domains and is essential to several RTK-mediated signalling pathways (Maignan et al., 1995). Grb2 mediates signalling from RTKs to the mitogen activated protein (MAP) kinase signalling pathway (Margolis and Skolnik, 1994). Here, the SH2 domain allows for binding to phosphorylated Y residues on RTKs and docking proteins. The SH3 domains interact with proline-rich sites on many intracellular signalling proteins, the most notable being son of sevenless (SOS), which is integral for RTK-mediated Ras-MAP kinase signal transduction (Li et al., 1993; Rozakis-Adcock et al., 1993).

Downstream signalling from the Fibroblast Growth Factor receptor (FGFR) regulates proliferation, migration and differentiation depending on the cell-type. There are seven FGFRs which are derived from alternative splicing (Manning et al., 2002). FGFR2 in particular recruits a docking protein called FGF receptor substrate 2 (FRS2) in a ligand-activated dependent manner (Ahmed et al., 2008). Activation of FGFR2 results in the phosphorylation of FRS2 which serves as a docking site for a number of intracellular proteins including Grb2 (Hadari et al., 1998) (**Figure 1.4a**). The formation of the Grb2/FRS2 complex initiates MAP Kinase activation. Grb2 can also recruit Gab1 leading to the activation of the phosphatidylinositol 3-kinase (PI3K)/Protein kinase B (PKB/Akt) pathway, which may mediate an anti-apoptotic effect (Eswarakumar et al., 2005).

In the absence of extracellular GF stimulus, dimeric Grb2 can bind to FGFR2 via its SH3 domain. This interaction occurs through the Grb2 C-terminal SH3 domain (C-SH3) and a C-terminal proline-rich region of FGFR2 (807-PSLPQYPHINGSVKT-821) (Ahmed et al., 2010). Here, dimeric Grb2 recruits two FGFR2 receptor molecules into a heterotetramer**.** This holds the FGFR2 receptors in a heterotetrameric complex, whereby the receptor activation loop Y residues are autophosphorylated and is therefore primed for external activation, but downstream signalling is inhibited (Lin et al., 2012) (**Figure 1.4b**). Thus, Grb2 controls the level of FGFR2 phosphorylation through controlled inhibition of the kinase activity of the receptor. Upon ligand-binding to FGFR2, receptor dimerisation is stabilised and autophosphorylation of the intracellular domain is upregulated. Grb2 is phosphorylated on Y residue Y-209 by the fully active FGFR2. This results in its dissociation from the complex with the receptor and dimer dissociation. Release of this interaction with Grb2 allows for additional Y residues to be phosphorylated within the C-terminal domain of FGFR2 and therefore, allows the recruitment of signalling molecules required for signal transduction (Ahmed et al., 2013). The phosphorylation of Grb2 through FGFR2 activation, leads to a monomeric Grb2 molecule which is capable of binding to SOS and upregulating MAP kinase signalling. Grb2 phosphorylation at Y160 has been associated with malignant forms of human prostate, colon and breast cancers (Ahmed et al., 2015).

This heterotetrameric binding event also regulates the function and phosphatase activity of SH2 domain–containing protein tyrosine phosphatase 2 (Shp2) in the FGFR2 signalling pathway (Ahmed et al., 2010; Ahmed et al., 2013). Here, the Grb2-dependent regulation of FGFR2 phosphorylation affects the kinase activity of FGFR2 required to phosphorylate Shp2 and hence, the phosphatase activity directed at FGFR2 and Grb2. Therefore, Grb2 is an important positive and negative regulator of receptor phosphorylation and thus, downstream FGFR2 signal transduction (Ahmed et al., 2013).

1.3.2 Evidence of Tier 2 signalling

In the absence of GFs, many Tier 2 cell signalling mechanisms have been found to occur in cells in response to growth under non-stimulated conditions. The relevance of these mechanisms in non-stimulated cells is likely to be associated with the requirement of cells to maintain metabolic and homeostatic ‘house-keeping’ function in the absence of any extracellular stimulation.

When under the absence of GF stimulus, the non-active form of the docking protein Shc-transforming protein 1 (Shc) can sequester the oncoprotein extracellular signal-regulated kinase 1/2 (Erk) activity by the direct interaction between the PTB domain of Shc and N-terminal lobe of Erk. Therefore, acting as a key negative regulator of MAP kinase signalling in non-stimulated cells. As a consequence, Shc suppresses Erk phosphorylation and, potentially, undesirable cellular outcomes such as oncogenic cellular proliferation. Upon external stimulation, recruitment of the Shc-Erk complex to phosphorylated RTKs through Shc’s PTB domain causes a conformational change within Shc which releases Erk from the inhibitory complex, allowing Erk to activate downstream signal transduction events (Suen et al., 2013). The particular binding site of Shc to Erk is evolutionary conserved, providing evidence that the maintenance of the Shc-Erk complex under GF-deprived conditions is important for maintaining cellular homeostasis.

Under GF deprived conditions, non-phosphorylated Grb2 exists in a concentration-dependent dimer-monomer equilibrium in the cytosol (Ahmed et al., 2015). The depletion of intracellular levels of Grb2 results in increased concentrations of monomeric Grb2. Therefore, in the absence of GF

stimulation, Grb2 cycles between the phosphorylated monomeric Grb2 and the non-phosphorylated, typically dimeric Grb2. The former is dependent on constitutive background RTK activity and the latter from intracellular Shp2 activity. The binding of dimeric Grb2 to FGFR2 in the absence of extracellular GF stimulus and when Grb2 levels are high within the cell to form a heterotetrameric complex is also a Tier 2 mechanism response to growth under GF-deprived stress conditions (Lin et al., 2012). Under GF-deprived conditions and when intracellular Grb2 levels are depleted, monomeric Grb2 concentrations are increased within the cytosol (Ahmed et al., 2015). In this state, monomeric non-phosphorylated Grb2 can bind to Shp2, via a bidentate interaction which enhances Shp2 phosphatase activity and downstream signal transduction. The binding of non-phosphorylated monomeric Grb2 releases Shp2 from its autoinhibited state and results in increased phosphatase activity and thus, Shp2 signal transduction. This activation of Shp2 is independent of phosphatase phosphorylation and in the absence RTK activation (Lin et al., 2021). In view of the fact that non-phosphorylated Grb2 exists in a concentration-dependent monomer-dimer equilibrium in cells, the activation of Shp2 is therefore cycled alongside the Grb2 monomer-dimer fluctuations and therefore, maintains homeostasis within the cell.

The intracellular enzyme phospholipase C g-1 (Plcg1) can also bind to the same proline-rich Grb2 binding site on FGFR2, under GF-deprived conditions. The competition between Grb2 and Plcg1 binding to the same site on the C-terminal tail of FGFR2 under serum-deprived conditions was found to have homeostatic relevance when both protein levels were in balance in the cell (Timsah et al., 2014). When the relative intracellular protein levels were changed and Grb2 intracellular levels were low and Plcg1 intracellular levels were high, the prevalence of Plcg1 binding to FGFR2 increased and aberrant Tier 2 cell signalling occured (Timsah et al., 2016) (**Figure 1.4c**).

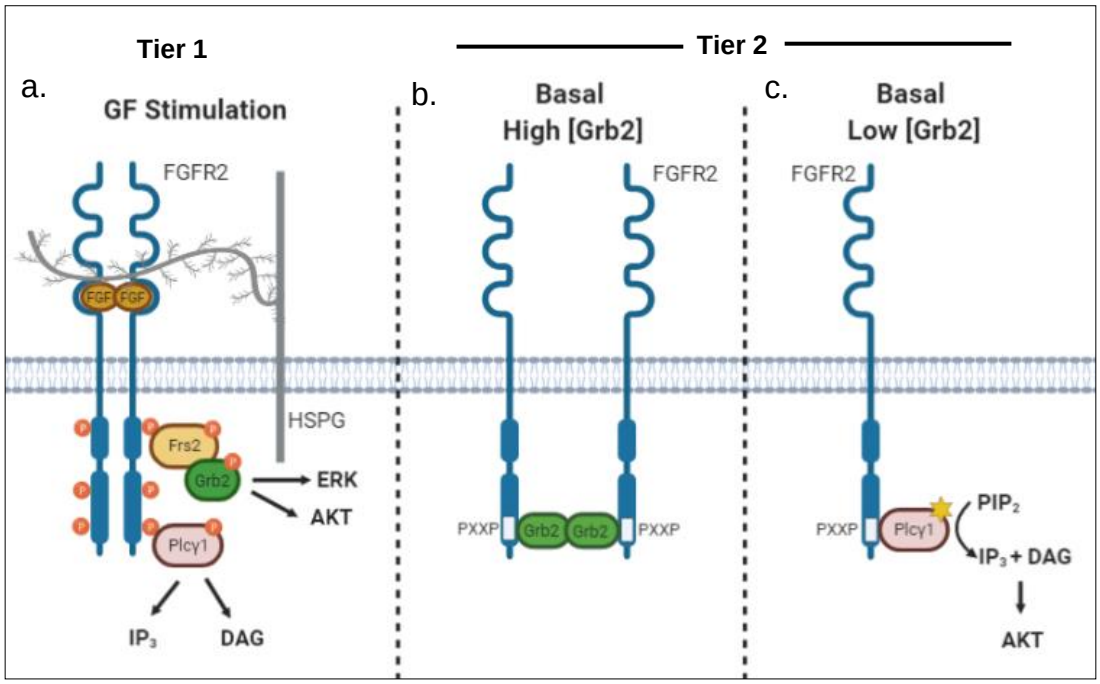

Figure 1.4 FGFR2 Tier 1 and Tier 2 signalling mechanisms.

a. Under growth factor stimulation of fibroblast growth factor (FGF), the FGFRs undergo receptor dimerisation and subsequent transphosphorylation of their TKDs. Docking proteins, including Frs2 and Plcg1, bind to these phosphosites, which leads to the activation of downstream signalling pathways. These include the MAP kinase (MAPK/Erk pathway and the PI3K/Akt pathway. **b.** Under serum-deprived, basal conditions and when Grb2 levels are high within the cell, FGFR2 is held in a heterotetramer with Grb2-dimer binding to the C-terminal PxxP motifs of FGFR2 via its SH3 domain. Here, it is held in a primed position with Grb2, ready to be phosphorylated once the receptor becomes activated. Phosphorylated Grb2 is no longer capable of dimerisation and is dissociated from the FGFR2 complex. **c.** Under basal conditions and when the Grb2 concentration is low, Plcg1 can bind to monomeric FGFR2 at a higher frequency and activate alternative signalling pathways. The binding of Plcg1 to the PxxP motif of FGFR2 changes the conformation of Plcg1 to an active form. Plcg1 activation initiates the excessive hydrolysis of PIP2 to inositol triphosphate (IP3) and diglyceride (DAG). This excessive depletion in PIP2 concentration results in the inhibition of phosphatase and tensin homologue deleted on chromosome 10

(PTEN), and results in the phosphorylation of Akt. Made using BioRender.com.

1.3.3 Evidence of aberrant Tier 2 signalling in cancer

Aberrancies in Tier 2 signalling have been associated with tumorigenesis and cancer progression. Proteomic changes resulting from environmental change-related stress can drive tumorigenesis through perturbation of the homeostatic Tier 2 signalling pathways.

In the absence of GF and when intracellular Grb2 levels were depleted, monomeric Grb2 interacts with the adaptor protein, Shp2. This interaction causes a conformational change in Shp2, whereby the autoinhibition of Shp2 is disrupted upon non-phosphorylated monomeric Grb2 binding and in turn, upregulates Shp2 activity in a phosphorylation-independent manner (Lin et al., 2021). The non-canonical activation of Shp2 under basal conditions was found to upregulate MAP kinase signalling in the triple-negative MDA-MB-468 breast cancer cell line through binding to activated Shp2, without the need for Shp2 phosphorylation. In the absence of external stimulation, the expression of non-phosphorylated monomeric Grb2 was associated with an enhanced level of cellular proliferation in the MDA-MB-468 breast cancer cell line compared with the expression of wildtype Grb2. It is hypothesised that cells which are depleted for a given RTK, as is found in triple negative breast cancer (TNBC), proliferative or metastatic signalling could be driven by the uncontrolled impact of monomeric Grb2-mediated Shp2 activation. Further study is needed to elucidate whether monomeric Grb2 levels are perturbed in response to RTK expression levels and environmental stress conditions and to determine the cellular and phenotypic outcome of monomeric Grb2-mediated upregulated Shp2 activation in cancer cells and whether this plays a role in tumorigenesis and progression.

Aberrant or non-homeostatic Tier 2 signalling has also been identified with FGFR2 and Plcg1, when homeostatic Tier 2 interactions with Grb2 and FGFR2 are out competed (Timsah et al., 2014; Timsah et al., 2016; Timsah et al., 2015). Here, the competition of binding to the same proline-rich site in the C-terminal tail of FGFR2 was dependent on the relative protein expression levels of Grb2 and Plcg1 within the cell. In Grb2 depleted cells and when Plcg1

intracellular levels were high, Plcg1 bound to FGFR2 at a higher frequency via its SH3 domain in the absence of FGF ligand. This led to changes in its protein conformation to an active form (Timsah et al., 2014). This conformational shift exposed the Y783 residue of Plcg1, which plays a critical role in Plcg1 signalling. When this residue is exposed it can interact with its own C-terminal SH2 domain which relieves the autoinhibition of Plcg1. GF-independent Plcg1 activation led to the excessive hydrolysis of the membrane-bound PIP_2 and induced intracellular calcium (Ca^{2+}) release. PIP_2 is an important molecule for the recruitment of effector molecules and canonical signalling.

Grb2 depletion, and thus promoting aberrant Plcg1 activity, in GF-deprived cells with FGFR2 expression, led to the inhibition of PTEN by drastically decreasing the cellular levels of PIP_2. PTEN is an antagonist to PI3K and dephosphorylates phosphatidylinositol 3, 4, 5-triphosphate (PIP_3) to PIP_2 and is conformally affected by cellular levels of PIP_2. As a result of PTEN inhibition, PIP_3 was not converted to PIP_2 and thus, PIP_3 accumulated in the plasma membrane. The accumulation of PIP_3 led to the consequent recruitment and phosphorylation of Akt at the plasma membrane. The fluctuations in proteomic expression levels of FGFR2, Grb2 and Plcg1 influenced the membrane lipid concentration of PIP_3, which in turn modulated cellular proliferation. The observation of tumour formation and progression was also seen in a xenograft mouse model in cells expressing FGFR2 with low Grb2 expression levels. The different expression levels of FGFR2, Grb2 and Plcg1 were seen to correlate with Akt phosphorylation and a highly proliferative outcome in ovarian cancer cell lines and a lower ovarian cancer patient survival (Timsah et al., 2016). The relative expression levels were also prognostic factors in lung adenocarcinoma patients (Timsah et al., 2015).

In addition to Akt activation, the hydrolysis of PIP_2 to IP_3 and DAG led to an influx of intracellular Ca^{2+}, which activates protein kinase C (PKC). This increased the cellular motility and cell-invasive behaviour in these cells under serum-deprived conditions (Timsah et al., 2014). Therefore, an oncogenic outcome can be dictated by the relative protein expression levels of the SH3 domain-containing proteins Grb2 and Plcg1 and FGFR2 RTK, in tumour cells.

1.4 Breast cancer (BC)

BC is the most commonly diagnosed cancer worldwide and accounts for 24.5% of all female cancers. It is the largest cause of cancer death in women, due to the high rates of BC metastases (Sung, Hyuna et al., 2021). BC is a solid tumour malignancy (Gupta, 2003) and is driven by the aberrant expression and regulation of cell signalling pathways in mammary epithelial cells (Butti et al., 2018). These aberrant changes are used as both prognostic and predictive markers for BC therapies. Receptor positive BC typically has a better outcome for patients than receptor-negative disease. This is due to there being no ‘specific’ target for therapy for patients with hormone-negative, human epidermal growth factor receptor-2 (HER2) negative (triple-negative) BC (TNBC). Receptor subtypes of BC patients have distinct gene expression patterns which are used to determine the best course of patient therapy (Finn, 2008).

New biomarker combinations are emerging which include immuno-histochemical markers (estrogen receptor (ER), progesterone receptor (PR), HER2 and proliferation marker Ki-67, genomic markers (e.g. BRCA1, BRCA2 and PIK3CA) and immunomarkers (e.g. tumour-infiltrating lymphocytes and programmed death-ligand-1 (PD-L1). The combination of all these biomarkers are the basis for increasingly complex diagnostic treatment algorithms. Neoadjuvant combination therapy, which often includes targeted drug agents, is the standard of care for BC patients. Radiotherapy is also an important aspect of BC therapy. Metastatic BC patients standard of care include targeted approaches such as PARP inhibitors, CDK4 and CDK6 inhibitors, PI3K inhibitors and PD-L1 immunotherapy, depending on the tumour type and the tumour molecular profile. The range of treatment options for different subtypes of BC patients reflects the complexity of BC therapy today and the heterogeneity of BCs (Loibl et al., 2021).

1.4.1 Aberrant RTK activation in BC

The overexpression and aberrant activation of many RTKs are found in many cancer types, including the breast (Tomiguchi et al., 2016; Palmieri et al., 2007; Lemmon and Schlessinger, 2010; Templeton et al., 2014). RTKs have been found to play an important role in BC progression. RTK pathways

aberrantly activated include pathways which induce cancer stemness, angiogenesis and metastasis (Butti et al., 2018). High levels of RTK expression in BC patients have been associated with a worse patient prognosis, including association with increased BC aggressiveness and decreased overall and disease-free survival (Templeton et al., 2014). Aberrantly activated RTK signalling pathways induces a cancer stem cell (CSC) phenotype which exhibits resistance to BC therapeutics (Wise and Zolkiewska, 2017; Ibrahim et al., 2017).

Since RTKs play important roles in BC progression, RTK-targeted therapy has been useful for BC treatment. Several RTK inhibitors have been tested and approved for use in BC patients. These include, trastuzumab (or otherwise known as Herceptin) and lapatinib (both HER2 inhibitors) and bevacizumab (anti-VEGF inhibitor, therefore targeting the vascular endothelial growth factor receptor (VEGFR)). RTK inhibitors have been found to improve disease-free survival in metastatic BC patients (He and Wei, 2012). Despite there currently being many advances in the detection, prevention, and the use of anti-RTK therapy, unfortunately many BC patients go on to develop *de novo* or acquired resistance, which limits the use of RTK-targeted therapy for BC treatment (Jemal et al., 2010; Huang, L. and Fu, 2015). The mechanisms behind the development of resistance to anti-RTK therapy needs to be elucidated for successful therapeutic regimens for BC treatment and anti-RTK therapy-resistant BCs.

1.5 Src kinase

Src is a 60 kDa membrane-associated non-receptor TK, belonging to the Src family of kinases (SFK) (Yeatman, 2004). Src plays a central and crucial role in maintaining cellular homeostasis of a large range of important cell signalling pathways which control a vast range of physiological functions. These include cell proliferation, survival, adhesion, invasion and migration (Mayer, E.L. and Krop, 2010). Given Src's important role in many cellular functions that are involved in malignant transformation, its aberrant activation has been strongly implicated in the development, growth, progression and metastasis of many

types of human cancers. These include those of the breast, brain, pancreas and colon (Irby and Yeatman, 2000).

1.5.1 Src structure

A hallmark of Src kinases is a short C-terminal tail in which there is an autoinhibitory phosphorylation site (Y527) (**Figure 1.5 and 1.6**). The inactivating phosphorylation at this Y site is carried out by Src-specific kinase (Csk). The phosphorylation of the C-terminal tail promotes the assembly of the SH2, SH3 and kinase domains to be in their autoinhibited conformation, whereby the SH2 domain binds to the phosphorylated C-terminal tail Y527. The SH3 domain interacts with the linker domain at the back of the catalytic domain, promoting a 'closed' conformation which prevents the interaction with other substrates (**Figure 1.6**) (Boggon and Eck, 2004; Guarino, 2010). Src can be activated by the dephosphorylation of Y527 residue (Roskoski, 2005). Through SH2/SH3-mediated intramolecular interactions, Src can undergo conformational changes which accompany different activation states (**Figure 1.6**) (Guarino, 2010).

As with all kinases, Src family members have an activation loop in their TKD that, when phosphorylated, gives the kinase full catalytic activity. In Src this site is Y416 (**Figure 1.5 and 1.6**) (Boggon and Eck, 2004). Src can become phosphorylated at Y416 by cytoplasmic proteins such as focal adhesion kinase (FAK) which plays a role in integrin signalling and by activated RTKs (Thomas and Brugge, 1997). This activation leads to Src being in an 'open' conformation (**Figure 1.6**), which enables the protein to interact with other substrates and downstream signalling molecules within many signalling pathways (**Figure 1.7**) (Finn, 2008).

Src has an N-terminal region which contains a myristic acid moiety which is essential for localisation at the cell membrane. This region also has a unique domain (also known as a src homology-4 (SH4) domain) that is believed to provide unique functions and specificity to each member of the Src family (Finn, 2008; Yeatman, 2004; Boggon and Eck, 2004).

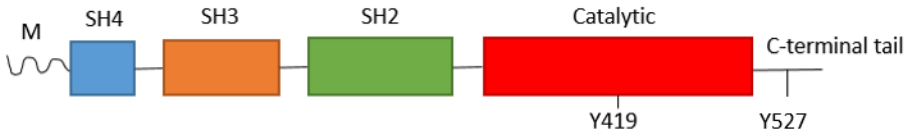

Figure 1.5 Src domain structure.

Src kinase architecture consists of four domains, an N-terminal myristoylation site which is used to anchor the protein into the cell membrane. The SH4 domain, otherwise known as the unique region is a varied region among SFK members. The SH3 domain allows for proline-rich motif recognition and binding. The SH2 domain recognises and binds to pY sites and contains a conserved R residue at R175. Between the SH2 and the catalytic domain there is a type II helix linker. The catalytic domain contains the TKD and activation loop, where Y416 can be phosphorylated and gives Src its full catalytic activity. Src contains a short C-terminal tail which has an autoinhibitory Y527 phosphorylation site which promotes the protein to be in an inactive conformation. Adapted from (Boggon and Eck, 2004).

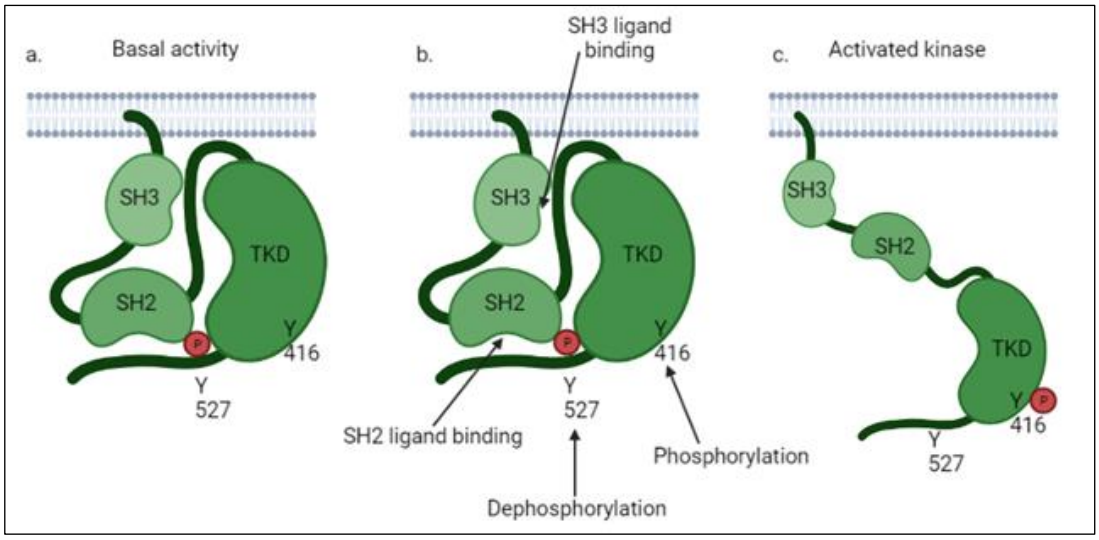

Figure 1.6 Different modes of Src activation.

a. Basal Src is inactive when phosphorylated at Y527 and thus, in its closed conformation. The SH3 domain binds to the linker domain on the back side of the catalytic domain, which promotes the 'closed' conformation and prevents the interaction of Src with other substrates. **b.** Src can be activated by multiple ways. These include through SH3 domain-binding, SH2 domain-binding, the dephosphorylation of Y527 and the activating phosphorylation of Y416. **c.** Src in its active and 'open' conformation, including the phosphorylation of Y416. Adapted from (Martin, 2001). Made using BioRender.com.

1.5.2 Src downstream signalling

Src has a role in multiple cell signalling pathways including those promoting cell proliferation, survival, metastasis, invasion and migration. Activated Src leads to the phosphorylation of downstream target proteins including PI3K, FAK, Ras and signal transducers and activators of transcription-3 (STAT3), which are all implicated in promoting tumorigenesis and progression. Src also plays a crucial role in the regulation of cell motility, adhesion and invasion through interactions with integrin's, FAK, the catenin-cadherin complex and RhoA (**Figure 1.7**) (Mayer, E.L. and Krop, 2010; Finn, 2008; Summy and Gallick, 2003). Src also promotes the epithelial to mesenchymal transition (EMT) and therefore, induces tumour cell metastasis (Guarino, 2010). In human cancers, the majority of Src dysregulation occurs via non-genetic events, which includes the aberrant maintenance of activation status,

association with stimulatory binding proteins and increased activation of RTK signalling (Summy and Gallick, 2003; Parsons and Parsons, 2004).

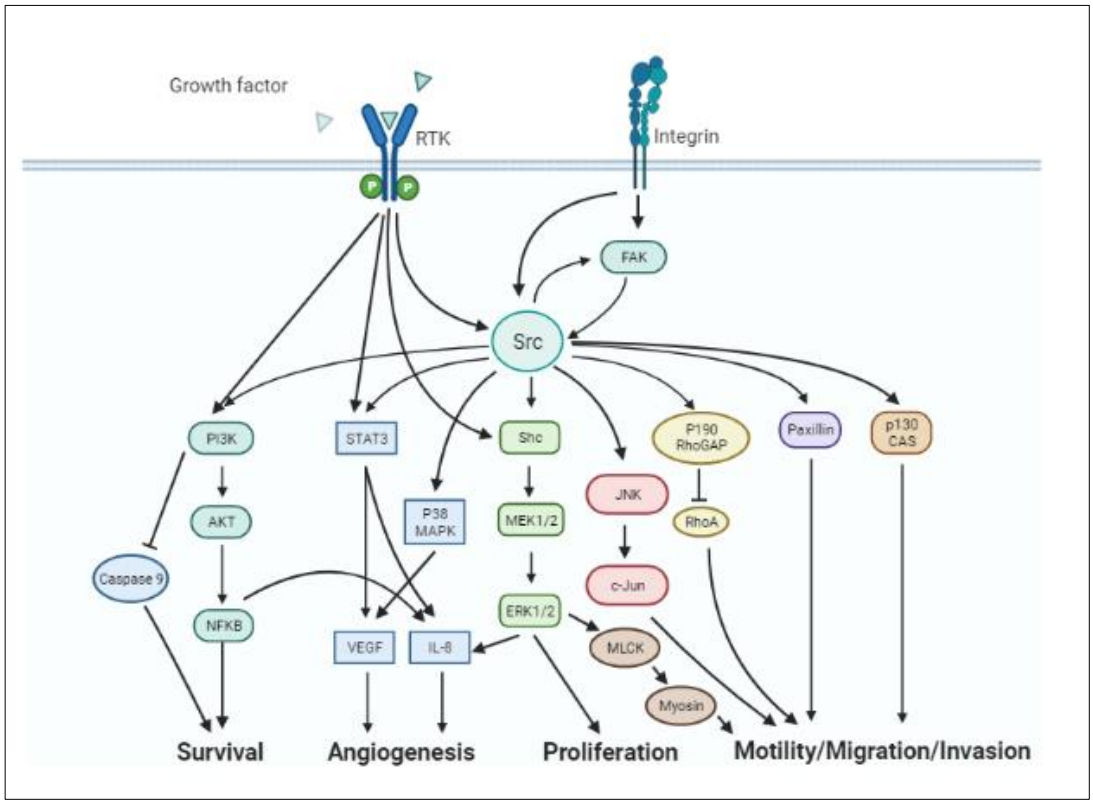

Figure 1.7 Src downstream signalling cascade.

Src has a central homeostatic role in many cellular functions including cell survival, angiogenesis, proliferation, motility, migration and invasion. Due to its central role in many tumorigenic pathways, Src can promote tumorigenesis and progression through its aberrant activation. Adapted from (Summy and Gallick, 2003). Made using BioRender.com.

1.5.3 Src activation in BC

Many studies have suggested an association between Src activation and the development, progression and metastasis of BC (Finn, 2008). The profound elevation of activated Src levels have been observed in human breast tumours compared to benign breast tumours or adjacent normal breast tissue (Ottenhoff-Kalff et al., 1992). Increased levels of activated Src have also been correlated with a low metastasis-free survival in BC patients and has been associated with an increased propensity for metastases in animal models of

BC (Myoui et al., 2003). Src activation has been implicated in BC therapeutic resistance pathways, including that of Herceptin treatment for HER2-positive BC patients. Here, Src activation was found to be a central node to *de novo* and acquired resistance to Herceptin (Zhang, S. et al., 2011; Zhou et al., 2020). The data linking the overexpression and/or increased activation of Src with a more malignant phenotype, indicates that Src is an important therapeutic target in BC.

Several Src inhibitors therefore have or are being developed to treat BC patients (Mayer, E.L. and Krop, 2010; Belli and Esposito, 2020; Lou et al., 2018). Src inhibitors appear to be most effective and potent to treat TNBC. This group of BC patients represents 15-20% of all BC patients and they have a high rate of relapse and metastasis compared to other BC types (Carey et al., 2010; Anders and Carey, 2009). The lack of receptor expression means that these patients cannot benefit from endocrine or HER2-targeted therapy and thus, there is a need for the discovery of specific therapies to treat these patients.

1.5.4 Thesis hypothesis, aims and objectives

Hypothesis:

Breast cancer progression is driven by the aberrant expression and regulation of cell signalling pathways (Butti et al., 2018). This can be driven by irregular receptor tyrosine kinase expression. Breast cancer is a solid tumour malignancy and thus, cells within the middle of the tumour mass are GF and nutrient deprived (Gupta, 2003). Under these microenvironmental conditions, breast cancer cells could utilise aberrant Tier 2 signalling mechanisms through the elevated expression levels of receptor tyrosine kinases, in breast cancer progression and in drug-resistance mechanisms.

Aims:

To determine whether receptor tyrosine kinase expressing breast cancer cells activate an aberrant Tier 2 signalling response to growth under conditions simulating that of the microenvironment of the middle of a tumour mass and under anti-receptor tyrosine kinase therapy.

Objectives:

1. To investigate whether receptor tyrosine kinase overexpression in response to growth under serum (GF)-deprivation/hypoxia/anti-receptor tyrosine kinase therapy leads to Tier 2 (non-canonical) activation of SH3 domain-containing proteins in breast cancer cells.

Breast cancer cells SkBr3 and/or MCF7 will be grown under serum-deprived and/or hypoxic conditions (simulating the tumour microenvironment of cancer cells within the middle of a tumour mass) and/or under anti-receptor tyrosine kinase therapy. The activation state of the SH3 domain-containing proteins hypothesised to be involved in these interactions will be investigated through obtaining phosphorylation levels via immunoblotting and cellular assays. The SH3 domain-containing proteins of interest will be used in further study to determine whether the aberrant Tier 2 activation is through a non-canonical binding event between the receptor tyrosine kinase and the SH3 domain-containing protein.

2. To determine whether Tier 2 activation of SH3-domain containing proteins is via a non-canonical protein-protein interaction between proline-rich regions of receptor tyrosine kinases and the SH3 domains of the SH3 domain-containing proteins, in response to growth under serum-deprivation/hypoxia/anti-receptor tyrosine kinase therapy in breast cancer cells.

Candidate Tier 2 protein-protein interactions will be determined between receptor tyrosine kinases and SH3 domain-containing proteins under serum-deprived and/or hypoxic conditions and/or under anti-receptor tyrosine kinase therapy via the use of domain mutant protein constructs obtained through site-directed mutagenesis, immunoprecipitation and pull-downs and fluorescence microscopy. These interactions will be the forefront of study to determine whether this non-canonical binding event can activate downstream signalling pathways.

3. To establish whether downstream aberrant Tier 2 signalling mechanisms are activated as a consequence of non-canonical activation of SH3-domain containing proteins in response to growth under serum-deprived/hypoxic/anti-receptor tyrosine kinase therapy, which could lead to cancer progression and receptor tyrosine kinase drug-resistance in breast cancer cells.

Phosphorylation levels of potential downstream signalling proteins activated in response to non-canonical Tier 2 activation of SH3 domain-containing proteins will be determined via immunoblotting and the prospective cellular and phenotypic outcome of this investigated through the use of phenotypic cellular assays, when simulating the effect of overexpression of the receptor tyrosine kinase of interest under serum-deprived conditions and/or hypoxic and/or under anti-receptor tyrosine kinase therapy in breast cancer cells. The outcome will determine whether aberrant Tier 2 signalling and a cellular/phenotypic effect can be upregulated in cancer cells overexpressing receptor tyrosine kinases under GF-deprived and/or hypoxia (simulating the microenvironment of the middle of a solid

tumour mass) and/or receptor tyrosine kinase inhibited conditions. This could therefore be a way that cancer cells can maintain viability and undergo cancer progression by upregulating oncogenic cellular pathways under these stress conditions. Thus, this research could impact future therapeutic regimens for receptor tyrosine kinase overexpressing breast cancer patients.

Chapter 2 Methods

2.1 Cell culture

2.1.1 Mammalian cell culture

2.1.1.1 Cell lines and maintenance

The well characterised BC cell lines SkBr3 (mammary gland, breast; derived from metastatic site: pleural effusion) and MCF7 (mammary gland, breast; derived from metastatic site: pleural effusion) were used in this study. SkBr3 cells were maintained in Dulbecco's modified eagle's medium (DMEM) (ThermoFisher, 11054001), supplemented with 10% v/v foetal bovine serum (FBS) (Sigma-Aldrich, F7524) and 1% penicillin-streptomycin (pen-strep) (ThermoFisher, 15070063). MCF7 cells were maintained in DMEM Glutamax medium (ThermoFisher, 21885108), supplemented with 10% v/v FBS and 1% pen-strep. Cells were grown in plastic tissue culture flasks (Corning, 430641U and 430639). Human cell lines were cultured in a Sanyo humidified incubator at 37°C with 5% CO_2 and normoxic conditions (21% O_2), unless stated otherwise.

When cells reached confluency, the cells were harvested by washing the cells with phosphate buffered saline (PBS) (Lonza, 17-516F) and dissociated with 1% trypsin (Gibco, 15400054)) for up to 5 minutes. Cells were collected and centrifuged at 500 x g for 5 minutes and the pelleted cells re-suspended in serum-supplemented media. The cells were passaged 1:4 for SkBr3 cells and 1:6 for MCF7 cells. The cells were added to fresh tissue-culture flasks containing serum-supplemented media and placed back into the incubator. Cells were viewed and imaged using an EVOS fluorescence microscope (Invitrogen). To count cells trypan blue and a cell counting chamber were used (Bio-Rad, 1450003). Mycoplasma was frequently tested in house by members of the Ladbury Laboratory via polymerase chain reaction (PCR).

2.1.1.2 Freezing cell stocks

Cells were frozen for long term storage at -80°C or in liquid nitrogen. Cells were dissociated from flasks using trypsin digestion (**2.1.1.1**). Pelleted cells were re-suspended in 1ml of the relevant serum-containing media with 10%

dimethyl sulfoxide (DMSO) (Sigma, D8418-50ML) and transferred to a cryogenic storage vial (ThermoFisher, 5000-1012). Cells were stored at -80°C for up to 3 months and transferred to liquid nitrogen for long term storage.

2.1.1.3 Cell transfection

Cells were seeded onto a 96 well plate (ThermoScientific, 167008), 12 well plate (Corning, 3513), 6 well plate (Corning, CLS3506) or 10cm² petri dishes (Corning, CLS430167) and cultured in serum-supplemented media to 70-80% confluency. Fresh serum-containing media was added to each well or plate before transfection. Lipofectamine 3000 (ThermoFisher, L3000001) was diluted in Opti-MEM medium (Gibco, 31985062) and a master-mix of purified plasmid DNA (**Table 2.1**) was prepared in Opti-MEM medium and an addition of P3000 reagent (Thermofisher, L3000001), where concentrations were adjusted to the culture vessel used (**Table 2.2**). The diluted DNA was added to the diluted Lipofectamine 3000 in a 1:1 ratio. The mixture was incubated for 15 minutes at room temperature and then added dropwise to the cells. After 24-48 hours the cells were visualised under the EVOS fluorescence microscope (Invitrogen) to determine the rate of transfection of fluorescent constructs. The cells were then used in further experiments.

Table 2.1 Plasmids for mammalian transfection

Plasmid	Encoded gene	Selection	Origin	Tag
SYFP2 (pSYFP2-C1) (Addgene plasmid #22878)	YFP-tag only	Kanamycin	Gifted by Beech Lab, University of Leeds	YFP
WT-VEGFR2-YFP (pcDNA4_TO_VEGFR2_SYFP2)	Wildtype VEGFR2	Ampicillin	Gifted by and made by Beech Lab, University of Leeds	YFP
KD-VEGFR2-YFP	Kinase dead VEGFR2 (K868M)	Ampicillin	Made by Eleanor Cawthorne, Ladbury Laboratory, University of Leeds	YFP
KD-P908A-VEGFR2-YFP	Kinase dead (K868M) and proline-rich motif (P908AP911A) VEGFR2 mutant	Ampicillin	Made by Eleanor Cawthorne, Ladbury Laboratory, University of Leeds	YFP

KD-P1195A-VEGFR2-YFP	Kinase dead (K868M) and proline-rich motif (P1195AP1198A) VEGFR2 mutant	Ampicillin	Made by Eleanor Cawthorne, Ladbury Laboratory, University of Leeds	YFP
KD-2XPXXP-VEGFR2-YFP	Kinase dead (K868M) and proline- rich motif (P908AP911A and P1195AP1198A) VEGFR2 mutant	Ampicillin	Made by Eleanor Cawthorne, Ladbury Laboratory, University of Leeds	YFP
Cerulean-C1 (Addgene plasmid #54604)	CFP-tag only	Kanamycin	Ladbury Laboratory, University of Leeds	CFP
Src-SH3-CFP	Src-SH3 domain only	Kanamycin	Made by Eleanor Cawthorne, Ladbury Laboratory, University of Leeds	CFP
Src-SH2-CFP	Src-SH2 domain only	Kanamycin	Made by Eleanor Cawthorne, Ladbury Laboratory, University of Leeds	CFP
WT-Src-CFP	Wildtype full length Src	Kanamycin	Made by Eleanor Cawthorne, Ladbury Laboratory, University of Leeds	CFP
Plcg1-SH3-CFP	Plcg1-SH3 domain only	Kanamycin	Made by Eleanor Cawthorne, Ladbury Laboratory, University of Leeds	CFP
Plcg1-SH2-N-CFP	Plcg1-SH2-N domain only	Kanamycin	Made by Eleanor Cawthorne, Ladbury Laboratory, University of Leeds	CFP
Plcg1-SH2-C-CFP	Plcg1-SH2-C domain only	Kanamycin	Made by Eleanor Cawthorne, Ladbury Laboratory, University of Leeds	CFP

Table 2.2 Scaling of Lipofectamine 3000 reagent mix

Culture vessel	Multiplication factor	Growth medium for complexing	Opti-MEM medium for complexing	DNA	P3000 reagent	Lipofectamine 3000 reagent
96 well	0.2	100µl	2 x 5µl	100ng	0.2µl	0.1µl
12 well	2	1ml	2 x 50µl	1µg	2µl	1µl
6 well	5	2ml	2 x 125µl	2.5µg	5µl	2.5µl
10 cm dish	28.95	10ml	2 x 500µl	14µg	28µl	14µl

2.1.1.4 Cell lysis

Cell lysates were obtained by washing the cells three times with ice-cold PBS (Lonza, 17-516F). Cells grown on 10cm^2 petri dishes or 6 well plates were then placed on ice and 1X mammalian cell lysis buffer (Cell Signalling, #9803) plus 1X protease and phosphatase inhibitor (ThermoFisher, A32963) was added to the cells and coated the whole dish with buffer. The cells were left to incubate for 20 minutes on ice. The cells were then scraped, collected and centrifuged at 15,000 rpm for 10 minutes at 4°C. After centrifugation, the supernatant of the cell lysate was retained into a clean Eppendorf tube and the pellet discarded. Lysates were stored at -80°C until use.

2.1.1.5 Serum-starvation

Cells were washed three times with PBS (Lonza, 17-516F) and then grown under fresh DMEM (SkBr3 cells) or DMEM glutamax (MCF7 cells) media only with no FBS supplementation (0% FBS), to induce nutrient and serum-deprived stress on the cells for 24 hours.

2.1.1.6 Hypoxic incubation

Cells were incubated in a hypoxic incubator (ESBE Scientific) to induce hypoxia-mediated stress on the cells for 24 hours. Here, the cells were incubated at 37°C with 1% O_2 and 5% CO_2.

2.1.2 Bacterial cell culture

2.1.2.1 Storage and growth of bacteria

Plasmids were amplified using the competent *E.Coli* strains XL1-Blue (Agilent, 200236) and DH5α (New England Biolabs (NEB), C2987H) and grown in

lysogeny broth (LB) (Sigma, L3522) with 1X antibiotic (Ampicillin - Sigma, A9518 or Kanamycin - Sigma, K1876) in a MaxQ 6000, ThermoScientific shaking incubator at 37°C or on 1X antibiotic containing plates (Corning, CLS430167) overnight at 37°C. For long term storage glycerol stocks of transformed bacteria were made using 50:50 v/v overnight culture: 50% glycerol (Sigma, G5516) and stored at -80°C.

Protein expression was performed using the competent *E.Coli* strain BL21 (DE3) (NEB, C2527H). Similar growth conditions were performed with BL21 (DE3), XL1-Blue and DH5α strains of bacteria, unless otherwise stated.

2.1.2.2 Bacterial transformation

Bacteria were transformed using 50µl competent cells and 100ng of purified plasmid DNA. The cells were incubated with the plasmid DNA on ice for 30 minutes, followed by a heat shock of 42°C for 45 seconds for both XL1-Blue and DH5α cells, and BL21 (DE3) for 10 seconds. The bacterial cells were recovered on ice for 2 minutes and 1ml super optimal broth (SOC) medium (NEB, B9020S) added. The cultures were incubated for 1 hour shaking at 37°C. Each culture was then plated on 1X antibiotic containing LB agar (Sigma, L3147) plates (Corning, CLS430167) and incubated at 37°C overnight for growth of bacterial colonies.

2.1.2.3 Plasmid purification

Qiagen plasmid miniprep (Qiagen, 27104) and midiprep kits (Qiagen, 12143) were used to purify small and medium-scale plasmid DNA for the use in further experiments, using the manufacturers guidelines. Overnight cultures were made in 5ml LB broth (Sigma, L3522) (miniprep) or 50ml LB broth (midiprep) with appropriate 1X antibiotic, containing inoculated bacterial colonies or glycerol stocks. Once the purified plasmid DNA was eluted using elution buffer (EB) from the kits, DNA was stored at -20 degrees for further use.

2.2 Bacterial protein expression and purification

Overnight cultures of transformed (**2.1.2.2**) BL21 (DE3) cells with bacterial protein expression plasmids (**Table 2.3**) were made in 5ml of LB and 1X antibiotic (Ampicillin - Sigma, A9518) at 37°C. 1ml of overnight culture was

added to 50ml LB and 1X antibiotic in a 250ml flask and grown to OD_{600} = 0.6. Expression was induced by adding 0.1mM Isopropyl β-D-1-thiogalactopyranoside (IPTG) (Sigma, I1284) to each culture and grown overnight at 20°C, 200rpm in a shaking incubator (ThermoScientific). Cells were then centrifuged at 3900rpm at 4°C for 20 minutes and the pellets stored at -20°C or re-suspended in 1X bacterial cell lysis buffer (1X bacterial cell lysis buffer recipe: 20mMTris pH8.0, 150mM NaCl, 1mM β-Mercaptoethanol in 1L dH_2O). The re-suspended bacteria were then sonicated for 2 minutes (5 seconds on, 10 seconds off, at 80% amplitude) to break open the bacterial cells and centrifuged at 3900rpm for 30 minutes at 4°C to get rid of cell debris. Bacterial supernatant containing the expressed protein of interest was retained and 5µl of supernatant and 5µl 2X laemmli sample buffer (Bio-Rad, 1610747) were boiled for 10 minutes at 95°C and protein expression determined via Sodium Dodecyl Sulphate-Polyacrylamide Gel Electrophoresis (SDS-PAGE) (**2.4.2**) on a pre-cast gel (Bio-Rad, 4561094). The gel was then stained using coomassie reagent (Bio-Rad, 161-0436) to detect protein bands of the correct size.

Table 2.3 Plasmids for bacterial protein expression

Plasmid	Encoded gene	Selection	Origin	Tag
MBP-tag	MBP-tag only	Ampicillin	Ladbury Lab, University of Leeds	MBP
MBP-VEGFR2-C-terminal- tail-WT	Wildtype VEGFR2-C-terminal-tail only	Ampicillin	Ladbury Lab, University of Leeds	MBP
MBP-VEGFR2-C-terminal-tail-PxxP mutant	VEGFR2-C-terminal-tail-P1195AP1198A mutant	Ampicillin	Eleanor Cawthorne, Ladbury Lab, University of Leeds	MBP

2.2.1 Maltose binding protein (MBP) purification

After bacterial protein expression was analysed (**2.2**), expressed MBP-tagged proteins were purified using amylose MBP-binding beads (NEB, E8021S). 200µl of amylose bead slurry were washed three times using 1ml 1X bacterial cell lysis buffer (recipe in **2.2**) by centrifuging at 4000rpm for 5 minutes,

discarding the supernatant, and washing again. The wash buffer was then discarded and the washed beads added to the retained bacterial supernatant (**2.2**) containing the expressed MBP-tagged protein of interest. The bacterial lysate and bead mixture were then incubated overnight, rotating at 4°C. The protein-bound amylose beads were pelleted via centrifugation (4000rpm for 5 minutes) and the supernatant discarded. The protein-bound amylose beads were washed five times by centrifugation, using 1ml 1X bacterial cell lysis buffer and the last wash step was exchanged to 1X mammalian cell lysis buffer (Cell Signalling, #9803), for use in an MBP pull-down with mammalian cell lysates (**2.6.3**).

2.3 Molecular cloning

2.3.1 Agarose gel electrophoresis, gel extraction and PCR purification

1% agarose gels were made using 1g Agarose (Sigma, A9539) and 100ml 1X TAE buffer (ThermoFisher, B49) and 1X Sybr safe (Invitrogen, S33102), to determine the success of PCR reactions. The agarose-TAE mixture was boiled until clear and allowed to set in a gel tank. DNA samples were diluted in 6X gel loading dye (NEB, B7024S) and 1Kb DNA ladder (NEB, N3232S) was also loaded to indicate the size of DNA molecules. The agarose gel was ran at 80V for 1 hour in 1X TAE buffer. DNA bands were extracted using a QIAquick gel extraction kit (Qiagen, 28704). If PCR reactions were not run on a gel, they were purified using a QIAquick PCR purification kit (Qiagen, 28104). The purified PCR products were then transformed into competent cells (**2.1.2.2**) and the DNA isolated and purified (**2.1.2.3**). All PCR products were sent for sequencing to determine whether the correct sequence was made in the reaction (Genewiz).

2.3.2 Site-directed mutagenesis (SDM)

A reaction mixture using specific primers to implement the mutation (**Table 2.4**) was made in a PCR tube (**Table 2.5**). The reagents were then ran on a PCR thermocycler (1000 Touch Thermocycler, BioRad) SDM programme (**Table 2.6**). 1µl DPNI (NEB, R0176S) was added to each reaction to digest the parental methylated DNA and incubated overnight at 37°C and

transformed straight into competent cells (**2.1.2.2**) and the plasmid DNA isolated and purified (**2.1.2.3**). All DNA was sent for sequencing (Genewiz) to determine whether the correct mutation had been implemented.

Table 2.4 SDM primers

Mutation	Forward primer	Reverse primer
VEGFR2 kinase dead (K868M)	CTT GCA GGA CAG TAG CAG TCA TGA TGT TGA AAG AAG GAG CAA CAC	GTG TTG CTC CTT CTT TCA ACA TCA TGA CTG CTA CTG TCC TGC AAG
VEGFR2 PxxP #1 (P908AP911A)	CTA GGT GCC TGT ACC AAG GCA GGA GGG GCA CTC ATG GTG ATT GTG G	CCA CAA TCA CCA TGA GTG CCC CTC CTG CCT TGG TAC AGG CAC CTA G
VEGFR2 PxxP #2 (P1195AP1198A)	GAT TCT GGA CTC TCT CTG GCT ACC TCA GCT GTT TCC TGT ATG GAG G	CCT CCA TAC AGG AAA CAG CTG AGG TAG CCA GAG AGA GTC CAG AAT C

Table 2.5 SDM PCR reagent mix

Reagent	Volume/concentration
dNTPs (ThermoFisher, R0191)	20mM
dH_20	Up to 25µl
Betaine (Sigma, B0300)	5µl
10x reaction buffer (Agilent, #600670)	2.5µl
DNA plasmid template	250ng
Forward primer (**Table 2.3**) (IDT)	0.6µM
Reverse primer (**Table 2.3**) (IDT)	0.6µM
Pfu UltraII (Agilent, #600670)	5 units

Table 2.6 SDM PCR thermocycler steps

Step	Number of cycles	Temperature	Time
Initial denaturation	1	92°C	30 seconds
Denaturation	18	92°C	30 seconds
Annealing	18	Dependent on primer Tm	1 minute
Elongation	18	68°C	2 minutes/Kb
Final Elongation	1	68°C	10 minutes
Held	1	4°C	∞

2.3.3 Cloning into Cerulean-C1 vector

Primers were designed to insert into the Cerulean-C1 vector at the restriction sites HindIII and EcoRI (**Table 2.7**). Phusion PCR was used to amplify the insert DNA using a Phusion PCR reagent mix (**Table 2.8**) on the PCR thermocycler (**Table 2.9**). After the insert DNA had been amplified, the PCR product was isolated via a PCR purification kit (**2.3.1**). Restriction digests were made of both the purified PCR insert and the Cerulean-C1 vector in parallel. The entire PCR reaction was used and 1µg Cerulean-C1 vector (**Table 2.10**). The reaction was incubated at 37°C overnight. The digest was ran on a 1% agarose gel and the DNA purified using a QIAquick gel extraction kit (**2.3.1**) to isolate the cut vector and insert DNA bands. The concentration of DNA was determined using a nanodrop 2000 (ThermoScientific). DNA ligation was performed with 100ng total DNA using a recipient plasmid to insert molar ratio of 1:3 (**Table 2.11**). The reaction was left to occur overnight at 16°C. Transformation was performed using the ligated DNA in XL-1 blue competent cells (**2.1.2.2**). Individual bacterial colonies were picked, their DNA isolated and purified (**2.1.2.3**), and sequenced (Genewiz) to check for successful ligations. Full sequencing results obtained of each CFP-construct can be found in **Supplementary 1.1**.

Table 2.7 Cerulean-C1 primers

Insert	Forward primer (HindIII)	Reverse primer (EcoRI)
Src SH2 domain	TAA GCA AAG CTT ATT GGT ATT TTG GCA AG	TGC TTA GAA TTC ATG CAC ACG GTG GTG AG
Src SH3 domain	TAA GCA AAG CTT ATG GTG GAG TGA CCA CC	TGC TTA GAA TTC ATG GAG TCG GAG GGC GC
Src WT full length	TAA GCA AAG CTT ATA TGG GTA GCA ACA AG	TGC TTA GAA TTC ATC TAG AGG TTC TCC CCG GG
Plcg1 SH2-N domain	TAA GCA AAG CTT ATT GGT TCC ATG GGA AG	TGC TTA GAA TTC ATG ACA GGC TCT GAA AG
Plcg1 SH2-C domain	TAA GCA AAG CTT ATT GGT ACC ACG CGA GC	TGC TTA GAA TTC ATG ATG GGA TAG CGC AG
Plcg1 SH3 domain	TAA GCA AAG CTT ATA CTT TCA AGT GTG CA	TGC TTA GAA TTC ATG TTG ACC ATC TCT TC

Table 2.8 Phusion PCR reagents mix

Reagent	Volume/concentration
Phusion® High-Fidelity PCR Master Mix with GC Buffer (NEB, M0532L)	12.5µl (1X)
Betaine (Sigma, B0300)	5µl
Forward primer (**Table 2.6**) (IDT)	1.25µl (10µM)
Reverse primer (**Table 2.6**) (IDT)	1.25µl (10µM)
DNA	<250ng
dH_2O	>25µl

Table 2.9 Phusion PCR thermocycler steps

Step	**Temperature**	**Time**
Initial denaturation	98°C	30 seconds
Denaturation (30 cycles)	98°C	5 seconds
Annealing (30 cycles)	Dependent on primer Tm	10 seconds
Elongation (30 cycles)	72°C	15 seconds/kb
Final Extension	72°C	10 minutes
Hold	4°C	∞

Table 2.10 Restriction enzyme double digestion reagents

Reagent	Volume
DNA	1µg
10X CutSmart Buffer (NEB, B7204S)	5µl (1X)
HindIII-HF (NEB, R3104S)	1µl
EcoRI-HF (NEB, R3101S)	1µl
Nuclease-free water	to 50µl

Table 2.11 DNA ligation reaction mix

Reagent	Volume/concentration
Digested vector DNA	100ng total DNA (Vector 1:3 insert DNA molar ratio)
Digested insert DNA	
T4 DNA Ligase Reaction Buffer (NEB, B0202S)	1µl (1X)
T4 DNA ligase (NEB, M0202S)	1µl
dH_2O	To 10µl

2.4 Immunoblotting

2.4.1 Determining protein concentration

Protein concentration was determined using the Bicinchoninic acid assay (BCA) (Pierce, 23225), whereby 10µl of pre-prepared bovine serum albumin (BSA) standards and unknown cell lysate samples were added to a microwell 96 well plate (ThermoScientific, 167008) and 200µl of working reagent (50:1 v/v, reagent A:B) to each well. The plate was covered, mixed thoroughly on a plate shaker for 30 seconds and incubated at 37°C for 30 minutes. The plate was allowed to cool to room temperature and the absorbance measured at 562nm on a plate reader (BioTek Powerwave, ThermoFisher).

A standard curve was produced using the BSA protein standards absorbance values and their known protein concentration. The unknown sample protein concentration was calculated in µg/ml using the linear equation calculated from the standard curve.

2.4.2 SDS-PAGE

For western blotting applications the appropriate protein concentration of cell lysate, which was determined by BCA assay (**2.4.1**), was added to 1X laemmli sample buffer (Bio-Rad, 1610747) and boiled for 10 minutes at 95°C in a heat block. The denatured samples were pelleted and added to a 4-20% TGX stain-free precast gel (Bio-Rad, 4561094) with pre-stained protein ladder (NEB,

P7719) to indicate protein size. Proteins were then separated via SDS-PAGE at 130V for 70 minutes in a gel tank (Bio-Rad) filled with 1X running buffer (Bio-Rad, #1610732).

2.4.3 Western blot

The protein bands were transferred to a polyvinylidene fluoride (PVDF) membrane (Bio-Rad, 1620177) using 250mAmp over 120 minutes in a tank filled with 1X transfer buffer (Bio-Rad, 1610771) and an ice pack. Once transferred, the membrane was blocked for 1 hour in 5% BSA (Sigma, B2518) diluted in 1X tris-buffered saline (TBS) (10X TBS: 24g Tris-Base (Sigma, T8524), 88g NaCl (sigma, S9888), dissolved in 900ml dH_2O. The pH was adjusted to 7.6 with hydrochloric acid (HCL) (Thermofisher, 10053023) and the final volume of TBS adjusted to 1L with dH_2O) with 1% Tween-20 (Sigma, P9416) (TBST) for 1 hour at room temperature. The membrane was then probed overnight with primary antibody (**Table 2.12**) diluted in 5% BSA, rocking at 4°C. The PVDF membrane was then washed four times in 1X TBST for 5 minutes, rocking, and incubated with a secondary horseradish peroxidase (HRP)-conjugated antibody (**Table 2.12**) diluted in 5% BSA for 1 hour at room temperature. Following a further four washes with 1X TBST, the protein bands were detected using enhanced chemiluminescence (ECL) substrate (Bio-Rad, 170-5060) and visualised using a G-box system (Syngene) to detect emitted light. Protein band intensity was determined and normalised (**2.8**).

Table 2.12 Antibody datasheet

Antibody	Molecular weight (KDa)	Source (IgG)	Manufacturer/catalogue number
pSrc Y416	60	Rabbit	Cell Signalling, #2101
pSrc Y527	60	Rabbit	Cell Signalling, #2105
Src	60	Rabbit	Cell Signalling, #2109
pHER2 Y877	185	Rabbit	Cell Signalling, #2241
pHER2 Y1221/1222	185	Rabbit	Cell Signalling, #2249
HER2	185	Rabbit	Cell Signalling, #2165
β-actin	45	Rabbit	Cell Signalling, #4970
pHER3 Y1289	185	Rabbit	Cell Signalling, #4791
VEGFR2	210, 230	Rabbit	Cell Signalling, #9698
pVEGFR2 Y1175	230	Rabbit	Cell Signalling, #3770
Plcg1	150	Rabbit	Cell Signalling, #5690
Nck1	47	Rabbit	Cell Signalling, #2319
GFP (YFP/CFP cross-reactivity)	27	Rabbit	Cell Signalling, #2956
MBP	42	Mouse	Cell Signalling, #2396
pAKT T308	60	Rabbit	Cell Signalling, #9275
Total AKT	60	Rabbit	Cell Signalling, #9272
pERK1/2 T202, Y204	42, 44	Rabbit	Cell Signalling, #9101
Total ERK	42, 44	Rabbit	Cell Signalling, #9102

VEGF	22	Mouse	Santa Cruz, (C-1) sc-7269
HRP-linked anti-Rabbit secondary	-	Goat	Cell Signalling, #7074
HRP-linked anti-Mouse secondary	-	Horse	Cell Signalling, #7076
Anti-rabbit IgG (Alexa Fluor® 594 Conjugate)	Rabbit	Goat	Cell Signalling #8889
Anti-rabbit IgG (Alexa Fluor® 488 Conjugate)	Mouse	Goat	Cell Signalling #4408

2.4.4 Human Phospho-Kinase Antibody Array

A Human Phospho-Kinase Antibody Array kit was purchased from R&D Systems (ARY003B) to analyse the phosphorylation profiles of human kinases in cell lysates. Pre-made nitrocellulose membranes spotted with capture antibodies were blocked for one hour using R&D blocking buffer and then incubated with the same protein concentration of cell lysate (**2.4.1**) (600µg) for each different cell culture condition sample, which was diluted in blocking buffer. The membranes were incubated with cell lysate overnight, rocking at 4°C. The membranes were then washed 3X for 10 minutes in R&D washing buffer and a detection antibody cocktail incubated with the membranes for 2 hours, rocking, at room temperature. The membranes were washed 3X for 10 minutes in washing buffer and then incubated with streptavidin-HRP for 30 minutes, rocking at room temperature. The blots were then washed 3X for 10 minutes with washing buffer and an R&D chemi-reagent added to the membranes for 1 minute. The membranes were then visualised using a G-box

system (Syngene) to detect emitted light. The intensity of dots was determined and normalised (**2.8**).

2.5 Fluorescence microscopy

2.5.1 Immunofluorescence (IF)

SkBr3 cells were grown on sterile 25x25 coverslips (Corning, CLS285525) in 6 well plates and grown to a confluency of around 50%. The cells were then serum starved prior to drug treatment (**2.1.1.5**). The media was removed and replaced with fresh serum-free medium containing PBS (Lonza, 17-516F) only (vehicle-control) or serum-free medium with Herceptin (Cambridge Biosciences, HY-P9907-1mg) at a concentration of 4µg/ml and incubated for 3 or 6 hours. The media was then aspirated and the cells washed three times with PBS. The cells were then covered with 4% paraformaldehyde (PFA) (Boster Biological Technology, AR1068) diluted in PBS (Lonza, 17-516F) by a depth of 2-3mm. The cells were fixed for 15 minutes at room temperature and then washed three times with PBS. The cells were blocked using 5% goat serum (Sigma, G9023) diluted in PBS, for 60 minutes at room temperature. The blocking buffer was then aspirated and diluted primary antibody (**Table 2.12**) was added to the cells according to the antibody data sheet, diluted in 5% goat serum and left to incubate overnight at 4°C. The cells were washed three times with PBS and probed with RFP-conjugated (α-rabbit) and GFP-conjugated (α-mouse) secondary antibodies (**Table 2.12**) for 2 hours at room temperature in the dark. The cells were washed three times in PBS and mounted onto coverslips using mountant medium with DAPI (Sigma, F6057) and added to glass slides (Sigma, S8902-1PAK). The slides were allowed to dry overnight in the dark at room temperature and stored at 4°C until imaged under the confocal microscope. Slides were imaged using an LSM700 Inverted Confocal Microscope (Zeiss) in the RFP (excited at 594nm and detected at 614nm) and GFP channel (excited at 488nm and detected at 510nm). Gain = 1.0.

2.5.2 Förster resonance energy transfer (FRET)

Cells were seeded onto sterile 25x25 coverslips (Corning, CLS285525) in a 12 well plate and left to grow overnight in 2ml fresh serum-supplemented

media. The cells were co-transfected (**2.1.1.3**) with each plasmid encoding the protein constructs with a yellow fluorescent protein (YFP) tag (acceptor) and cerulean fluorescent protein (CFP) tag (donor), where these fluorescent tags were used as a FRET pair. After transfection, the cells were serum starved (**2.1.1.5**), prior to fixation. The cells were then washed three times with PBS and fixed in the 12 well plate, coating the cells in 0.5ml 4% PFA for 20 minutes. The coverslips were washed three times with PBS and mounted onto a glass slide (Sigma, S8902-1PAK) using mounting media (Sigma, 03989). The slides were left to dry overnight in the dark, at room temperature and stored at 4°C.

Fluorescent signals were detected on a Zeiss LSM880 + airyscan inverted confocal microscope. CFP fluorescence was measured by exciting CFP at 436nm and emission detected between 470-510nm. YFP fluorescence was measured by exciting YFP at 516nm and emission detected at 520-540nm. FRET signal was excited at 436nm and detected at 520-540nm. Gain = 1.0.

2.6 Immunoprecipitation (IP) and pull-downs

2.6.1 Endogenous co-immunoprecipitation (Co-IP)

50µl of protein G sepharose bead slurry (Sigma, GE17-0618-01) were washed three times with PBS via centrifugation (1000g for 5 minutes) at 4°C. Cell lysates of 1mg total protein concentration (**2.4.1**) were pre-cleared with the washed protein G sepharose beads for 1 hour rotating at 4°C, to eradicate any non-specific binding. The samples were then centrifuged and the pre-cleared supernatant added to 4µg of antibody (**Table 2.12**) and incubated for 4 hours at 4°C, rotating. 50µl bead slurry of protein G sepharose beads were washed three times with PBS via centrifugation and added to the lysate-antibody mixture and left to incubate overnight at 4°C, rotating. The beads were pelleted and the supernatant discarded. The beads were washed three times with ice-cold 1X mammalian cell lysis buffer (Cell Signalling, #9803) via centrifugation. 20µl of 4X laemmli sample buffer (Bio-rad, 1610747) was added to the beads and bound proteins eluted by boiling at 95°C for 10 minutes. The samples were then centrifuged to pellet the beads and the eluted bound proteins analysed by SDS-PAGE (**2.4.2**) and western blotting (**2.4.3**).

2.6.2 YFP/CFP pull-down

GFP-TRAP agarose beads (ChromoTek, gtak-20) were used to pull-down YFP and CFP tagged proteins in cell lysate due to the multi-specificity of the beads. 25µl bead slurry was washed with 500µl ice-cold dilution buffer (ChromoTek, gtak-20) and centrifuged (2500g for 5 minutes) at 4°C. The beads were washed three times and cell lysate containing CFP or YFP tagged proteins were added to the equilibrated beads. The beads and lysate mixture were left to rotate for 1 hour at 4°C. The beads were pelleted and the supernatant discarded. The beads were then washed three times with 500µl ice-cold dilution buffer via centrifugation and the bound proteins dissociated with 100µl of 2X laemmli sample buffer (Bio-rad, 1610747). Proteins were eluted by boiling at 95°C for 10 minutes and the beads pelleted via centrifugation. The supernatant containing bound proteins was analysed via SDS-PAGE (**2.4.2**) and western blotting (**2.4.3**).

2.6.3 MBP pull-down

Mammalian cell lysate (1mg total protein) was pre-cleared for 1 hour at 4°C, rotating, with washed amylose beads (**2.2.1**), to eradicate any non-specific binding. The mammalian cell lysate-bead mixture was centrifuged and the pre-cleared mammalian cell lysate supernatant was added to the purified MBP-tagged protein bound amylose beads (**2.2.1**). The MBP-bound-beads and cell lysate mixture was left to incubate overnight, rotating at 4°C. The beads were then washed three times via centrifugation (4000rpm for 5 minutes) with 1ml 1X mammalian cell lysis buffer (Cell Signalling, #9803). 100µl of 2X laemmli sample buffer (Bio-Rad, 1610747) was added to the isolated beads and boiled at 95°C to elute bound proteins from the beads. The eluted protein was used for SDS-PAGE (**2.4.2**) and western blot (**2.4 3**) analysis.

2.7 Cellular assays

2.7.1 MTT cell viability assay

SkBr3 cells were seeded at a density of $5x10^3$ cells per well in a 96 well plate (Corning, 3599) and incubated overnight in 200µl of serum-supplemented or serum-free media. The plates were drug treated with the 100µl replacement

method, 100µl of media was aspirated and 100µl of media containing Herceptin (Cambridge Biosciences, HY-P9907-1mg) or Lapatinib (Biovision, #1624) was added to each well in 5 times serial dilutions. At each concentration were four replicate wells. A row of control wells containing media with PBS only (Lonza, 17-516F) or DMSO only (Sigma, D8418-50ML) (vehicle-control) and a row with media only as a background control, were also plated. The plates were incubated for 72 hours at 37°C. 20µl of 3-(4,5-dimethylthiazol-2-yl)-2,5-diphenyl tetrazolium bromide (MTT) was added to each well at a stock concentration of 5mg/ml, giving a final concentration of 0.5mg/ml per well and incubated for 4 hours at 37°C. All media was then aspirated and 150µl of DMSO was added to each well. The plate was mixed on a shaker for 30 seconds to dissolve the formazan crystals and the relative viability detected via spectrophotometry, at a wavelength of 570nm and detection absorbance normalised to the vehicle-treated control wells (DMSO only).

2.7.2 Scratch wound migration assay

A 96 well gridded plate (Essen, 4379) was pre-coated with 5µg/cm^2 collagen (ThermoFisher, A1048301). 70,000 SkBr3 cells or 50,000 MCF7 cells were seeded into each coated well with serum-supplemented media and incubated overnight at 37°C. The cells were washed three times and fresh media added with serum (10% FBS) or without serum (0% FBS) and incubated for a further 24 hours at 37°C to allow for serum starvation (**2.1.1.5**). After this incubation, the cells were either drug treated with Herceptin at the appropriate concentrations (Cambridge Biosciences, HY-P9907-1mg) or transfected (**2.1.1.3**) in each well, alongside a vehicle-treated control. The scratch was then made using a wound maker 96 (Essen) to create a uniform scratch across the surface. The cells were washed three times with PBS. The plates were then placed in an incubator at optimum cell conditions (37°C and normoxia (21% O_2), 5% CO_2). Images were taken at every hour over a 48 hour period at 10x magnification using the IncuCyte system (Sartorius). The average wound closure (µM) and average wound confluence (%) was determined (**2.8**)

2.7.3 Src phosphorylation assay

A PathScan Phospho-Src (Y416) Sandwich Elisa Kit (Cell Signalling, #7953) was used to determine relative endogenous phosphorylated Src at Tyrosine 416 (Y416) Src levels in SkBr3 cells that had been treated with Herceptin. Here, pY416 Src rabbit antibody had already been pre-coated onto microwells and were incubated with pre-Herceptin treated SkBr3 cell lysate (1mg of total protein in each sample) overnight at 4°C. After incubation with cell lysates, the wells were washed 4X to eradicate any unbound proteins. A reconstituted mouse Src detection antibody was added to each well to recognise the bound protein and incubated at 37°C for 1 hour. After a second wash step (4X washes), 100µl of HRP-linked anti-mouse secondary antibody was added to each well and incubated at 37°C for 30 minutes. The plates were then washed 4X and 100µl of 3,3',5,5'-tetramethylbenzidine (TMB) substrate added to each well and incubated for 10 minutes at 37°C. 100µl of stop solution was added to the wells and the absorbance detected using a plate reader at 450nm. The magnitude of the absorbance for each well was proportional to the quantity of pY416 Src in each sample.

2.8 Kaplan-Meier plotter analysis

The prognostic value of VEGFR2 (KDR) and Src protein expression levels in BC patient data was analysed using the Kaplan-Meier Plotter database (http://kmplot.com/analysis/). The database integrates protein expression data of BC patients with clinical data. To date, the Kaplan-Meier plotter only has protein expression correlation data in BC patients but can also be used to look into gene expression correlations with clinical data with other cancer types. The database contains information on 1064 BC patients and their protein expression and clinical survival data. The analysis in this study focused VEGR2 and Src independent expression levels on OS of BC patients. Using this software the hazard ratio (HR), 95% confidence interval (CI) and log-rank p value were calculated to determine whether there was a significant relationship between protein expression levels and OS.

2.9 Data analysis

Blot intensity was determined via densitometry analysis which was quantified using Image Studio Lite analysis software (Licor). The intensity of each dot or band was normalised to a total protein loading control. All scratch assays were analysed using IncuCyte Base Analysis Software (Sartorius) for both wound closure (µM) and wound density (%). Differences between control cells and treated cells were compared using a two-tailed T-test (GraphPad Prism). P-values ≤0.05 were considered statistically significant. A significant difference was denoted by * = P≤0.05, ** = P≤0.01, *** = P≤0.001, **** = P≤0.0001 between the two values.

Chapter 3
The effect of inhibition of the HER2-RTK via Herceptin in HER2-positive BC cells

3.1 Introduction

3.1.1 ErbB/HER family

The ErbB family of RTKs are responsible for multiple diverse biological responses including cell proliferation, differentiation and motility. There are four closely related members of the ErbB family, epidermal growth factor receptor (EGFR) or human epidermal growth factor receptor-1 (HER1/ErbB1), human epidermal growth factor receptor-2 (HER2/ErbB2) human epidermal growth factor receptor-3 (HER3/ErbB3) and human epidermal growth factor receptor-4 (HER4/ErbB4) (Baselga and Swain, 2009).

Individual ErbBs and specific ErbB dimers activate particular downstream signalling pathways. The three best characterised pathways induced by ErbB signalling include, Ras–MAPK, PI3K–Akt and PLC-PKC. All ErbB receptors couple to activate the Ras-MAPK pathway either through SH2 domain recruitment of Grb2 or indirectly through PTB domain-mediated binding of the adaptor protein Shc (Marmor et al., 2004; Yarden and Pines, 2012).

3.1.1.1 ErbB structure

ErbB receptors contain an extracellular ligand-binding domain and a single hydrophobic transmembrane domain. The intracellular domain encompasses a highly conserved TKD. Upon ligand binding, the ErbB receptors hetero- or homo- dimerise with each other, resulting in the transphosphorylation of the receptors and the activation of intrinsic TK activity. The resulting autophosphorylation within the C-terminal tail of the receptor molecules enables the recruitment and activation of particular signalling effector proteins (Olayioye et al., 2000; Marmor et al., 2004).

There are four extracellular binding domains. Cysteine-rich domains II and IV, and the ligand-binding domains I and III. Domain II participates in homo or heterodimer formation with other ErbB family members (Appert-Collin et al., 2015) (**Figure 3.1.1b**). ErbB1, ErbB3 and ErbB4 all exist in a monomeric

‘closed’ confirmation under basal conditions, in which the dimerisation domain cannot make contact with other ErbB receptors in the absence of ligand. ErbB2 or HER2 is unique in that it exists in an ‘open’ conformation under basal conditions and is therefore always readily available for ErbB receptor dimerisation (Baselga and Swain, 2009) (**Figure 3.1.1a**).

Upon ligand-binding, the ErbB receptors (1, 3 and 4) re-orientate their extracellular domains such that domain I binds to domain III and thus, changes the conformation of the receptor to an ‘open’ and active state. When the ErbB receptors change their conformation to an active form, they can hetero- or homo- dimerise with other ErbB receptors, including HER2 which is in a constitutively ‘open’ and active state, primed ready for dimerisation (**Figure 3.1.1b**) (Baselga and Swain, 2009).

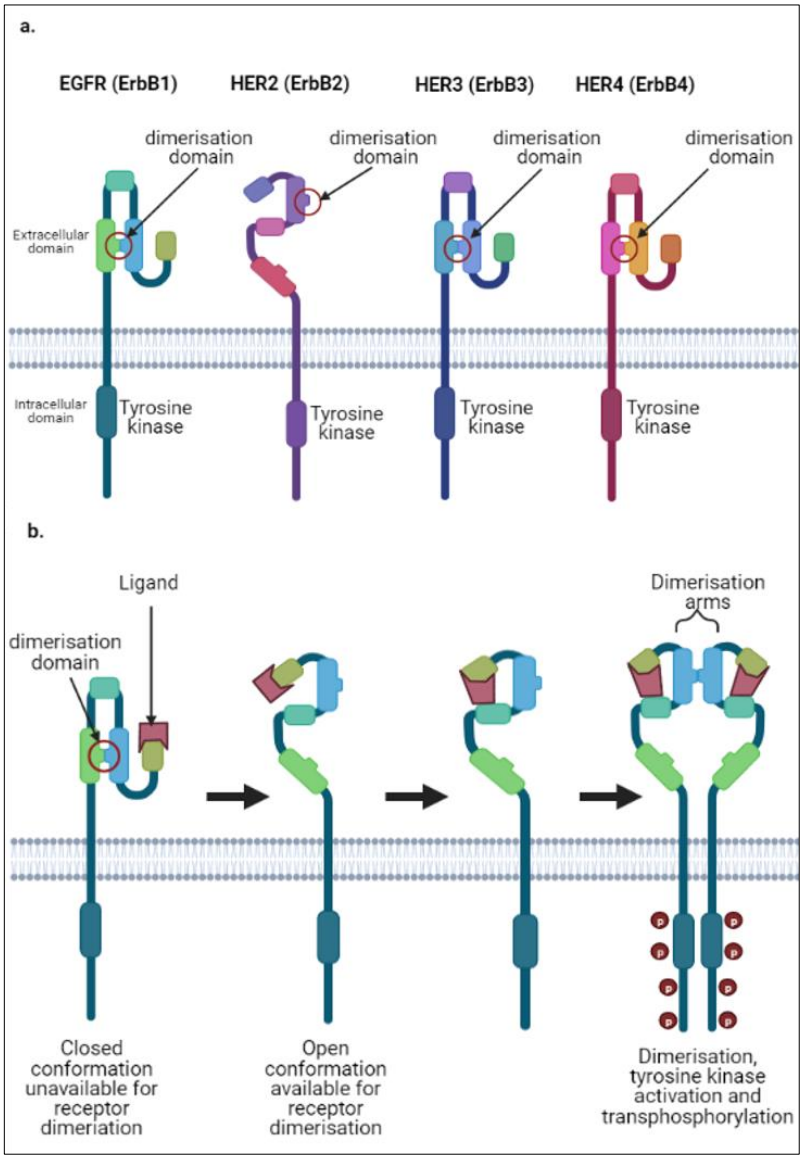

Figure 3.1.1 ErbB family structure and dimerization.

a. The structures of the four ErbB receptors, including their sub-domains and conformation when under basal, serum-deprived conditions. HER2 is in a constitutively 'open' conformation with the dimerisation domain in an extended state. This allows HER2 to be available to heterodimerise with any ErbB receptor upon ligand-induced ErbB activation. **b.** The mechanism of activation of ErbBs 1, 3 and 4 upon ligand binding and the resulting dimerisation of two ErbB receptors through contact of the exposed dimerisation domains. Adapted from (Baselga and Swain, 2009), using BioRender.com.

3.1.2 HER2

HER2 or ErbB2 is a unique member of the ErbB family and is encoded by the HER2/*neu* gene. The receptor does not bind to any known ligands and the protein conformation is in a constitutively extended state (Yarden and Sliwkowski, 2001). The strong interaction between domains I and III closes the binding pocket, and thus, the ligand binding region is inaccessible and thus, HER2 has no known binding-ligand (Baselga and Swain, 2009). As HER2 exists in a constantly active state, it renders HER2 to always be available for hetero- or homo- dimerisation with other ErbB receptors. HER2 is therefore the preferred binding partner of other ErbB receptors, as it is always primed, ready for hetero-dimerisation (Appert-Collin et al., 2015; Baselga and Swain, 2009).

Overexpression of HER2 by gene amplification is usually seen in multiple malignancies including breast, ovarian, gastric and salivary gland tumours (Baselga and Swain, 2009). The overexpression of HER2 is correlated with patient chemoresistance and a poor prognosis (Olayioye et al., 2000; Appert-Collin et al., 2015). It is assumed that high levels of HER2 may result in constitutive HER2 homo-dimerisation. On the other hand, it may be that overexpressed HER2 may promote oncogenesis by spontaneous ligand-induced hetero-dimerisation with other ErbBs (Citri et al., 2003). HER2 is amplified in 20-25% of invasive BCs and is associated with a shorter disease-free interval and reduced survival in patients with early and advanced disease (Pohlmann et al., 2009). HER2 overexpression is found both in the primary breast tumour and in the metastatic sites (Valabrega et al., 2007).

As well as the function as a cell surface receptor it has also been reported that HER2 can be transported to the nucleus and regulate gene expression directly (Schillaci et al., 2012). In addition to its proposed function in the nucleus, HER2 has also been found in many human cancers in an amino-terminally truncated form, known as p95 HER2 or C-terminal fragments, by α-secretases. This form of HER2 appears to be an active form and can upregulate cell-signalling pathways. p95 HER2 expression in BC cells which were injected into transgenic mice led to the development of aggressive and invasive mammary tumours (Pedersen et al., 2009).

3.1.2.1 HER2 C-terminal region

The HER2 C-terminal domain is predicted as an intrinsically disordered domain and contains five pY binding sites. These sites serve for PTB and SH2 domain-containing adaptor proteins, including Shc, Grb2 and Grb7 (Jones et al., 2006). Disordered domains are associated with flexibility and a lack of tertiary structure. This flexibility also allows the C-terminal of HER2 to interact with multiple targets via linear motifs (Goh et al., 2007). These include proline-rich motifs, either in conserved sequences or in flanking regions. The side chain atoms of P form a pyrrolidine ring with the backbone atoms, which facilitates sequence specific recognition in the absence of a high affinity interaction (Kay et al., 2000). These areas are therefore used for specific and moderate-weak interactions that are essential for cell signalling and communication which require fast, reversible reactions. Seven proline-rich motifs have been found in the C-terminal tail of HER2 (**Figure 3.1.2**). The identification of a SFK SH3 binding site within the C-terminal domain of HER2 RTK has been found via biophysical techniques. Here, the proline-rich SH3-binding site was found to be R_{1146}PQPPSP_{1152} within HER2 C-terminal tail (Bornet et al., 2014). The SFK member Fyn was found to interact with HER2 proline-rich motif via its SH3 domain with a K_D of around 0.9mM, which is within the range of moderate-weak interactions already reported for other SH3:ligand complexes (Yu et al., 1994).

> P04626-ERBB2_HUMAN|P04626|676-1255

```
LTSIISAVVG ILLVVVLGVV FGILIKRRQQ KIRKYTMRRL LQETELVEPL
       710        720        730        740        750
TPSGAMPNQA QMRILKETEL RKVKVLGSGA FGTVYKGIWI PDGENVKIPV
       760        770        780        790        800
AIKVLRENTS PKANKEILDE AYVMAGVGSP YVSRLLGICL TSTVQLVTQL
       810        820        830        840        850
MPYGCLLDHV RENRGRLGSQ DLLNWCMQIA KGMSYLEDVR LVHRDLAARN
       860        870        880        890        900
VLVKSPNHVK ITDFGLARLL DIDETEYHAD GGKVPIKWMA LESILRRRFT
       910        920        930        940        950
HQSDVWSYGV TVWELMTFGA KPYDGIPARE IPDLLEKGER LPQPPICTID
       960        970        980        990       1000
VYMIMVKCWM IDSECRPRFR ELVSEFSRMA RDPQRFVVIQ NEDLGPASPL
      1010       1020       1030       1040       1050
DSTFYRSLLE DDDMGDLVDA EEYLVPQQGF FCPDPAPGAG GMVHHRHRSS
      1060       1070       1080       1090       1100
STRSGGGDLT LGLEPSEEEA PRSPLAPSEG AGSDVFDGDL GMGAAKGLQS
      1110       1120       1130       1140       1150
LPTHDPSPLQ RYSEDPTVPL PSETDGYVAP LTCSPQPEYV NQPDVRPQPP
      1160       1170       1180       1190       1200
SPREGPLPAA RPAGATLERP KTLSPGKNGV VKDVFAFGGA VENPEYLTPQ
      1210       1220       1230       1240       1250
GGAAPQPHPP PAFSPAFDNL YYWDQDPPER GAPPSTFKGT PTAENPEYLG

LDVPV
```

Figure 3.1.2 HER2 amino acid cytoplasmic sequence.

The cytoplasmic amino acid sequence of HER2 RTK is highlighted in yellow and the 8 proline rich motif sequences highlighted in red. Sequence from (UniProt, 2021).

3.1.3 Herceptin

The HER2 inhibitor, Herceptin (trastuzumab, Genentech Inc.) is a humanized IgG1 monoclonal antibody (mAb) and is the standard-of-care to treat HER2-positive BC patients. Herceptin works by binding to HER2 at the C-terminal portion of the extracellular domain IV, at a site that contains the binding pocket for the extended domain II loop (Rockberg et al., 2009).

Herceptin combined with chemotherapy increases response rates, time to disease progression and survival. However, a large majority of BCs that initially respond to Herceptin treatment begin to relapse within 1 year (Nahta

and Esteva, 2006b). The mechanisms of action of Herceptin have not been fully elucidated to date and is likely to be multifaceted. The proposed mechanisms of action includes inhibiting HER2 signalling via blocking homo- and/or hetero-dimerisation with other ErbBs, initiating G1 cell cycle arrest, induction of apoptosis, inhibition of angiogenesis, inhibition of DNA repair, internalisation of HER2 inducing degradation, blocking HER2 extracellular domain cleavage and an increased immune response via cell-mediated cytotoxicity (Baselga et al., 2001; Nahta and Esteva, 2006b) (**Figure 3.1.3**)

There is inconclusive evidence to Herceptin's optimal use. One of the reasons behind this is the lack of conclusive data about the mechanisms of action and a lack of knowledge on how primary and acquired resistance to Herceptin occurs. Therefore, research into this area will contribute towards the use of more selective patient treatments, how to prevent resistance and how to manage patients whose breast tumours progress during Herceptin treatment (Valabrega et al., 2007).

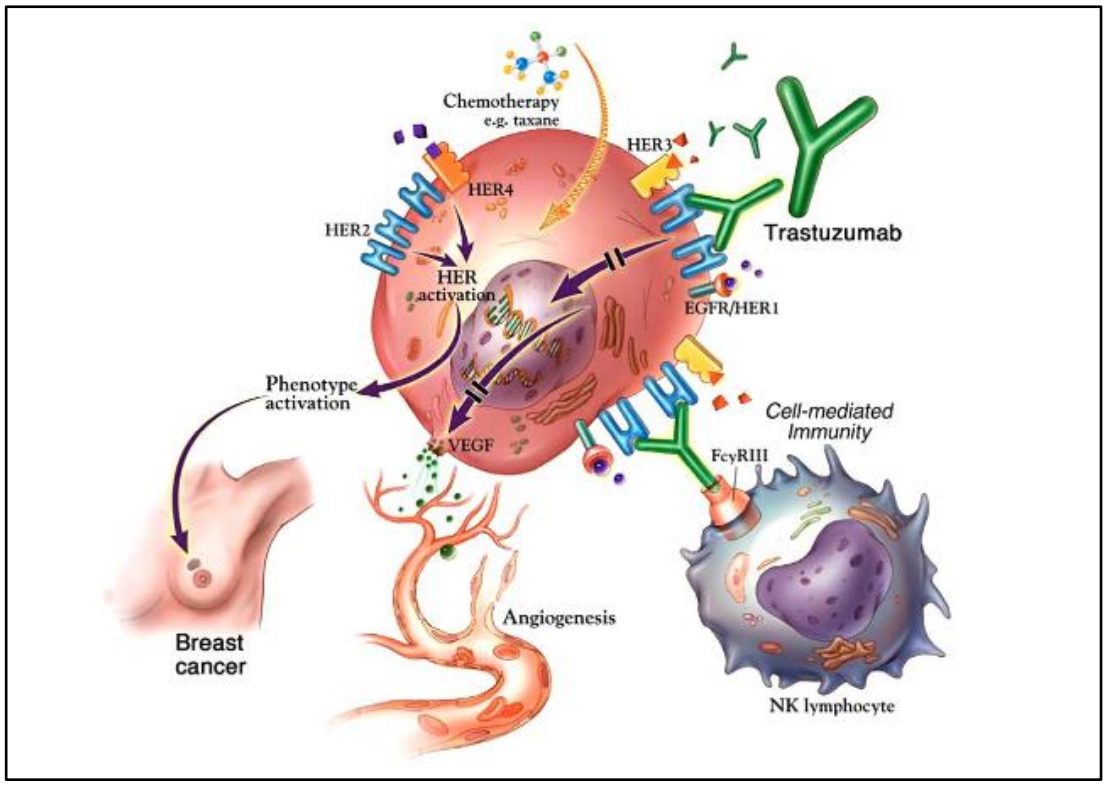

Figure 3.1.3 The proposed mechanisms of action of Herceptin.

The many different proposed mechanisms of action of Herceptin binding to HER2 include the disruption of receptor dimerisation and downstream signalling, inhibition of DNA repair, initiation of G1 cell-cycle arrest and reduced proliferation, internalisation of HER2 for degradation, induction of apoptosis, suppression of angiogenesis, the inhibition of HER2 extracellular domain proteolysis and the stimulation of natural killer cells by cell-mediated cytotoxicity (Nahta and Esteva, 2006b).

3.1.3.1 Herceptin resistance

Although Herceptin considerably improves the outcomes of both early stage and metastatic BCs, some patients do not respond to Herceptin at all (*de novo* HER2 resistance). The rate of *de novo* resistance to single-agent Herceptin has been found to be as high as 66-88% for HER2-overexpressing metastatic BC patients (Baselga et al., 1996; Cobleigh et al., 1999; Vogel et al., 2002). Some patients respond initially but become resistant over time (acquired HER2 resistance) (Ross et al., 2009; Nahta and Esteva, 2006b). Acquired resistance was found in around 70% of patients who initially responded to the drug (Vu and Claret, 2012). Most patients with an initial response to Herceptin

develop resistance within one year of treatment (Nahta and Esteva, 2006a). There is an increased risk of brain metastasis (BM) as the first site of disease recurrence in patients with HER2-positive BC, who have been treated with Herceptin (Kaplan et al., 2015; Olson et al., 2013a). BM at the time of metastatic diagnosis occurs in around 8% of patients with no previous exposure to Herceptin treatment. However, after prolonged use of anti-HER2 therapy, brain metastatic tumours are observed to increase to around one third to one half of all cases (Olson et al., 2013a; Olson et al., 2013b; Lin, N.U. and Winer, 2007).

Proposed hypotheses for the brain being the first site of relapse after Herceptin treatment includes that the brain is a sanctuary site for metastatic tumour cells, that Herceptin cannot penetrate the blood brain barrier (BBB) or that some tumour cells lose HER2 overexpression when migrating to the brain (Bria et al., 2008). Therefore, it is important to determine the patients who will not respond to Herceptin treatment and will develop resistance to the drug, as there is an increased risk of central nervous system (CNS) metastasis associated with Herceptin use. Determining the particular proteins and signalling pathways involved in both *de novo* and acquired resistance will lead to more patient selected therapy and possible drug targets in combination with Herceptin.

3.1.3.2 The roles of PTEN and Src in Herceptin resistance

The expression of tumour suppressor proteins and oncoproteins have been identified as playing a role in both *de novo* and acquired resistance. These include the tumour suppressor protein PTEN and the oncoprotein Src (Vu and Claret, 2012). PTEN activity antagonises PI3K function and thus, negatively regulates Akt activity. Decreased PTEN expression was found to correlate with a lower overall response rate to Herceptin in HER2-positive BC patients. A loss of PTEN is observed in 36% of HER2-positive BC patients with stage IV disease (Nagata et al., 2004). In a cohort of 55 HER2-overexpressing BC patients, 25% had a PI3K activating mutation and 20-25% had a PTEN deficiency. Furthermore, patients with activating PI3K mutations had a significantly shorter progression-free survival than those without mutations (Berns et al., 2007).

PTEN deficiency confers resistance to therapy and Src is activated in BC cell lines that are associated with *de novo* and acquired resistance to Herceptin (Zhang, S. et al., 2011). A novel mechanism of Src regulation was found which involved the activity of PTEN. PTEN was found to directly dephosphorylate Src at Y416 when active, and thus Src pY416 levels were higher in cells with PTEN deficiency. Therefore, the loss of PTEN phosphatase activity led directly to Src activation, which contributed to *de novo* Herceptin resistance. Src was found to be hyperactivated in various Herceptin resistance models. Patients with phosphorylated Src correlated with both a lower response to Herceptin and poorer survival rates. Src was found to be a central node of multiple Herceptin resistance pathways, indicating a promising global therapeutic target for patients who are resistant to Herceptin (Zhang, S. et al., 2011).

3.1.4 Breast cancer brain metastasis (BCBM)

BM is an end stage of BC progression and has a very poor prognosis, with a median overall survival (OS) ranging from 4-25 months after diagnosis (Darlix et al., 2019). The incidence of BCBM differs based on the BC subtype of the patient. Between 5 and 10% of patients with oestrogen receptor (ER)-positive, HER2-negative tumours (around 70% of BCs) go on to develop BCBM. Those with TNBC or HER2-positive tumours have a BM incidence of 20% and 25-50% respectively (Aversa et al., 2014; Kennecke et al., 2010).The increased incidence of BCBM in HER2-positive BC patients is most likely due to the use of anti-HER2 chemotherapies, which expands the lifespan of the patients and thus, allows time for the cancer cells, which are resistant to the chemotherapy, to migrate and metastasise to other areas of the body (Brufsky et al., 2011; Gori et al., 2007; Olson et al., 2013a). How the BC cells initially develop metastatic properties and in which manner the cells become resistant remains relatively unknown.

3.1.4.1 The BCBM cascade

Preclinical studies have provided important protein targets within the metastatic cascade, from initial primary BC to BM. This cascade includes cellular dissemination of metastasis from the primary tumour, intravasation into the blood, active and passive migration to the brain, embedding into a

capillary bed and attachment to the endothelium, extravasation through the BBB and tumour expansion into the brain microenvironment (Eichler et al., 2011). Most of the preclinical studies carried out investigate the early stages of BCBM. These include gene expression analysis of brain seeking and primary parental cells arisen from BCBM animal models (Kodack et al., 2015). RTKs appear to play roles in multiple stages of BCBM, including HER2, vascular endothelial growth factor receptor-2 (VEGFR2), EGFR, insulin-like growth factor receptor-1 (IGF-1R), hepatocyte growth factor receptor (HGFR/c-Met) and the TK Src, all play a role in BCBM. The brain microenvironment appears to be a unique 'safe haven' for metastatic cells to survive and proliferate (Kodack et al., 2015). Knowing the protein expression signature and particular cellular pathways which alter the cancer cells to complement tumour growth in the brain microenvironment, will be important therapeutic targets for BC patients with increased risk of BM.

3.1.5 Other HER2 targeted therapeutics

Other HER2 targeted therapies currently in the clinic include the use of small-molecule TK inhibitors (TKIs), which directly inhibit the kinase activity of HER2. They bind to the ATP-binding site of the TK, preventing downstream signal transduction. The most clinically advanced TKI used to target HER2-positive BCs is Lapatinib (Tykerb, GlaxoSmithKline) (Spector et al., 2005). Lapatinib has been approved for use in combination with another chemotherapeutic, Capecitabine (an anti-metabolite drug used to treat many cancer types) to treat BC patients. In a Phase III trial this combination of drugs given to HER2-positive advanced BC patients increased the progression-free survival rate. It was also found that fewer patients that were treated with Lapatinib developed BM (Geyer et al., 2006). Due to the small size of Lapatinib, it is thought that it can penetrate the BBB and thus, leads to fewer cases of BCBM (Iwata et al., 2013).

It has been suggested that Lapatinib may work for some HER2-positive BC patients with Herceptin resistant tumours. This may be due to the fact that Lapatinib can bind and stop signalling with truncated versions of HER2 (p95 HER2) or HER2 C-terminal fragments which lack the extracellular binding

domain (Pedersen et al., 2009). Approximately 20% of human BC tumours express this truncated version of HER2 (Baselga et al., 1996).

Pertuzumab (Perjeta, Roche) is another anti-HER2 immunotherapeutic given to treat HER2-positive BC patients. Pertuzumab is a recombinant humanized mAb which binds to the dimerisation domain II of HER2. This binding inhibits heterodimerisation of HER2 with other ErbB family members. Dual HER2 blockade of Herceptin treatment with the addition of Pertuzumuab has improved the outcome of patients with HER2-positive metastatic BC. This dual treatment is the standard of care as first-line therapy for patients with advanced HER2-positive disease. This form of treatment has been shown to significantly prolong both progression-free survival and OS rates (Hurvitz et al., 2018).

3.1.6 HER2-Src interaction hypothesis

Our laboratory group has previously shown that non-homeostatic interactions between proline-rich regions within the C-terminal tail of non-activated monomeric RTKs and the SH3 domains of signalling proteins, under basal conditions, is important in the development of certain cancers. These interactions occur when the relative levels of the proteins involved are at high expression concentrations. It has also been established that an interaction occurs between the proline-rich motif of HER2 and the SH3 domain of SFK member, Fyn (Bornet et al., 2014). Fyn bound to the proline rich motif, R_{1146}**P**QP**P**SP_{1152}, within the C-terminal tail of HER2. Fyn shares a high level of homology to Src (74.4%) (Ulmer et al., 2002). Src signalling is known to stimulate invasion, migration and metastasis (Summy and Gallick, 2006) and Src activation has been found to be a central node in Herceptin resistance pathways in BC cells (Zhang, S. et al., 2011). Therefore, under HER2 inhibition via Herceptin, when it is proposed that HER2 receptor co-dimerisation is abrogated and thus, HER2 is in a monomeric state, may trigger the non-canonical activation of a Tier 2 mechanism under HER2-therapeutic stress-conditions. Here, the non-canonical activation of Src-kinase under basal conditions, is investigated within this chapter. BC cells with HER2 overexpression and a high Src expression level (SkBr3 cells) were used in all the following experiments.

Therefore, the possibility of aberrant Tier 2 signalling pathways being activated downstream of non-canonical Src activation in response to HER2-inhibition, may contribute towards anti-HER2 drug-resistance and cancer progression in BC through this mechanism.

If our hypothesis is correct, this research could explain the increased risk of metastasis seen in HER2-positive BC patients, after treatment with Herceptin via the aberrant activation of Tier 2 Src signalling pathways (Olson et al., 2013a; Kaplan et al., 2015).

3.1.7 Experimental objectives

In this chapter the following objectives were investigated:

1) To determine the effective concentration of Herceptin to administer to SkBr3 cells (HER2-overexpressing breast cancer cells), by choosing a dose which gives a phenotypic effect but not a lethal dose.
2) To identify whether the inhibition of HER2 RTK via Herceptin treatment in SkBr3 cells, upregulates pY416 Src levels using immunoblotting to determine relative phosphorylation levels in SkBr3 cells after treatments with Herceptin and compared to vehicle-treated control cells.
3) To determine if Herceptin treatment of HER2-overexpressing BC cells leads to a change in the cellular localisation of HER2 and Src via fluorescence microscopy.
4) To establish if changes in non-canonical Src activation via Herceptin treatment leads to a migratory outcome in HER2-overexpressing BC cells, through the use of a scratch migration assay.
5) To identify the time-point at which Src becomes phosphorylated after treatment with Herceptin in SkBr3 cells via the use of immunoblotting and Src phosphorylation assay.

3.2 Results

3.2.1 Effective concentration of Herceptin determined via MTT assay

To investigate the effect of Herceptin treatment on non-canonical activation of pY416 Src, via the inhibition of HER2 RTK, the HER2 overexpressing cell line, SkBr3, which also has a high level of Src expression, was utilised in all the following experiments within this chapter.

The optimal concentration of Herceptin was determined using an MTT cell viability assay, with the SkBr3 cell line. This assay determines the number of viable cells in each well by the conversion of MTT into formazan crystals, which occurs as a consequence of metabolic activity. The presence of crystals can be determined calorimetrically by dissolving the crystals in DMSO and using a plate reader at a wavelength of 570nm to detect this. The varying concentrations of Herceptin were dosed as a five-fold decrease in concentration to SkBr3 cells, ranging from 20µg/ml to $2.56x10^{-4}$ µg/ml. This assay was used to determine the concentration of drug to use in future experiments whereby, the drug would not be administered to the SkBr3 cells at a toxic dose.

Following a drug incubation of 72 hours in serum-deprived media, at 37°C (21% O_2, 5% CO_2), cell viability was measured in SkBr3 cells to obtain a dose-response curve (**Figure 3.2.1**). Absorbance values were normalised to the vehicle-treated control (PBS only) cells. All cells were serum-starved 24 hours prior to drug treatment, to allow for serum-deprivation to take effect before the addition of Herceptin. A dose-dependent decrease in cell viability was observed, with a maximum cell reduction of around 60%. This was in agreement with other studies (Sun et al., 2018; Tseng et al., 2006). 4µg/ml concentration was determined as a suitable concentration to use in further experiments as this gave the highest phenotypic effect on the cells but 60% of them were still viable.

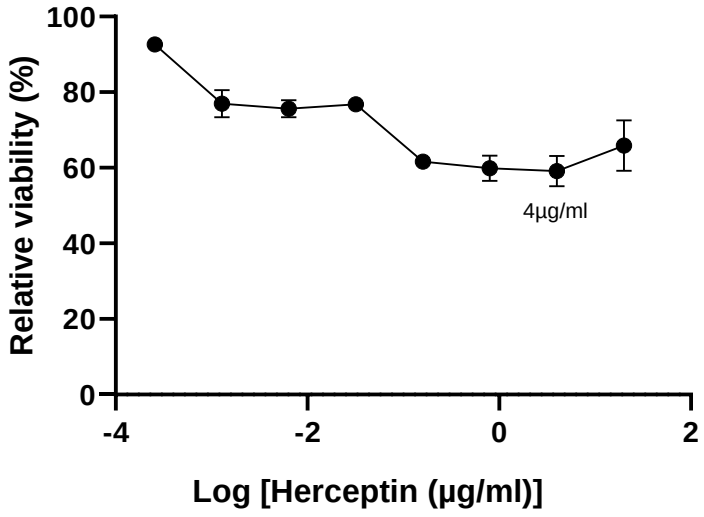

Figure 3.2.1 Dose-response curve of SkBr3 cells treated with Herceptin, under serum-deprived conditions, n=4.

A dose-response curve obtained by MTT cell viability assay, where five-fold serial dilutions of Herceptin were administered in serum-deprived (0% FBS) media to SkBr3 cells for 72hrs and normalised to the vehicle-treated control (PBS only) cells. SkBr3 cells were serum-starved for 24 hours prior to the addition of Herceptin. Each individual point was an average of n=4 +/- SD.

3.2.2 Herceptin treatment activates Src-kinase in SkBr3 cells, under serum-deprived conditions

The effect of Herceptin treatment on the cellular protein levels of HER2 and Src was investigated via immunoblotting of SkBr3 cells, treated with increasing concentrations up to a maximum dose of 4µg/ml of Herceptin, under serum-deprived (0% FBS) conditions. The cells were serum-starved for 24 hours prior to drug treatment. SkBr3 cells were dosed with the drug for 72 hours at 37°C (21% O_2, 5% CO_2), (**Figure 3.2.2a.**). This length of incubation was chosen to correlate with the viable cells observed in the MTT assay. The data was then quantified by densitometry (**Figure 3.2.2b.-d.**).

In the vehicle-control treated SkBr3 cells, it was observed that there was a basal phosphorylation maintained on the HER2 receptor, which was phosphorylated at Y877 (**Figure 3.2.2c.**) and Y1221 (**Figure 3.2.2d.**) when grown under serum-deprived conditions. To obtain visible bands a long exposure of the blots was required. Src expression was observed, but no Src phosphorylation at Y416 was visualised in the vehicle-treated control cells (**Figure 3.2.2b.**). Basal HER2 phosphorylation was maintained in the Herceptin treated SkBr3 cells at all concentrations, but a fairly lower total protein expression of HER2 was observed after drug treatment, compared to the vehicle-control. The phosphorylation of Src at Y416 was visualised in SkBr3 cells upon treatment with Herceptin at all concentrations up to 4µg/ml. Total Src expression levels remained relatively the same at all concentrations of Herceptin treatment, compared to the vehicle-treated control. Densitometry was performed to normalise the phosphorylated protein levels to the total amount of protein and to the loading control, β-actin. The overall trend showed that activated Src phosphorylation at Y416 was found to occur, following Herceptin treatment in HER2-overexpressing SkBr3 BC cells.

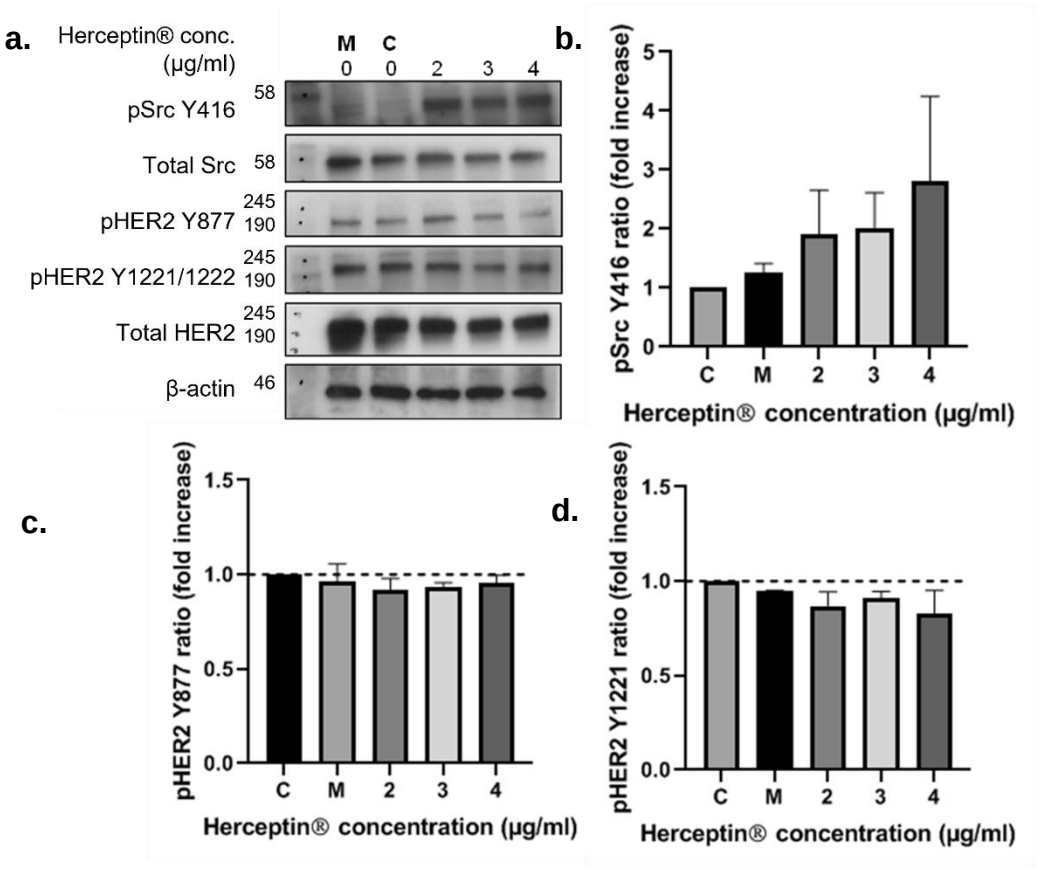

Figure 3.2.2 The effect of Herceptin treatment on Src and HER2 protein levels in SkBr3 cells, under serum-deprived conditions, n=3.

a. A representative blot of Src and HER2 phosphorylation and total protein levels in SkBr3 cells, grown under serum-deprived (0% FBS) conditions, after the addition of Herceptin at increasing concentrations. The cells were treated with 0 (**C** and **M**), 2, 3 and 4µg/ml Herceptin for 72 hours. The cells were serum-starved for 24 hours prior to the addition of Herceptin. **C** shows the vehicle-treated control (PBS only) cells and **M** shows cells grown in serum-free media only. Representative of n=3 blots. **b.-d.** Levels of phosphorylated protein were compared to total protein expression levels and normalised to the β-actin loading control. Phosphorylated Src and HER2 levels were calculated as a fold increase from the vehicle-treated control (**C**). Densitometry results were obtained from n=3 repeats of Herceptin treated SkBr3 cells with the same batch of Herceptin.

3.2.3 HER2 TKI, Lapatinib, has no effect on activated Src levels in SkBr3 cells, under serum-deprived conditions

Having observed that the activating pY416 of Src occurs under Herceptin treatment in SkBr3 cells, we wanted to investigate the effects of another clinically relevant HER2 inhibitor, Lapatinib. Lapatinib is known to abrogate HER2 autophosphorylation, either alone or when paired with Herceptin in SkBr3 and BT474 BC cells (Zhang, D. et al., 2008; Diermeier-Daucher et al., 2011). Lapatinib is a dual inhibitor of EGFR and HER2 and an approved treatment for HER2-positive metastatic BC patients. This drug differs to Herceptin in that it is a direct kinase inhibitor, which binds intracellularly to the ATP-binding pocket of the TKD, rather than externally to HER2 (Baselga and Swain, 2009). We carried out these experiments to investigate whether Src was activated at Y416 in the absence of basal phosphorylation of HER2, after treatment with Lapatinib.

To determine the correct dose of Lapatinib to treat SkBr3 cells an MTT cell viability assay was firstly performed to obtain a dose-response curve. Lapatinib was dosed to SkBr3 cells at a five-fold decrease in concentration ranging from 65nM to $8.32X10^{-4}$ nM in serum-deprived media (0% FBS), and the cell viability determined after 72 hours of drug treatment. The cells were serum-starved for 24 hours prior to addition of the drug. The dose response curve obtained (**Figure 3.2.3a.**) showed a large reduction in cell viability compared to that of Herceptin. Absorbance values were normalised to the vehicle-treated control (DMSO only) cells. The cells were reduced to around 40% viability compared to the vehicle-treated control cells, with the highest concentration of Lapatinib used, 65nM. The full viability curve was not established, as higher concentrations were needed, however, a dose-dependent decrease in cell viability was observed in the SkBr3 cells. This was enough to show that at the recommended concentration from the vendor, 13nM (BioVision), gave an effect on the SkBr3 cells but was not a toxic dose and thus, could be used in further experiments.

13nM Lapatinib was dosed to SkBr3 cells under serum-deprived conditions to determine at which time-point HER2 phosphorylation was abrogated and to determine whether Src phosphorylation at Y416 occured in response to this

(**Figure 3.2.3b.**). SkBr3 cells were serum-starved for 24 hours prior to the addition of Lapatinib. We observed that HER2 phosphorylation at Y877 and Y1221/Y1222 was reduced after 1 hour of incubation with Lapatinib and was eradicated after around 3 hours of incubation, compared to the vehicle-treated control. The total HER2 protein expression level remained the same after Lapatinib treatment at all the different time-points of the experiment, compared to the vehicle-control. Phosphorylation of Src at Y416 and total Src levels did not differ to the vehicle-treated control at all time-points of Lapatinib addition, even when HER2 basal autophosphorylation was abrogated. This indicated that inhibiting the basal phosphorylation of HER2 via Lapatinib does not activate Src kinase.

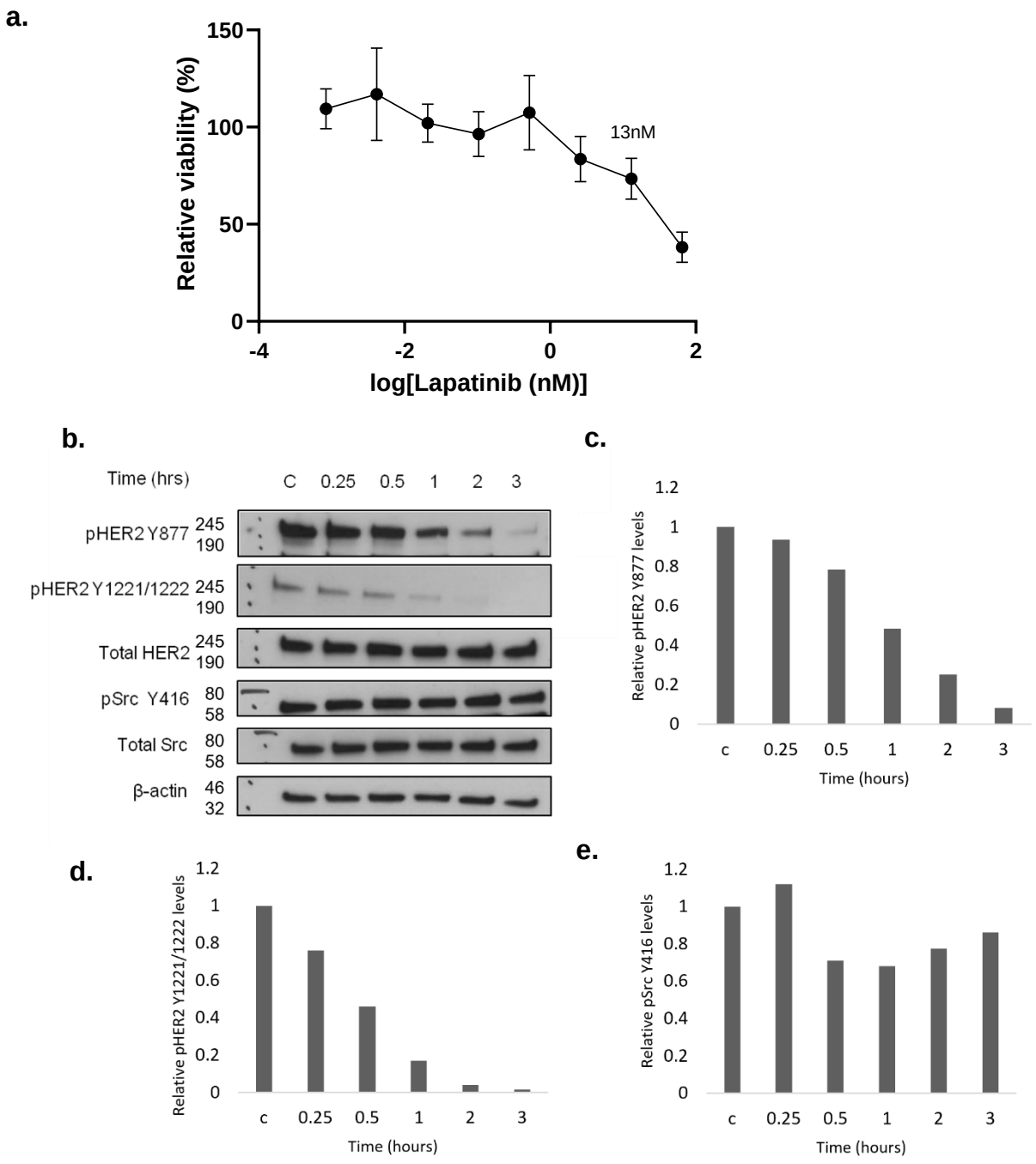

Figure 3.2.3 Dose-response curve and protein expression of SkBr3 cells treated with Lapatinib, under serum-deprived conditions.

a.Serial dilutions of Lapatinib were dosed to SkBr3 BC cells for 72 hours, under serum-deprived conditions and a dose-response curve obtained via MTT cell viability assay. Here, each concentration was normalised to the vehicle-treated control (DMSO only) cells. Cells were serum-starved for 24 hours prior to drug treatment. Each individual point was an

average of n=4 +/- SD. **b.** Immunoblot of SkBr3 cell lysates to determine the protein expression and phosphorylation levels of HER2 and Src after exposure to 13nM Lapatinib treatment, under serum-starved conditions. The cells were serum-starved for 24 hours prior to drug treatment. The cells were incubated for 0.25, 0.5, 1, 2 and 3 hours with Lapatinib and compared to the vehicle-treated control (DMSO only) cells. **c.** – **e.** show the relative protein expression levels of pY877 HER2, pY1221/1222 HER2 and pY416 Src obtained via densitometry. Phosphorylation levels were normalised to total protein and β-actin levels, n=1.

3.2.4 Herceptin treatment induces HER2 internalisation after 6 hours in SkBr3 cells, under serum-deprived conditions

The effect of Herceptin on the cellular distribution of HER2 and Src and thus, whether HER2 and Src could co-localise after treatment with Herceptin was investigated in SkBr3 cells. It has been proposed that HER2 is internalised upon Herceptin exposure, which is thought to increase the levels of HER2 degradation (Nahta and Esteva, 2006b; Baselga et al., 2001). However, it is unknown what happens to Src-kinase once Herceptin has been administered to HER2-positive BC cells. Thus, the localisation of Src and HER2 were determined via IF.

The cells were treated with 4ug/ml Herceptin (a fresh vial of Herceptin was used) for 3 and 6 hours in serum-deprived media, to see whether changes to the cellular localisation of HER2 and Src occurs rapidly after Herceptin treatment. The treated cells were compared to vehicle-treated control (PBS only) cells. The cells were serum-starved for 24 hours prior to drug treatment. The cellular localisation of Src and HER2 was investigated by probing the Herceptin-treated SkBr3 cells with anti-Src (mouse) and anti-HER2 (rabbit) primary antibodies and GFP-conjugated (anti-mouse) and RFP-conjugated (anti-rabbit) secondary antibodies. The cell nucleus was stained using DAPI stain mountant medium. The localisation of HER2 and Src was visualised using IF via an inverted confocal microscope (Zeiss). HER2 localisation was visualised by exciting the RFP conjugate at 594nm and emission detected at 614nm and Src localisation visualised by exciting the GFP conjugate at 488nm and emission detected at 510nm (**Figure 3.2.4.**).

The vehicle-control cells showed distinct expression of HER2 within the plasma cell membrane of SkBr3 cells and Src was mainly distributed within the cytosol. Upon Herceptin treatment, after 3 hours of treatment there appeared to be no difference in the cellular localisation of both HER2 and Src, compared to the vehicle-treated control. At 6 hours of treatment with Herceptin, the distribution of HER2 changed compared to the vehicle-treated control and HER2 was distributed both within the cytosol and at the plasma membrane. Src was visualised to remain mainly within the cytosol. These results demonstrate that the cellular distribution of HER2 is altered upon Herceptin treatment and that both HER2 and Src are localised within the cytosol after 6 hours of Herceptin treatment in SkBr3 BC cells.

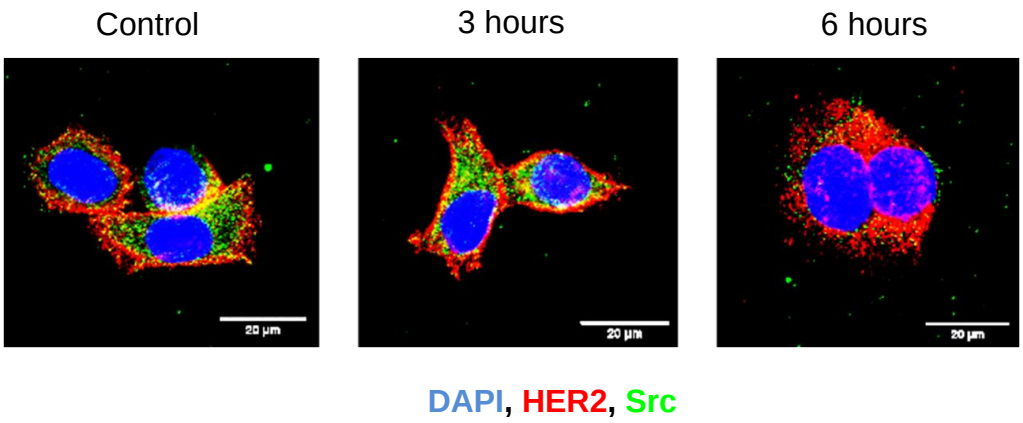

Figure 3.2.4 The effect of Herceptin treatment on HER2 and Src cellular localisation in SkBr3 cells, under serum-deprived conditions, n=1.

SkBr3 cells were serum-starved for 24 hours prior to the treatment of Herceptin. Cells were dosed with 4µg/ml Herceptin in serum-deprived media for 3 and 6 hours, compared to vehicle-treated control (PBS only) cells. Cells were fixed and probed with anti-HER2 (rabbit) and anti-Src (mouse) primary antibodies and their corresponding secondary fluorophores (anti-rabbit RFP and anti-mouse GFP), following with DAPI. IF images were taken using an inverted LSM700 confocal microscope. Scale bar = 20µm, n=1.

3.2.5 Herceptin treatment inhibits SkBr3 cell migration

HER2-positive BC patients have prevalent rates of both *de novo* and acquired resistance to Herceptin treatment (Baselga et al., 1996; Cobleigh et al., 1999; Vogel et al., 2002). The activation of Src-kinase has been found to be centrally implicated in activating resistance pathways to Herceptin treatment (Zhang, S. et al., 2011). The activation of Src is implicated in upregulating migration and invasion cell signalling pathways, which can contribute towards tumour metastasis (Mayer, E.L. and Krop, 2010; Finn, 2008; Summy and Gallick, 2003). HER2-positive BC patients who are treated with Herceptin also have a higher risk of BCBM (Kaplan et al., 2015; Olson et al., 2013a). Therefore, the migratory effects of Herceptin treatment on HER2-overexpressing SkBr3 cells was investigated via a scratch wound migration assay, using an IncuCyte (Sartorius).

A scratch was made to confluent SkBr3 cells in a collagen coated 96 well plate after growth under serum-supplemented conditions for 24 hours to confluency, prior to the addition of Herceptin (a fresh vial of Herceptin was used). The cells were then washed with PBS. Herceptin was then dosed to the cells at 2 different concentrations, 4µg/ml and 20µg/ml, in serum-deprived (-) or serum-supplemented (+) media and compared to the vehicle-treated control (PBS only) cells. The scratched cells in the 96 well-plate were then added to the IncuCyte incubator and images of the SkBr3 cells were taken every hour (**Figure 3.2.5a.**). The average wound confluence (%) and average wound closure (µM) was calculated over 48 hours of Herceptin treatment (**Figure 3.2.5b. and c.** respectively).

The vehicle-treated control cells grown under serum-supplemented or serum-deprived conditions were observed to have a higher overall wound closure and percentage wound confluence compared to BC cells treated with Herceptin. Cells treated with 4µg/ml Herceptin under serum-supplemented conditions did not give a significant difference in average wound closure or wound confluence compared to the serum-supplemented vehicle-control cells. At 20µg/ml Herceptin treatment under serum-supplemented conditions there was a significant difference compared to the serum-supplemented vehicle-control cells with regards to average wound closure, but no significant

difference seen in wound confluence (121.7µM +/- 19.18) (P=0.031) and (17.48% +/-3.40) (P=0.182) respectively. SkBr3 cells treated with 4µg/ml Herceptin under serum-deprived conditions showed a significant difference in average wound closure, but no significant difference seen in wound confluence compared to the serum-deprived vehicle-control cells, (68.79µM +/- 16.41) (P=0.030) and (21.36% +/-7.32) respectively. SkBr3 cells treated with 20µg/ml of Herceptin under serum-deprived conditions showed no significant difference for both average wound closure and wound confluence compared to the serum-deprived vehicle-control cells. These results establish that SkBr3 cell migration is inhibited upon Herceptin treatment.

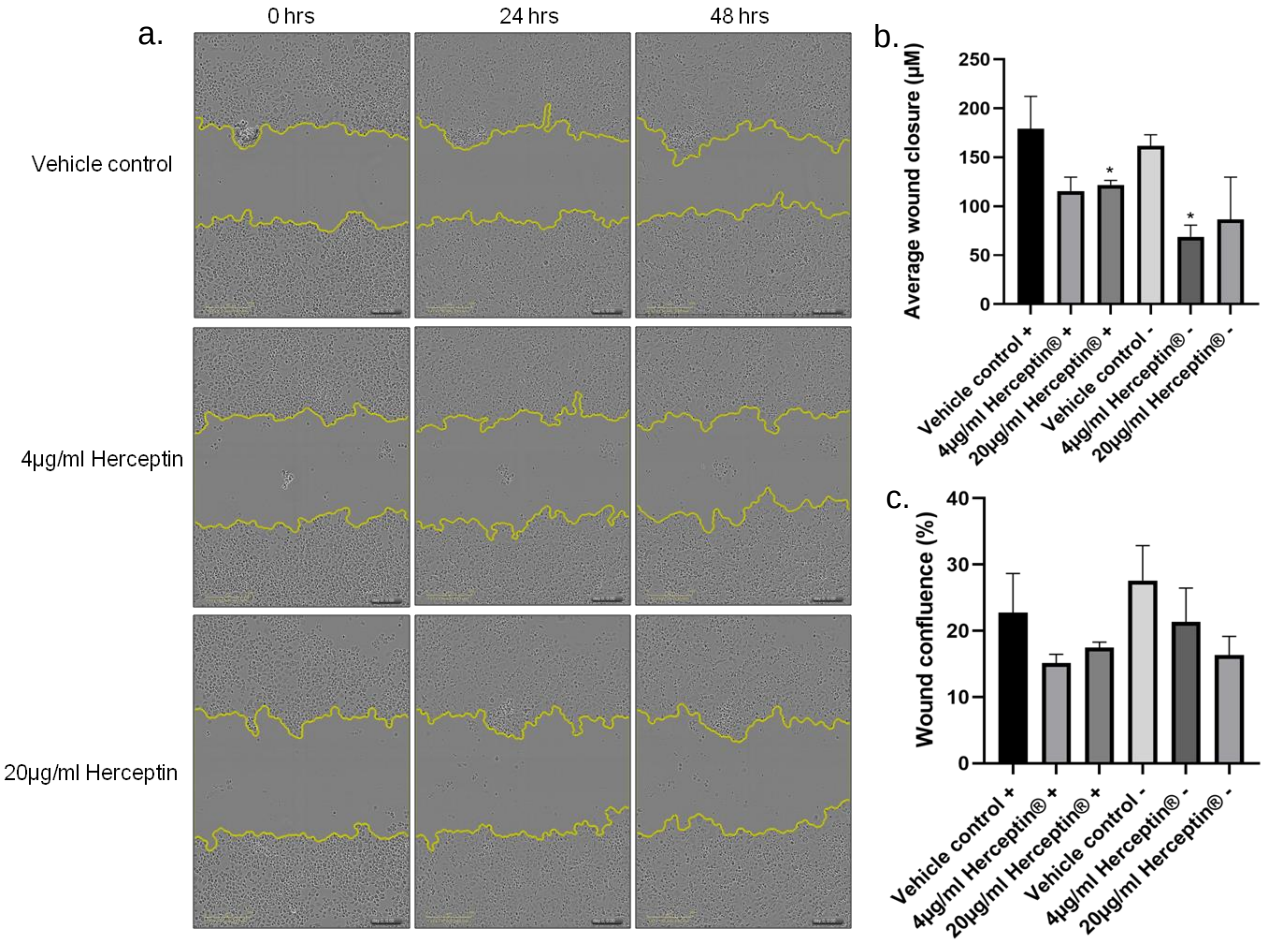

Figure 3.2.5 The effect of Herceptin treatment on SkBr3 cell migration, n=3.

a. Representative images of SkBr3 cells grown in a collagen-coated 96 well plate under serum-deprived (-) conditions. Cells were serum-starved for 24 hours prior to Herceptin treatment. The cells were scratched and dosed with 4µg/ml or 20µg/ml of Herceptin in serum-deprived media for 48 hours and compared to vehicle-treated control (PBS only) cells. The representative images were taken at 0hrs, 24hrs and 48hrs after Herceptin treatment using an IncuCyte. Representative of n=3 repeats. **b.** Average wound closure (µM) was determined for Herceptin-treated SkBr3 cells after 48 hours of drug treatment, grown under serum-supplemented (+) or serum-deprived (-) conditions compared to vehicle-treated control (PBS only) cells. A

significant difference was observed at 20µg/ml Herceptin treatment grown under serum-supplemented conditions (*=P=0.031) compared to the serum-supplemented vehicle-control cells and at 4µg/ml Herceptin treatment grown under serum-deprived conditions (*=P=0.030) compared to the serum-deprived vehicle-control cells, n=3. **c.** Percentage wound confluence (%) of SkBr3 cells grown with (+) and without (-) serum, after the addition of Herceptin at both 4µg/ml and 20µg/ml concentration, compared to the serum-supplemented and serum-deprived vehicle-treated control cells, n=3.

3.2.6 Herceptin time-point treatment of SkBr3 cells gives no effect on activated Src levels, under serum-deprived conditions

Having observed that Src phosphorylation at Y416 occurs in the SkBr3 BC cells, after Herceptin treatment (**Figure 3.2.2**), we wanted to investigate the specific time-point after dosage that this phosphorylation event occurred.

The specific time-point that Src was phosphorylated at Y416 in response to Herceptin treatment was investigated via immunoblotting SkBr3 cell lysates grown under serum-deprived conditions, after Herceptin dosage of 4µg/ml at different drug-incubation times (a new vial of Herceptin was used). The time-course ranged between 6 and 96 hours of drug incubation. Cells were serum-starved for 24 hours prior to drug treatment. Herceptin treated SkBr3 cells were compared to vehicle-treated control (PBS only) cells (**Figure 3.2.6a.**). Src activation is also implicated in inducing a proliferative cellular outcome, via the activation of the downstream Erk/MAPK signalling pathway (Mayer, E.L. and Krop, 2010; Finn, 2008; Summy and Gallick, 2003). Therefore, the relative cell viability was also determined via MTT assay at the different time points post Herceptin treatment, to see if there was any correlation with the time Herceptin was administered to the cells and whether this had an effect on SkBr3 cellular proliferation (and thus, a higher cell viability compared to the vehicle-treated control cells) and if a proliferative outcome was possibly correlated with the time of Src activation via pY416.

In the vehicle-treated control cells (**Figure 3.2.6a.**) a basal phosphorylation of Src was present at Y416 and at the inhibitory site of Y527. There was also a basal phosphorylation of HER2 at Y877 and Y1221/Y1222, which was seen previously (**Figure 3.2.2**). The HER3 receptor was also phosphorylated in the vehicle-treated control, which suggests possible co-dimerisation with the HER2 receptor. After treatment with Herceptin, the phosphorylated Src levels at both Y416 and Y527 seemed to remain relatively the same at all time-points of Herceptin treatment, compared to the vehicle-control (**Figure 3.2.6b.** and **Figure 3.2.6c.**). The total levels of Src were also maintained after drug treatment compared the vehicle-treated control. Phosphorylation of HER2 at Y877 and Y1221/Y1222 remained the same as the vehicle-control after Herceptin treatment and only seemed to be reduced slightly after around 72

to 96 hours of Herceptin treatment. The total HER2 protein levels were slightly reduced after Herceptin treatment. Phosphorylated HER3 levels were lower after Herceptin treatment which suggests that the HER2 inhibitor blocks co-dimerisation with the HER3 receptor, which is a proposed Herceptin mechanism of action (Baselga et al., 2001; Nahta and Esteva, 2006b). These results contrast with the findings at the beginning of the study in **Figure 3.2.2**, as activated Src, visualised via Y416 phosphorylation, was not observed after Herceptin treatment at any time-point in the SkBr3 cells, under serum-deprived conditions.

SkBr3 cells were then treated with 4µg/ml Herceptin under serum-deprived conditions and incubated for 6, 24, 48, 72, and 96 hours in a 96 well plate and an MTT assay performed. Cells were serum-starved for 24 hours prior to drug treatment. The viability results (**Figure 3.2.6d.**) show that there was no significant difference observed in viability rates of SkBr3 cells at the different incubation times at which Herceptin was administered, compared to the vehicle-control cells. At all time-points, except for 24 hours of Herceptin treatment, the relative cell viability was lower than the vehicle-treated control cells. At 24 hours of Herceptin treatment the relative cell viability increases to 123.2% +/- 14.51%, which suggests that cellular proliferation of SkBr3 cells may increase at this time-point after Herceptin treatment.

Overall, these results demonstrated that Herceptin treatment of SkBr3 cells appeared to not effect pY416 Src levels under serum-deprived conditions as was seen previously in **Figure 3.2.2**. The cells also appeared to have higher proliferation rates at 24 hours of Herceptin treatment. Therefore, the differences seen between **Figure 3.2.6** and **Figure 3.2.2** was investigated further.

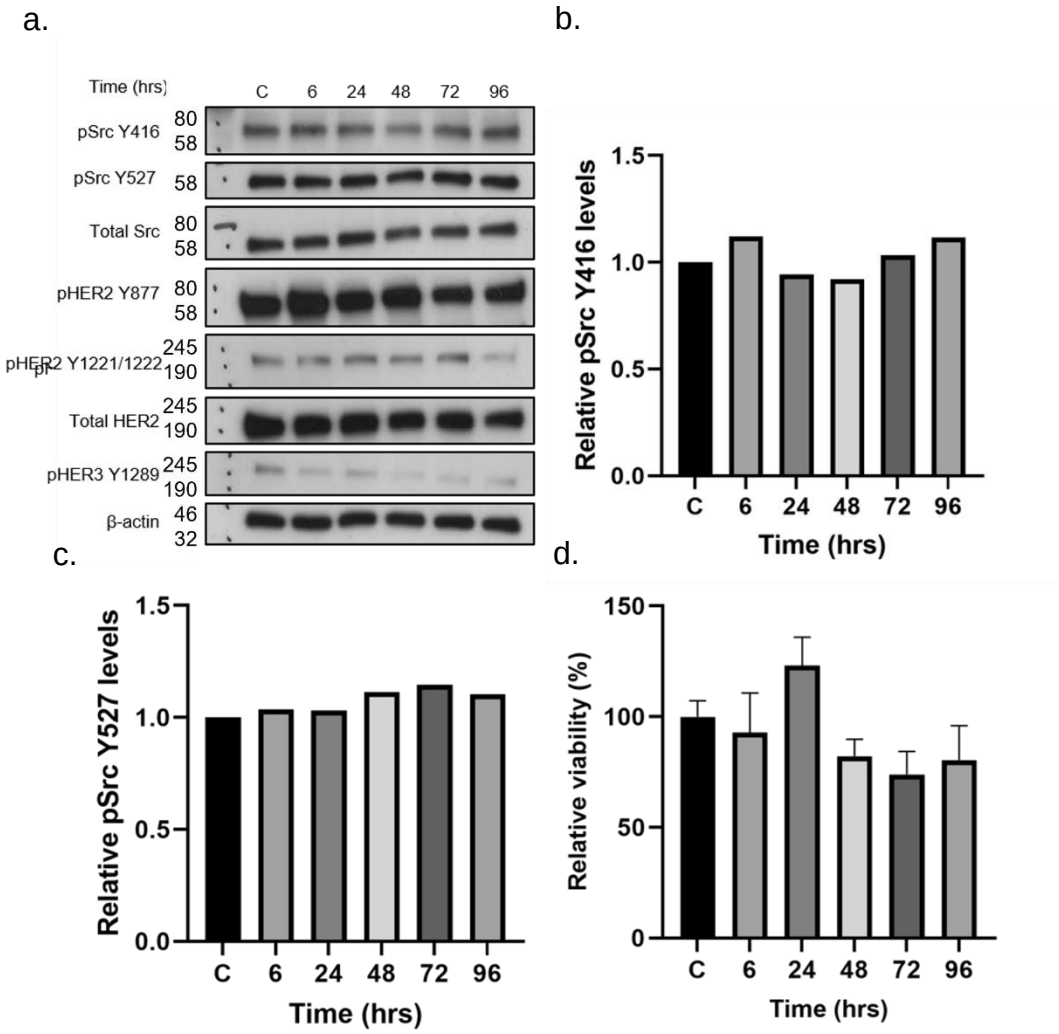

Figure 3.2.6 Relative protein expression levels and the effect of cellular proliferation after time-point Herceptin treatment of SkBr3 cells, under serum-deprived conditions.

a. Immunoblot of SkBr3 cell lysates after exposure to 4µg/ml Herceptin incubated for 6, 24, 48, 72 and 96 hours compared to the vehicle-control (PBS only) cells. Here, the cells were treated under serum-deprived conditions, after growing in serum-deprived media for 24 hours prior to drug-treatment, n=1. **b.** Relative densitometry of pSrc Y416 levels and **c.** Relative densitometry of pSrc Y527 levels in the Herceptin treated SkBr3 cells. Phosphorylation levels were compared to total Src expression levels and normalised to the β-actin loading control. Phosphorylated Src levels were calculated as a fold change from the vehicle-treated control

(**C**) cells, n=1. **d.** Relative cell viability determined via MTT assay of SkBr3 cells grown under serum-deprived conditions, after the treatment of Herceptin at concentrations of 4µg/ml for 6, 24, 48, 72 and 96 hours, compared to the vehicle-control (PBS-only) cells, n=4 +/- SD. All cells were serum-starved for 24 hours prior to the addition of Herceptin.

3.2.7 Herceptin treatment of SkBr3 cells gives no effect on activated Src levels determined via sandwich ELISA

After the contrast in results seen with regards to activated pY416 Src levels in time-point Herceptin treated SkBr3 cells (**Figure 3.2.6**) to those obtained at the beginning of the study (**Figure 3.2.2**), activated Src levels in response to Herceptin treatment were further examined. A different method was utilised to determine Src pY416 levels in SkBr3 cells after treatment with Herceptin. An Enzyme-linked immunosorbent assay (ELISA) Pathscan Phospho-Src (Y416) Sandwich kit (Cell Signalling) was used to colorimetrically determine the pY416 Src levels in Herceptin-treated SkBr3 cell lysates. ELISA is known for its high sensitivity levels and is a quantitative technique compared to immunoblotting which is semi-quantitative. Thus, this technique was used to validate the results found via western blot.

Here, a 96 well plate was pre-coated with pSrc Y416 capture antibody and incubated with 1mg/ml SkBr3 cell lysates after treatment with 4µg/ml Herceptin (using a fresh vial of Herceptin) for 3 and 6 hours alongside vehicle-treated control (PBS-only) cells. The cells were grown under serum-deprived (-) or serum-supplemented (+) conditions. Cells grown under serum-deprived conditions were serum-starved for 24 hours prior to drug treatment. A second capture antibody and a HRP-linked antibody was used to amplify the signal and visual detection of Src phosphorylation at Y416 was determined using a plate reader. The magnitude of absorbance at 450nm was directly proportional to the levels of pY416 Src in each sample.

No significant difference was observed with regards to phosphorylated Y416 Src levels compared to the vehicle-treated control cells, for both the SkBr3 cells grown under serum-deprived or serum-supplemented conditions for 3 and 6 hours of Herceptin treatment (**Figure 3.2.7**). Thus, the treatment of SkBr3 cells with Herceptin for up to 6 hours has no effect on pY416 Src activation levels.

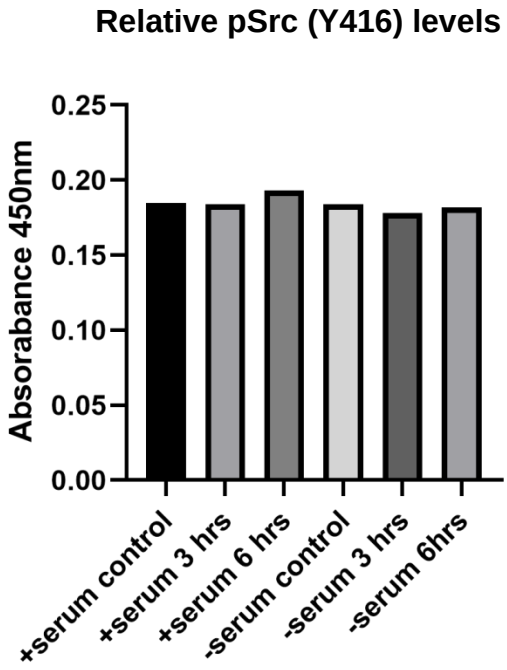

Figure 3.2.7 Phosphorylated Y416 Src levels in SkBr3 cells, after 3 and 6 hours of Herceptin treatment, n=1.

Phosphorylated Src (Y416) levels were determined via colorimetric sandwich ELISA in SkBr3 cell lysates treated with 4µg/ml Herceptin. The SkBr3 cells were treated for 3 and 6 hours compared to vehicle-treated control (PBS only) cells, under serum-deprived (-) and serum-supplemented (+) conditions. Cells treated under serum-deprived conditions were serum-starved for 24 hours prior to drug treatment. The level of pY416 Src in each sample is proportional to the magnitude of absorbance at 450nm, n=1.

3.2.8 Herceptin treatment of SkBr3 cells with new vials of Herceptin shows batch-to-batch variability

The contrasting results regarding phosphorylated Src levels at Y416 from the ELISA (**Figure 3.2.7**) and the time-point immunoblot (**Figure 3.2.6**) using different vials of Herceptin, led us to repeat the initial immunoblotting experiments to determine if the same results are observed with a fresh vial, and thus, batch of Herceptin.

A new vial and batch of Herceptin was used to determine SkBr3 cell viability following a drug incubation of 72 hours in serum-deprived media and incubated at 37°C (21% O_2, 5% CO_2). Herceptin was dosed to SkBr3 cells as a five-fold decrease in concentration, ranging from 20µg/ml to $2.56x10^{-4}$ µg/ml (the same concentrations used in **Figure 3.2.1**). A dose-response curve was obtained (**Figure 3.2.8a.**) to clarify whether the new vial of Herceptin gives the same concentration-dependent viability response as seen in **Figure 3.2.1**. Absorbance values were normalised to the vehicle-treated control (PBS only) cells. SkBr3 cells were serum-starved 24 hours prior to the addition of Herceptin. It was observed that the SkBr3 cells gave the same dose-dependent decrease in cellular viability to increasing concentrations of Herceptin treatment as those found previously (**Figure 3.2.1**) giving a maximum cell reduction of around 60%. This suggests that this new batch of Herceptin produces reproducible toxicity of SkBr3 cells.

Immunoblotting of SkBr3 cell lysates treated with increasing concentrations of the new vial of Herceptin, grown under serum-deprived conditions was also performed (**Figure 3.2.8b**). Cells were serum-starved for 24 hours prior to drug treatment. SkBr3 cells were dosed with Herceptin for 72 hours at 37°C (21% O_2, 5% CO_2), under serum-deprived conditions. Total and phosphorylated HER2 and Src levels were determined and compared to the β-actin loading control. The results obtained here displayed a very different immunoblotting outcome to those seen previously, in **Figure 3.2.2**. HER2 phosphorylation at Y877 and total HER2 levels were slightly lower after Herceptin treatment, compared to the vehicle-control, which is similar to the results seen previously (**Figure 3.2.2**). There was no difference seen in comparison to the vehicle-treated control cells in regards to Src

phosphorylation levels at Y416 and total Src protein levels, in cells treated with Herceptin at any concentration for 72 hours. This suggested that there was batch-to-batch variability of Herceptin, from the first vial utilised in **Figure 3.2.1** and **Figure 3.2.2**. Therefore, the activation of Src first observed in **Figure 3.2.2** in response to Herceptin treatment, in HER2-overexpressing SkBr3 cells under serum-deprived conditions, was found to be an anomaly.

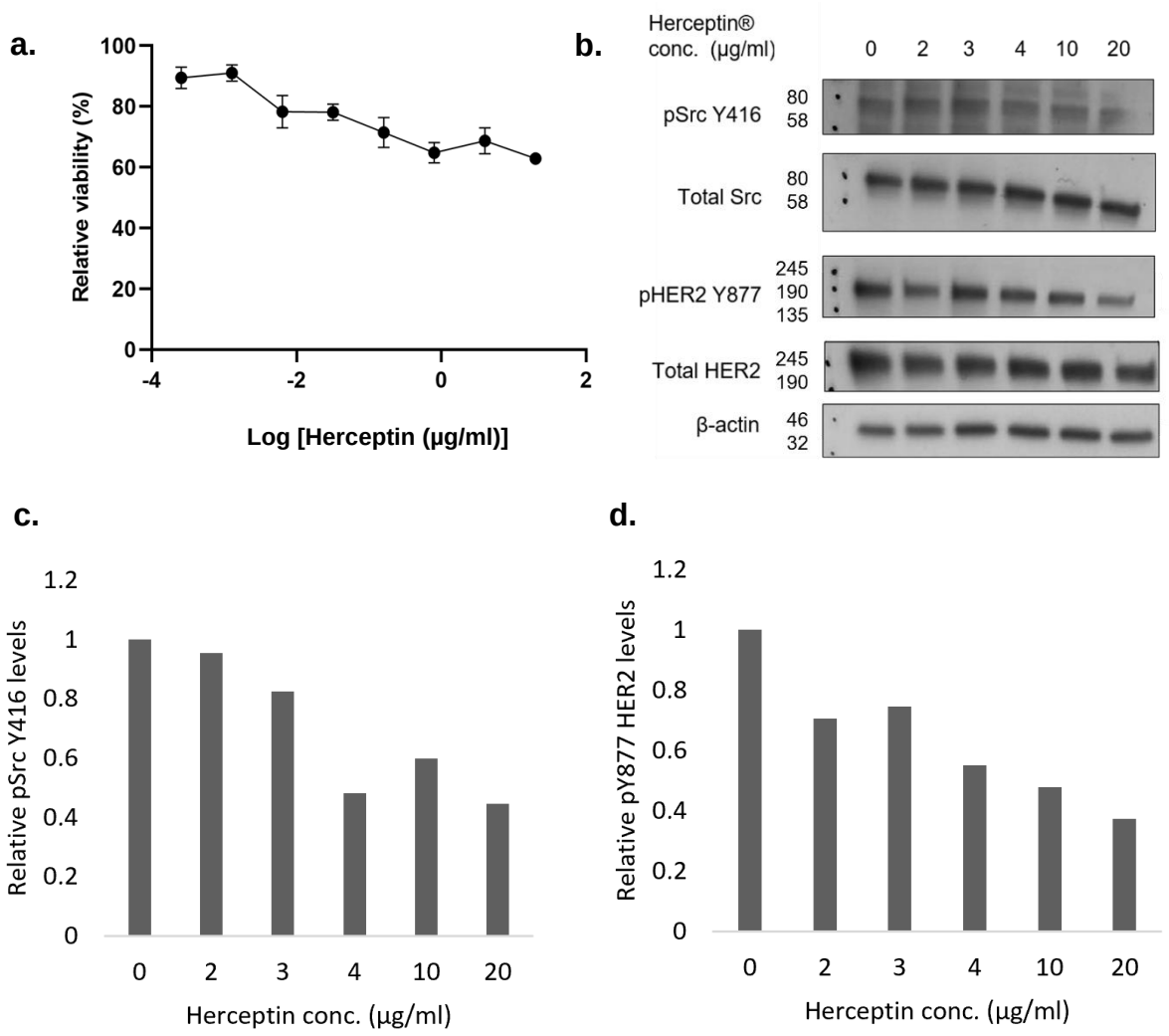

Figure 3.2.8 Repeated dose-response curve and immunoblotting of SkBr3 cells after treatment with a new vial and batch of Herceptin, under serum-deprived conditions.

A dose-response curve obtained via MTT cell viability assay of SkBr3 cells treated with five-fold serial dilutions of Herceptin for 72 hours, in serum-deprived media with a new vial and new batch of Herceptin. The cells were serum-starved for 24 hours prior to drug treatment. Relative cell viability (%) was normalised to the vehicle-treated (PBS-only) control cells, n=4. **b.** Immunoblot of SkBr3 cells treated with increasing concentrations of the new vial of Herceptin, under serum-deprived conditions for 72 hours. The cells were serum-deprived for 24 hours prior to drug treatment. Concentrations of Herceptin administered to

the SkBr3 cells include, 0 (vehicle-treated control), 2, 3, 4, 10 and 20µg/ml. Src and HER2 phosphorylation and total protein levels were probed and the β-actin loading control, n=1.

3.3 Discussion

Herceptin therapy is the standard of care used to treat patients with HER2-positive BC. Herceptin targets an external domain of the HER2 receptor and the proposed mechanism of action prevents the binding to other ErbB family members and thus, inhibits canonical HER2 signalling (Baselga et al., 2001). However, around 50% of HER2-positive BC patients go on to develop BM (Aversa et al., 2014; Kennecke et al., 2010), with a higher incidence of BM observed in HER2-positive BC patients, after treatment with Herceptin (Olson et al., 2013a). BM is an end-stage of BC progression, where only 20% of patients survive up to 1 year after diagnosis (Leyland-Jones, 2009). A significant proportion (66-88%) of HER2-positive BC patients have *de novo* resistance to Herceptin treatment (Baselga et al., 1996; Cobleigh et al., 1999; Vogel et al., 2002). Around 70% of patients who respond initially, become resistant to Herceptin over time (acquired HER2 resistance) (Ross et al., 2009; Nahta and Esteva, 2006b). There is a lack of conclusive evidence on the specific deterministic factors of the high rates of *de novo* and acquired resistance in HER2-positive BC patients after treatment with Herceptin and also a lack of conclusive data about Herceptin's mechanism of action (Valabrega et al., 2007). Herceptin *de novo* and acquired resistance has been associated with the expression and activation of the oncoprotein, Src (Zhang, S. et al., 2011). Src plays a vital role in many cell signalling pathways, which when aberrantly activated can promote tumorigenesis and metastasis (Summy and Gallick, 2003).

The novel mechanism of Tier 2 signalling demonstrates how aberrant activation of oncogenic signalling pathways can be initiated by interactions between non-activated RTKs and SH3-domain-containing proteins, under serum-deprived stress conditions. These interactions occur depending on the relative proteome of the cell (Timsah et. al., 2016). Previous research from our laboratory has shown that a non-homeostatic Tier 2 mechanism is utilised via other types of cancers, whereby the SH3 domain of Plcg1 was found to

interact with a proline-rich motif within FGFR2 C-terminal tail. This interaction occurred under conditions that promoted the non-canonical binding of Plcg1 to FGFR2, when relative cellular Grb2 levels were low and when cells were under serum-deprived stress (Timsah et al., 2016b). This PPI induced the non-canonical activation of Plcg1, which in turn, upregulated the Akt signalling pathway. The activation of Akt gave a highly proliferative outcome in ovarian cancer cells. It was also found that this Tier 2 signalling mechanism was of particular importance as a prognostic factor in lung adenocarcinoma patient pathological outcome (Timsah et al., 2015).

Furthermore, HER2 has already been found to interact with a close family member of Src (Fyn) in a HER2 phosphorylation independent manner, via HER2 C-terminal proline-rich motif (R_{1146}PQPPSP$_{1152}$) to the SH3 domain of Fyn (Bornet et al., 2014). Src displays a large percentage of homology to Fyn (74.4%) (Ulmer et al., 2002). Therefore, Src may also be able to bind via its SH3 domain to this same proline-rich binding site when HER2 is in a non-activated state (under Herceptin inhibition) and under serum-deprived stress. The propensity of other RTKs to bind to SH3-domain containing proteins via a Tier 2 mechanism is likely, due to the significant levels of RTKs containing proline-rich sequences within their intracellular domains and the high levels of SH3 domain-containing proteins within cells (Mayer, B.J. and Gupta, 1998). Therefore, the aberrant activation of a Tier 2 mechanism via HER2 RTK and Src-SH3 domain could be a possible chemoresistance mechanism utilised by BC cells and implicated in BC progression, when under HER2-inhibited stress via Herceptin treatment.

The potential for aberrant Tier 2 signalling to be driven by the possible interaction and activation of Src-kinase via HER2 RTK, when under the inhibition of Herceptin, was investigated. We found in initial experiments that the key oncoprotein, Src, was phosphorylated at Y416 in response to Herceptin treatment of SkBr3 BC cells. To our knowledge there has not been any studies on direct Herceptin mediated activation of Src. Src activation is known to be involved in invasion and migration signalling pathways (Summy and Gallick, 2003) and has been found to be a common node in Herceptin resistance in HER2-positive BCs (Zhang, S. et al., 2011). The non-canonical activation of Src, therefore, could be utilised as a mechanism of Herceptin

resistance when cancer cells are under Herceptin treatment and under serum-deprived stress.

The results presented in this chapter also showed that a basal phosphorylation of HER2 RTK was maintained after Herceptin treatment. This was in accordance to the findings of Gijsen *et al.,* where they found that HER2 phosphorylation was maintained by a PKB (Akt) negative feedback loop after Herceptin treatment in both SkBr3 cells and BT474 cells (Gijsen et al., 2016). HER2 total expression levels were found to decrease after Herceptin treatment, which could be via Herceptin mediated HER2 internalisation (Nahta and Esteva, 2006b). The internalisation of HER2 in SkBr3 cells was also visualised by IF after 6 hours of Herceptin treatment, under serum-deprived conditions. Further investigation into the co-localisation of Src and HER2 needs to be investigated via the use of a higher microscope magnification. Here, the use of FRET may have been useful to determine whether the two proteins are in close proximity and to further validate whether a PPI occurs between Src and HER2, under basal conditions.

The effect of the TKI HER2-inhibitor, Lapatinib, was investigated in SkBr3 cells, to determine whether there was an effect on Src activation via phosphorylation at Y416. Lapatinib treatment of SkBr3 cells showed a larger maximum cell reduction in cellular viability compared to the vehicle-treated control (~40%), than seen with Herceptin (~60%). Lapatinib treatment also abrogated HER2 autophosphorylation after a few hours of incubation, but it did not give any effect on Src phosphorylation at Y416. Thus, the inhibitor was not used in further experiments as there was no effect on Src activation in SkBr3 cells via Lapatinib induced HER2-inhibition. The results from this experiment indicated that basal phosphorylation of HER2 may play a role in activating Src at Y416 when under Herceptin inhibition. It would have been interesting to see whether dual treatment of both Lapatinib and Herceptin had an effect on pY416 Src levels. The effect of Pertuzumab, another approved mAb HER2-targeting treatment for HER2-positive BC patients, on SkBr3 BC cells would also have been interesting. The mechanism of action of Pertuzumab is known and includes that of inhibiting all heterodimerisation with other ErbB receptors (Hurvitz et al., 2018). Therefore, it would have been interesting to see if abrogation of co-dimerisation (which is a proposed but not

validated mechanism of action of Herceptin also) has an effect on Src and HER2 phosphorylation and protein levels, in HER2-overexpressing BC cells.

Unfortunately, later experiments of Herceptin-treated SkBr3 cells showed contradictory results to those originally obtained. When the initial experiments were repeated with a fresh vial and new batch of Herceptin, different results were obtained to those found previously. These initial results were found to be anomalous when repeated with further batches of the drug. The first batch of Herceptin was used in the initial experiments determining the dose-response curve of Herceptin-treated SkBr3 cells and the immunoblotting results, where Src activation at pY416 was observed upon Herceptin treatment of SkBr3 cells over 72 hours, with n=3 repeats. This difference in experimental results may have been due to a possible contaminant in the first batch of the drug. The vials of Herceptin used in these experiments were only of lab grade, compared to the high sterile grade that would be used to treat HER2-positive BC patients in hospitals. For further use of Herceptin in experiments, a sample could be sent to be analysed via mass spectrometry to indicate whether there would be any unknown peaks and thus, unknown contaminants in the vial before experimentation.

The migration assay results also support that the original findings of Src activation upon Herceptin treatment were an anomaly, as Src activation is implicated in the upregulation of migration signalling pathways (Mayer, E.L. and Krop, 2010). Therefore, the expected results would have been to see an increase in cellular migration upon Herceptin-mediated non-canonical Src-activation in SkBr3 cells. The results found here were the opposite, whereby Herceptin treatment inhibited cell migration of SkBr3 cells.

Further work into this project would have been to validate whether Src activation occurs through an aberrant Tier 2 mechanism in SkBr3 BC cells, via Herceptin inhibition. Here, the utilisation of HER2 protein constructs with mutated proline-rich motifs would have been expressed in BC cells. Therefore, it would be determined whether the mutation of the proline-rich motif of HER2 would abrogate the activation of Src-kinase, when HER2 is under the inhibition of Herceptin. FRET and co-localisation experiments would have been used to validate a PPI between Src-SH3 domain and HER2 proline-rich motif, under

Herceptin inhibition. The utilisation of other BC cell lines would have also been used to determine whether the same effects are seen in other HER2-expressing BC cell lines.

Even though Src was not found to be activated in response to Herceptin treatment of HER2-positive SkBr3 cells, it is possible that there could be other intracellular SH3 domain-containing proteins which are non-canonically activated via a Tier 2 signalling mechanism in HER2-positive BC cells, in response to Herceptin treatment. The aberrant activation of a Tier 2 mechanism in BC cells in response to Herceptin-induced HER2 inhibition could contribute towards the high levels of resistance and metastasis observed in HER2-positive BC patients, after treatment with Herceptin. The SkBr3 cells gave a maximum cell reduction of 60% after drug-treatment with Herceptin and thus, many SkBr3 BC cells are able to survive Herceptin treatment. The SkBr3 cell line is known to be heterogeneous, therefore, it would have been interesting to investigate whether the cells which survive Herceptin treatment have something in common, in particular the expression and/or activation of SH3 domain-containing proteins. To investigate this, a HER2 Co-IP could be performed in BC cell lysates after treatment with Herceptin. The elute which would include bound proteins to HER2 would be sent for mass spectrometry analysis. Here, any bound proteins containing an SH3 domain would be identified and the results could be used for further investigation of a possible Tier 2 mechanism occurring in HER2-overexpressing BC cells under Herceptin-mediated HER2-inhibition and to determine whether this possibility contributes to the survival, progression and resistance to Herceptin therapy.

3.3.1 Conclusion

The findings from this chapter conclude that the original results obtained showing non-canonical Src activation via the phosphorylation of Y416 in response to Herceptin-inhibition of HER2 in SkBr3 cells, was found to be an anomaly. The phenotypic migration assay and subsequent immunoblotting and ELISA results contradicted the initial immunoblotting results obtained with the first batch of drug used in these experiments. The vials of Herceptin used here were only of lab grade and thus, not the sterile high-grade Herceptin used

to treat patients in hospitals. Therefore, a possible contaminant in the first vial of Herceptin may have given these anomalous results and induced the activation of Src-kinase in SkBr3 cells. Due to these original findings being an anomaly, a new project was initiated looking at non-canonical Tier 2 signalling via VEGFR2 RTK in BC cells, under serum-deprived microenvironmental stress.

Chapter 4 Exploring the potential of non-canonical Tier 2 PPIs via VEGFR2-RTK in BC cells

4.1 Introduction

4.1.1 Vascular Endothelial Growth Factor Receptor (VEGFR) Family

The VEGFR family of proteins are members of the RTK superfamily and consist of three RTKs which are crucial regulators of vascular development during embryogenesis (vasculogenesis) and blood vessel formation (angiogenesis) (Olsson et al., 2006). VEGFRs are expressed in endothelial, stromal cells and are aberrantly expressed in cancer (Butti et al., 2018). In mammals, there are five vascular endothelial growth factor (VEGF) ligands which bind to the three VEGFRs and co-receptors (e.g. heparan sulphate proteoglycan (HSPG) and Neuropilin) in an overlapping fashion (**Figure 4.1.1**). The binding of VEGF ligand to a particular VEGFR induces receptor co-dimerisation and activation of the TKD. This leads to the subsequent phosphorylation of docking sites within the intracellular domain for the binding and activation of signal transducers. VEGFRs activate many cellular processes that are common to GF receptors, including cell migration, survival and proliferation (Shibuya, Masabumi and Claesson-Welsh, 2006).

VEGFR1 and VEGFR2 canonically bind to VEGF-A ligand (Ferrara, N. et al., 2003). VEGFR1 also binds to VEGF-B and placental growth factor (PLGF) and has an established role in mediating chemotaxis in monocytes and macrophages (Barleon et al., 1996). VEGFR1 is both a positive and negative regulator of VEGFR2. A splice-variant of VEGFR1 is known to bind to and sequester VEGF-A and prevent the binding of VEGF-A to VEGFR2 (Kendall and Thomas, 1993). VEGFR2 also binds to VEGF-E and is the main mediator of mitogenic signals of the VEGF-A ligand and is involved in both normal and pathological vascular-endothelial-cell-biology (Ferrara, N. et al., 2003). VEGFR3 on the other hand, does not bind to VEGF-A but binds to VEGF-C and VEGF-D (Karkkainen et al., 2002). VEGFR2 can also bind to VEGF-C and VEGF-D after proteolytic processing, but with a lower affinity than

VEGFR3 (Olsson et al., 2006). VEGFR3 is important for lymphatic-endothelial-cell development and function.

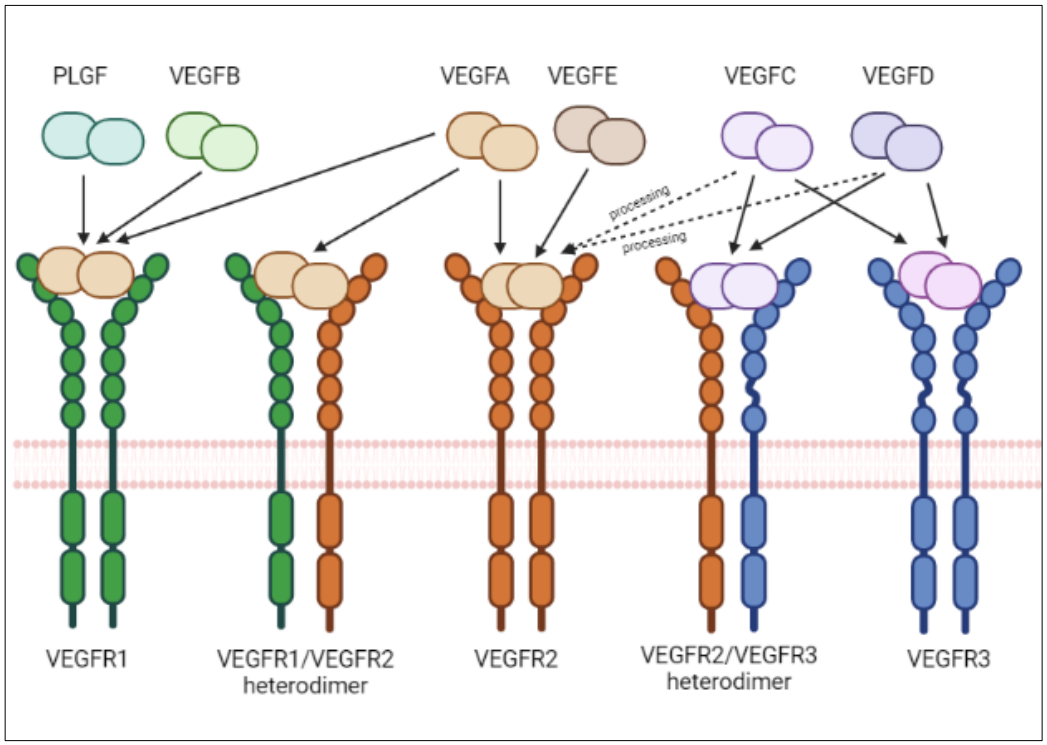

Figure 4.1.1 Canonical VEGFR ligand-binding and consequent signalling complexes.

VEGF ligands bind to three VEGFR RTKs in an overlapping fashion to induce homo- or hetero-dimerisation, leading to the activation of different downstream signalling pathways. Proteolytic processing of VEGF-C and VEGF-D allows for binding to VEGFR2. Adapted from (Olsson et al., 2006) using BioRender.com.

4.1.2 VEGFR structure and activation

VEGFRs contain a large extracellular domain of approximately 750 amino acid residues, which makes up seven immunoglobulin (Ig)-like folds. Ig domain-2 of VEGFR1 constitutes the ligand binding domain (Christinger et al., 2004) and Ig domains-2 and -3 of VEGFR2 are important for ligand-binding specificity (Fuh et al., 1998). VEGFR3 extracellular domain slightly differs in that the fifth Ig domain is replaced by a disulphide bridge. The extracellular domain is followed by a single transmembrane domain (TMD), a juxta-

membrane domain (JMD) and a split TKD, which is interrupted by a 70-amino-acid kinase insert (KI) and a C-terminal tail (Olsson et al., 2006; Guo, S. et al., 2010).

Following ligand-binding, interactions between Ig-like domains 4 and 7, the TMD and the JMD between a VEGFR dimerisation pair, stabilise the VEGF-VEGFR complex (Stuttfeld and Ballmer-Hofer, 2009). Dimerisation of the receptors leads to the activation of the TKD, and to the consequent autophosphorylation of Y residues within the KI and C-terminal region of the receptors (Shibuya, M., 2011). Subsequently, a variety of signalling molecules, including SH2 and PTB-containing proteins, are recruited to VEGFR dimers and bind to phosphorylated Y residues within the intracellular domains. The activation of these signalling effector proteins go on to upregulate signal transduction events downstream of VEGFR activation (Stuttfeld and Ballmer-Hofer, 2009).

4.1.3 VEGFR2

VEGFR2 (also known as kinase domain region (KDR) or Flk-1), encoded by the VEGFR2 gene, is a 210-230 kDa glycoprotein that plays a significant role in angiogenesis and is the major mediator of the mitogenic, angiogenic and permeability-enhancing effects of VEGF in endothelial cells (Ferrara, N. et al., 2003; Shibuya, Masabumi and Claesson-Welsh, 2006). VEGFR2 has a 10-fold lower affinity to VEGF-A than VEGFR1 but VEGFR1 TK activity is approximately 10-fold weaker than VEGFR2 (Shibuya, M., 2011). VEGFR2 can form homo-dimers and hetero-dimers with VEGFR1 and VEGFR3, which gives substantial differences in signal transduction events, due to the different downstream substrates that they activate (Huang, K. et al., 2001). VEGFR2 is also found in non-endothelial cells such as pancreatic duct cells, retinal progenitor cells, megakaryocytes and haemopoietic cells. VEGFR2 expression is also aberrantly expressed in pathological processes, such as cancer (Koch et al., 2011).

The VEGFR2 gene encodes a full-length receptor (**Figure 4.1.2**) of 1356 amino-acid residues. Within the cell, the VEGFR2 protein is translated as a 150kDa protein without any significant glycosylation. It is then processed, by

a series of glycosylations, to a mature 210-230kDa form, that is expressed on the plasma membrane (Takahashi, Tomoko and Shibuya, 1997).

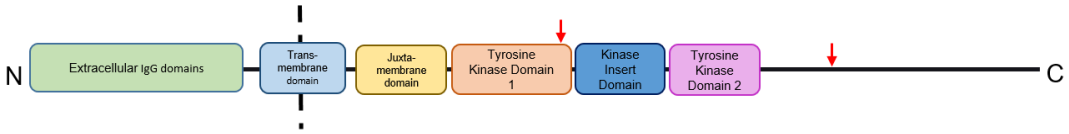

Figure 4.1.2 VEGFR2 domain structure.

VEGFR2 full-length domain structure (proline-rich motif regions are indicated by red arrows).

4.1.3.1 Canonical VEGFR2 signalling

Ligand-dependent activation and subsequent Y phosphorylation of VEGFR2 results in the upregulation of mitogenic signalling pathways which mediates many different cellular outcomes including cell survival, migration, proliferation and permeability (**Figure 4.1.3**). A unique feature of VEGFR2 activation is the upregulation of the Raf-Mek-Erk pathway through the phosphorylation of Plcg1 and the subsequent activation of PKC, rather than through the activation of Ras. This pathway is preferentially and highly activated by ligand-activated VEGFR2 and upregulates proliferation signalling pathways in endothelial cells (Takahashi, T. et al., 1999; Takahashi, T. et al., 2001). Plcg1 binds to the pY1175 site specifically within the VEGFR2 C-terminal tail. This signalling pathway is important for pro-angiogenic signalling.

The pY951 site within the KI is important for cell migration signals and is phosphorylated in active angiogenesis (Matsumoto et al., 2005). T-cell-specific adaptor molecule (TSAd) binds to this site, which is implicated in actin reorganisation and migration signalling pathways. TSAd forms a complex with Src in a ligand-dependent manner. The PI3K/Akt pathway is also activated downstream which upregulates cell survival and cell permeability pathways via the activation of B-cell lymphoma-1 associated death promoter (BAD) and caspase-9 and the activation of endothelial nitric-oxide synthase-3 (eNOS). The pY1059 site has been shown to bind and activate Src-kinase. The activation of Src phosphorylates other residues in VEGFR2 intracellular domain, including Y1175 and downstream signal transducers, including IQ-

motif-containing GTPase-activating protein-1 (IQGAP1) (Meyer et al., 2008). IQGAP1 has been implicated in the regulation of cell-cell contacts, proliferation and migration (Yamaoka-Tojo et al., 2006). The phosphorylation of the Y1175 site has also been known to bind and activate SH2-domain containing adaptor protein B (SHB), SHC-transforming protein B (SCK) and Shc. The binding of these molecules may recruit the nucleotide exchange factor son of sevenless (SOS) to VEGFR2 and therefore, control downstream Ras activation (Warner et al., 2000; Kroll and Waltenberger, 1997). The phosphorylation of the Y1214 site allows the recruitment of non-catalytic region of TK adaptor protein (Nck) to VEGFR2. An Nck-Fyn complex mediates the phosphorylation of p21-activated protein kinase (PAK) and the activation of cell division cycle 42 (Cdc42) and p38MAPK (Lamalice, Laurent et al., 2006; Lamalice, L. et al., 2004).

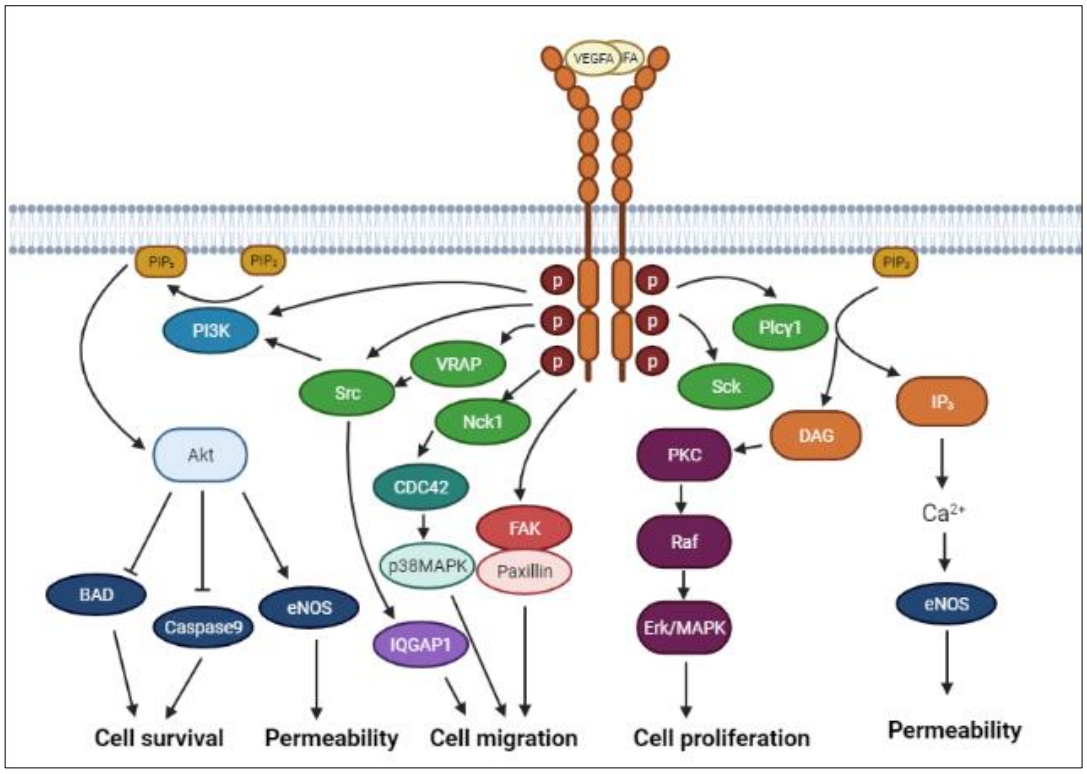

Figure 4.1.3 Canonical VEGFR2 signalling.

Canonical VEGFR2 activation and signalling after ligand-binding of VEGF-A, showing important downstream signal transduction pathways. Ligand-binding induces VEGFR2 co-dimerisation. Upon receptor dimerisation, the TKD is activated and autophosphorylation of particular Y residues within the KI and C-terminal tail occurs. SH2 and PTB domain-containing proteins bind to particular pY sites in the intracellular domain. Downstream signal transduction of these molecules is upregulated, which activate signalling pathways leading to the outcome of cellular functions including cell survival, migration, permeability and proliferation. The canonical activation of PKC via Plcg1 plays a crucial role in mitogenic signalling via the Raf-Mek-Erk pathway inducing cellular proliferation and permeability. Cell survival and permeability is mediated through PI3K-mediated activation of Akt. The activation of Src, FAK and p38 MAPK is implicated in cell migration signalling. Adapted from (Matsumoto and Claesson-Welsh, 2001; Koch et al., 2011), using BioRender.com.

4.1.3.2 VEGFR2 C-terminal region

There are five major pY sites within the C-terminal tail of VEGFR2, which include Y951 in the KI domain, Y1054 and Y1059 within the TKD and Y1175 and Y1214 in the C-terminal domain (**Figure 4.1.4**) (Matsumoto et al., 2005; Takahashi, T. et al., 2001; Koch et al., 2011). These phosphosites serve as SH2 and PTB binding-sites for effector proteins, which activate canonical downstream signalling pathways. VEGFR2 also contains two proline-rich motifs (PxxP) within the intracellular domain of the receptor. The first PxxP motif is located within the first TKD of VEGFR2 at residues P908xxP911. The second proline-rich motif is located at residue P1195xxP1198 within the C-terminal tail of VEGFR2 (**Figure 4.1.4**).

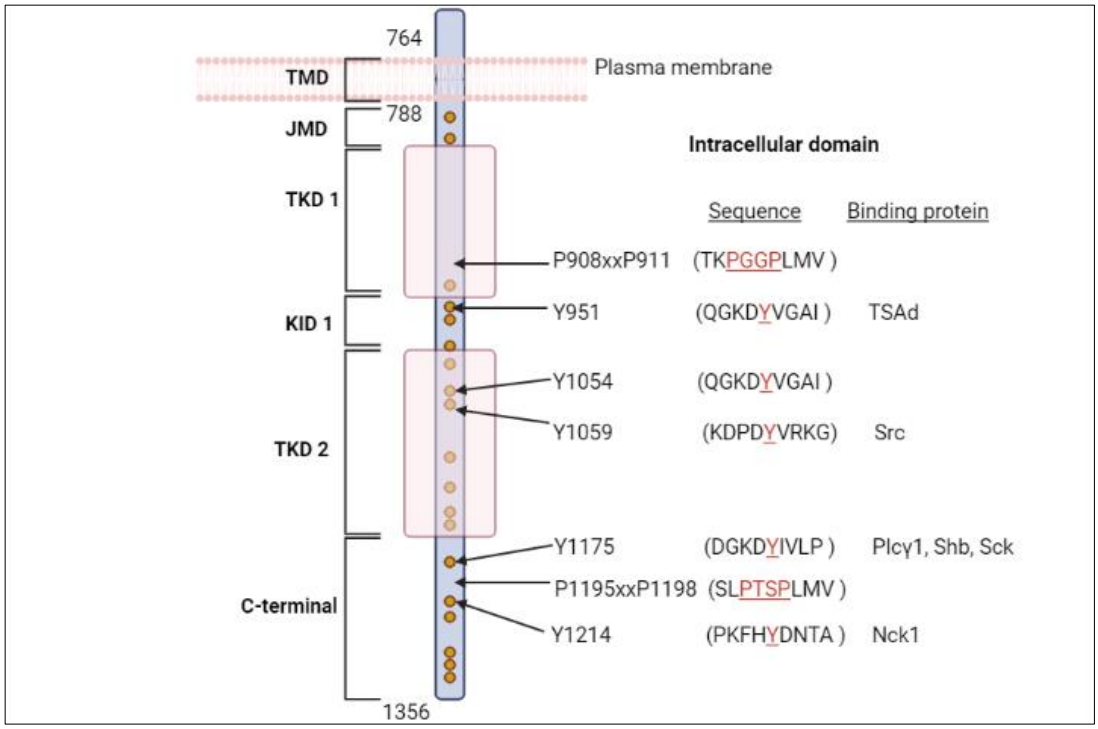

Figure 4.1.4 VEGFR2 intracellular domain structure and protein binding sites.

The intracellular domain consists of a JMD, a split TKD (TKD 1 and TKD 2), a KI domain (KID) and a C-terminal tail. pY sites which occur due to ligand-activation of the receptor are shown in yellow dots. The significant binding sites, their corresponding sequence and their known binding proteins are labelled. Adapted from (Holmes et al., 2007), made using BioRender.com.

4.1.4 VEGFR2 expression in cancer

Due to the potential role of VEGFR2 in tumour angiogenesis, the expression was investigated in cancers soon after it was identified as a RTK for VEGF (Waltenberger et al., 1994). Besides the initiation of angiogenesis via VEGFR2 signalling in different malignancies, the impact of VEGFR2 expression on cancer cell signalling is lesser known (De Palma et al., 2017). The overexpression of VEGFR2 occurs in many cancer types and the expression levels directly relate to the disease stage, recurrence and outcome of cancer patients (Guo, S. et al., 2010; Xia et al., 2006; Kim et al., 2008). VEGFR2 overexpression has been reported in various cancer types such as ovarian (Jang et al., 2017; Chen et al., 2004), brain (Lu-Emerson et al., 2015; Puputti et al., 2006), liver (Kim et al., 2008), renal (Pengcheng et al., 2017), colon (Takahashi, Y. et al., 1995; Mahfouz et al., 2017), bladder (Zhong et al., 2017; Xia et al., 2006) and lung cancer (Riquelme et al., 2014; Carrillo de Santa Pau et al., 2009) as well as in BCs (Guo, S. et al., 2010; Nakopoulou et al., 2002; Rydén et al., 2003; Weigand et al., 2005). VEGFR2 expression was detected in 64.5% of invasive breast carcinomas (Nakopoulou et al., 2002). Other cancers have different VEGFR2-positive expression levels (**Table 4.1.1**) including oesophageal adenocarcinoma and squamous-cell cancer where the VEGFR2-positive expression rate was found to be 94% and 100% respectively (Gockel et al., 2008).

Table 4.1.1 VEGFR2 expression levels in human cancers and cancer cell lines.

Adapted from (Guo, S. et al., 2010).

Tissue	Subtype	VEGFR2 expression level	Reference
Bladder	Carcinoma	50%	(Xia et al., 2006)
Brain	Glioma	6-17%	(Puputti et al., 2006)
Breast	Adenocarcinoma	64.5%	(Nakopoulou et al., 2002)
Cervix	Adenosquamous carcinoma	73.3%	(Longatto-Filho et al., 2009)
Colon	Adenocarcinoma	40%	(Takahashi, Y. et al., 1995)
Oesophagus/ Squamous-cell	Carcinoma	94%/100%	(Gockel et al., 2008)
Kidney	Clear cell cancer	35%	(Badalian et al., 2007)
Lung	Non-small-cell carcinoma	54.2%	(Carrillo de Santa Pau et al., 2009)
Oral	Carcinoma	Overexpressed	(Sato and Takeda, 2009)

Ovary	Carcinoma	Overexpressed	(Chen et al., 2004)
Pancreas	Carcinoma	Overexpressed	(Itakura et al., 2000)
Prostate	Cancer cell lines	100%	(Stadler et al., 2004)
Skin	Melanoma	Overexpressed	(Straume and Akslen, 2003)

4.1.4.1 VEGFR2 expression and significance in BC

VEGFR2 has been found to be overexpressed in BC tissues and is directly correlated with the pathogenesis of BC patients (Guo, S. et al., 2010). In malignant breast carcinoma patient tissues, VEGFR2 expression was found in all samples, independent of tumour stage and histological grade. When malignant BC tissue was compared with the neighbouring non-neoplastic tissue, activated VEGFR2 was at a much higher level in the malignant tissue samples compared to the non-neoplastic tissue (Kranz et al., 1999). Ligand-activated VEGFR2 via VEGF has been found to promote breast and lung CSC self-renewal via VEGFR2 downstream activation of STAT3. STAT3 activation upregulates Myc and Sox2 in TNBC (Zhao, D. et al., 2015). The co-expression of VEGF and VEGFR2 have been found in BC (Rydén et al., 2003) and an autocrine-loop between secreted VEGF and the activation of VEGFR2 was found in BC cell lines and primary BC cultures *in vitro* (Weigand et al., 2005). In another study, the expression levels of VEGFR2 were correlated with lymph node metastasis of BC and patients with a high VEGFR2 expression had a significantly worse OS. The expression of EMT markers, Twist1 and Vimentin was also found to be higher in BC tumours with a high VEGFR2 expression, while the epithelial marker, E-cadherin was lower in the same tumours. This suggested that VEGFR2 may be a possible mediator of the EMT in BC (Yan et al., 2015). VEGFR2 expression levels in BC patient samples were found to be significantly correlated with the expression of the proliferation indices Ki-

67 and Topo-Iiα (Nakopoulou et al., 2002). High levels of VEGFR2 expression was found to be a significant characteristic of TNBC. The high levels of VEGFR2 in TNBC was found to be significantly correlated with decreased BC-specific survival (Rydén et al., 2010). Taken together, these data suggests that high levels of VEGFR2 may aid in cancer progression and is a potential biomarker for BC patients.

4.1.4.2 Clinical significance and targeting of VEGFR2

Solid tumour malignancies, including BC, are considered angiogenesis dependent (Gupta, 2003). However, anti-angiogenic therapies have shown various results due to the different and distinct panel of anti-angiogenic factors and expression levels of angiogenesis-specific proteins in different tumour types. Tumours develop resistance to anti-angiogenic therapy by turning to alternate survival pathways when one is therapeutically inhibited. Therefore, research into how cancer cells develop resistance to anti-angiogenic therapy and the particular resistance pathways upregulated are important for patient selected treatment (Roy and Perez, 2009; Hayes et al., 2007).

Some anti-angiogenic treatment strategies have entered the clinic to date. These agents include Bevacizumab (anti-VEGF-A humanised mAb, Avastin; Genentech) which has been approved for the treatment of breast, colorectal, lung, renal and glioblastoma cancer patients (Ferrara, Napoleone and Kerbel, 2005; Diaz, R.J. et al., 2017). The VEGFR2-targeting mAb, Ramucirumab (Cyramza, ImClone Stystems Inc) has been approved for the treatment of solid tumours, including stomach, colorectal and non-small cell lung cancer. Apatinib (Rivoceranib, Elevar Therapeutics), a TKI which also targets VEGFR2 directly, was shown when in combination with Ramucirumab to have a more favourable benefit in patients when compared to the direct block of angiogenesis stimuli by bevacizumab, in the treatment of gastric cancer (Pinto et al., 2017). Several other orally active small-molecule TKI of VEGFR2 are now in clinical use, including Sunitinib (Sutent) a dual-targeted RTK inhibitor to VEGFR2 and PDGFR-β and more in clinical trials (Jiang et al., 2020; Holmes et al., 2007). However, many have serious side-effects which limits their long-term use.

4.1.5 The tumour microenvironment of solid tumours

Within the tumour microenvironment of solid tumours, the lack of sufficient vasculature leads to the development of nutrient and GF deprived conditions and hypoxia (**Figure 4.1.5**). These conditions elicit the activation of different signalling pathways which modify the characteristics and behaviour of tumour cells (Efeyan et al., 2015; Anastasiou, 2017). Hypoxia is a reduction in the normal level of tissue oxygen tension and occurs in cancer. Solid tumours develop a severely hypoxic microenvironment (Pugh and Ratcliffe, 2003), due to the increasing metabolic demand of the growing mass of tumour cells and insufficient tumour vascularisation. Advanced tumours are conditioned to survive these harsh growth environments during intravasation, extravasation and migration during metastasis when they move away from the vasculature to a secondary site and during anti-angiogenic therapy (White, ElShaddai Z. et al., 2020). Cancer cells growing under these conditions adapt by activating signalling pathways to allow tumour cells to survive and proliferate. These processes contribute to a more malignant phenotype and aggressive tumour behaviour (Harris, 2002).

Nutrient deprivation has been correlated to a poorer patient survival, suggesting that the lack of nutrients can induce tumour cell survival pathways (Moscat et al., 2015). A high expression of Akt was found to be correlated with cancer cell line survival under nutrient and serum-deprived conditions (Izuishi et al., 2000). In the MCF7 BC cell line, serum-deprivation was found to increase cell migration and a number of migration marker mRNA levels (Ahmadiankia et al., 2019). In prostate cancer cell lines, serum-deprivation initiated the adaptation of cancer cells to oxidative stress and a survival mechanism to anti-tumorigenic agents (White, ElShaddai Z. et al., 2020). The prolonged serum-deprivation of both MCF7 BC cells and H460 lung cancer cells displayed a multi-drug resistance phenotype by activating alternative and multiple cell signalling mechanisms (Yakisich et al., 2017). This was found to be an important adaptive mechanism for survival under harsh growth conditions such as serum-deprivation and exposure to therapeutic drugs. The aberrant activation of the Tier 2 mechanism between FGFR2 and Plcg1 in ovarian cancer cells is an example of the upregulation of an oncogenic

signalling pathway implicated in cancer progression, when tumour cells are under serum-deprived stress conditions (Timsah et al., 2016b).

Tumour hypoxia is associated with a poor patient prognosis and resistance to radio- and chemo-therapy (Harris, 2002). Pathways that are regulated by hypoxia include angiogenesis, glycolysis, GF-signalling, immortalisation, genetic instability, tissue invasion and metastasis, apoptosis and pH regulation (Harris, 2002). A key regulator of hypoxic response is the upregulation of hypoxia inducible factor-1 (HIF-1). When activated, HIF-1 activates the transcription of a series of genes including VEGF, erythropoietin and anaerobic glycolysis (Izuishi et al., 2000). *In situ* hybridisation studies have shown that VEGF mRNA is up-regulated in human tumours in response to hypoxia (Ferrara, N. and Davis-Smyth, 1997). VEGFR2 expression is also upregulated during hypoxia, but how expression is regulated remains to be clarified (Olsson et al., 2006). Cellular proliferation, migration and angiogenesis are linked by signalling pathways that operate physiologically to preserve oxygen and nutrient homeostasis (Pugh and Ratcliffe, 2003). Thus, tumour growth under these stress conditions can induce the activation of signalling pathways involved in angiogenesis, migration and proliferation signalling, which can contribute towards cancer progression and chemoresistance. The role of VEGFR2 expression in tumour cells under tumour microenvironmental stress appears relatively unknown.

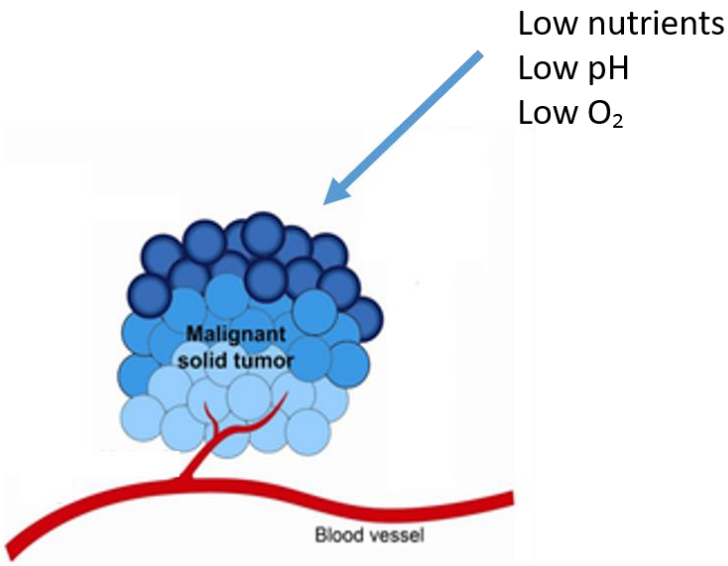

Figure 4.1.5 The tumour microenvironment of solid tumours.

Cancer cells within a tumour mass are at different gradients of nutrient and oxygen deprivation depending on the distance from the vasculature. The cells furthest away from the vasculature have a severe lack of GFs, nutrients and are under hypoxia. Nutrient and oxygen deprivation is a universal phenomenon in solid tumours, due to the increasing growth of the tumour mass and the poor tumour vasculature. Under these stress conditions tumour cells adapt by triggering the activation of cell signalling pathways, allowing tumour cells to survive, proliferate and metastasise from the tissue. Picture adapted from (Graham and Unger, 2018).

4.1.6 Plcg1

Phosphoinositide-specific phospholipase C γ-1 (Plcg1) is part of the phospholipase C (PLC) family of proteins and plays an important role as a downstream effector protein in transmembrane signalling (Singer et al., 1997). The multi-domains of Plcg1 cooperate to integrate multiple signals in response to extracellular stimuli. Plcg1 is activated by both binding to and being phosphorylated by TKs and RTKs. Plcg1 plays a critical role in growth, survival, motility, and proliferation pathways in cells (Wells and Grandis, 2003; Yamaguchi and Condeelis, 2007; Emmanouilidi et al., 2017). Therefore, the regulation of Plcg1 activity is of crucial importance to maintain cellular homeostasis.

4.1.6.1 Plcg1 structure

Plcg1 is a 145 kDa effector protein with various different binding-domains (Wang et al., 1998) (**Figure 4.1.6**). The catalytic domain is composed of two regions (X and Y boxes) which are separated by an extended linker region (X-Y linker). Plcg1 is unique among phospholipases in that the X-Y linker comprises of a series of discrete binding domains (two SH2 domains and an SH3 domain, in-between a split pleckstrin homology (PH) domain) (Timsah et al., 2014). The N-terminal SH2 domain (N-SH2) is responsible for complex formation with activated RTKs. The C2 and PH domains cooperate with the SH2 domain to translocate Plcg1 to the plasma membrane (Lemmon and Schlessinger, 2010).

Figure 4.1.6 Plcg1 domain structure.

The multiple domains of Plcg1 which co-operate to integrate various different signals at the plasma membrane. RTK-mediated phosphorylation of Plcg1 at Y775 and Y783 (red arrows), leads to the binding of the C-terminal SH2 domain to Y783. This change in protein conformation stimulates the enzymatic activity of Plcg1. The C2 and PH domains cooperate with the SH2 domain to facilitate the translocation of Plcg1 to the membrane. The N-terminal PH domain facilitates binding to the membrane by binding to PIP_3. Adapted from (Lemmon and Schlessinger, 2010; Fearon and Grose, 2014) using BioRender.com.

4.1.6.2 Plcg1 downstream signalling

RTK-mediated Y phosphorylation of Plcg1 leads to the intramolecular binding of the C-terminal SH2 domain to pY783. This releases Plcg1 autoinhibition and changes the conformation, which stimulates the enzymatic activity of Plcg1 (Lemmon and Schlessinger, 2010; Gresset et al., 2010). The relocation of Plcg1 to the cell membrane is facilitated by the N-terminal PH domain binding to PIP_3 at the plasma membrane. Plcg1 activation leads to the

hydrolysis of PIP_2 to generate the secondary messengers IP_3 and DAG. These secondary messengers are known to stimulate the release of intracellular Ca^{2+} and activate PKC respectively (Nishizuka, 1992; Wahl and Carpenter, 1991). IP_3 diffuses into the cytosol and initiates Ca^{2+} release from the endoplasmic reticulum. DAG remains in the membrane and goes on to activate PKC. Both the increase in intracellular Ca^{2+} release and activation of PKC induces the activation of many signalling pathways and particular cellular outcomes. Downstream signalling of Plcg1 activation includes cell survival, actin remodelling, migration and chemotaxis, proliferation, differentiation and apoptosis (Rebecchi and Pentyala, 2000; Rhee, 2001; Kölsch et al., 2008; Hao et al., 2009; Emmanouilidi et al., 2017). Cancer progression and metastasis can therefore occur under the aberrant activation of Plcg1 (Sala et al., 2008).

As discussed in part **1.3,** Plcg1 can also undergo non-canonical activation via the aberrant activation of a Tier 2 mechanism, binding via its SH3 domain to FGFR2 C-terminal proline-rich motif, under serum-deprived conditions. Plcg1 activation occurred via a change in Plcg1 conformation, exposing the Y783 residue and thus, was able to activate downstream oncogenic signalling pathways. Plcg1 expression levels were found to correlate with Akt phosphorylation and a lower patient survival in ovarian cancer patients (Timsah et al., 2016). The expression levels of Plcg1, FGFR2 and Grb2 were also prognostic factors in lung adenocarcinoma patient outcome (Timsah et al., 2015).

4.1.6.3 Plcg1 expression in BC

Plcg1 is highly expressed in various tumours, including BCs, and has been found to be involved in tumour progression and metastasis (Eccles, 2005; Emmanouilidi et al., 2017; Wells and Grandis, 2003). A high expression of activated Plcg1 has been found to be associated with worse clinical outcome in terms of incidence of distant metastases. The analysis of BC patient samples showed an increase in Plcg1 expression in tumour metastases compared with the primary tumour in 50% of tissues analysed. The down-regulation of Plcg1 expression in BC cell lines impaired the activation of small GTP-binding protein Rac and cell invasion *in vitro* and inhibited lung

metastasis formation in nude mice (Sala et al., 2008). Plcg1 overexpression was also found to be a strong predictive marker in the development of metastases in early luminal-A and –B BC patients (Lattanzio et al., 2019). The expression levels of PLC enzymes in BC was found to positively correlate with patient grade and tumour differentiation. Moderately and poorly differentiated breast tumours (grade 2 and 3) had a significantly higher levels of Plcg1 expression compared with well differentiated breast tumours (Cai et al., 2017). Taken together, these findings suggest that Plcg1 plays a role in metastatic progression of early stage BC and that Plcg1 could be a potential biomarker for BC metastatic progression.

4.1.7 Nck

The Nck family consists of Nck1/α and Nck2/β and referred to as Nck. Both Nck protein isoforms share an overall 68% amino acid identity (Chen et al., 2004) and are widely believed to have overlapping functions (Bladt et al., 2003). Most of the literature does not define Nck1 or Nck2 in their findings but use the term Nck to define both proteins. Nck acts as a downstream effector protein involved in the transduction of signals from a number of activated RTKs and TKs to downstream proline-rich effector molecules which regulate cytoskeletal movement (Castello et al., 2013; Aryal et al., 2015). Thereby, Nck regulates activation-dependent processes during cell polarisation and migration (Lettau et al., 2009). Nck activation is also involved in T-cell receptor activation, invadopodia formation and cell adhesion and motility (Chaki and Rivera, 2013).

4.1.7.1 Nck structure

Nck adaptor proteins are 47kDa and consist of three N-terminal SH3 domains followed by a single C-terminal SH2 domain (**Figure 4.1.7**). The SH2 domain binds to a number of activated RTKs and Y phosphorylated docking proteins. On the other hand, the Nck SH3 domains engage in binding to proline-rich binding sites on a host of effector proteins implicated in cytoskeletal regulation (Li et al., 2001; Park et al., 2006).

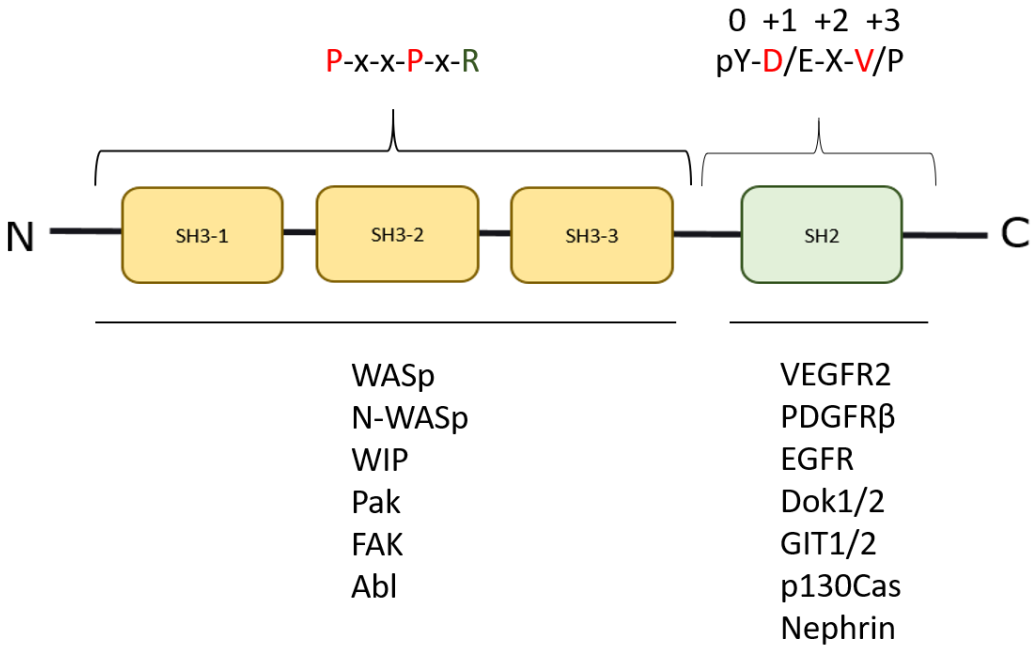

Figure 4.1.7 Nck structure and specific binding partners.

Schematic of Nck domain structure consisting of three N-terminal SH3 domains and one C-terminal SH2 domain. The known SH3 and SH2 domain-specific binding partners are labelled with the particular consensus sequences found within the proteins which bind to Nck. Adapted from (Chaki and Rivera, 2013).

4.1.7.2 Nck downstream signalling

Nck links ligand-activated RTKs and integrin's with the cytoskeleton. Once activated, Nck regulates planar cell polarity and directional migration. Nck stimulates actin related protein (Arp) 2/3 dependent polymerisation through the activation of Wiskott-Aldrich Syndrome protein (WASp) and WASp-family verprolin-homologous protein (WAVE) proteins at the leading edge/lamellipodium (Eden et al., 2002; Ditlev et al., 2012; Donnelly et al., 2013). Nck contributes to directional migration through the spatiotemporal regulation of Rho GTPases (e.g. Cdc42) and stabilisation of newly formed protrusions at the leading edge by strengthening cell-matrix adhesions (Chaki et al., 2013). Nck may play an indirect role in the differential distribution/activation of polarity complexes at the leading edge through

modulation of Rho GTPases. Nck may also contribute to cell polarity through the modulation of vesicular/membrane trafficking (Chaki and Rivera, 2013).

4.1.7.3 Nck expression in BC

Nck expression was found to be required for the growth and progression to metastatic disease of primary BC tumours. The expression of Nck promoted lung metastases in a BC xenograft model and extravasation following injection in the tail vein. Nck was also found to direct the polarisation of cell-matrix interactions for efficient BC cell migration in a 3D matrix. The expression of Nck advanced BC cell invasion by regulating actin dynamics at invadopodia and enhanced focalised extracellular matrix proteolysis by the accumulation of matrix metalloproteinase-14 (MMP-14) at the cell surface, through the Nck activation of Cdc42 and transforming protein RhoA (Morris et al., 2017). Nck1 has also been found to co-localise with cortactin in matrix-degrading invadopodia in a metastatic BC cell line, MDA-MB-231 (Oser et al., 2011). The overexpression of Nck was also evident in breast carcinoma patient tissue samples compared to normal tissue (Chaki et al., 2019). Overall, Nck1 expression and activation appears to play a role in BC metastasis and invasion. Therefore, Nck1 could be a potential biomarker for BC patients who may progress to metastatic disease.

4.1.8 Project rationale

Under serum-deprived conditions, our laboratory has shown that a secondary tier of signalling can occur between SH3 domains of intracellular signalling proteins and proline-rich motifs of RTKs, depending on the proteome of the cell. This mechanism has been hypothesised to be incorporated in maintaining cellular homeostasis when under periods of cell stress. When this signalling is perturbed it can lead to pathological outcomes. Aberrant Tier 2 signalling involving the non-canonical activation of Plcg1 through the RTK FGFR2, under serum-deprived conditions, has been shown to contribute to poorer outcomes in ovarian cancer, but it has not been widely explored for other RTKs or other types of cancers (Timsah et al., 2016b).

Cancer cells within the middle of a tumour mass have no access to ligand stimulation and have limited access to nutrients, a low pH and low O_2 levels due to insufficient tumour vascularisation (Harris, 2002). Nutrient and serum-

deprivation has been found to contribute to a more malignant and aggressive tumour phenotype with a poorer patient prognosis and resistance to therapeutics (Yakisich et al., 2017). Nutrient and O_2 deprived cancer cells are known to express VEGFR2 RTK, which has been hypothesised to induce angiogenesis under these stress conditions (Olsson et al., 2006; Guo, S. et al., 2010). VEGFR2 overexpression has been found in many types of cancer, including the breast (Guo, S. et al., 2010) but the role of VEGFR2 expression in cancer cell signalling has not been fully elucidated.

Here, some of the response to growth under tumour microenvironmental stress (such as within the middle of a tumour mass) could be through the activation of a non-canonical Tier 2 signalling mechanism via VEGFR2 to aid in maintaining viability and towards cancer progression. Under stress conditions simulating that of the microenvironment of a solid tumour mass, the relative protein concentrations of VEGFR2 and the SH3 domain-containing proteins Plcg1, Src and Nck1, which are known to bind to VEGFR2 canonically, may change in response to BC growth under stress. This change in relative protein concentration could allow the binding of these proteins to occur without the need for VEGFR2 activation, through a Tier 2 mechanism. If the non-canonical activation of the SH3 domain-containing proteins occurs via a non-canonical PPI via VEGFR2 proline-rich motif, under microenvironment-induced stress conditions, aberrant oncogenic signalling mechanisms may be upregulated in adaptation to growth under these conditions. Thus, these mechanisms may contribute towards BC progression and anti-VEGFR2 resistance. This area of research may open new avenues to how breast cancer cells can survive and progress under tumour microenvironmental stress conditions and when under anti-angiogenic therapy. This understanding therefore, may lead to the identification of specific patient prognostic factors and towards selective patient treatment. A summary of this hypothesis is visualised in **Figure 4.1.8**.

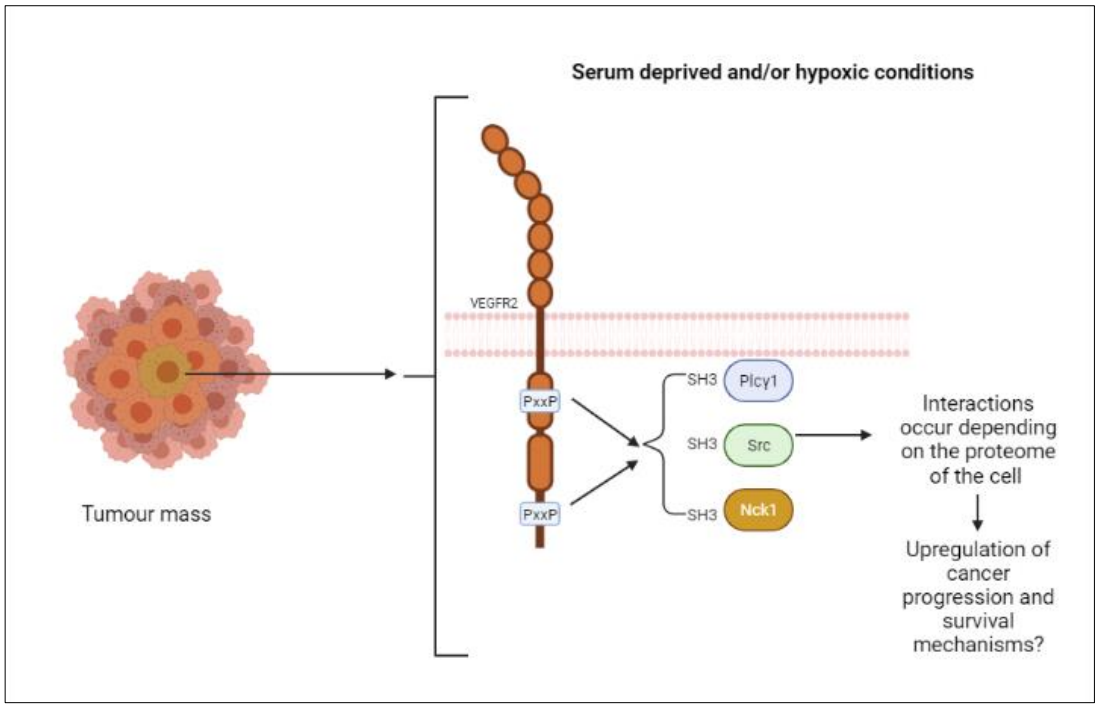

Figure 4.1.8 VEGFR2 aberrant Tier 2 signalling hypothesis, in BC cells under solid tumour microenvironmental stress conditions.

Within a solid tumour mass, BC cells are under serum deprived and/or hypoxic conditions. The relative concentrations of VEGFR2 and the three SH3 domain-containing proteins, which are known to bind to VEGFR2, may change in response to growth under these microenvironmental stress conditions. This change in relative protein concentration could allow the binding of these proteins to occur without the need for VEGFR2 activation through an aberrant Tier 2 mechanism. If the non-canoncal activation of these proteins occurs through this mechanism, aberrant oncogenic signalling may be upregulated in adaptation to growth under microenvironmental stress conditions and contribute towards cancer progression and anti-RTK (anti-VEGFR2) drug-resistance. Made using BioRender.com.

4.1.9 Experimental objectives

In this chapter the following objectives were investigated:

1) To determine whether there are changes in cellular morphology and therefore, in the proteome of breast cancer cells in response to growth under conditions simulating the tumour microenvironment of cancer cells within the middle of a tumour mass (serum (GF)-deprived and under hypoxia). This will be evaluated using phase contrast microscopy of the breast cancer cells under the different tumour microenvironmental conditions and changes to protein expression observed through immunoblotting.

2) To identify whether the three SH3 domain-containing proteins, which are known to bind to ligand-activated VEGFR2, also bind to basal VEGFR2 under GF-deprived conditions, in breast cancer cells. This will be determined via immunoprecipitation experiments between endogenous VEGFR2 and endogenous SH3-domain containing proteins in breast cancer cells and analysed using immunoblotting.

3) To generate yellow fluorescent protein (YFP) tagged VEGFR2 mutant protein constructs for the use of pull-down experiments. Here, the use of site-directed mutagenesis will be used to mutate key domain residues within the proline-rich motifs on the C-terminal tail of VEGFR2. To determine whether the correct mutation were incorporated, the plasmids will be validated through sequencing.

4) To generate cerulean fluorescent protein (CFP) tagged domain protein constructs of the SH3 domain-containing proteins for use in FRET. Here, each binding domain (SH2, SH3 etc.) will be cloned into a CFP vector and the correct sequence of residues validated through sequencing of the plasmids and the correct open reading frame (ORF) observed through successful transfection.

5) To establish whether binding of the SH3 domain-containing proteins to VEGFR2, observed under serum-deprived conditions in breast cancer cells, is via a non-canonical interaction via the SH3 domains of the SH3 domain-containing proteins to a proline-rich motif within VEGFR2 C-

terminal tail. This will be analysed by overexpressing mutant VEGFR2-YFP protein constructs in breast cancer cells and conducting immunoprecipitation and pull-down experiments. Protein-protein interactions will be examined via immunoblotting. Förster resonance energy transfer (FRET) will be performed in intact breast cancer cells grown under serum-deprived conditions, using CFP-tagged domain constructs and the VEGFR2-YFP mutant constructs to further validate protein-protein interactions found through immunoprecipitation experiments. This will also confirm that the interactions are occurring through the SH3 domain of the SH3-domain containing proteins to a particular proline-rich motif within VEGFR2 C-terminal tail.

4.2 Results

4.2.1 The effect of microenvironmental stress on BC cell morphology

The two epithelial BC cell lines SkBr3 and MCF7 were utilised in all the following experiments. Both cell lines express VEGFR2 RTK endogenously, with SkBr3 having a higher endogenous expression compared to MCF7 cells. The cell lines were both derived from the metastatic site of a female caucasian BC patient but have different expression profiles (**Table 4.2.1**) and cellular morphologies. SkBr3 cells display a rounded epithelial morphology and grow to have a heterogeneous morphology, with both small rounded and larger 'cobble-stone' appearance cells when grown in the presence of serum. MCF7 cells on the other hand grow in clusters and have a polygonal morphology. Under growth, the clusters join each other to form an even layer of cells.

Table 4.2.1 BC cell line receptor status and subtype.

The ER, PR and HER2 expression status defines the BC subtype. Adapted from (Dai et al., 2017).

Cell line	ER	PR	HER2	Subtype	Tumour type
SkBr3	-	-	+	HER2 positive	Invasive Ductal Carcinoma
MCF7	+	+	-	Luminal A	Adenocarcinoma

The morphology of both BC cell lines was investigated under microenvironmental stress of both serum-deprivation (0% FBS) and hypoxia (1% O_2, 5% CO_2) for 24 hours (**Figure 4.2.1**), using phase contrast images obtained using an EVOS microscope (LifeTech) FL system at X20 magnification. In response to growth under serum-deprivation and under normoxic conditions (18% O_2, 5% CO_2), SkBr3 cells displayed an elongated and enlarged cellular morphology, with some rounded cells (**Figure 4.2.1a**). When grown under hypoxia and in the presence of serum (10% FBS), the SkBr3 cells appeared to have an enlarged nuclei and an elongated, irregular shape. In response to growth under both serum-deprived and hypoxic

conditions, the SkBr3 cells displayed prominent protrusions and filopodia, which is typical of a more fibroblastic phenotype.

The MCF7 cell line showed a stark difference in cellular morphology in response to serum-deprivation (**Figure 4.2.1b**). When grown under serum-deprived conditions and under normoxia, the MCF7 cells appeared smaller but elongated with prominent cellular protrusions. In response to growth under hypoxia and under the presence of serum, the MCF7 cells did not appear to look much different to the cells grown under normoxic conditions in the presence of serum, except for a slightly larger cell nuclei. The MCF7 cells grown under serum-deprived and hypoxic conditions displayed a fibroblastic phenotype with protrusions and filopodia extending from the cells.

In summary, SkBr3 cells appear to respond morphologically to growth under serum-deprivation and hypoxia and MCF7 cells appear to respond morphologically to growth under serum-deprivation.

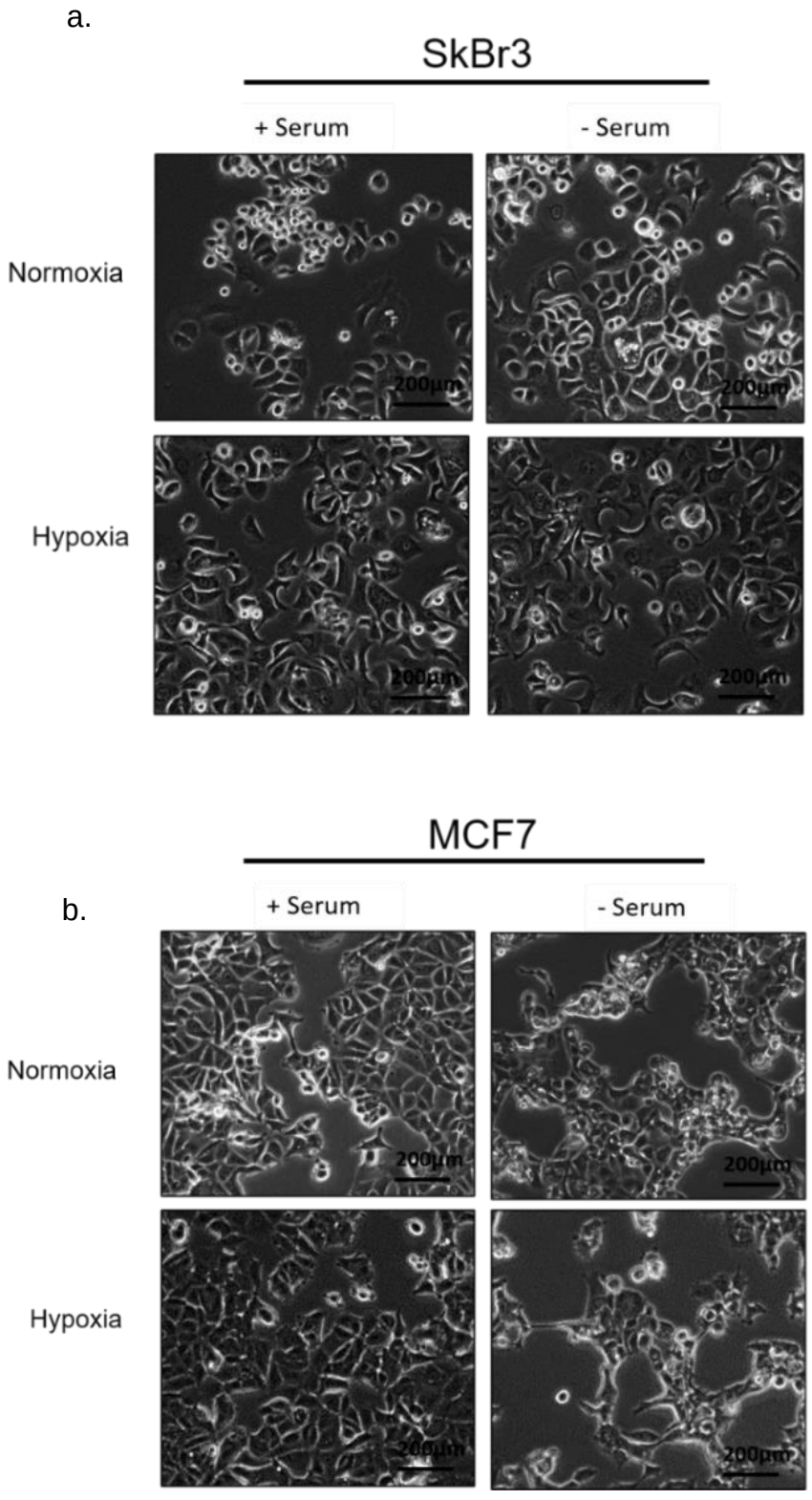

Figure 4.2.1 The cellular morphology of SkBr3 and MCF7 BC cells grown under microenvironmental stress conditions.

a. SkBr3 cells and **b.** MCF7 cells were grown under normoxic (18% O_2,

5% $CO_{2,}$), hypoxic (1% $O_{2,}$ 5% CO_2), serum-supplemented (+, 10% FBS) and serum-deprived (-, 0% FBS) conditions at 37°C for 24 hours. Representative images were taken under an EVOS microscope at X20 magnification.

4.2.2 The effect of microenvironmental stress on protein expression levels in BC cells

The BC cell lines showed a stark difference in their cellular morphology in response to serum-deprivation and hypoxic stress. VEGFR2 expression is upregulated in response to tumour growth under conditions when cancer cells are deprived of the vasculature (Olsson et al., 2006). It is therefore of interest to determine whether these microenvironmental stress conditions have an effect on the relative protein expression and phosphorylation levels of VEGFR2. The Ladbury laboratory have previously shown that PPIs between SH3 domains of intracellular signalling proteins and proline-rich motifs within the C-terminal tail of RTKs is important to maintain homeostasis within the cell, in periods where there is no external stimulation. Growth under stress conditions can have a major impact on the relative expression levels of proteins. Interactions between proline-rich sequences on RTKs and the SH3 domains from effector proteins are dictated by the respective concentrations of the interactants. Under stress conditions, normal signalling which is associated with maintaining cell homeostasis and with 'house-keeping' functions can be out-competed by other interactions involving proteins that are expressed at elevated levels. The signalling outcome of these interactions can give rise to an aberrant oncogenic outcome (Timsah et al., 2016b). Thus, the relative protein expression levels of the three SH3 domain-containing proteins which are known to bind to VEGFR2 were also investigated, to see if the relative protein expression levels change in response to growth under microenvironmental stress conditions, simulating the environment of a solid tumour mass.

The effect of serum-deprivation (0% FBS) and/or hypoxia (1% O_2, 5% CO_2) on total protein expression and phosphorylation levels of VEGFR2 was determined via immunoblotting in SkBr3 cells (**Figure 4.2.2a**) and MCF7 cells (**Figure 4.2.2b**) and compared to growth in the presence of serum (10% FBS) and under normoxia (18% O_2, 5% CO_2). The cells were grown under these conditions for 24 hours. SkBr3 cells endogenously express a higher total protein level of VEGFR2 compared to that of MCF7 cells. The total protein of the three SH3 domain-containing proteins Plcg1, Src and Nck1, was also determined when grown under each condition. Densitometry was performed

to determine the relative protein levels in each cell line under the different growth conditions, via normalisation to the β-actin loading control (**Figure 4.2.2c-l**).

Immunoblotting of the SkBr3 cells showed that total VEGFR2 protein levels were vastly increased in response to growth under hypoxic conditions (**Figure 4.2.2c.**). An increase in VEGFR2 levels was also observed in SkBr3 cells in response to growth under serum-deprived conditions. In MCF7 cells, the relative total VEGFR2 protein levels were increased in response to growth under serum-deprived conditions (**Figure 4.2.2d**). The levels of VEGFR2 phosphorylation at Y1175 in SkBr3 cells and in MCF7 cells showed a general trend of receptor phosphorylation observed in response to growth in the presence serum (**Figure 4.2.2e** and **Figure 4.2.2f** respectively). In response to growth under serum-deprived conditions, the VEGFR2 receptor Y1175 phosphorylation levels in both BC cell lines was drastically reduced.

Relative total Plcg1 levels went down slightly in SkBr3 cells in response to growth under microenvironmental stress, from either serum-deprivation or hypoxia (**Figure 4.2.2g**). In MCF7 cells, the Plcg1 total protein levels remained the same, if not at slightly increased levels in response to growth under serum-deprivation or hypoxia stress (**Figure 4.2.2h**). SkBr3 cells showed that they express a similar total expression level of Src under any growth condition, except in response to growth under serum-deprived stress and under normoxia, where the total levels of Src were observed to increase (**Figure 4.2.2i**). MCF7 cells showed an increase in relative total Src levels in response to growth under hypoxic conditions (**Figure 4.2.2j**). Relative levels of Nck1 showed a slight increase in total protein expression levels in SkBr3 cells in response to growth under hypoxia and in the presence of serum. Total Nck1 levels were seen to be lower in SkBr3 cells in response to growth under serum-deprivation (**Figure 4.2.2k**). MCF7 cells showed that Nck1 total protein levels had a similar trend to that of total Src expression levels, in that the total Nck1 levels went up in response to growth under hypoxia (**Figure 4.2.2l**). A significant difference between protein expression and phosphorylation levels was shown via * = $P<0.05$, ** = $P<0.01$, *** = $P<0.001$, **** = $P<0.0001$ between the two indicated values. Phosphorylation levels were normalised to the total protein and the β-actin loading control.

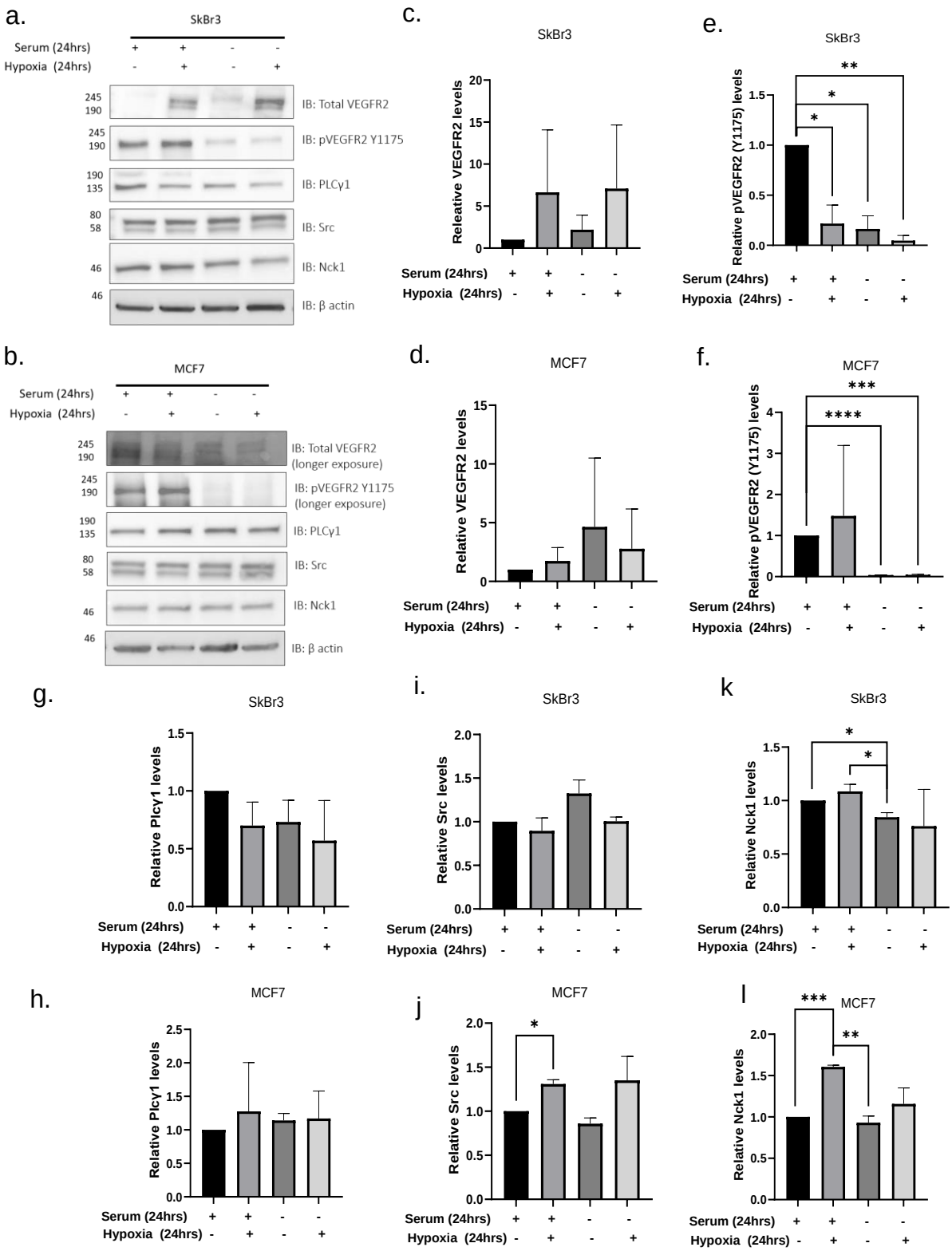
a.
SkBr3
Serum (24hrs) + + - -
Hypoxia (24hrs) - + - +
245
190
IB: Total VEGFR2
245
190
IB: pVEGFR2 Y1175
190
135
IB: PLCγ1
80
58
IB: Src
46
IB: Nck1
46
IB: β actin
b.
MCF7
Serum (24hrs) + + - -
Hypoxia (24hrs) - + - +
245
190
IB: Total VEGFR2
(longer exposure)
245
190
IB: pVEGFR2 Y1175
(longer exposure)
190
135
IB: PLCγ1
80
58
IB: Src
46
IB: Nck1
46
IB: β actin
c.
SkBr3
Releative VEGFR2 levels
Serum (24hrs) + + - -
Hypoxia (24hrs) - + - +
d.
MCF7
Relative VEGFR2 levels
Serum (24hrs) + + - -
Hypoxia (24hrs) - + - +
e.
SkBr3
Relative pVEGFR2 (Y1175) levels
Serum (24hrs) + + - -
Hypoxia (24hrs) - + - +
f.
MCF7
Relative pVEGFR2 (Y1175) levels
Serum (24hrs) + + - -
Hypoxia (24hrs) - + - +
g.
SkBr3
Relative Plcγ1 levels
Serum (24hrs) + + - -
Hypoxia (24hrs) - + - +
h.
MCF7
Relative Plcγ1 levels
Serum (24hrs) + + - -
Hypoxia (24hrs) - + - +
i.
SkBr3
Relative Src levels
Serum (24hrs) + + - -
Hypoxia (24hrs) - + - +
j
MCF7
Relative Src levels
Serum (24hrs) + + - -
Hypoxia (24hrs) - + - +
k
SkBr3
Relative Nck1 levels
Serum (24hrs) + + - -
Hypoxia (24hrs) - + - +
l
MCF7
Relative Nck1 levels
Serum (24hrs) + + - -
Hypoxia (24hrs) - + - +

Figure 4.2.2 Relative protein expression and phosphorylation levels of SkBr3 and MCF7 cells grown under microenvironmental stress conditions.

a. A representative immunoblot of SkBr3 cells and **b**. MCF7 cells grown under different microenvironmental stress conditions of serum-supplementation (5% FBS), serum starvation (0% FBS), normoxic (18% O_2, 5% CO_2) and hypoxic conditions (1% O_2, 5% CO_2) for 24 hours, to determine total protein and phosphorylation levels. Graphs **c**.-**l.** show the normalised densitometry levels of proteins. Phosphorylated protein was normalised to the total protein levels and all compared to the β-actin loading control. All levels were calculated as a fold increase/decrease to cells grown with serum and under normoxic conditions, (n=3).

4.2.3 Changes in the proteome of BC cells is VEGF independent when grown under serum-deprived conditions

Due to the known effects of microenvironmental stress on the induction of VEGF expression and autocrine secretion in BC cells (Rydén et al., 2003; Zhao, D. et al., 2015), the presence of VEGF-A was investigated in SkBr3 and MCF7 cell growth media. The corresponding media after growth under each microenvironmental stress condition in **Figure 4.2.2** was ran on an SDS gel and immunoblotted for the presence of secreted autocrine VEGF-A (22 kDa) (**Figure 4.2.3**). Here, an anti-VEGF monoclonal IgG against VEGF-A was utilised. VEGF-A was found in serum-supplemented media of the growing BC cells, which was expected as FBS contains many different GFs. Under serum-deprived conditions, VEGF-A was not found and thus, not secreted by the BC cells. This confirms that the changes to the proteome observed in **Figure 4.2.2** is VEGF-A independent and that VEGFR2 is not ligand-activated via VEGF-A under serum-deprived conditions.

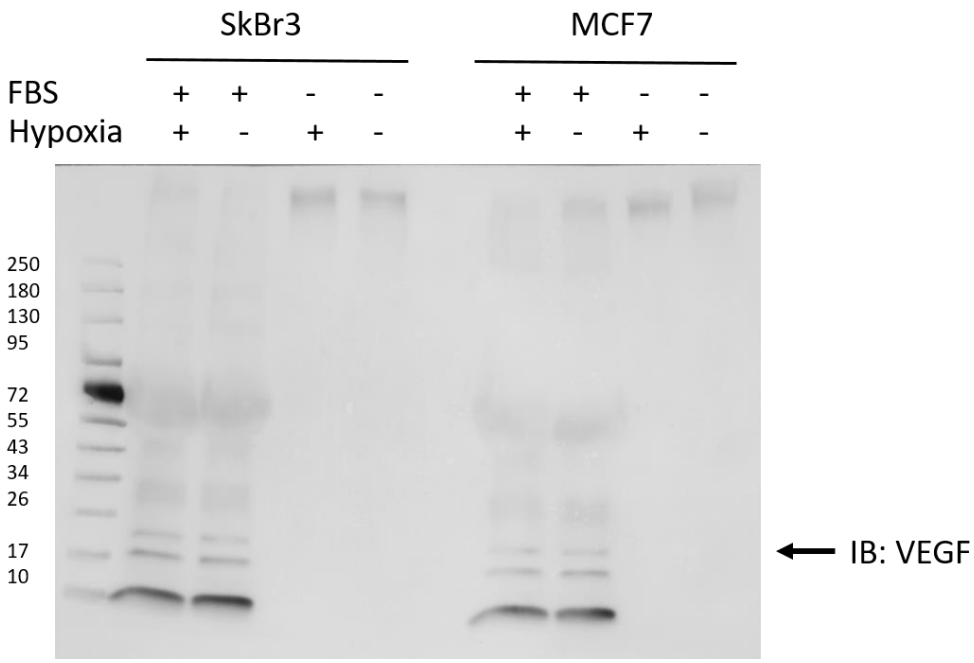

Figure 4.2.3 The presence of VEGF-A in the growth media of BC cells grown under conditions simulating micro-environmental stress.

Representative immunoblot of the corresponding growth media after the growth of SkBr3 and MCF7 BC cells grown under serum-supplemented (10% FBS), serum-starved (0% FBS), normoxic (18% O_2, 5% CO_2) and hypoxic (1% O_2, 5% CO_2) conditions for 24 hours and probed for the presence of secreted VEGF-A, (n=3).

4.2.4 The effect of microenvironmental stress on SkBr3 downstream kinase signalling

After concluding that the cellular morphology and protein expression levels of BC cells is drastically changed in response to growth under microenvironmental stress conditions, the SkBr3 BC cell line was further investigated to see whether growth under serum-deprived and/or hypoxia had an effect on downstream kinase signalling. SkBr3 cells were grown under the different stress conditions of serum-supplementation (10% FBS), serum-deprivation (0% FBS), normoxia (18% O_2, 5% CO_2) and hypoxia (1% O_2, 5% CO_2) for 24 hours and corresponding cell lysates obtained. A human phospho-kinase array kit (R&D systems) was utilised to determine the relative phosphorylation levels of 37 human protein kinases and 2 related total proteins used as a loading control. SkBr3 cell lysate of the same protein concentration (600µg) from growth under each stress condition was determined by BCA assay, and was incubated with the membranes. The relative phosphorylated protein levels were detected using biotinylated antibodies that recognises the phosphorylated sites of bound kinases within the particular cell lysate and was visualised using chemiluminescent reagents. The intensity of the dot produced on the blot was proportional to the phosphorylation levels of the bound analyte from the particular cell lysate sample.

Dot blots were obtained from SkBr3 cell lysates grown under the four different microenvironmental stress conditions (**Figure 4.2.4a)** and compared to growth under serum-supplemented and normoxic conditions. The relative phosphorylated protein levels were analysed via densitometry and normalised to the total protein loading-control on each nitrocellulose membrane (**Figure 4.2.4b)**.

The phosphorylation levels of several protein kinases went up in response to growth under microenvironmental stress conditions in BC cells. Comparing the levels of phosphorylation in response to growth under serum-deprived conditions only (and under normoxia), the major changes in phosphorylation levels include that of STAT3 and heat shock protein 60 (HSP60) which showed lower levels of phosphorylation in response to growth under serum-

deprivation (and under normoxia) compared to growth with the presence of serum (and under normoxia). Upregulated phosphorylation of kinases in response to growth under serum-deprived conditions (and under normoxia) include Checkpoint kinase-2 (Chk-2), cAMP-response element binding protein (CREB), 70kDa ribosomal protein S6 kinase (p70 S6 kinase), p53, proline-rich tyrosine kinase-2 (PYK2) and c-Jun compared to the response to growth under the presence of serum (and under normoxia). Many kinases were phosphorylated in response to growth under hypoxia and in the presence of serum and thus, the hyperactivation of intracellular kinases may be via receptor activation from GFs present in the serum. This is consistent with cellular adaptation of activating cell signalling survival pathways in response to growth under hypoxic stress (Harris, 2002). BC cells in response to growth under both serum-deprived conditions and under hypoxia, they lose the activation of many kinases. This could be due to the cell needing to 'switch off' non-important signalling pathways to preserve cellular energy, to maintain cell survival under serum-deprivation and hypoxic stress. Interestingly, the BC cells grown under these conditions mimicking the tumour microenvironment of cancer cells within the middle of a solid tumour mass, maintains a high level of phosphorylation of FAK, proline-rich Akt substrate of 40kDa (PRAS40) and CREB compared to kinase phosphorylation levels in response to growth under normoxia and serum-supplemented conditions. The elevated levels of FAK phosphorylation in particular are increased by around 80% compared to the levels in BC cells grown under normoxia and with serum. FAK activation is implicated in Src signalling pathways, in particular within promoting cell motility, migration and invasion (Mayer, E.L. and Krop, 2010; Finn, 2008; Summy and Gallick, 2003). In response to growth under hypoxia, and both in the presence or deprivation of serum the levels of phosphorylation of target of rapamycin (Tor or mTOR) is shown to be depleted in SkBr3 cells.

a.

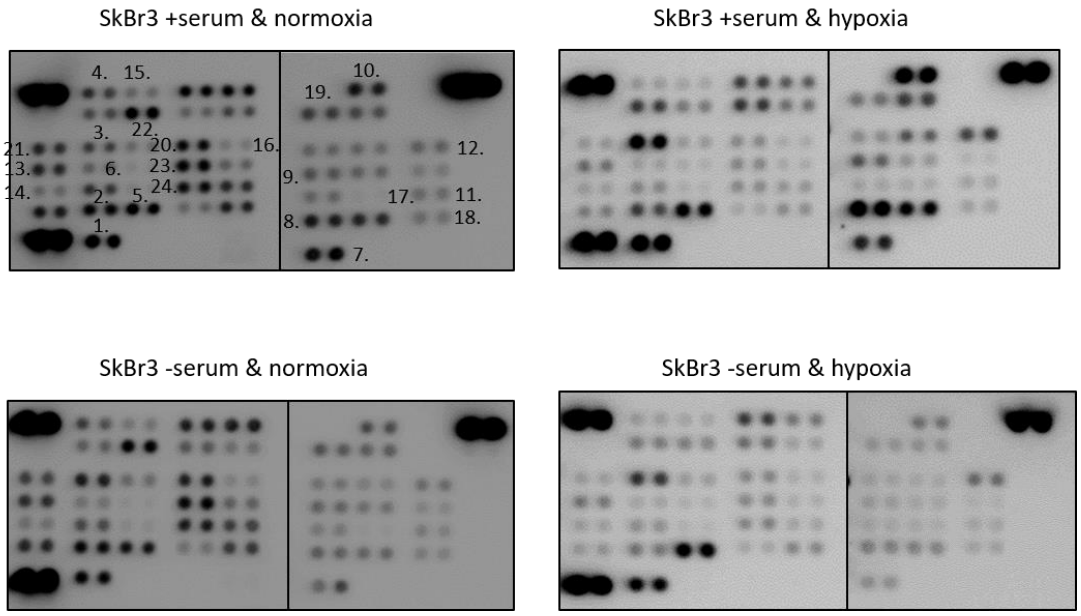

b.

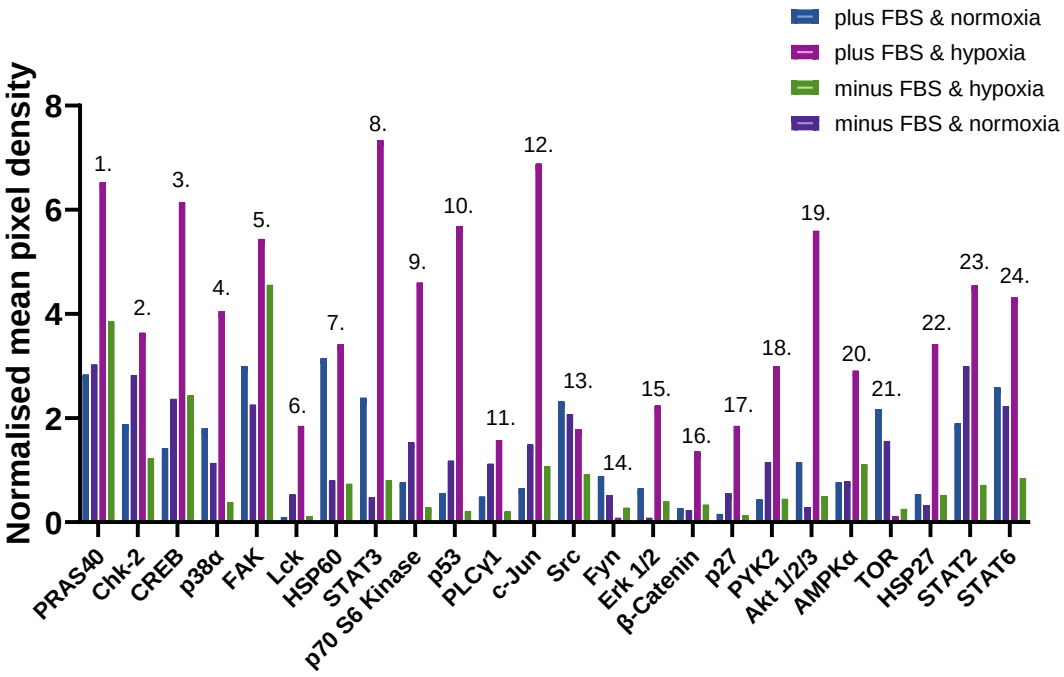

Figure 4.2.4 Changes in kinase phosphorylation levels in SkBr3 BC cells in response to growth under microenvironmental stress conditions.

a. Human phospho-kinase array of SkBr3 cell lysates grown under different stress conditions of serum-supplemented (+, 10% FBS), serum-deprived (-, 0% FBS), normoxic (18% O_2, 5% CO_2) and hypoxic (0%

O_2, 5% CO_2) conditions for 24 hours. The intensity of the dots is directly proportional to the kinase phosphorylation levels within the cell lysate **b.** Normalised levels of kinase phosphorylation via densitometry were compared to the total protein loading-control. The numbers to each peak correspond with the particular paired dots on each blot.

4.2.5 SH3 domain-containing proteins bind to VEGFR2 in BC cells, under serum-deprived conditions

Our laboratory has shown that non-canonical Tier 2 signalling occurs in cells under serum-deprived conditions, when RTKs are non-stimulated. Under microenvironmental stress conditions, the proteome of tumour cells can significantly change and therefore, homeostatic Tier 2 signalling could be out-competed by other interactions of proteins with elevated levels of protein expression (Timsah et al., 2016b). In both BC cell lines, VEGFR2 expression levels were found to be elevated in response to growth under nutrient and serum-deprived stress, therefore the following experiments were carried out under serum-deprivation conditions and under normoxia.

To determine whether non-canonical interactions occur between the VEGFR2 receptor and the SH3 domain-containing proteins that are known to bind to VEGFR2, an endogenous Co-IP of VEGFR2 was performed in BC cells. Here, the interaction with the SH3 domain-containing proteins was determined. A VEGFR2 antibody was bound to IgG binding agarose beads and added to SkBr3 and MCF7 cell lysates after growth under both serum-deprived (0% FBS) and serum-supplemented (10% FBS) conditions for 24 hours, under normoxia (18% O_2, 5% CO_2). Endogenous VEGFR2 in the BC cell lysates were pulled down with the beads using centrifugation and the bound beads denatured and the eluted bound proteins ran on an SDS gel. An immunoblot was then performed and probed for the binding of VEGFR2 and SH3 domain-containing proteins (**Figure 4.2.5**).

When the two BC cell lines were grown under serum-supplemented conditions, it was expected to see that all three SH3 domain-containing proteins (Plcg1, Src and Nck1) bind to the activated VEGFR2 receptor, as GFs are present within the FBS serum. An interaction was observed in both BC cell lines, with all three SH3 domain-containing proteins to endogenous VEGFR2, under growth in the presence of serum. Interestingly, when the BC cells were grown under serum-deprived conditions, an interaction was also observed with all three SH3 domain-containing proteins to endogenous VEGFR2, in both BC cell lines. The beads only control in both BC cell lines showed that there was only a small amount of background binding to the

beads and therefore, that the interaction bands observed are due to the binding to VEGFR2 not to the agarose beads. The PPIs observed under serum-deprived growth conditions between the SH3 domain-containing proteins and VEGFR2 suggest that this binding could be via a non-canonical PPI, whereby the SH3 domains of the intracellular signalling proteins bind to a proline-rich motif within the C-terminal tail of the receptor, under serum-deprived conditions.

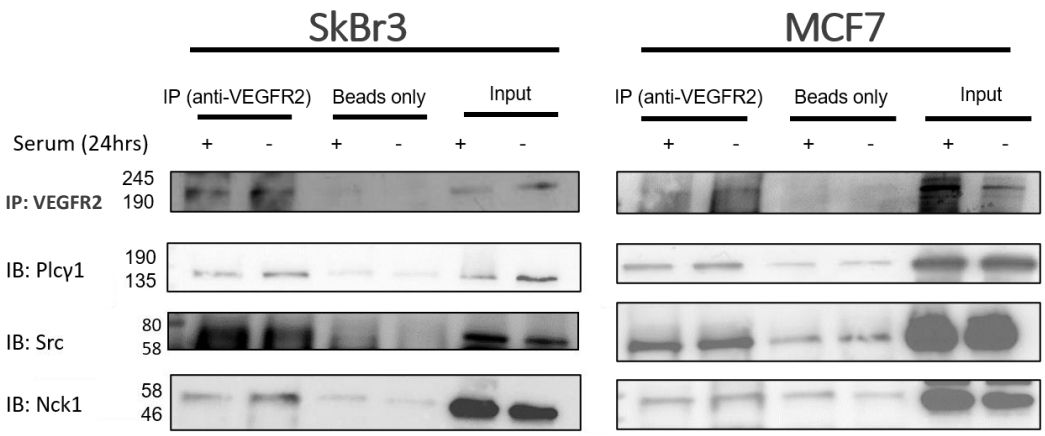

Figure 4.2.5 SH3 domain-containing proteins bind to endogenous VEGFR2 in BC cells, under serum-starved and serum-supplemented conditions.

A representative blot of endogenous VEGFR2 Co-IP performed in SkBr3 and MCF7 cell lysates when grown under serum-supplemented conditions (+, 10% FBS) and serum-deprived conditions (-, 0% FBS), for 24 hours. The interaction of SH3 domain-containing proteins, Plcg1, Src and Nck1 were probed to determine if there was a PPI with VEGFR2 under both serum-supplemented and/or serum-deprived conditions, (n=3).

4.2.6 Generation of VEGFR2-YFP mutant constructs

To determine whether the interaction occurring between the SH3 domain-containing proteins Plcg1, Src and Nck1 and VEGFR2 under serum-deprived conditions is via a non-canonical Tier 2 PPI, mutant protein constructs of VEGFR2 were made using 3 different mutations via SDM.

Specific primers containing the particular mutation were designed and implemented into a VEGFR2-YFP vector, kindly gifted and made by the Beech Laboratory, University of Leeds. This plasmid encoded a full-length wildtype VEGFR2 protein with a YFP tag. Three mutations were made to the VEGFR2-YFP construct. Firstly, a lysine (K) to methionine (M) at amino acid residue 858 to make a kinase-dead (KD) mutant, which abrogates VEGFR2 phosphorylation and thus, abrogates canonical downstream signalling to pY sites within VEGFR2 intracellular domain (**Figure 4.2.6 and Figure 4.2.7**). This particular mutation has previously been found by Takahashi *et al.* where it was shown through immunoblotting experiments that this mutation generated a kinase-inactive VEGFR2 which showed no autophosphorylation of the receptor and no signal transduction was observed through tyrosine phosphorylation of Plcg1 or MAPK after VEGF-A stimulation. It was also shown that the K868M VEGFR2 mutant could not initiate DNA synthesis in response to VEGF-A (Takahashi et al., 2001). Therefore, this mutation was chosen to generate a KD VEGFR2 mutant with no autophosphorylation within the intracellular domain, abrogating any potential binding to VEGFR2 through SH2 or PTB domains of intracellular proteins.

Secondly, a mutation was made to the first proline-rich motif within the intracellular domain of VEGFR2. The two important P residues, P908 and P911 of the PxxP motif were mutated to an alanine (A) (P908AP911A) (**Figure 4.2.6**). The final mutation was made to the second proline-rich motif within the C-terminal tail of VEGFR2. Again, both of the important P residues, P1195 and P1198, of the PxxP motif were mutated to A (P1195AP1198A) (**Figure 4.2.6 and Figure 4.2.8**).

a.

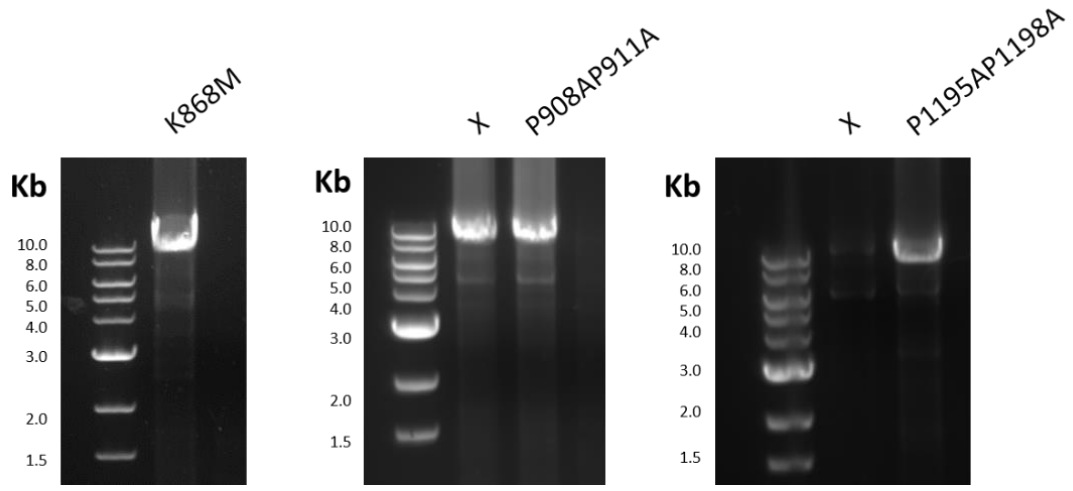

b.

```
WT_VEGFR2                ACTTGCAGGACAGTAGCAGTCAAAATGTTGAAAGAAGGAGCAACACACAGTGAGCATCGA  2640
VEGFR2_SDM_K868M_1_FOR_6 ACTTGCAGGACAGTAGCAGTCATGATGTTGAAAGAAGGAGCAACACACAGTGAGCATCGA  258
                         ********************  ************************************

WT_VEGFR2                GCTCTCATGTCTGAACTCAAGATCCTCATTCATATTGGTCACCATCTCAATGTGGTCAAC  2700
VEGFR2_SDM_K868M_1_FOR_6 GCTCTCATGTCTGAACTCAAGATCCTCATTCATATTGGTCACCATCTCAATGTGGTCAAC  318
                         ************************************************************
```

K868M

```
WT_VEGFR2                GCTCTCATGTCTGAACTCAAGATCCTCATTCATATTGGTCACCATCTCAATGTGGTCAAC 2700
VEGFR2_P908A_2_FOR_6     GCTCTCATGTCTGAACTCAAGATCCTCATTCATATTGGTCACCATCTCAATGTGGTCAAC 320
                         ************************************************************

WT_VEGFR2                CTTCTAGGTGCCTGTACCAAGCCAGGAGGGCCACTCATGGTGATTGTGGAATTCTGCAAA 2760
VEGFR2_P908A_2_FOR_6     CTTCTAGGTGCCTGTACCAAGGCAGGAGGGGCACTCATGGTGATTGTGGAATTCTGCAAA 380
                         ******************** ******** ****************************
```

P908P911A

```
WT_VEGFR2                GGAAATCTCTTGCAAGCTAATGCTCAGCAGGATGGCAAAGACTACATTGTTCTTCCGATA  3540
P1195A_VEGFR2_2_2_FOR_8  GGAAATCTCTTGCAAGCTAATGCTCAGCAGGATGGCAAAGACTACATTGTTCTTCCGATA  347
                         ************************************************************

WT_VEGFR2                TCAGAGACTTTGAGCATGGAAGAGGATTCTGGACTCTCTCTGCCTACCTCACCTGTTTCC  3600
P1195A_VEGFR2_2_2_FOR_8  TCAGAGACTTTGAGCATGGAAGAGGATTCTGGACTCTCTCTGGCTACCTCAGCTGTTTCC  407
                         ************************************ ******** ********
```

P1195AP1198A

Figure 4.2.6 SDM of VEGFR2-YFP vector to implement KD and PxxP mutations.

a. A 1% agarose gel of stained DNA PCR product bands after using different Tm annealing temperatures to incorporate SDM mutations into the VEGFR2-YFP vector. The mutations incorporated by the specific primers include a KD (K868M), first VEGFR2 proline rich motif (P908AP911A) and the second VEGFR2 proline rich motif (P1195AP1198A) on separate VEGFR2-YFP plasmids. The plasmid bands which were successful in implementing the desired mutation and their corresponding sequencing results determined are labelled. Unsuccessful SDM DNA bands are denoted by an X. **b.** The corresponding sequencing results from the plasmid bands isolated from **a.** using Clustal Omega (EMBL-EBI) software against the full-length wild-

type VEGFR2 sequence. The successful mutations implemented are highlighted in yellow.

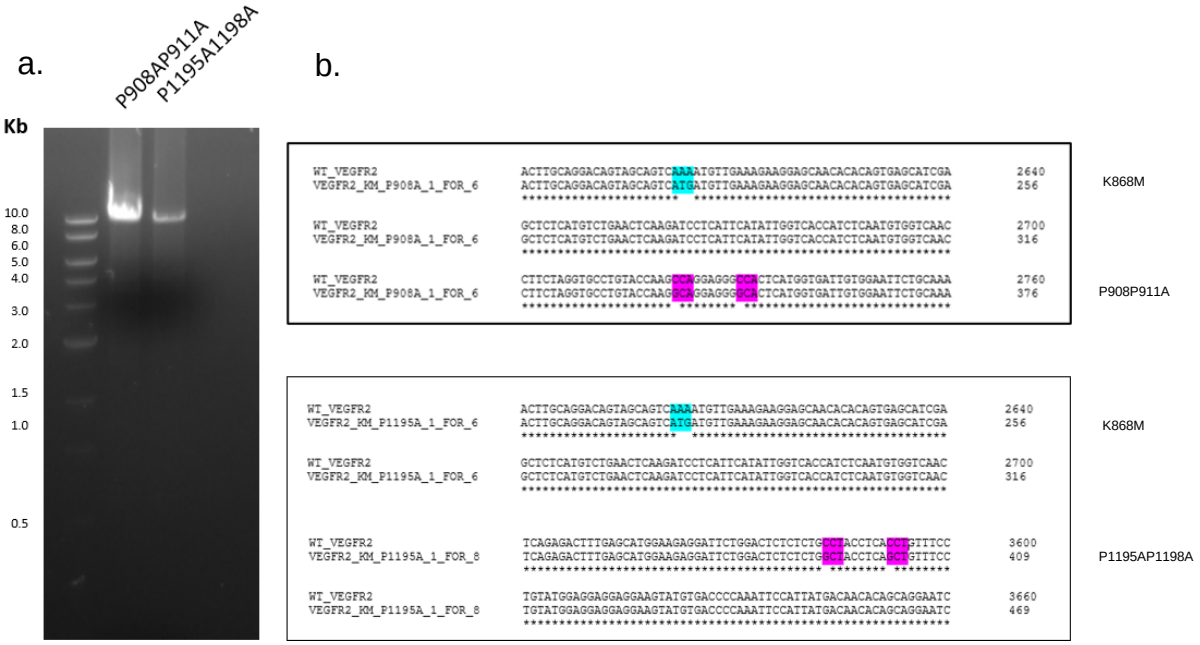

Figure 4.2.7 Insertion of the KD mutation into both proline-rich motif mutant VEGFR2-YFP construct vectors via SDM.

a. The PCR DNA products of SDM were ran on a stained 1% agarose gel. The mutation incorporated by the SDM primers was a KD mutation (K868M) into each VEGFR2-YFP proline-rich motif mutant of VEGFR2-YFP (P908AP911A and P1195AP1198A respectively). **b.** The isolated plasmid from **a.** was sent for sequencing and determined via Clustal Omega (EMBL-EBI) against the full length wildtype VEGFR2 sequence. Successful K868M mutation is highlighted in blue for both the P908AP911A VEGFR2-YFP mutant and the P1195AP1198A VEGFR2-YFP mutant (both previous PxxP mutations are highlighted in pink).

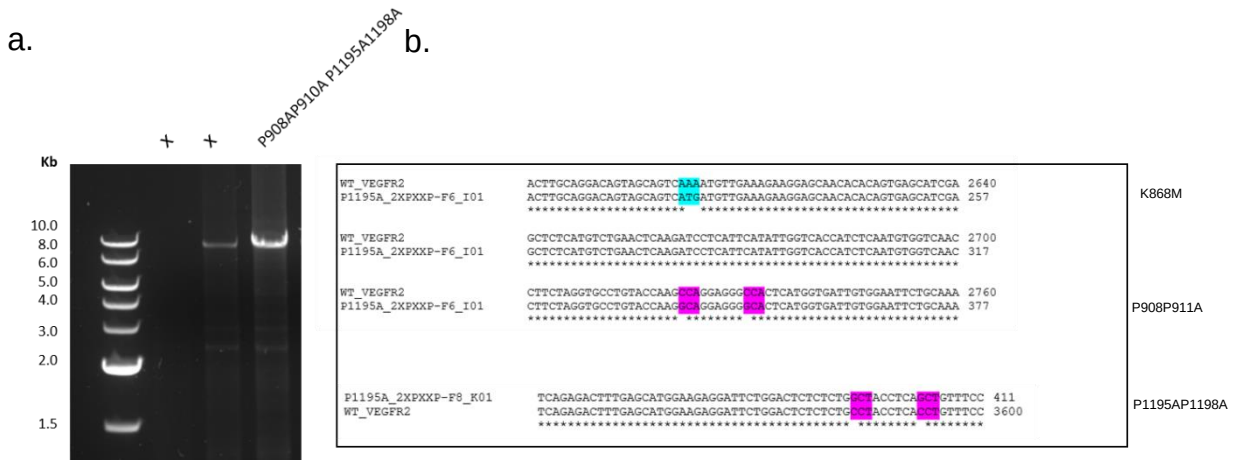

Figure 4.2.8 Insertion of the second proline-rich motif mutation (P1195AP1198A) into the KD P908AP911A VEGFR2-YFP construct vector to make a KD double PxxP mutant VEGFR2-YFP construct via SDM.

a. A stained 1% agarose gel was ran with the SDM DNA PCR products. The primers incorporated the second proline-rich motif mutation (P1195AP1195A) which was implemented into the KD P908AP911A VEGFR2-YFP construct plasmid. A band was visualised in Lane 3. The DNA band was isolated, purified and sent for sequencing. An X denoted unsuccessful SDM PCR products **b.** The corresponding sequencing results from the DNA band in Lane 3 (**a.**) for the implementation of the P1195AP1198A mutation was determined using Clustal Omega (EMBL-EBI) against the full length wildtype VEGFR2 sequence. The successful mutations within this KD double PxxP motif mutant VEGFR2 construct plasmid are highlighted in blue (KD) and pink (proline rich motif).

4.2.7 SH3 domain-containing proteins interact with VEGFR2 via the second PxxP motif within VEGFR2 C-terminal tail in BC cells, under serum-deprived conditions

To determine whether the SH3 domain-containing proteins Plcg1, Src and Nck1, interact with VEGFR2 via binding to a proline-rich motif within the intracellular domain of VEGFR2 under serum-deprived conditions, a Co-IP was performed via a YFP-pull down, using the VEGFR2-YFP mutant constructs (**Figure 4.2.9a**). The mutant VEGFR2 constructs were transfected into both BC cell lines along with a YFP only control (SYFP2). After successful transfection, the cells were serum-starved for 24 hours (normoxia) and then lysed. A GFP TRAP-A Kit (ChromoTek) was utilised to pull down the YFP-tagged proteins in the BC cell lysates, as the GFP-TRAP agarose beads cross-react with YFP.

The elute of bound proteins to the GFP-TRAP agarose beads was visualised on an immunoblot and probed for binding of the VEGFR2-YFP constructs and the SH3 domain-containing proteins (**Figure 4.2.9b**). In both BC cell lines the SYFP2 expressing vehicle-control cells showed no non-specific binding to any of the SH3 domain-containing proteins, which validates that the proteins did not bind to the YFP tag alone. Phosphorylated VEGFR2 was also determined to check whether the KD mutation abrogated the basal phosphorylation of the VEGFR2 receptor. Both SkBr3 cells and MCF7 cells showed that basal phosphorylation of VEGFR2 was abrogated upon implementation of the KD mutation. This mutation was implemented so that the binding of SH3-domain containing proteins could not be via their SH2/PTB domains to a phosphorylated site within VEGFR2 C-terminal tail. In both BC cell lines, an interaction was found to occur with Plcg1, Src and NCK1 with the wildtype (WT) VEGFR2-YFP construct, the KD VEGFR2-YFP construct and the KD P908AP911A (#1 PxxP) VEGFR2-YFP construct, under serum-deprived conditions. The interactions found to occur with the KD VEGFR2-YFP constructs indicated that the SH3 domain-containing proteins were binding via their SH3 domains to the C-terminal tail of the receptor, when the receptor was dephosphorylated. Upon mutation of the second proline rich motif (P1195AP1198A) (#2 PxxP) the interactions with all three SH3 domain-

containing proteins in both cell lines was abrogated. The same abrogation of binding was also visualised with the double proline-rich motif KD VEGFR2-YFP mutant construct. This suggests that the interactions occurring between VEGFR2 and the three SH3 domain-containing proteins, under serum-deprived conditions, occurs via interactions with the second PxxP motif (P1195P1198) within VEGFR2 C-terminal tail in BC cells.

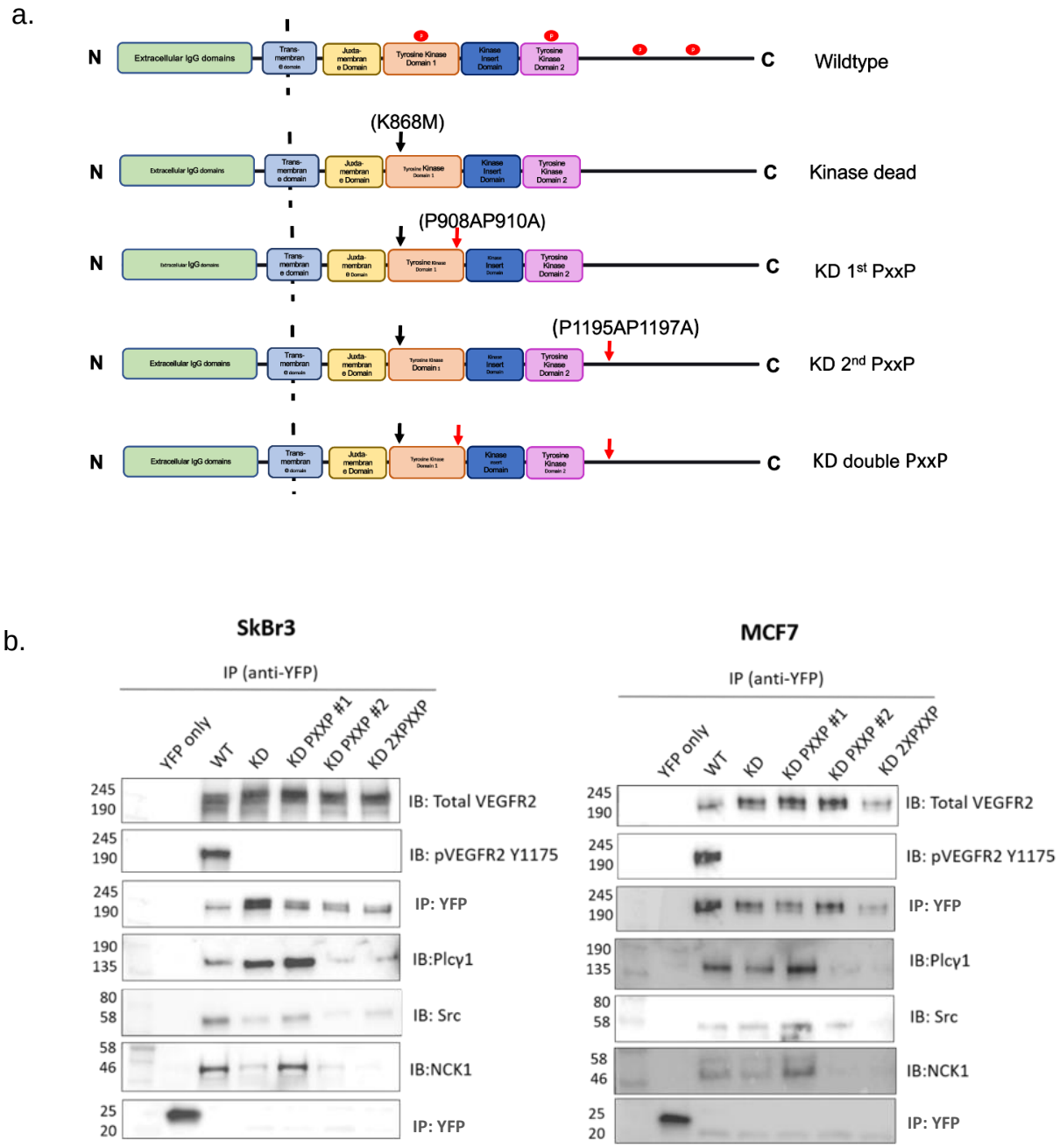

Figure 4.2.9 VEGFR2-YFP constructs and interactions with SH3 domain-containing proteins, in BC cells under serum-deprived conditions.

a. Schematic of the VEGFR2-YFP constructs with their particular mutations marked by the black arrow (K868M) and red arrows showing the corresponding PxxP mutation site (P908AP911A and/or P1195AP1195A) **b.** Representative immunoblots of a Co-IP performed

in SkBr3 and MCF7 cells after transfection with the VEGFR2-YFP constructs and compared to the YFP-only vehicle-control (SYFP2). The cells were serum-starved after transfection for 24 hours. The blots were probed for the binding of SH3 domain-containing proteins Plcg1, Src and Nck1 to the VEGFR2-YFP constructs (n=3).

4.2.8 Generation of mutant VEGFR2 C-terminal tail peptide

To further validate the finding that Plcg1, Src and Nck1 interact with VEGFR2 via the second C-terminal proline-rich motif under serum-deprived conditions, a plasmid which encodes the protein expression of a 193 residue-long C-terminal tail peptide of VEGFR2 was utilised. This peptide contained the second proline-rich motif only. An N-terminal maltose binding protein (MBP) tag was attached to the VEGFR2 C-terminal peptide and was expressed in BL21 (DE3) *E.Coli* cells. In addition a mutant VEGFR2 C-terminal proline-rich motif peptide construct was made from this vector using SDM (P1195AP1198A), to make a mutant proline-rich motif VEGR2 C-terminal tail peptide (**Figure 4.2.10**).

a.

N-terminal MBP tag - L L Q A N A Q Q D G K D Y I V L P I S E T L S **M** E E D S G L S L P T S P V S C **M** E E E E V C D P K F H Y D N T A G I S Q Y L Q N S K R K S R P V S V K T F E D I P L E E P E V K V I P D D N Q T D S G **M** V L A S E E L K T L E D R T K L S P S F G G **M** V P S K S R E S V A S E G S N Q T S G Y Q S G Y H S D D T D T T V Y S S E E A E L L K L I E I G V Q T G S T A Q I L Q P D S G T T L S S P P V Stop

b.

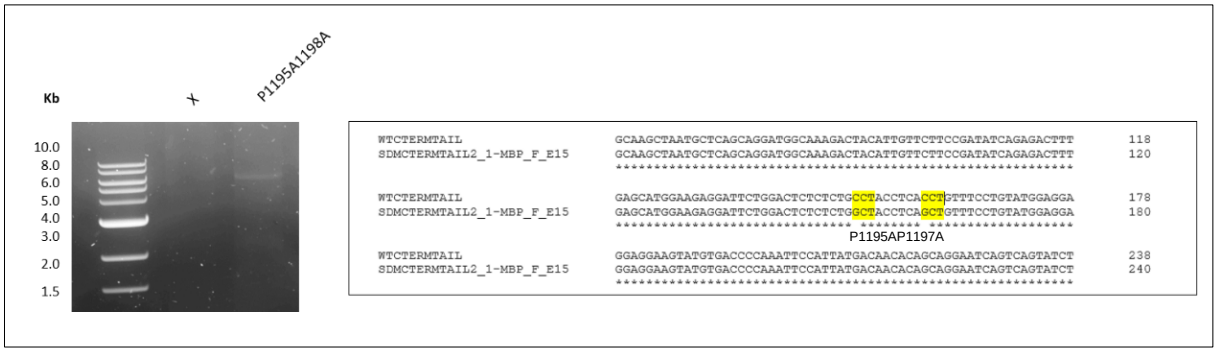

Figure 4.2.10 C-terminal VEGFR2 peptide sequence and the insertion of the proline-rich motif mutation via SDM.

a. The wildtype amino acid residue sequence of the VEGFR2 C-terminal tail peptide with an N-terminal MBP tag containing an intact proline-rich motif, highlighted in red. **b.** A 1% stained agarose gel ran with the PCR DNA products of SDM to implement the P1195AP1198A proline-rich motif mutation into the VEGFR2 C-terminal tail peptide vector. A DNA band was visualised in Lane 2. Unsuccessful PCR DNA products are denoted using an X. The DNA band from Lane 2 was sent for sequencing and compared to the VEGFR2 wildtype sequence using Clustal Omega (EMBL-EBI). The successful mutation implemented within the C-terminal VEGFR2 sequence is highlighted in yellow.

4.2.9 Validation of SH3 domain-containing proteins binding to the second proline-rich motif within VEGFR2 C-terminal tail in BC cells, under serum-deprived conditions

To further investigate and to validate the interaction observed between the SH3 domain-containing proteins and the second proline-rich motif within VEGFR2 C-terminal tail (residues P1195P1198), under serum-deprived conditions, an Co-IP was performed via an MBP-pull down, using the MBP-tagged VEGFR2 C-terminal peptides. The wildtype and mutant PxxP VEGFR2 C-terminal tail peptide was expressed in BL21 (DE3) *E.Coli* cells alongside an MBP-tag only vehicle-control. The peptides were isolated and purified using amylose MBP-binding beads. After serum-starvation of the BC cells for 24 hours (under normoxia), SkBr3 and MCF7 cell lysates were added to the purified MBP-tagged-proteins and incubated overnight. The MBP-bound beads were isolated and any bound protein eluted. The bound proteins were determined via immunoblotting and the SH3 domain-containing proteins were probed for the binding to the MBP-tagged peptides (**Figure 4.2.11**).

In both BC cell lines, an interaction was observed with Plcg1, Src and Nck1 with the wildtype C-terminal tail, which had an intact proline-rich motif (P1195P1198). There was no binding observed with the MBP-tag only vehicle-control, therefore validating that the binding of these proteins is through interactions with the C-terminal peptide and not the MBP-tag alone. When the proline-rich motif within the VEGFR2 C-terminal tail peptide was mutated, this mutation abrogated the interactions observed with all three SH3 domain-containing proteins to the wildtype VEGFR2 C-terminal tail peptide, in both BC cell lines. Thus, this experiment gives further validation that the SH3 domain-containing proteins interact with VEGFR2 via the second proline-rich motif (P1195P1198) within the C-terminal tail, under serum-deprived conditions in both BC cell lines.

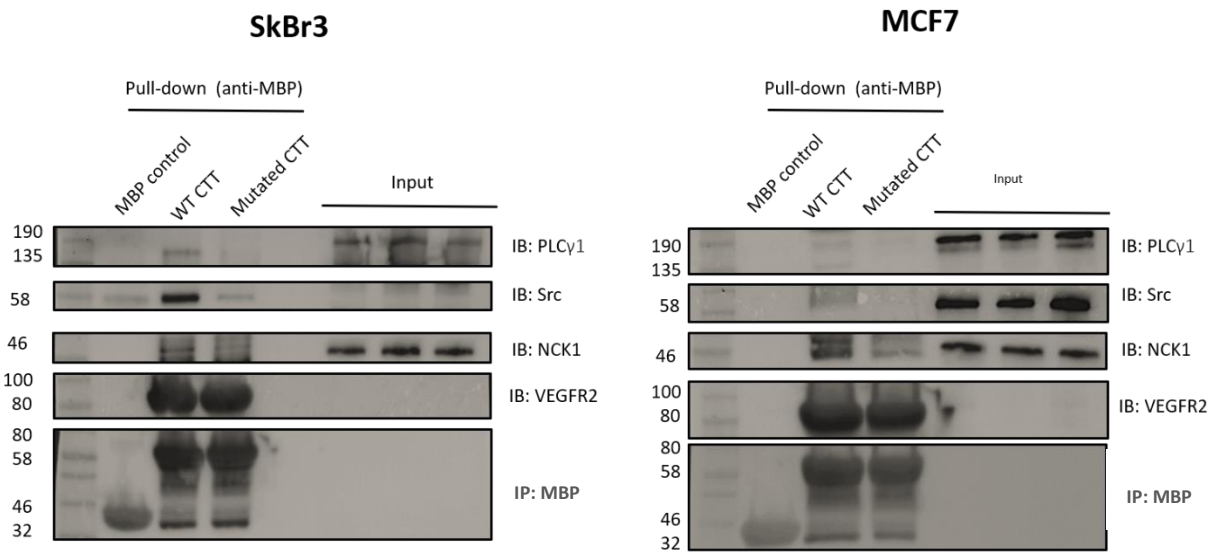

Figure 4.2.11 Mutation of the second proline-rich motif within the C-terminal tail (CTT) of VEGFR2 abrogates interactions with SH3 domain-containing proteins, in serum-starved BC cells.

Expressed and purified MBP-tagged peptides including MBP-tag only (MBP control), MBP-tagged wildtype VEGFR2 C-terminal tail (WT CTT) and MBP-tagged P1195AP1198A motif mutated VEGFR2 C-terminal tail (Mutated CTT) were incubated in serum-starved (0% FBS for 24 hours) SkBr3 and MCF7 cell lysates. An MBP Co-IP was performed using amylose MBP-binding beads and bound proteins were eluted and visualised via immunoblotting. An interaction with SH3 domain-containing proteins Plcg1, Src and Nck1 were probed to determine whether an interaction occurred with the MBP-tagged peptides. Representative blots of n=3.

4.2.10 Generation of CFP-tagged Plcg1 and Src domain constructs

The PPIs between SH3 domain-containing proteins Plcg1, Src and Nck1 and VEGFR2 was elucidated to occur via the second proline-rich motif within VEGFR2 C-terminal tail, under serum-deprived conditions. This suggests that the proteins were interacting with VEGFR2 via their SH3-domains which are known to bind to proline-rich regions (Cicchetti et al., 1992; Ren et al., 1993). To validate that the interactions with VEGFR2 occur via their SH3 domains, specific protein domains of Src and Plcg1 were cloned into a cerulean fluorescent protein (CFP) vector (Cerulean-C1) which expresses an N-terminal CFP tag. A CFP vector was chosen as CFP-tag is a well-known FRET pair with YFP and thus, could be used in further experiments. The constructs were made via the insertion of HindIII and EcoRI restriction sites to flank the insert domains using designed primers, via Phusion PCR. Restriction digests were made of both the construct inserts with the flanking restriction sites and the Cerulean-C1 vector in parallel. Both the open Cerulean-C1 plasmid and the insert DNA bands (**Figure 4.2.12**) were purified via gel extraction and ligated to reform the plasmid with the specific domain insert. The resulting plasmid was sent for sequencing and successful CFP expression was determined via transfection in cells (**Figure 4.2.13** and **Figure 4.2.14**). Full length Plcg1 was not used in this study as the full Plcg1 sequence from the plasmid obtained was not correct, however the corresponding SH2 and SH3 domains were of the correct sequence. The sequencing results obtained for each CFP-domain construct can be found in **Supplementary 1.1**.

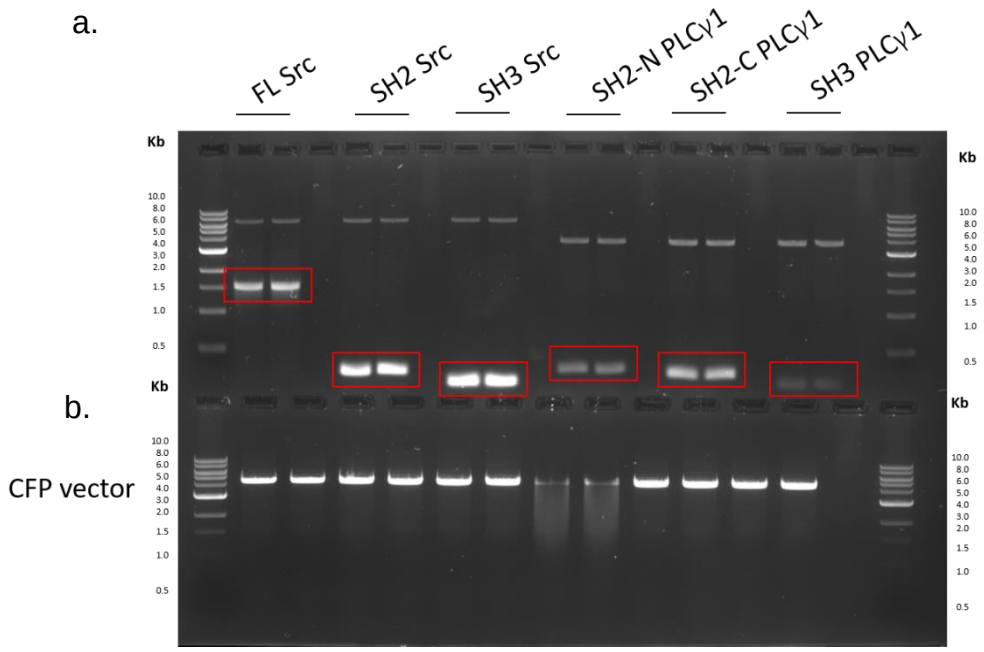

Figure 4.2.12 Restriction digest of Plcg1 and Src domain constructs and Cerulean-C1 vector.

a. The HindIII and EcoRI restriction digest products of the different domains of Src (Full length (FL), SH2 domain (SH2) and SH3 domain (SH3) and Plcg1 (N-terminal SH2 domain (SH2-N), C-terminal SH2 domain (SH2-C) and SH3 domain (SH3)). The DNA bands were isolated and gel purified. **b.** Restriction digested Cerulean-C1 plasmid via HindIII and EcoRI, to be used in a ligation reaction with the purified insert products observed in **a.**

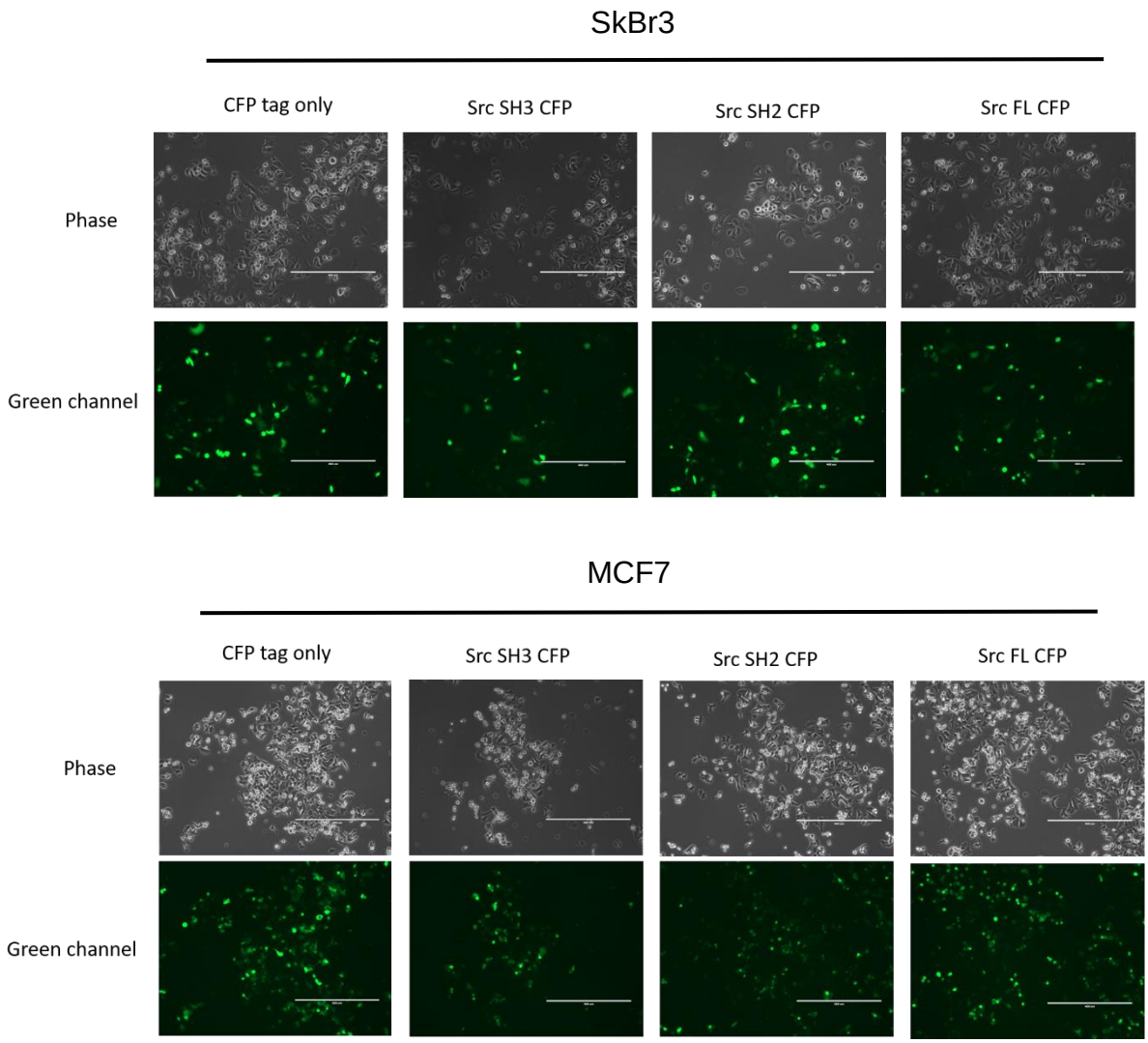

Figure 4.2.13 Successful transfection of the Src Cerulean-C1 cloned plasmids in BC cells.

The successful ligation and sequence open reading frame (ORF) was determined via the transfection of each cloned Src domain plasmid into SkBr3 and MCF7 cells and the fluorescence visualised in the green channel (470-525nm) on an EVOS (LifeTech) FL system at X10 magnification. The domains transfected include CFP-tag only (Cerulean-C1), Src SH3 domain-CFP (Src SH3 CFP), Src SH2 domain-CFP (Src SH2 CFP) and full length wildtype Src-CFP (Src FL CFP) via Lipofectamine 3000. Scale bar = 400nM**.**

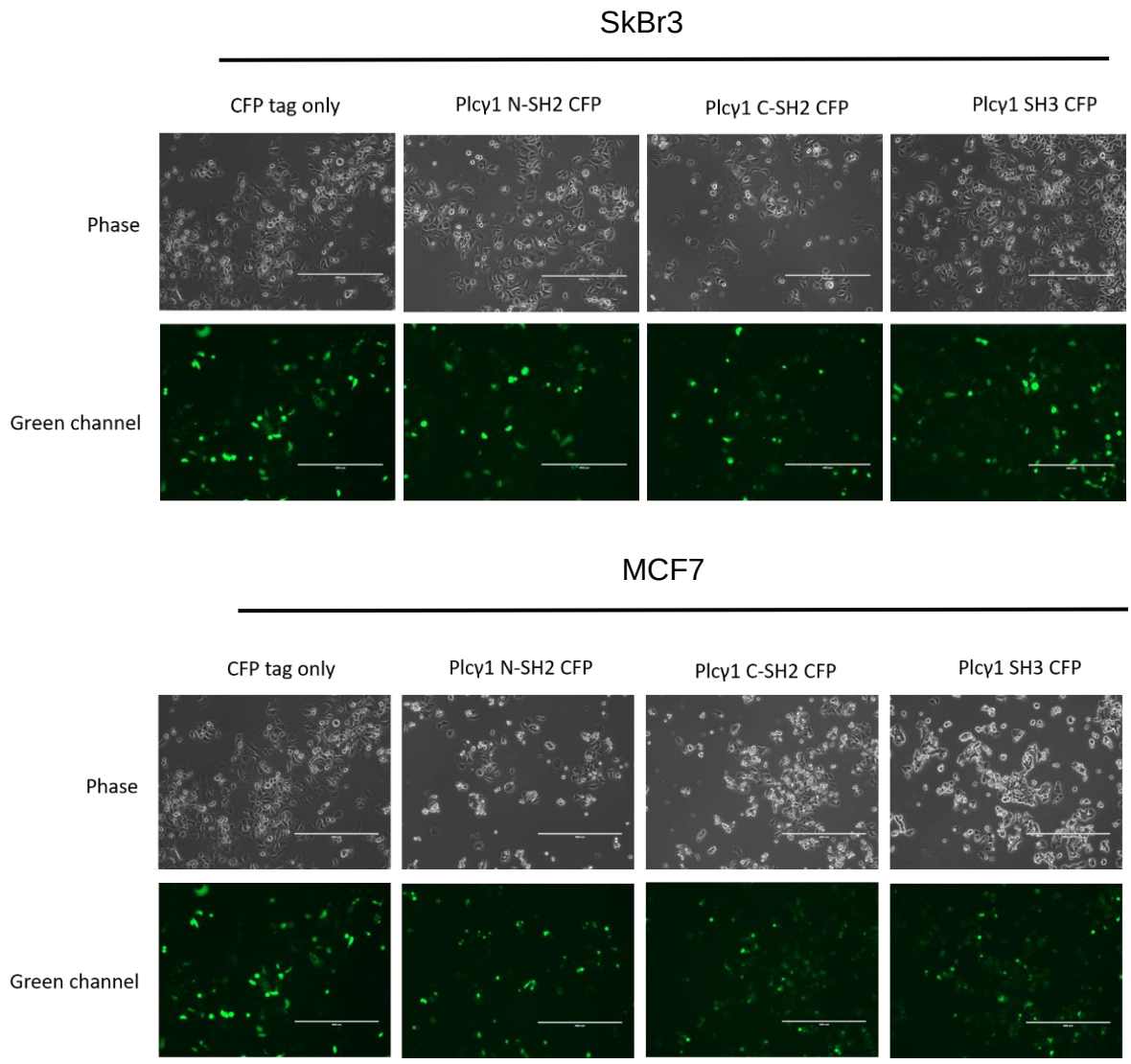

Figure 4.2.14 Successful transfection of the Plcg1 Cerulean-C1 cloned plasmids.

The successful ligation and sequence open reading frame (ORF) was determined via the transfection of each cloned Plcg1 domain plasmid into SkBr3 and MCF7 cells and the fluorescence in the green channel (470-525nm) detected on an EVOS (LifeTech) FL system at X10 magnification. The domains transfected include CFP-tag only (Cerulean-C1), Plcg1 N-terminal SH2 domain CFP (Plcg1 N-SH2 CFP) CFP, Plcg1 C-terminal SH2 domain CFP (Plcg1 C-SH2 CFP) and Plcg1 SH3 domain CFP (Plcg1 SH3 CFP) via Lipofectamine3000. Scale bar = 400nM.

4.2.11 Src SH3 domain binds to endogenous VEGFR2 in BC cells, under serum-deprived conditions

To determine the specific binding domain of the SH3 domain-containing proteins in the interaction observed between Plcg1 and Src to VEGFR2, under serum-deprived conditions, a Co-IP was performed via a CFP pull-down. The SkBr3 and MCF7 BC cells were transfected with the CFP-tagged domain constructs (**Figure 4.2.13** and **Figure 4.2.14**) and serum-starved for 24 hours (under normoxia) and lysed. A CFP pull-down was performed using a GFP-TRAP-A kit (ChromoTek). The GFP-TRAP agarose beads also cross-react with CFP-tagged proteins and was utilised to pull down the CFP-tagged domains expressed in the BC cell lysate. The elute of bound proteins was visualised on an immunoblot and probed for VEGFR2 binding to each CFP-tagged domain construct. Phosphorylated VEGFR2 at Y1175 was also probed, to determine if the domains bind to basal phosphorylated wildtype VEGFR2 endogenously expressed in BC cells (**Figure 4.2.15**).

In both BC cell lines an interaction was observed between C-terminal SH2 domain of Plcg1 to basal phosphorylated VEGFR2 at Y1175. In SkBr3 cells the binding of full length Src was observed to bind to phosphorylated VEGFR2 at Y1175 and a faint band visualised in MCF7 cells. Endogenous VEGFR2 was observed to interact with Src SH2 domain, Src SH3 domain, full length Src, Plcg1 N-terminal SH2 domain and Plcg1 C-terminal SH2 domain in both SkBr3 cells and MCF7 cells. The bands indicating an interaction with VEGFR2 appear fainter in MCF7 cells than those seen in SkBr3 cells as they have a lower endogenous expression level of VEGFR2 protein. It was observed that the CFP-tag vehicle-control showed no binding to VEGFR2 and thus, validating that the binding effects observed with VEGFR2 and the CFP-domain constructs are not due to non-specific binding to the CFP-tag only. A band for Plcg1 SH3 domain interacting with VEGFR2 was absent in both BC cell lines. Therefore, this PPI may be weaker than the PPI interaction observed with Src-SH3 domain. Thus, the interaction observed in this experiment between Src-SH3 domain and VEGFR2 was further investigated.

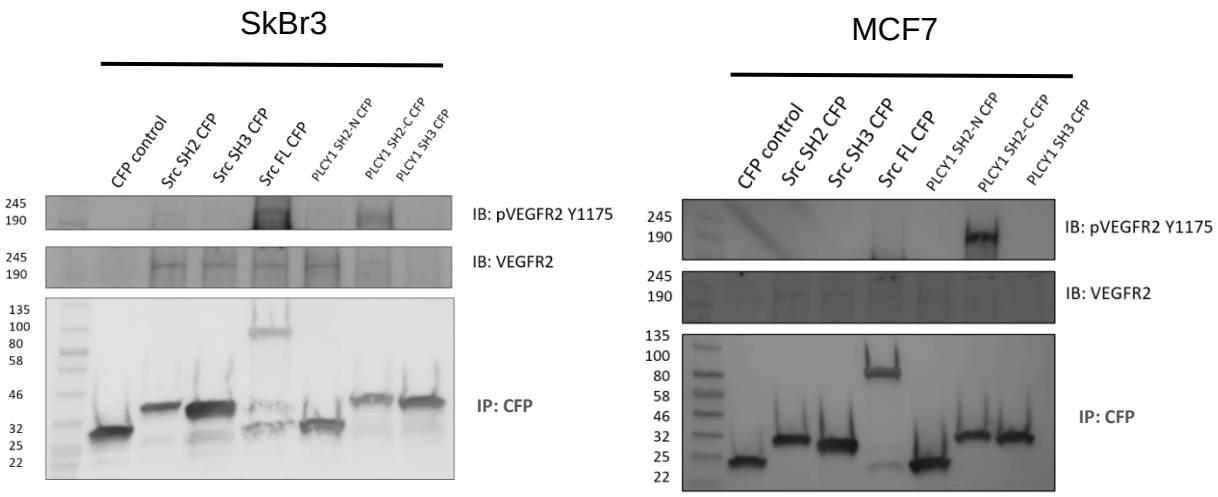

Figure 4.2.15 Src and Plcg1 domain binding to endogenous VEGFR2 in BC cells, under serum-starved conditions.

A representative immunoblot of SkBr3 and MCF7 cells transfected with CFP-Plcg1 and CFP-Src domain constructs and a CFP-tag only vehicle-control, after serum-starvation of 24 hours. A GFP-TRAP pull-down of the CFP-tagged constructs was performed with the BC cell lysates. The agarose GFP-binding beads cross-react to bind to CFP-tagged proteins. The blots were probed for the binding of the particular protein domains to phospho-VEGFR2 (Y1175) and total VEGFR2 under serum-deprived conditions (n=3).

4.2.12 Src SH3 domain interacts with the second proline-rich motif of VEGFR2 in SkBr3 cells, under serum-deprived conditions

To investigate further the non-canonical PPI between Src-SH3 domain and VEGFR2 seen in **Figure 4.2.15**, Förster resonance energy transfer (FRET) was utilised to assess the interaction between the Src-CFP constructs and the VEGFR-YFP constructs in SkBr3 BC cells, under serum-deprived conditions.

FRET is a very sensitive technique to study molecular interactions occurring in intact cells, therefore the technique allows for spatial resolution and localisation of molecular protein-protein interactions (Sekar and Periasamy, 2003). The technique is distance-dependent by which energy is transferred from an excited donor fluorophore to an acceptor fluorophore by intermolecular long-range dipole-dipole coupling. FRET is an accurate measurement of molecular proximity when positioned within the Förster radius (the distance at which half the excitation energy of the donor is transferred to the acceptor, typically within 3-6nm). YFP and CFP are a widely-used and well-known FRET donor-acceptor pair, with YFP as the acceptor molecule and CFP as the donor. The pairing works well due to the spectroscopic properties of the two fluorophores. These are selected based on their sufficient separation in excitation spectra for selective stimulation of the donor fluorophore, an overlap (>30%) with the emission spectrum of the donor and the excitation spectrum of the acceptor to obtain efficient energy transfer and sufficient separation in emission spectra between the donor and acceptor, to allow independent measurement of each fluorophore (Pollok and Heim, 1999). If FRET occurs, the donor channel signal will be quenched and the acceptor channel signal will be sensitised or increased. This therefore, gives validation that the proteins associate and interact within a very small distal range, in intact cells.

Before carrying out the FRET experiments, control measurements were taken to validate that the interactions we observed through the FRET channel were correct and to determine the YFP and CFP crosstalk into the FRET channel. Here, cells expressing YFP construct only were used and measured the signal intensity in each channel (YFP_{ex}/YFP_{em}, CFP_{ex}/CFP_{em}, CFP_{ex}/YFP_{em}). In this

case YFP only was visualised with minimal bleed through into the CFP channel. There was no/very low signal in the FRET channel (CFP_{ex}/YFP_{em}) determining that there is no crosstalk from the YFP into the FRET channel. Cells expressing CFP construct only were used and measured the signal intensity in each channel. In this case, a signal was only observed in the CFP channel and very minimal/low signal seen in the YFP channel. Signal in the FRET channel was also not observed and thus, the signals in the FRET channel were not due to crosstalk of the CFP into the FRET channel. The same exposure time was used in all three channels and cells expressed the same level of fluorescent protein as the same amount of DNA was transfected of each fluorescent vector for each independent experiment in the BC cells.

The CFP fluorescence was excited at 436nm and the emission detected at 470-510nm. The YFP fluorescence was excited at 516nm and the emission detected at 520-540nm. FRET was thus measured by exciting the donor (CFP) and if the YFP-tagged proteins were in close enough proximity (within 10nM) to the CFP-tagged proteins, emission from the acceptor (YFP) FRET channel was observed. SkBr3 cells were transfected with each plasmid (YFP-tagged and CFP-tagged) and the cells were then grown under serum-deprived conditions for 24 hours. The cells were fixed on coverslips and mounted on slides to be imaged under the inverted LSM880 + airyscan confocal microscope (Zeiss).

When full length wildtype VEGFR2-YFP (VEGFR2-WT-YFP) was expressed alongside the different Src-CFP constructs (**Figure 4.2.16**), FRET was observed and thus a PPI detected, between wildtype VEGFR2-YFP and full length wildtype Src-CFP (Src-WT-CFP). A FRET signal was also visualised between wildtype VEGFR2-YFP and Src-SH2 domain-CFP (Src-SH2-CFP) and Src-SH3 domain-CFP (Src-SH3-CFP). This indicates that the binding of Src to wildtype VEGFR2 can occur via both the SH2 and SH3 domain of Src. when the wildtype VEGFR2 receptor has basal phosphorylation, under serum-deprived conditions. The vehicle-control vector CFP-tag only (CFP-control) showed no background FRET signal.

When the VEGFR2 KD construct (VEGFR2-KD-YFP) was expressed in SkBr3 BC cells alongside the Src-CFP domain constructs a different pattern of FRET

signal was visualised within the SkBr3 cells (**Figure 4.2.17**). FRET signal was observed between the VEGFR2 KD-YFP construct and full-length Src wildtype-CFP and Src SH3 domain-CFP. A very low or no FRET signal was detected between Src SH2-domain-CFP and VEGFR2-KD-YFP when there is no basal phosphorylation of the VEGFR2 receptor. The CFP-tag only vehicle-control (CFP-control) showed no background FRET signal.

After determining that Src binds to VEGFR2 under serum-deprived conditions via its SH3 domain in a VEGFR2-phosphorylation independent manner, we wanted to validate that the binding of the SH3 domain of Src to VEGFR2 was via the second proline rich motif (P1195P1198). To investigate this, the VEGFR2-YFP construct containing a KD mutation and mutated proline-rich motif (P1195AP1198A) was transfected into SkBr3 BC cells alongside the Src-CFP domain constructs (**Figure 4.2.18**). No FRET signal was observed between the KD + P1195AP1198A mutant VEGFR2-YFP construct (VEGFR2-PXXP-#2-YFP) and any of the Src-CFP constructs. This confirmed that the binding of Src SH3 domain occurs via binding to the second proline rich motif (P1195P1198) within VEGFR2 C-terminal tail, under serum-deprived conditions, as the interaction observed is abrogated via the implementation of the P1195AP1198A mutation. The vehicle-control vector CFP-tag only (CFP-control) showed no background FRET signal.

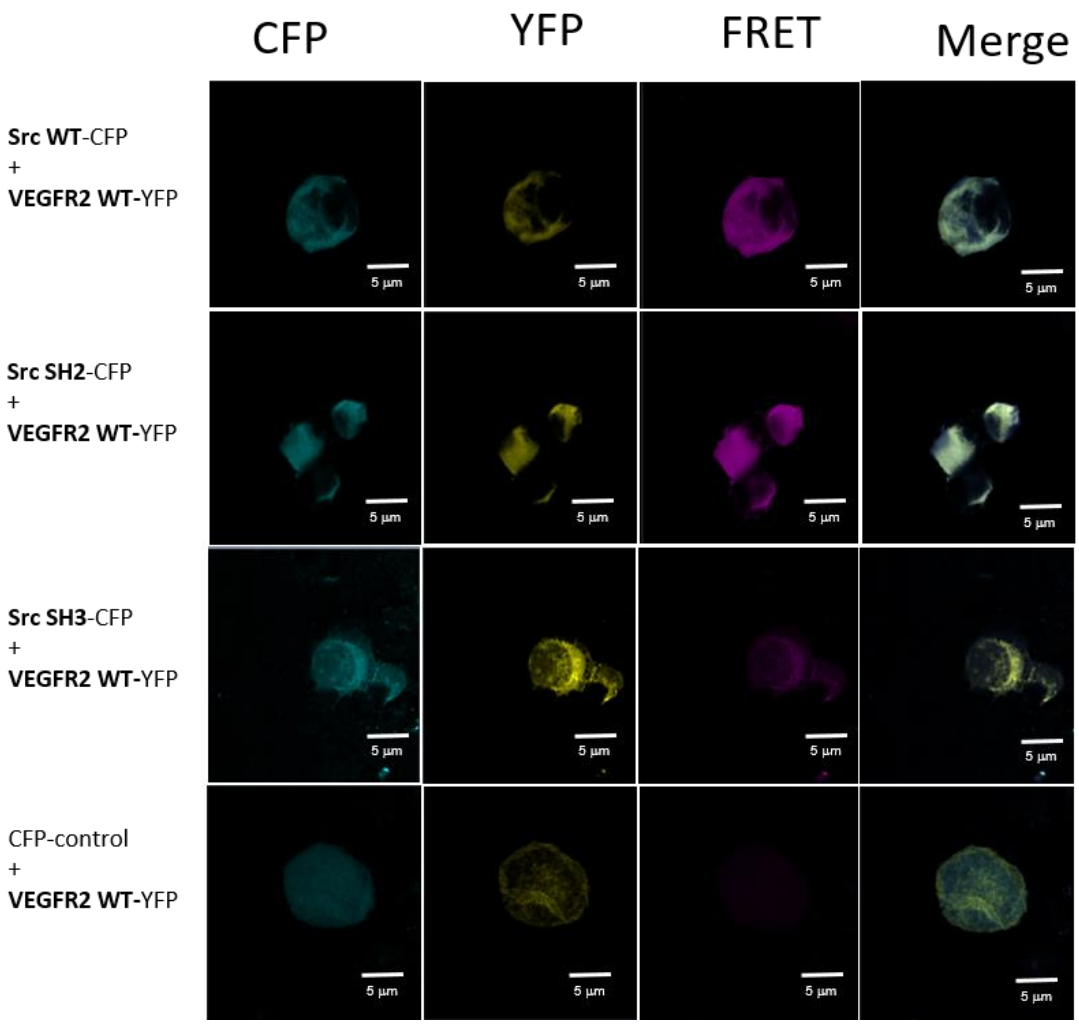

Figure 4.2.16 Wildtype VEGFR2 binds to Src SH3 and SH2 domain in SkBr3 cells, under serum-deprived conditions.

Förster Resonance Energy Transfer of SkBr3 cells transfected with both YFP-tagged full-length wildtype VEGFR2 (VEGFR2 WT-YFP) and CFP-tagged Src domain constructs alongside a CFP-tag only vehicle-control (CFP-control). CFP-constructs transfected include full-length wildtype Src-CFP (Src-WT-CFP), Src SH2 domain-CFP (Src-SH2-CFP) and Src SH3 domain-CFP (Src-SH3-CFP). The cells were serum-starved (0% FBS) for 24 hours, after transfection. The cells were fixed and imaged under an LSM880 + airyscan confocal microscope at X40 magnification. CFP signal was excited at 436nm and emission was detected at 470-510nm. YFP signal was excited at 516nm and emission was detected at

520-540nm. FRET signal was detected by the excitation of the CFP donor at 436nm and detection of the YFP emission at 520-540nm. Gain=1.0.

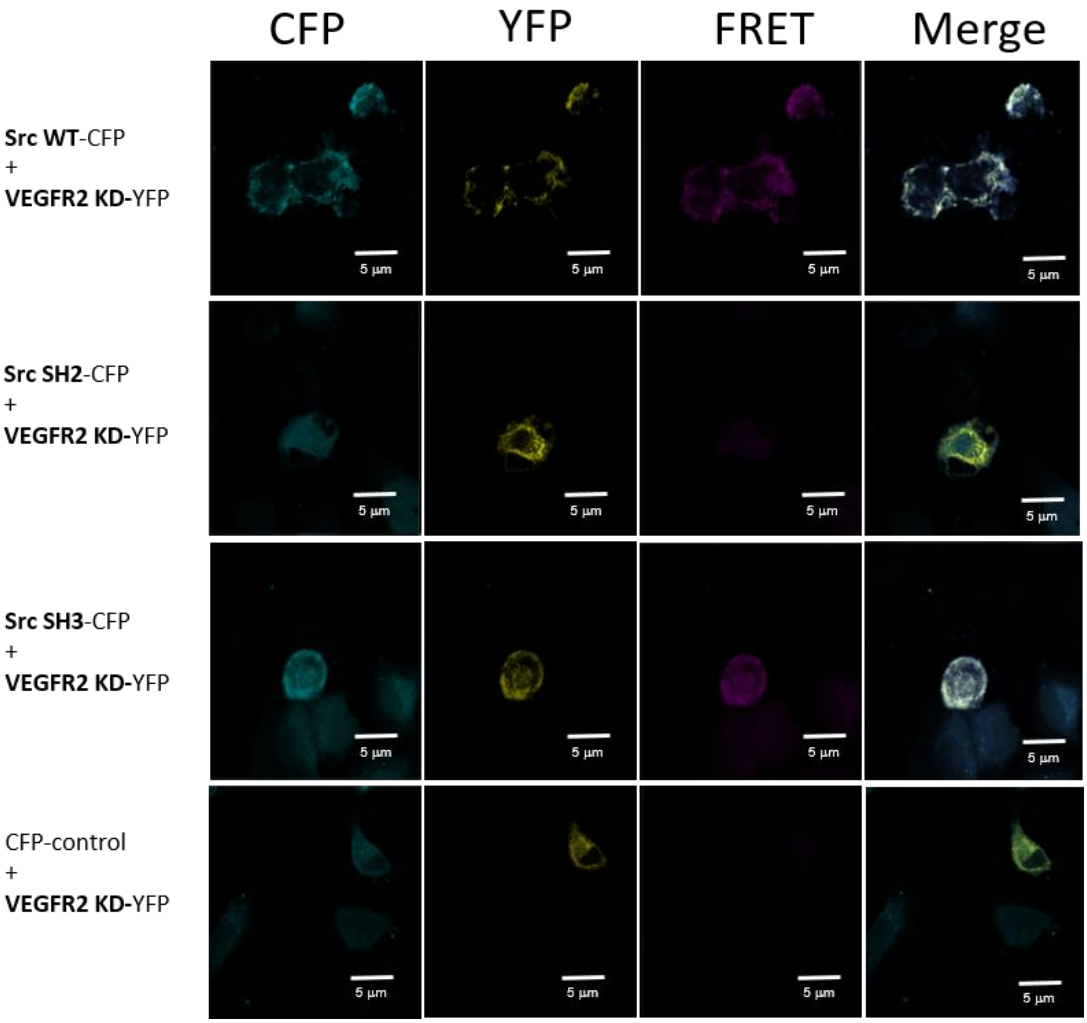

Figure 4.2.17 KD VEGFR2 binds to Src SH3 domain only in SkBr3 cells, under serum-deprived conditions.

Förster Resonance Energy Transfer of SkBr3 cells transfected with both YFP-tagged full-length KD VEGFR2 (VEGFR2 KD-YFP) and CFP-tagged Src domain constructs alongside a CFP-tag only vehicle-control (CFP-control). CFP-constructs include full-length wildtype Src-CFP (Src-WT-CFP), Src SH2 domain-CFP (Src-SH2-CFP) and Src SH3 domain-CFP (Src-SH3-CFP). The cells were serum-starved (0% FBS) for 24 hours, after transfection. The cells were fixed and imaged under an LSM880 + airyscan confocal micro-cope at X40 magnification. CFP

signal was excited at 436nm and emission was detected at 470-510nm. YFP signal was excited at 516nm and emission was detected at 520-540nm. FRET signal was detected by the excitation of the CFP donor at 436nm and detection of the YFP emission at 520-540nm. Gain=1.0.

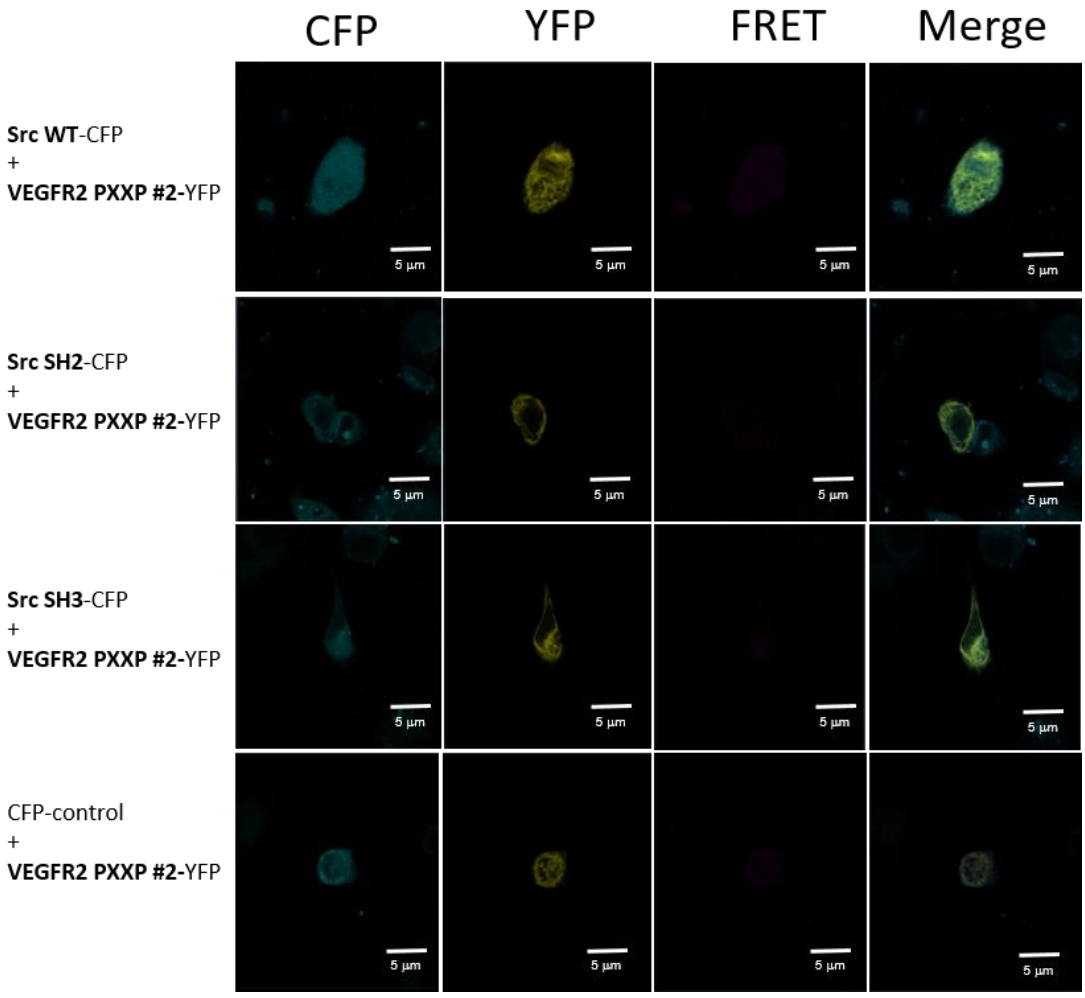

Figure 4.2.18 Mutation of the second proline rich motif (P1195P1198) of VEGFR2 abrogates the binding of Src in SkBr3 cells, under serum-deprived conditions.

Förster Resonance Energy Transfer of SkBr3 cells transfected with both YFP-tagged full-length KD VEGFR2 with a second proline rich motif mutation (P1195AP1198A) (VEGFR2-PxxP#2-YFP) and CFP-tagged Src domain constructs alongside a CFP-tag only vehicle-control (CFP-control). CFP-constructs include full-length wildtype Src-CFP (Src-WT-CFP), Src SH2 domain-CFP (Src-SH2-CFP) and Src SH3 domain-CFP

(Src-SH3-CFP). The cells were serum-starved (0% FBS) for 24 hours, after transfection. The cells were fixed and imaged under an LSM880 + airyscan confocal microscope at X40 magnification. CFP signal was excited at 436nm and emission was detected at 470-510nm. YFP signal was excited at 516nm and emission was detected at 520-540nm. FRET signal was detected by the excitation of the CFP donor at 436nm and detection of the YFP emission at 520-540nm. Gain=1.0.

4.3 Discussion

The uncontrolled growth of tumour cells can give rise to a mass of tumour cells that surpasses the aberrant tumour vasculature and thus, leads to nutrient and oxygen deprived tumour cells in the middle of a tumour mass (Hanahan and Weinberg, 2011). Nutrient and oxygen deprivation also occurs during tumour cell metastasis, when cancer cells disengage from the vasculature to move into a new secondary site and when patients are treated with anti-angiogenic therapy (White, ElShaddai Z. et al., 2020). Advanced tumour cells are known to survive and proliferate under these conditions via the activation of signalling pathways which contribute to a more malignant and aggressive phenotype (Harris, 2002; Izuishi et al., 2000). Nutrient deprivation has been found to be correlated to poor patient survival (Moscat et al., 2015) and hypoxia associated with a poor patient prognosis and chemoresistance (Graham and Unger, 2018). Therefore, tumour cells that survive and adapt to growth under microenvironmental stress are the particular tumour phenotype that progresses to malignancy.

Many cancer types express VEGFR2 (Guo, S. et al., 2010) and the expression is upregulated in response to hypoxia (Olsson et al., 2006). VEGFR2 is implicated in tumour angiogenesis but its impact in cancer cell signalling has not been fully elucidated (De Palma et al., 2017). The overexpression of VEGFR2 has been found to be directly linked to the pathogenesis of breast tumours (Guo, S. et al., 2010). High VEGFR2 expression levels in BC have been correlated with the expression of migration markers, proliferation markers and decreased survival in TNBC (Yan et al., 2015; Nakopoulou et al., 2002; Rydén et al., 2010). Our laboratory group have previously demonstrated that interactions between SH3 domain-containing proteins and proline-rich motifs of RTKS are important for maintaining cellular homeostasis. These interactions are determined upon the relative protein concentrations within the cell. Cellular stress can severely alter protein expression levels and thus, give rise to an aberrant signalling outcome when normal homeostatic signalling is out-competed by interactions involving proteins with elevated protein expression levels, in response to growth under microenvironmental stress. This aberrant Tier 2 signalling outcome was found to give a highly proliferative

phenotype in ovarian cancer cells and the invasive potential in lung cancer cells, upon conditions which promoted the non-canonical activation of Plcg1 (Timsah et al., 2015; Timsah et al., 2016b). The elevated protein expression levels of Plcg1 and FGFR2 were also correlated with a worse prognosis in ovarian cancer patients and a worse recurrence-free survival in lung adenocarcinoma cancer patients.

In this study we investigated the effect of nutrient and oxygen deprivation and thus, simulating microenvironmental tumour stress, on BC cell morphology and protein expression levels. Additionally, the presence of a non-canonical Tier 2 mechanism between VEGFR2 and SH3 domain-containing proteins, under serum-deprived conditions, was investigated. Aberrant activation of a Tier 2 mechanism under these conditions could aid in BC cell survival, progression and chemoresistance when under periods of microenvironmental stress and under anti-angiogenic therapy. We observed that in both BC cell lines the cellular morphology drastically changed when grown under microenvironmental stress conditions. SkBr3 cells tended to respond morphologically to growth under both hypoxia and serum-starved conditions, whereby the cells displayed an elongated, irregular shape with prominent protrusions and filopodia. MCF7 cells responded predominantly to serum-deprivation alone, showing a smaller, elongated morphology with protrusions and filopodia also visualised. Filopodia was observed in both BC cell lines when under microenvironmental stress, simulating growth within a tumour mass and are important for cell adhesion and migration. Filopodia are plasma membrane protrusions and are formed of tightly bundled parallel actin filaments (Mattila and Lappalainen, 2008). This process of actin elongation by actin polymerisation pushes the cell edge forward and thus, induces cellular migration (Arjonen et al., 2011). Ten filopodia linked genes were found to be upregulated in malignant human BCs, including MYO10 (Myosin-X) and ACTR2 (Arp2). Myosin-X translocation to filopodia is regulated by PIP_3 and PIP_2 and therefore implicated in the PI3K/Akt signalling pathway. Arp2 is activated downstream of Nck. Both Src and Nck have been implicated in activating cell motility and migration signalling pathways and thus, may be implicated in the formation of filopodia in BC cells (Aryal et al., 2015; Finn, 2008).

Moreover, our findings showed that BC cell growth under serum-deprivation and/or hypoxic conditions gave rise to differences in relative protein expression levels. Serum-deprivation abrogated VEGFR2 phosphorylation in both BC cell lines and thus, VEGFR2 is expected to be in its monomeric basal state under these conditions. Interestingly, the relative total levels of VEGFR2 changed in both cell lines in response to growth under microenvironmental stress conditions. SkBr3 cells showed a highly elevated increase in VEGFR2 expression levels in response to growth under hypoxia. An increase in VEGFR2 expression was also visualised in SkBr3 cells in response to growth under serum-deprivation. MCF7 cells however, showed an increase in VEGFR2 expression in response to growth under serum-deprivation conditions only. VEGFR2 expression has been implicated in BC patient metastasis (Yan et al., 2015) and the expression of proliferation markers (Nakopoulou et al., 2002), thus, the elevated VEGFR2 expression levels may upregulate proliferation and migration pathways in response to growth under a stress environment. The relative expression levels of Plcg1, Src and Nck1 all change in response to growth under serum-starvation and oxygen-deprivation. Most strikingly, both Src and Nck1 expression levels went up in response to growth under hypoxia in MCF7 cells and Src and Nck1 levels were elevated in response to serum-starvation in SkBr3 cells. These differences in protein expression levels in response to growth under microenvironmental stress shows the high tumour heterogeneity between BC subtypes (Aleskandarany et al., 2018). Thus, particular subtypes of BC respond differently to different environmental stress within the tumour microenvironment. Under serum-deprived conditions, VEGF was not present in the media and therefore, VEGF was not secreted in response to growth under microenvironmental stress. Thus, changes to the proteome of SkBr3 and MCF7 cells under serum-deprived conditions is VEGF independent. Tier 2 signalling occurs under nutrient and GF-independent conditions and can upregulate oncogenic signalling pathways in response to changes in protein expression levels, thus, this supports the presence of a Tier 2 signalling mechanism as a possible adaptation to growth under nutrient and serum-deprived stress conditions.

The activation of particular intracellular kinases in SkBr3 BC cells in response to growth under serum-deprivation and hypoxia was observed to be different for each growth condition. This indicates that growth under each particular stress condition elucidates a different cell signalling response. SkBr3 growth under hypoxia activated many cellular kinases, when in the presence of serum. This hyperactivation may be driven by the hyperactivation of GF receptors and thus, activation of their downstream signalling pathways by GFs present in serum, in response to hypoxia-mediated cell stress.

In response to growth under serum-deprivation (and under normoxia), the SkBr3 cells phosphorylation levels of STAT3 and HSP60, was found to be lower compared to growth in the presence of serum (and under normoxia). STAT3 is activated via GF activation, which are present in FBS. Thus, it appears to be only activated when serum is present, and plays a role in cell survival and proliferation (Bharti et al., 2018). STAT3 is also hyperactivated in response to growth under hypoxia and in the presence of serum and therefore, may be activated downstream of hyperactivated RTKs in the presence of GF to induce cell survival under oxygen-deprived stress conditions. HSP60 maintains protein homeostasis (Caruso Bavisotto et al., 2020) and therefore, may not be activated under serum-deprived conditions as the cell tries to adapt and ‘switch off’ certain cellular processes to conserve cellular energy into processes that the cell needs to adapt and survive without access to nutrients and GFs.

Chk-2 and C-Jun showed higher levels of phosphorylation in SkBr3 cells grown under serum-deprived conditions (and under normoxia) compared to growth under serum-supplemented conditions (and under normoxia). Chk-2 is phosphorylated in response to DNA-damage (Antoni et al., 2007), therefore, the activation of this protein could be via tumour cell survival through DNA-repair, due to microenvironmental induced DNA damage. C-Jun is a component of the transcription factor activator protein 1 (Vleugel, M. M. et al., 2006) and activates TRE/AP-1 elements. C-Jun was found to be expressed in 38% of BC cases and its expression was associated with activating proliferation and tumour angiogenesis in invasive BCs. C-Jun is also hyperactivated in response to SkBr3 cell growth under hypoxia and in the presence of serum (thus, GF) and therefore, may also be activated

downstream of RTK hyperactivation via GFs in response to growth under hypoxic-mediated stress. CREB is upregulated in response to growth under serum-deprivation and is a nuclear transcription factor which regulates cell differentiation, proliferation and survival pathways. CREB is involved in tumour initiation, progression and metastasis, and therefore, has a role as a proto-oncogene. The overexpression of CREB was implicated in inducing tumour proliferation in BC patients (Xiao et al., 2010). P70 S6 kinase was also activated under serum-deprived conditions (and under normoxia), compared to cells grown under serum-supplemented conditions (and under normoxia). P70 S6 kinase is a downstream effector of the PI3K signalling pathway and plays a role in cell survival signalling. The overexpression of p70 S6 kinase has been found to activate the EMT in ovarian cancers (Pon et al., 2008). P53 was observed to be highly phosphorylated in response to growth under serum-deprived conditions (and under normoxia) compared to growth in the presence of serum (and under normoxia). The tumour suppressor protein is activated in response to DNA-damage and cellular stress (Vogelstein et al., 2000). The activation of p53 in SkBr3 BC cells may contribute towards cell survival in response to growth under harsh microenvironmental stress conditions and in response to stress-induced DNA damage. Plcg1 activation was also observed in response to growth under serum-deprived conditions. Plcg1 phosphorylation and downstream signalling activates proliferation and survival pathways (Emmanouilidi et al., 2017) and the expression and activation is associated with BC metastatic progression. A high expression of Plcg1 has been correlated with a worse clinical outcome in terms of incidence of distant metastases in BC cells (Sala et al., 2008). When Plcg1 is activated via an aberrant Tier 2 signalling mechanism, via FGFR2, Plcg1 is not phosphorylated but it changes its protein conformation such that the protein is in an activated state. Thus, the phosphorylation of Plcg1 here may be downstream to other signalling pathways activated in response to serum-deprivation stress. It is possible, however, that the aberrant phosphorylation of Plcg1 could be though a non-canonical tier 2 interaction which exposes the Y783 site to be phosphorylated via intracellular TKs. PYK2 levels of phosphorylation are also elevated in response to growth under serum-deprivation compared to growth in the presence of serum. PYK2 is a well-

known mediator of signalling pathways involved in cell proliferation, migration and invasion. The expression of PYK2 in HER2-positive BC cells has been found to promote BC cell invasion and chemoresistance (Al-Juboori et al., 2019).

When the BC cells were grown under both serum-deprivation and hypoxic-mediated stress the cells were observed to lose the activation of many of their intracellular kinases. This may also be due to the cell needing to 'switch off' non-important signalling pathways under periods where there is no access to nutrients or GFs, as a way of preserving energy for the pathways the cells need to survive and progress.

Interestingly however, the cells do maintain a high level of phosphorylation of both FAK and PRAS40. The level of FAK activation increased by around 80% compared to the levels in BC cells grown under normoxia and in the presence of serum. FAK plays a crucial role in cell motility and survival and is implicated in the Src signalling pathway. Here, active FAK promotes cell migration and invasion downstream of Src activation (Mayer, E.L. and Krop, 2010; Finn, 2008; Summy and Gallick, 2003). FAK phosphorylated at Y397 can bind, phosphorylate and activate Src kinase itself through binding to Src-SH2 domain (Aleshin and Finn, 2010). Activated Src then in turn, fully activates FAK at Y576, Y577, Y861 and Y925 (Mitra and Schlaepfer, 2006). Several studies have noted that increased FAK expression and activation is correlated with enhanced tumour malignancy and poor prognosis (Avizienyte and Frame, 2005). In BC in particular, the activation of FAK has been correlated with BC initiation, progression and metastasis (Luo and Guan, 2009). FAK promotes cancer cell migration by regulating focal adhesion formation and turnover, through multiple signalling cascades (Mitra and Schlaepfer, 2006). Overall, this is an exciting and novel finding that growth under tumour microenvironmental stress conditions stimulates the activation of FAK and possible downstream signalling dynamics may play a role in BC cell migration when under tumour microenvironmental stress conditions of hypoxia and nutrient-deprivation. FAK activation can also promote cellular viability in response to stress and is commonly overexpressed in breast cancer (Dawson et al., 2021).

PRAS40 is a substrate of Akt and a component of the mammalian target of rapamycin (mTOR). PRAS40 phosphorylation is associated with tumour progression and mediates the signalling of the PI3K/Akt pathway. PRAS40 activation promotes tumorigenesis via the dysregulation of cellular proliferation, apoptosis, metastasis and senescence (Lv et al., 2017). In response to growth under both hypoxic-mediated stress and under serum-deprivation in SkBr3 showed a loss of phosphorylation of the kinase Tor or mTOR. mTOR phosphorylation occurs downstream of the PI3K/Akt pathway and plays a critical role in cell survival. mTOR proteins regulate protein synthesis and protein degradation and are active in response to the presence of sufficient nutrients to fuel protein synthesis. Thus, under hypoxic-stress and under nutrient-deprivation mTOR phosphorylation is downregulated.

Overall, it appears that SkBr3 BC cells respond to growth under hypoxia and in the presence of serum, and thus GF, by the elevated hyperactivation and phosphorylation of a number of intracellular kinases. These kinases may be activated through the hyperactivation of GF receptors in the presence of GFs in the serum. The kinases that are activated in response to serum-deprivation stress (and under normoxia) in SkBr3 cells, compared to cells grown under the presence of serum (and under normoxia) are proteins that are involved with DNA-repair, survival, proliferation, chemoresistance, migration, tumour angiogenesis and tumour progression. Proteins that are highly phosphorylated in SkBR3 cells in response to growth under both serum-deprivation and hypoxic stress conditions are involved with cell survival, motility, migration, apoptosis, senescence and proliferation signalling pathways. Therefore, these results show that different proteins are phosphorylated and thus, activated in response to growth under serum-deprivation and/or hypoxic stress conditions. The activation of these kinases may play a role in the survival and progression of tumour cells in response to adaptation of growth under the harsh conditions of the tumour microenvironment. It would have been interesting to compare the activation of kinases in MCF7 cells in response to growth under each microenvironmental stress condition also, but unfortunately due to lack of experimental time this experiment was not repeated in MCF7 cells.

SkBr3 and MCF7 BC cells express endogenous levels of VEGFR2, with SkBr3 cells showing an overexpression of the receptor. VEGFR2 has been found to have a possible role in the upregulation of BC cell migration, proliferation and survival (Yan et al., 2015; Nakopoulou et al., 2002; Rydén et al., 2010). Under GF and serum-deprived conditions, non-homeostatic Tier 2 signalling is dependent on relative protein concentrations and occurs when RTKs are non-activated. Non-canonical interactions can occur between proline-rich-motifs within RTK C-terminal tails and the SH3-domains of intracellular signalling molecules, and in turn, can non-canonically activate oncogenic signalling pathways (Timsah et al., 2014; Lin, C.C. et al., 2021). Growth under microenvironmental stress conditions has shown that the proteome of both SkBr3 and MCF7 BC cells change in response to adaptation of growth under serum-deprived and hypoxic conditions. In particular the elevation of VEGFR2 protein expression was observed in response to growth under serum-deprivation stress in both BC cell lines. Therefore, the aberrant utilisation of a Tier 2 mechanism, under serum-deprived conditions, could upregulate survival, resistance and progression pathways in BC cells in adaptation to growth under microenvironmental stress. Here, we investigated whether a non-canonical PPI occurs between VEGFR2 RTK and SH3 domain-containing proteins, known to bind to VEGFR2, in response to growth under nutrient and serum-deprived conditions, in BC cells.

The data presented here determined that the three SH3-domain containing proteins Plcg1, Src and Nck1, all interact with VEGFR2 RTK under serum-deprived conditions in BC cells. Non-canonical PPIs between SH3 domains and proline-rich motifs can occur without GF activation of the RTK (Timsah et al., 2014). Thus, this data suggests that the proteins may bind through a non-canonical Tier 2 SH3-domain:proline-rich interaction with VEGFR2, when under GF and nutrient-deprived conditions. VEGFR2 contains two proline-rich motifs within its intracellular domain, one within the TKD (P908P911) and one within the C-terminal tail (P1195P1198). To elucidate whether the proteins were interacting with VEGFR via binding to an intracellular proline-rich motif of VEGFR2, under serum-deprived conditions, different VEGFR2 constructs were made and utilised. These constructs were made to abrogate SH2-domain binding by implementing a KD mutation which inhibited the

phosphorylation of VEGFR2. Mutation of the two proline-rich motifs (whereby, the important P residues were mutated to A) within VEGFR2 intracellular domain were also implemented. P residues have a distinct structure in peptides and when found as a proline-rich motif exhibit a PPII helix structure that SH3 domains recognise and bind (Teyra et al., 2017). The mutation of P residues to A would abrogate this structure and therefore, SH3 domain binding to this specific SH3-binding site. Both P and A are small non-polar, hydrophobic, amino acid residues, therefore the substitution of P to A should not affect the whole protein conformation. Our findings show that Plcg1, Src and Nck1 all interact with dephosphorylated (KD) VEGFR2 under serum-deprived conditions, in both BC cell lines. The PPIs observed with all three SH3 domain-containing proteins with VEGFR2, under serum-deprived conditions, was abrogated via a second proline-rich motif mutation to the P1195P1198 motif, within the C-terminal tail of VEGFR2. This indicated that this was the protein binding site for the SH3 domain-containing proteins, under serum-deprived conditions. This binding event through the second proline-rich motif of VEGFR2 was further validated with the results obtained from the VEGFR2 C-terminal tail peptide Co-IP. The wildtype VEGFR2 C-terminal tail peptide, which has an intact P1195P1198 proline-rich motif, was observed to interact with all three SH3 domain-containing proteins in both BC cell lines, under serum-deprived conditions. The mutation of the same proline-rich motif (P1195P1198) within the C-terminal peptide of VEGFR2 abrogated the interactions observed between the SH3 domain-containing proteins to the wildtype VEGFR2 C-terminal tail peptide. Plcg1, Src and Nck1 expression have all been found to play a role in BC tumour progression and metastasis (Ottenhoff-Kalff et al., 1992; Lattanzio et al., 2019; Morris et al., 2017). Therefore, these non-classical binding events under serum-deprived stress conditions, via VEGFR2 RTK, may upregulate non-canonical signalling pathways that play a role in tumour cell survival, progression and motility.

It is well-known that SH3 domains bind to proline-rich motifs embedded in the structures of cellular proteins (Yu et al., 1994) and therefore, the results indicated that the binding observed via this proline-rich site of VEGFR2 was through their SH3 binding-domains, under serum-deprived conditions. Further experiments using CFP-tagged domain constructs of both Src and Plcg1 was

used to validate this. The protein expression and Co-IP pull down of CFP-Src domain constructs in both BC cell lines showed that Src SH3 domain was indeed binding to VEGFR2 under serum-starved conditions, in both SkBr3 and MCF7 cells. Src SH2 domain was also observed to bind to VEGFR2 under serum-deprived conditions, but the pY1059 site on VEGFR2 was not probed for, which is the known binding site of Src to VEGFR2 when phosphorylated. Therefore, the binding of Src SH2 domain may occur by binding to basal phosphorylation of pY1059 of VEGFR2 but this could not be elucidated from these results.

The results observed via FRET validated that a non-canonical PPI occurred between the SH3 domain of Src and the P1195P1198 proline-rich motif within VEGFR2 C-terminal tail, in SkBr3 cells, under serum-deprived conditions. The non-canonical PPI via Src SH3 domain was found to be abrogated upon mutation of the P1195P1198 proline-rich motif, further validating that this interaction occurs through this specific proline-rich motif within VEGFR2 C-terminal tail. FRET, is a well-known and validated technique in elucidating PPIs (Kenworthy, 2001) and allows the detection of PPIs via the energy transfer of one excited fluorescent molecule to a fluorescent acceptor molecule, when in the close proximity of up to 10nM in living or fixed cells, using carefully selected donor pairs. However, there are limitations of FRET as a technique to detect PPIs which includes the tag possibly altering the location, conformation and function of the protein of interest and the presence of signal contamination. The interaction between VEGFR2 and Src was via the C-terminal P1195P1198 proline-rich motif, therefore the YFP tag expressed at the N-terminal of the VEGFR2 protein would not disturb the PPI.

Therefore, the novel interaction between Src via its SH3-domain to VEGFR2 P1195P1198 proline-rich motif has been validated in BC cells, under serum-deprived conditions. The binding of Src via its SH3 domain is one of the mechanisms in which Src can become activated (Martin, 2001). Thus, the non-canonical activation of Src and the downstream activation of Src signalling pathways may occur in these BC cells, under serum-deprivation stress. Here, the aberrant activation of a Tier 2 mechanism via the non-canonical activation of Src may contribute towards BC survival, progression and chemoresistance.

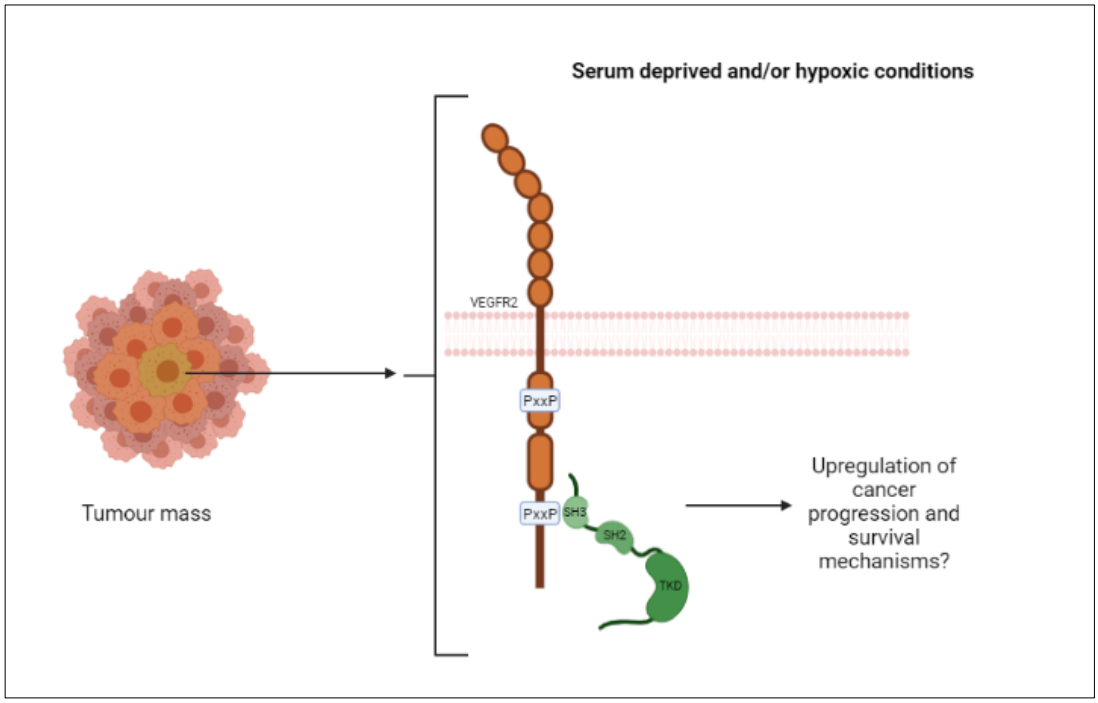

Figure 4.3.1 Proposed model for Src and VEGFR2 interaction under serum-deprived conditions

Src interacts via a non-canonical PPI through its N-terminal SH3 domain to the second proline rich motif, P1195P1198, within the C-terminal tail of VEGFR2, under serum-deprived conditions. This interaction may non-canonically activate Src-kinase through changes to its protein conformation to an active form, via SH3-domain binding to VEGFR2. Therefore, downstream Src-kinase signalling pathways may be upregulated under these microenvironmental stress conditions, in BC cells. The non-canonical activation of a Tier 2 signalling mechanism may contribute towards BC cell survival, progression and resistance.

The CFP Co-IP results showed that Plcg1 was interacting with VEGFR2 via its N-SH2-domain and C-SH2-domain under serum-deprived conditions, in BC cells. Plcg1 was also observed to bind via its C-SH2 domain to basal pY1175 VEGFR2, in both SkBr3 cells and MCF7 cells. This goes against the literature which states that Plcg1 binds through its N-SH2 domain to phosphorylated RTKs (Lemmon and Schlessinger, 2010; Timsah et al., 2016b), whereas the C-SH2 domain is utilised in the activation of Plcg1 via

binding to pY783 on the protein itself, to release autoinhibition and to give Plcg1 its active conformation (Lemmon and Schlessinger, 2010; Gresset et al., 2010). Although, it has not been fully elucidated which particular SH2-domain binds to pY1175 of VEGFR2 and is thus, possible that the binding could be through the C-SH2 domain of Plcg1 interacting with VEGFR2, to induce the activating Y783 and Y775 phosphorylation of Plcg1. The binding of Plcg1 SH3 domain to VEGFR2 was not evident in the CFP pull-down experiment. A limitation to the Co-IP CFP pull-down experiment was the use of a full-length Plcg1 construct and the use of Nck1 domain and full-length constructs. Both Src and Plcg1 constructs were available in the laboratory and after sequencing of the Src construct was found to be correct for all domains and the full-length construct (checked against REFSEQ: accession NM_005417.5). Therefore, these were utilised in making the CFP-tagged constructs to be used in FRET. The Plcg1 SH2-N, SH2-C and SH3 domain sequencing was found to be correct but the full length construct including the PH, X-box and Y-box domains were not and thus, the full length construct was not utilised in these experiments (checked against REFSEQ: accession NM_002660.3). Further study via the use of Nck1 domain constructs with VEGFR2 in BC cells needs to be performed, to further validate the PPI observed between Nck1 and VEGFR2, under serum-starved conditions.

4.3.1 Conclusion

Overall, evidence presented here shows that BC cells change their proteome in response to growth under nutrient-deprivation and hypoxic-induced stress conditions. These conditions simulate the tumour microenvironment of solid tumours, tumours under anti-angiogenic therapy and migrating cancer cells (White, E. Z. et al., 2020). Our results show that BC cells may utilise a Tier 2 mechanism in response to growth under serum-deprived stress conditions. Plcg1, Src and Nck1 are all implicated in oncogenic signalling pathways that upregulate cell survival, proliferation and migration in BC (Sala et al., 2008; Morris et al., 2017; Myoui et al., 2003). The novel non-canonical PPI between Src via its N-terminal SH3-domain to VEGFR2 C-terminal P1195P1198 proline-rich motif, under serum-deprived conditions, was validated from this study. SH3-domain binding of Src kinase is a mode of Src activation (Martin, 2001). Therefore, the non-canonical activation of Src-kinase and downstream

signalling may occur in these BC cells, under serum-deprived stress conditions. Thus, the aberrant activation of a Tier 2 mechanism, downstream of non-canonical Src activation, may contribute towards BC survival, progression and chemoresistance, under microenvironmental stress conditions.

Chapter 5 The downstream signalling and phenotypic effects of non-canonical Tier 2 activation of Src-kinase via VEGFR2-RTK in BC cells

5.1 Introduction

5.1.1 Erk

Extracellular signal-regulated kinase 1/2 (Erk 1/2), are ubiquitous serine-threonine kinases that belong to the MAPK family of proteins. Erk 1/2 (thereafter referred to as Erk) relay mitogen-activated and GF-induced signals as part of a phosphorylation cascade (Anjum and Blenis, 2008; Keshet and Seger, 2010). Erk is a central regulator of an array of cellular processes and activates a diverse cellular response with a large repertoire of downstream substrates. Erk is generally located within the cytoplasm and exists as a homologous dimer. Erk 1/2 are important members of the MAPK/Erk pathway, with molecular weights of 44 and 42kDa, respectively. The aberrant upregulation of this pathway is correlated to tumorigenesis as several upstream activators of Erk are frequently activated in human tumours. The hyperactivation of Erk plays a key role in activating oncogenic signalling pathways and contributes towards cancer progression (Guo, Y.J. et al., 2020).

5.1.1.1 The Erk signalling pathway

The Erk/MAPK signalling pathway has various different activating mechanisms. These include activation in response to changes in intracellular Ca^{2+} levels and through activated RTKs, activation of PKC and through G protein-coupled receptors (Lawrence et al., 2008). MAPK cascades are important cell signalling pathways which regulate many cellular processes, including proliferation, differentiation, apoptosis, and stress response (Keshet and Seger, 2010; Sabio and Davis, 2014; Plotnikov et al., 2011). There are three main kinases within the signalling pathway. These include, MAPK kinase kinase, MAPK kinase and MAPK, which activate downstream effector molecules to relay a signalling response. The Ras/Raf/MEK/Erk pathway is an important MAPK signalling cascade which is aberrantly activated in cancer and plays a crucial role in the survival and development of cancer cells (**Figure**

5.1.1) (Guo, Y.J. et al., 2020). MEK directly interacts with Erk and catalyses the phosphorylation of Y and threonine (T) residues in the 8 ‘TEY box’ of the sub-functional region of Erk, which gives full catalytic activity.

Upon activation of Erk via phosphorylation and dimerisation, Erk can translocate to the nucleus where it regulates transcription factor activity and gene expression (Boulton et al., 1991). Activated Erk also promotes cytoplasmic target protein phosphorylation and regulates the activity of other intracellular protein kinases and the further phosphorylation of downstream substrates. These include the phosphorylation of cytoskeletal components within the cytoplasm which regulate cell morphology and cytoskeletal distribution. Activated Erk within the cytoplasm can also phosphorylate a series of other protein kinases upstream of the Erk pathway in a negative feedback regulatory mechanism. In the nucleus, activated Erk induces the phosphorylation of nuclear transcription factors such as proto-oncogene c-Jun, c-Fos, ETS domain-containing protein (Elk-1), c-Myc and cyclic AMP-dependent transcription factor (ATF2). These factors activate gene expression which regulates cell proliferation, cell cycle progression, survival, migration, and invasion (Eblen, 2018; Kolch, 2000; Schulze et al., 2001; Deming et al., 2008; O'Neill and Kolch, 2004). The large repertoire of signalling pathways and proteins activated via Erk phosphorylation is summarised in **Figure 5.1.2**.

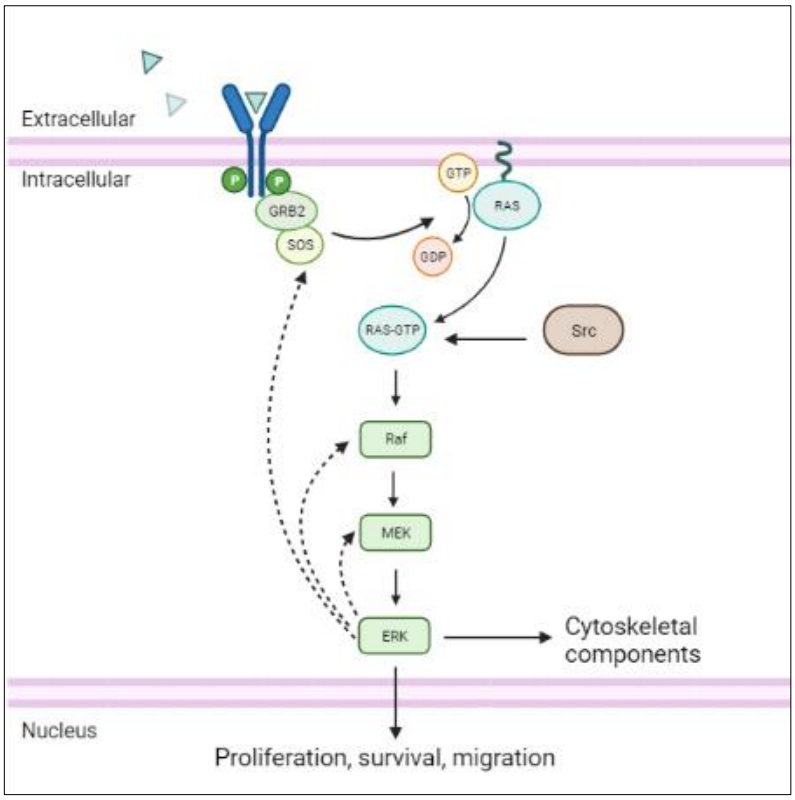

Figure 5.1.1 The Erk/MAPK signalling pathway.

RTK-RAS-induced activation of the kinase-mediated Erk/MAPK signalling cascade via phosphorylation. Erk is the terminal kinase activated within the MAPK cascade and can translocate to the nucleus to activate transcription programmes that mediate proliferation, survival and migration. Erk phosphorylation can activate upstream protein kinases by a negative feedback mechanism (dotted arrows). Cytoskeletal components are activated by pErk within the cytoplasm, which activates cell migration and motility. Adapted from (Guo, Y.J. et al., 2020; Liu, F. et al., 2018), using BioRender.com.

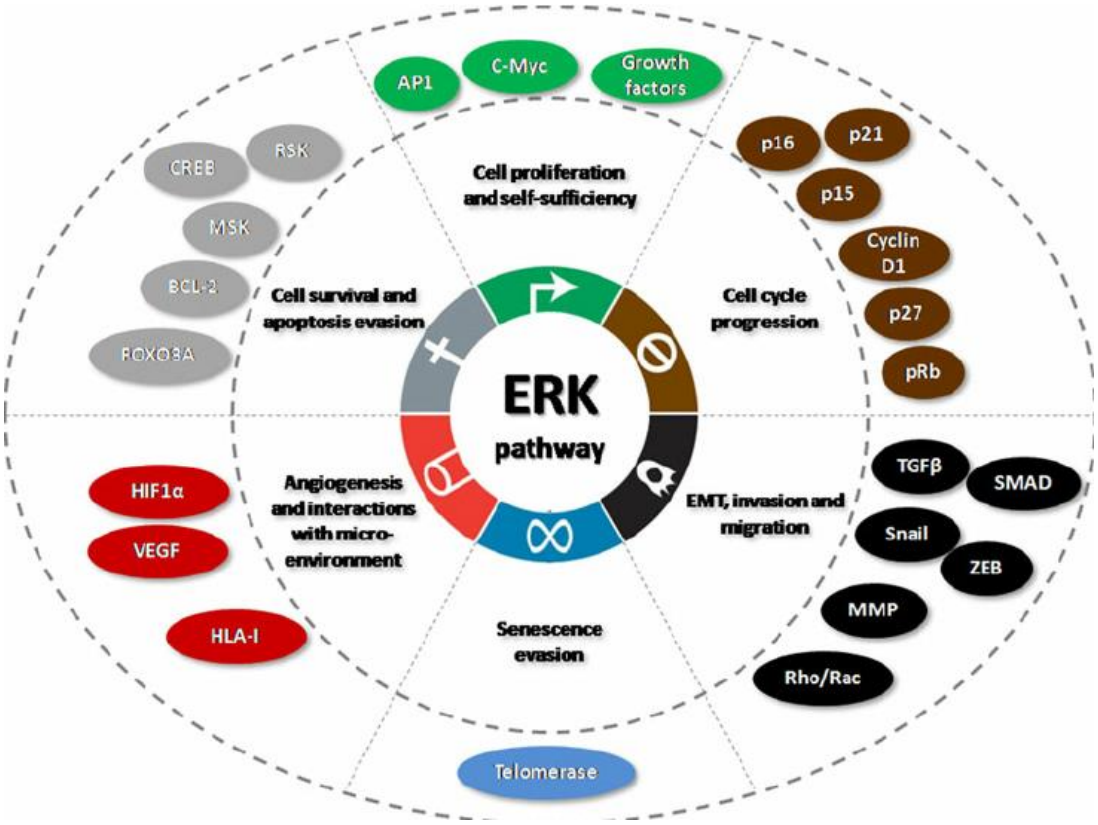

Figure 5.1.2 The diverse repertoire of downstream targets and cellular outcomes of Erk activation.

Erk activation is implicated in the upregulation of many different signalling mechanisms and cellular outcomes. These include cell proliferation and self-sufficiency, cell-cycle progression, EMT, invasion and migration, senescence evasion, angiogenesis and interactions with tumour microenvironment and cell survival and apoptosis evasion (Neuzillet et al., 2013).

5.1.1.2 Erk signalling in BC tumorigenesis

Elevated levels of Erk expression have been found in many different human tumours, including breast, ovarian, colon and lung cancers (Bhartiya and Singh, 2015; Bang et al., 1998; Rao and Herr, 2017; Tang et al., 2017). High Erk expression levels have been found to correlate with a lower survival in TNBC patients (Bartholomeusz et al., 2012). Erk expression has been reported to confer chemoresistance in breast and other cancers, utilising the activation of different evasion mechanisms including reduction of apoptosis, increased cellular proliferation and the up-regulation of drug efflux

transporters (Salaroglio et al., 2019). The expression and activation of Erk was found to be a key factor in patient BC tumorigenesis and BC progression. The expression of Erk increased significantly in BC tissue samples in comparison to the normal tissues. The overexpression of Erk was also found to be correlated with the clinical stage of BC, with higher levels of expressed and activated Erk present in patients of a higher stage of BC (Zhang, X.-m. et al., 2004). Taken together, these data suggests that Erk activation is implicated in BC progression and resistance.

5.1.2 Akt

Protein kinase B or Akt plays a pivotal role in multiple interconnected cell signalling pathways which are implicated in cell metabolism, cell growth, apoptosis suppression and angiogenesis (Bellacosa et al., 1995; Bellacosa et al., 2005; Fresno Vara et al., 2004; Zhao, G.X. et al., 2015; Duronio, 2008). Akt is a serine/threonine kinase consisting of three isoforms (Akt1, Akt2 and Akt3), with molecular weights of 60kDa. Akt plays a critical role downstream of activated RTKs and PI3K. The aberrant activation of Akt and its subsequent downstream signalling is implicated in human cancer and models of tumorigenesis. Akt activation has been found to be one of the most common molecular alterations in human malignancy (Bellacosa et al., 2005).

5.1.2.1 The Akt signalling pathway

The Akt cascade can be upregulated by various signals including through the activation of RTKs, integrins, B and T cell receptors, cytokine receptors and G-protein-coupled receptors. Upstream of Akt activation, PIP_3 is generated as an effect of PI3K activation (Scheid and Woodgett, 2003; Brazil et al., 2004). PIP_3 alters Akt protein conformation via binding to its PH domain and recruiting it to the plasma membrane. This allows phosphoinositide-dependent kinase 1 (PDK1) to phosphorylate Akt at the T308 residue within the TK domain. The full activation of Akt requires a second phosphorylation at regulatory Serine (S) 473 (Song et al., 2005; Altomare and Testa, 2005; Conus et al., 2002; Mora et al., 2004). A number of intracellular kinases have been found to activate Akt to full catalytic activity, including PDK1, integrin-linked kinase (ILK) or an ILK-associated kinase, mTOR and Akt itself (Memmott and Dennis, 2009). Activated Akt upregulates many different downstream signalling

pathways, including the control of cell growth and survival (**Figure 5.1.3**). Such downstream targets of Akt phosphorylation include PRAS40, Paladin, mTOR, cell cycle inhibitors p21 and p27 and Vimentin, all which enhance tumour motility, invasion and metastasis growth (Hers et al., 2011; Liu, P. et al., 2009).

mTOR is a key element in the Akt signalling network. mTOR is a downstream member of the Akt signalling pathway and a key regulator of cell growth and metabolism and can also act as an activator of Akt (Laplante and Sabatini, 2012). Akt directly regulates cell survival by inhibiting pro-apoptotic signals, such as BAD and Forkhead box O (FOXO) transcription factors (Zhang, X. et al., 2011). Tumour suppressor PTEN is the most important negative regulator of Akt function. The phosphatase activity of PTEN acts as an antagonist of PI3K, dephosphorylating PIP_3 to PIP_2 (Newton and Trotman, 2014; Haddadi et al., 2018). Mutations leading to amplification of proteins involved in the PI3K/Akt pathway also include the loss of function of PTEN and are found frequently in cancer tissues. This results in pathologically enhanced PI3K signalling and a loss of cell growth control by evasion of apoptosis (Ouyang et al., 2017).

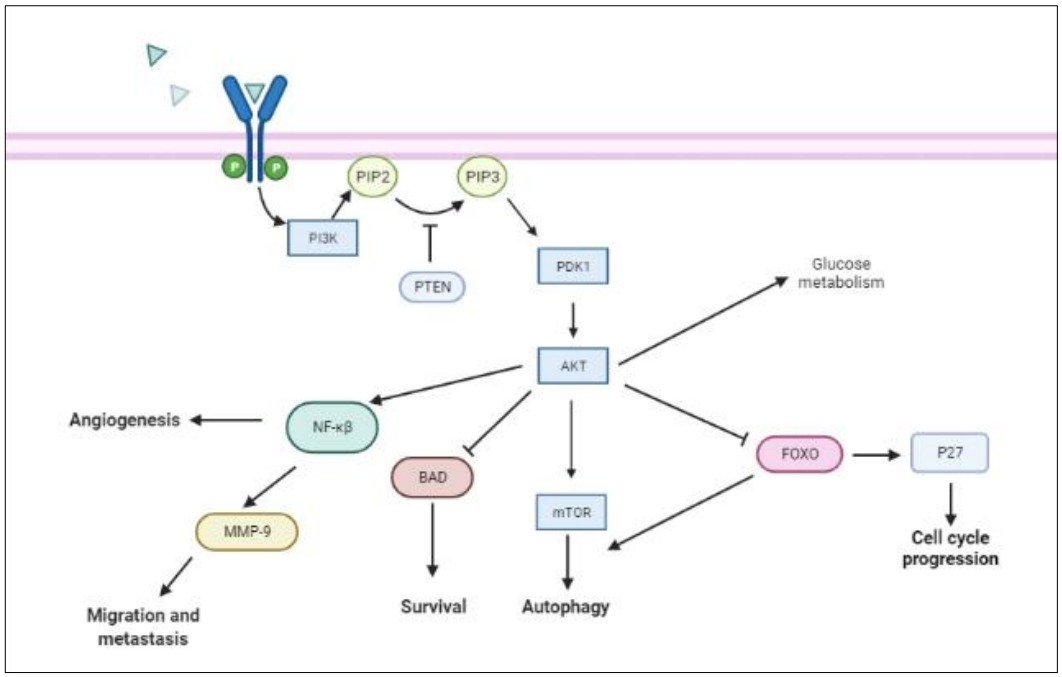

Figure 5.1.3 PI3K/Akt signalling pathway.

RTK activation of PI3K induces the hydrolysis of PIP_2 to PIP_3, which is antagonised by PTEN. PIP_3 within the plasma membrane allows the recruitment of Akt to the membrane and the consequent phosphorylation of Akt by PDK1. Activation of Akt mediates the activation of many different cell signalling pathways including those involved in cell survival migration, metastasis, autophagy, cell cycle progression and angiogenesis. Adapted from (Mitchell and Engelbrecht, 2017), using BioRender.com.

5.1.2.2 Akt signalling in BC tumorigenesis

The hyperactivation of Akt via different pathogenic mechanisms of the PI3K/Akt pathway, have been found in many different cancers and in some cases have been associated with tumour aggressiveness (Nitulescu et al., 2018). The PI3K/Akt pathway has been correlated with resistance to endocrine therapy, chemotherapy and cytotoxic therapy in BC (Nahta, 2012; Paplomata and O'Regan, 2013). Approximately 30-40% of BC patients present PI3K mutations, which induce hyperactivation of the α isoform of PI3K. High levels of Akt activation and PTEN loss have been associated with a poor disease outcome in BC patients (Miricescu et al., 2020). High activation levels

of Akt were found to correlate with increasing levels of cytoplasmic p53 and was associated with a reduced disease-free survival in BC patients (Vestey et al., 2005). BC patients with activated Akt overexpression were significantly correlated with a worse OS and disease-free survival. Activated AKT-overexpressing BC patients also had a 50% higher risk of death and a 30% higher risk of disease recurrence compared to those without phosphorylated Akt overexpression (Yang et al., 2015).

5.1.3 Project rationale

The non-canonical PPI observed between Src-SH3 domain and VEGFR2 P1195P1198 proline-rich motif was validated through the use of Co-IP experiments and FRET in BC cells under serum-deprived conditions in Chapter 4. SH3 domain binding of Src-kinase is known to be a mode of Src activation (Martin, 2001). Therefore, the possible Tier 2 downstream signalling and the physiological relevance of the non-canonical activation of Src is to be explored within this chapter.

Fully activated Src-kinase upregulates many different cellular mechanisms which lead to several phenotypic outcomes, including those promoting cell proliferation, survival, metastasis, invasion and migration (Summy and Gallick, 2006). Active Src leads to the phosphorylation and activation of downstream target proteins which include the PI3K/Akt and Erk/MAPK oncogenic signalling pathways. Thus, whether Src is fully activated through phosphorylation at Y416 (Martin, 2001) in response to the non-canonical binding event with VEGFR2 under serum-deprived conditions in BC cells, is to be elucidated. The aberrant downstream activation of Akt and Erk signalling pathways as a consequence of non-canonical Src activation, is also to be investigated.

High levels of activated Src-kinase have been associated with the development, progression and metastasis of BCs and correlated with a worse prognosis for BC metastasis-free survival (Ottenhoff-Kalff et al., 1992) and with the increased propensity of metastases in animal models of BC (Myoui et al., 2003). Elevated Src activity has also been found in invasive carcinoma BC patient tissues compared with the non-neoplastic tissues (Diaz, N. et al., 2006). These data suggests that high levels of Src activation may aid in a

more malignant and migratory phenotype in BC. Thus, the role of non-canonical Src activation in contributing towards the activation of a migratory phenotype in BC cells under serum-deprived stress is to be investigated. The aberrant activation of a Tier 2 signalling mechanisms as a consequence of the non-canonical activation of Src-kinase through VEGFR2, may contribute towards survival, progression and anti-RTK (ani-VEGFR2) drug-resistance in BCs, when under tumour microenvironmental stress conditions. A schematic of the chapter project rationale is shown in **Figure 5.1.4**.

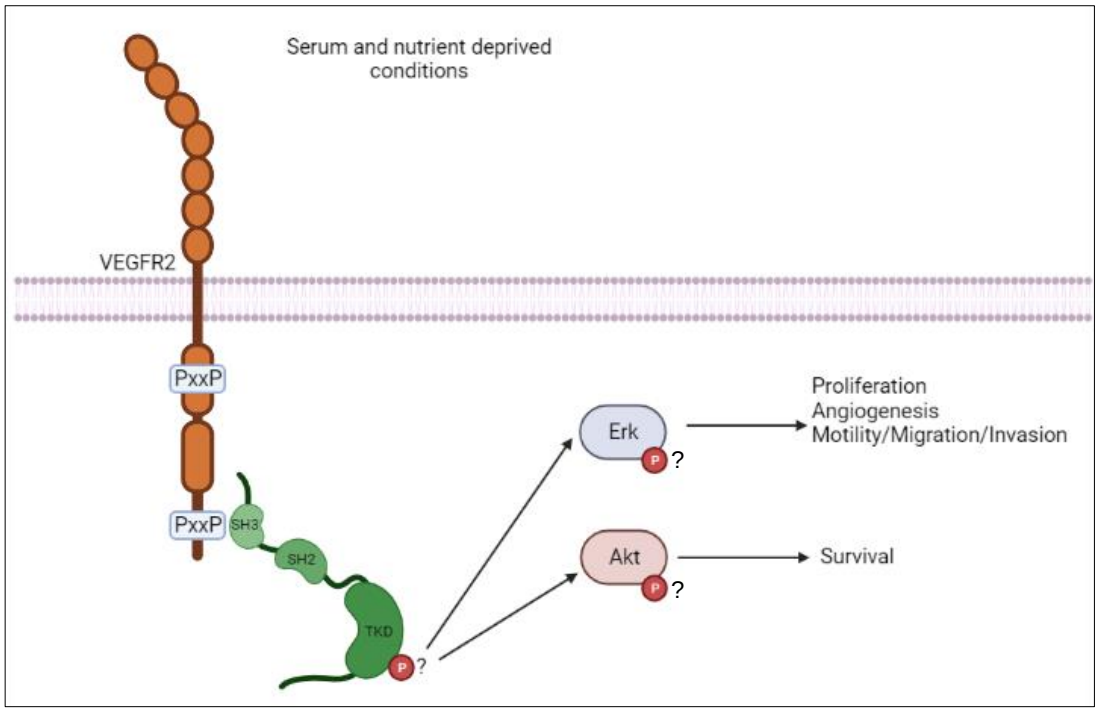

Figure 5.1.4 Hypothesised aberrant Tier 2 downstream signalling of non-canonical Src activation via VEGFR2 in BC cells.

Under serum-deprived conditions, VEGFR2 C-terminal P1195P1198 proline rich motif can interact with Src SH3 domain in BC cells. Therefore, the binding of Src via its SH3-domain could change the conformation of Src to an active form and allow the full activation of Src to occur via phosphorylation at Y416, this could be through a conformation change of Src allowing the phosphorylation of Src to occur via intracellular kinases. Active Src can lead to the upregulation of downstream signalling pathways, including the PI3K/Akt and Erk/MAPK mechanisms. The activation of a Tier 2 downstream signalling pathway via non-canonical Src activation could therefore lead to aberrant oncogenic phenotypic outcomes. These outcomes could be implicated in BC survival, progression and anti-VEGFR2 therapy-resistance, when under microenvironmental stress conditions.

5.1.4 Experimental objectives

In this chapter the following objectives were investigated:

1) To examine whether the non-canonical protein-protein interaction observed in Chapter 4 between Src-SH3 domain and VEGFR2 C-terminal P1195P1198 proline-rich motif, under serum-deprived conditions, leads to the full activation (phosphorylation) of Src-kinase in breast cancer cells. This will be conducted by determining relative active Src phosphorylation levels (Y416) in breast cancer cells overexpressing the mutant VEGFR2-YFP constructs and grown under serum-deprived conditions, via the use of immunoblotting experiments.
2) To determine whether the non-canonical interaction between Src and VEGFR2 observed under serum-deprived conditions in breast cancer cells activates aberrant Tier 2 downstream oncogenic signalling pathways, in particular the Erk and Akt signalling pathways which are both downstream of canonical Src activation. Here, the relative phosphorylation levels of both Erk and Akt will be determined in breast cancer cells with overexpression of the mutant VEGFR2-YFP protein constructs and grown under serum-deprived conditions via immunoblotting.
3) To establish whether the non-canonical interaction between Src and VEGFR2 under serum-deprived conditions in breast cancer cells incurs a migratory phenotypic outcome. To investigate this, a scratch wound migration assay will be performed using the breast cancer cells overexpressing both the VEGFR2-YFP mutant constructs and full length Src-CFP, when grown under serum-deprived conditions
4) To identify whether there is a prognostic significance between protein expression levels of VEGFR2 and Src and breast cancer patient overall survival (OS). Here, the Kaplan Meier Plotter database will be utilised to analyse whether there is any correlation between VEGFR2 and Src protein expression in breast cancer tissue specimens within The Cancer Genome Atlas (TCGA) database and the overall survival levels using clinical information obtained of the corresponding breast cancer patients.

5.2 Results

5.2.1 Src and Erk are activated in response to non-canonical Src:VEGFR2 PPI

The validation of the non-canonical PPI between Src SH3 domain and the second proline-rich motif (P1195P1198) within the C-terminal tail of VEGFR2 in BC cells, under serum-deprived conditions, was shown in Chapter 4 via molecular biology and biochemical techniques. The non-canonical interaction of the SH3-domain of Plcg1 and proline-rich motif within the FGFR2 C-terminal tail, under serum-deprived conditions, was found to activate the oncoprotein Akt and activate the Akt downstream signalling pathway, in ovarian cancer cells (Timsah et al., 2016b). This resulted in the excessive cellular proliferation of ovarian cancer cells and tumour progression observed in a xenograft mouse model. The activation of Akt through FGFR2-mediated non-canonical activation of Plcg1 and the consequent inhibition of PTEN was founded to be a novel cell signalling mechanism. Canonical activation of FGFR2 via FGF ligand-binding phosphorylates Plcg1, which canonically activates PKC and the downstream RAF/MEK/Erk pathway (Touat et al., 2015). Therefore, the non-canonical binding and possible activation of Src-kinase via VEGFR2, under serum-deprived conditions, may activate alternate signalling pathways than when canonically activated through ligand-activated VEGFR2. To determine whether SH3-domain binding of Src to VEGFR2 results in the activation of its full catalytic activity via Y416 phosphorylation (Martin, 2001), under serum-deprived conditions, the phosphorylation status of Src at Y416 was investigated. The overexpression of each mutant VEGFR2-YFP construct was utilised in MCF7 and SkBr3 BC cells. The phosphorylation status of oncoproteins Erk and Akt were also investigated, as their downstream signalling pathways are implicated in RTK oncogenesis (Lemmon and Schlessinger, 2010) and are both phosphorylated downstream of Src activation (Summy and Gallick, 2006).

The effect of overexpression of each mutant VEGFR2-YFP construct, and possible downstream activation was determined via immunoblotting of MCF7 cells (**Figure 5.2.1a.**) and SkBr3 cells (**Figure 5.2.2a.**) and compared to the overexpression of a YFP-tag only vehicle-control (SYFP2) in each cell line.

The cells were grown under serum-deprived conditions (0% FBS) and normoxia for 24 hours. The phosphorylation levels of VEGFR2, Src, Erk and Akt were determined. Densitometry was performed to normalise the relative phosphorylation levels in MCF7 (**Figure 5.2.1b.-e.**) and SkBr3 cells (**Figure 5.2.2b.-e.**) compared to total protein, total YFP and the β-actin loading-control.

Immunoblotting of the BC cells grown under serum-deprived conditions, showed that overexpression of the wildtype VEGFR2 construct gave a basal phosphorylation of VEGFR2 at Y1175 in both MCF7 (**Figure 5.2.1b.**) and SkBr3 cells (**Figure 5.2.2b.**), which has been seen previously **(Figure 4.2.9)**. In both BC cell lines, Src is phosphorylated at the activating phosphorylation site, Y416 at higher levels when the WT, KD and KD P908AP911A VEGFR2 constructs were overexpressed in both MCF7 (**Figure 5.2.1c)** and in SkBr3 cells (**Figure 5.2.2c.**), under serum-deprived conditions, compared to the YFP-only vehicle-control cells. In both BC cell lines, the relative levels of phosphorylated Src at Y416 goes down in cells when the KD P1195AP1198A and the KD 2X PxxP VEGFR2 mutant constructs were overexpressed and thus, when the non-canonical binding of Src SH3 domain to P1195P1198 proline-rich motif within the VEGFR2 C-terminal tail is abrogated, under serum-deprived conditions.

Relative phosphorylated Erk (T202/Y204) levels in MCF7 cells (**Figure 5.2.1d.**) and SkBr3 cells (**Figure 5.2.2d.**) were found to be higher when the WT, KD and KD P908AP911A VEGFR2 constructs were overexpressed, compared to the YFP-tag vehicle-control cells. In both BC cell lines, phosphorylated Erk levels at T202/Y204 was lower when both the KD P1195AP1198A and KD 2x PxxP motif VEGFR2 constructs were overexpressed in both BC cell lines, and thus, also in response to abrogated non-canonical binding of Src via its SH3 domain to the P1195P1198 VEGFR2 C-terminal proline-rich motif, under serum-deprived conditions.

The BC cells gave different results however, for the activation of Akt in response to the overexpression of the different VEGFR2 constructs, under serum-deprived conditions. In MCF7 cells, the relative phosphorylated Akt levels at T308 showed that the phosphorylation levels were higher when the WT VEGFR2 construct was overexpressed compared to the YFP-only

vehicle-control cells (**Figure 5.2.1e.**). Phosphorylated T308 Akt levels went down considerably in comparison to the overexpression of the WT VEGFR2 construct when the KD, KD P908AP911A, KD P1195AP1198A and KD 2x PxxP VEGFR2 mutant constructs were overexpressed. Thus, the phosphorylation of Akt at T308 was found to be at lower levels in response to the KD mutation of VEGFR2 in MCF7 cells. In SkBr3 cells however, the relative levels of phosphorylated T308 Akt levels went up when all VEGFR2 constructs were overexpressed, compared to the YFP-only vehicle-treated control cells (**Figure 5.2.2e.**). The overexpression of KD, KD P908AP911A and KD 2x PxxP VEGFR2 constructs showed very high levels of phosphorylated T308 Akt compared to the vehicle-control and WT VEGFR2 construct. Therefore, Akt phosphorylation at T308 appeared to go up in response to the KD mutation, and therefore, dephosphorylation of the VEGFR2 receptor in SkBr3 cells.

Overall, these results imply that Src is phosphorylated at Y416 in response to the VEGFR2-mediated non-canonical interaction of Src via its SH3 domain to VEGFR2 P1195P1198 proline-rich motif, under serum-deprived conditions. Erk also appears to be phosphorylated downstream of the VEGFR2-mediated non-canonical activation of Src-kinase.

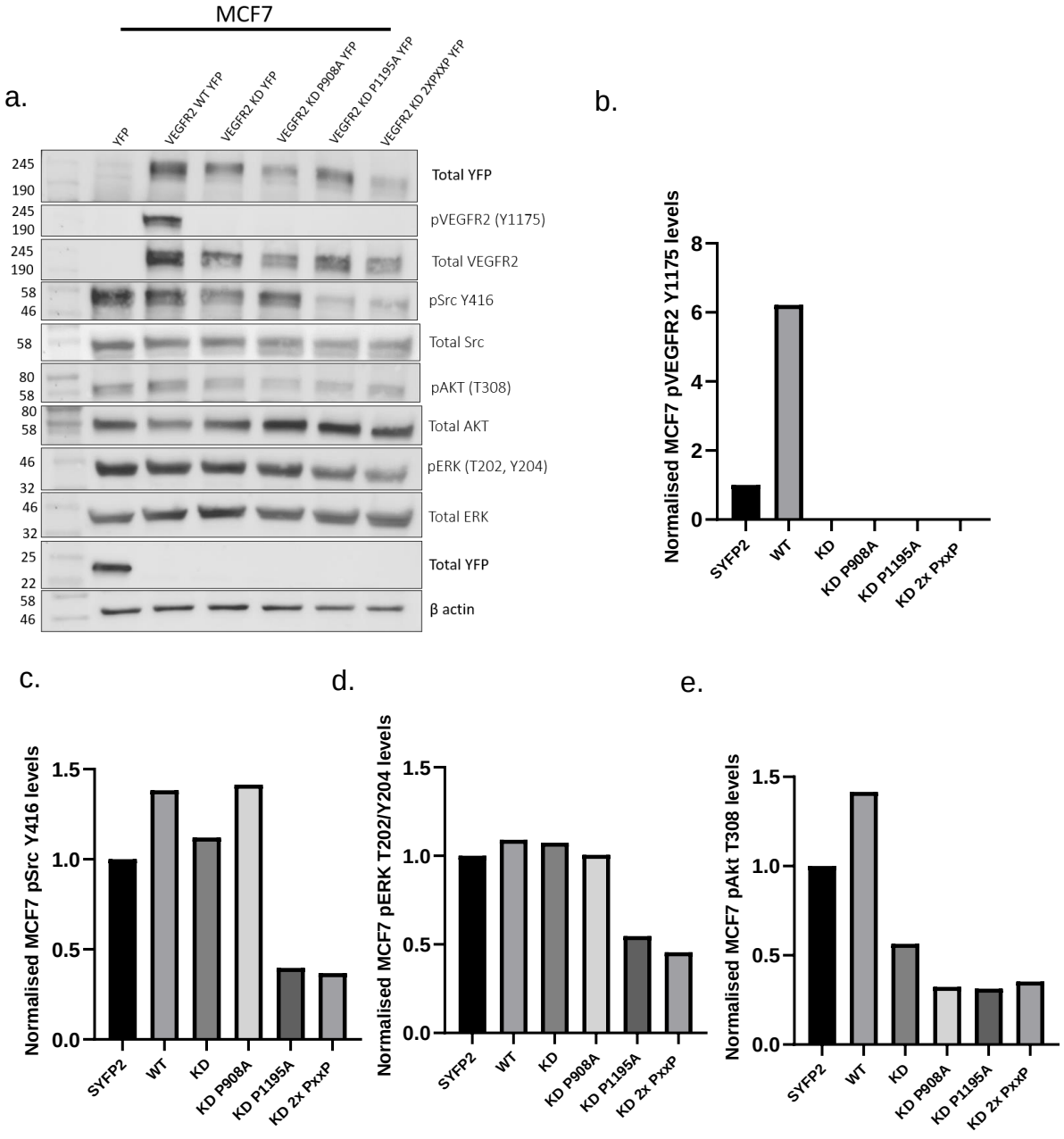

Figure 5.2.1 The effect of VEGFR2-construct overexpression on non-canonical downstream signalling in MCF7 cells, under serum-deprived conditions.

a. An immunoblot of transfected MCF7 cells with each VEGFR2 mutant YFP-construct, to simulate the overexpression of each VEGFR2 mutant variant, grown under serum-deprived (0% FBS) and normoxic (18% O2, 5% CO2) conditions, for 24 hours. The blots were probed for the phosphorylation levels of VEGFR2, Src, Erk and Akt. Graphs **b.**-**e.** show

the normalised densitometry of phosphorylation levels of proteins. Phosphorylated protein were normalised to the total protein expression levels, total YFP levels and all compared to the β-actin loading-control. All phosphorylation levels were calculated as a fold increase/decrease to cells transfected with the SYFP2-tag only vehicle-control.

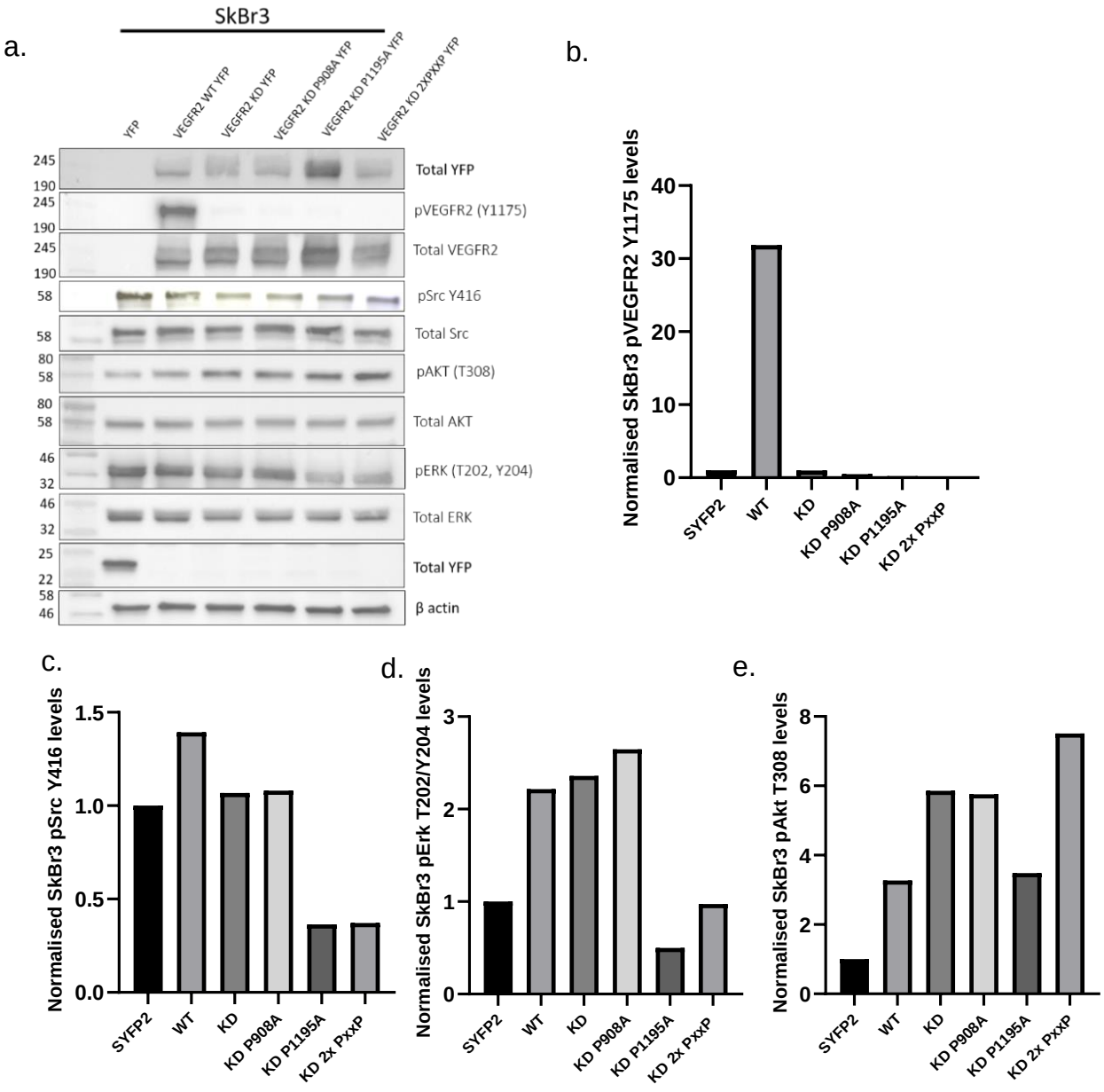

Figure 5.2.2 The effect of VEGFR2-construct overexpression on non-canonical downstream signalling in SkBr3 cells, under serum-deprived conditions.

a. An immunoblot of transfected SkBr3 cells with each VEGFR2 mutant YFP-construct, to simulate the overexpression of each VEGFR2 mutant variant, grown under serum-deprived (0% FBS) and normoxic (18% O_2, 5% CO_2) conditions for 24 hours. The blots were probed for the phosphorylation levels of VEGFR2, Src, Erk and Akt. Graphs **b.**-**e.** show the normalised densitometry of phosphorylation levels of proteins. Pho-

sphorylated protein were normalised to the total protein expression levels, total YFP levels and all compared to the β-actin loading-control. All phosphorylation levels were calculated as a fold increase/decrease to cells transfected with the SYFP2-tag only vehicle-control.

5.2.2 Non-canonical activation of Src via VEGFR2 activates a migratory response when VEGFR2 is dephosphorylated

The non-canonical full-catalytic activation of Src in response to binding via its SH3 domain to VEGFR2, under serum-deprived conditions, was found in both breast cancer cell lines. Src activation is implicated in many cell signalling pathways, including motility, migration, and invasion pathways (Mayer, E.L. and Krop, 2010). Erk activation which is downstream of Src activation has been implicated in different cellular outcomes including proliferation, angiogenesis, migration and invasion (Summy and Gallick, 2006). Erk phosphorylation can activate MLCK and Myosin to promote cellular migration and invasion (Webb et al., 2004). The elevation of activated Src levels have been associated with the development, progression and metastasis of BCs and have been correlated with a low metastasis-free survival in BC patients (Ottenhoff-Kalff et al., 1992) and increased metastasis of the lung and bone in animal models of human BC metastasis (Myoui et al., 2003). High levels of activated Src have also been found in invasive carcinoma BC patient tissues compared with the neighbouring non-neoplastic tissues (Diaz, N. et al., 2006). Therefore, the cellular response of VEGFR2-mediated non-canonical activation of Src and possible downstream activation of Erk in BC cells, under serum-deprived conditions, could be implicated in upregulating a migratory outcome. Thus, the relative migration of BC cells expressing each VEGFR2-YFP construct and full-length Src-CFP was performed using a scratch wound migration assay.

BC cells were transfected with VEGFR2-YFP constructs and a YFP only (SYFP2) vehicle-control, alongside full-length Src-CFP in a collagen-coated 96-well plate, growing in serum-supplemented conditions. After transfection, a scratch was made to confluent transfected MCF7 and SkBr3 cells and the cells were grown in serum-deprived media. Images of the MCF7 (**Figure 5.2.3a**) and SkBr3 cells (**Figure 5.2.4a**) were taken every hour via an IncuCyte. The average wound confluence (%) and wound closure (µM) was calculated over 48 hours of serum-deprivation.

The vehicle-control (SYFP2 + Src-CFP) cells showed the lowest percentage wound confluence for both MCF7 cells (**Figure 5.2.3b.)** and SkBr3 BC cells

(**Figure 5.2.4b.**), when grown under serum-deprived conditions. When both WT VEGFR2-YFP and Src-CFP constructs were co-expressed, the percentage wound confluence went up slightly in comparison to the vehicle control BC cells in MCF7 cells and stayed at a relatively similar level in SkBr3 cells. Interestingly, when both the KD VEGFR2-YFP and Src-CFP constructs were co-expressed and when both the KD P908A VEGFR2-YFP and Src-CFP constructs were co-expressed, the relative percentage wound confluence went up considerably in both BC cell lines, compared to the WT VEGFR2-YFP + Src-CFP BC cells and the vehicle-control BC cells. A significant difference was found with respect to the WT VEGFR2-YFP + Src-CFP cells compared to the KD P908A VEGFR2-YFP + Src-CFP cells in the MCF7 cell line (27.57% +/- 2.98) (P=0.045). When both the KD P1195AP1198A VEGFR2-YFP and Src-CFP constructs were co-expressed and when both the KD 2x PxxP VEGFR2-YFP and Src-CFP constructs were co-expressed, the relative percentage wound closure was found to be lower in both BC cell lines in comparison to the KD VEGFR2-YFP + Src-CFP and KD P908AP911A VEGFR2-YFP + Src-CFP BC cells and was at a similar percentage wound confluence to that seen by the WT VEGFR2-YFP + Src-CFP BC cells.

The average wound closure (μM) was also investigated in both BC cell lines. In MCF7 cells (**Figure 5.2.3c.)** they followed a similar pattern to the percentage wound confluence, showing the highest wound closure when both the KD VEGFR2-YFP and Src-CFP constructs were co-expressed and when both the KD P908AP910A VEGFR2-YFP and Src-CFP constructs were co-expressed in comparison to the WT-VEGFR2-YFP + Src-CFP BC cells and the vehicle-control BC cells. In SkBr3 cells (**Figure 5.2.4c.**) however a higher average wound closure was observed when both the WT VEGFR2-YFP and Src-CFP constructs were co-expressed and when the KD VEGFR2-YFP and Src-CFP constructs were co-expressed, but both had large standard error bars. When SkBr3 cells co-expressed KD P908A VEGFR2-YFP and Src-CFP a lower average wound closure was observed compared to both the WT VEGFR2-YFP + Src-CFP BC cells and the KD VEGFR2-YFP + Src-CFP constructs BC cells. When both the KD P1195A VEGFR2-YFP and Src-CFP constructs were co-expressed and when the KD 2x PxxP VEGFR2-YFP and Src-CFP constructs were co-expressed a lower average wound closure was

observed when compared to the KD-VEGFR2-YFP + Src-CFP cells in both cell lines. Therefore, these results appear to follow the same pattern to that seen with the average percentage wound closure results, whereby, the implementation of the P1195AP1198A mutation of VEGFR2 shows lower migration compared to the expression of the KD VEGFR2 mutant in both BC cell lines.

Overall, migration appears to be upregulated in BC cells upon implementation of the KD mutation and therefore, dephosphorylation of the VEGFR2 receptor, under serum-deprived conditions. Upon mutating the second proline-rich motif within VEGFR2, the migration of BC cells is observed to be much lower in comparison to the cells with expression of the KD and KD P908AP911A VEGFR2 receptor and are observed to be at similar levels to those seen with expression of the WT VEGFR2 receptor.

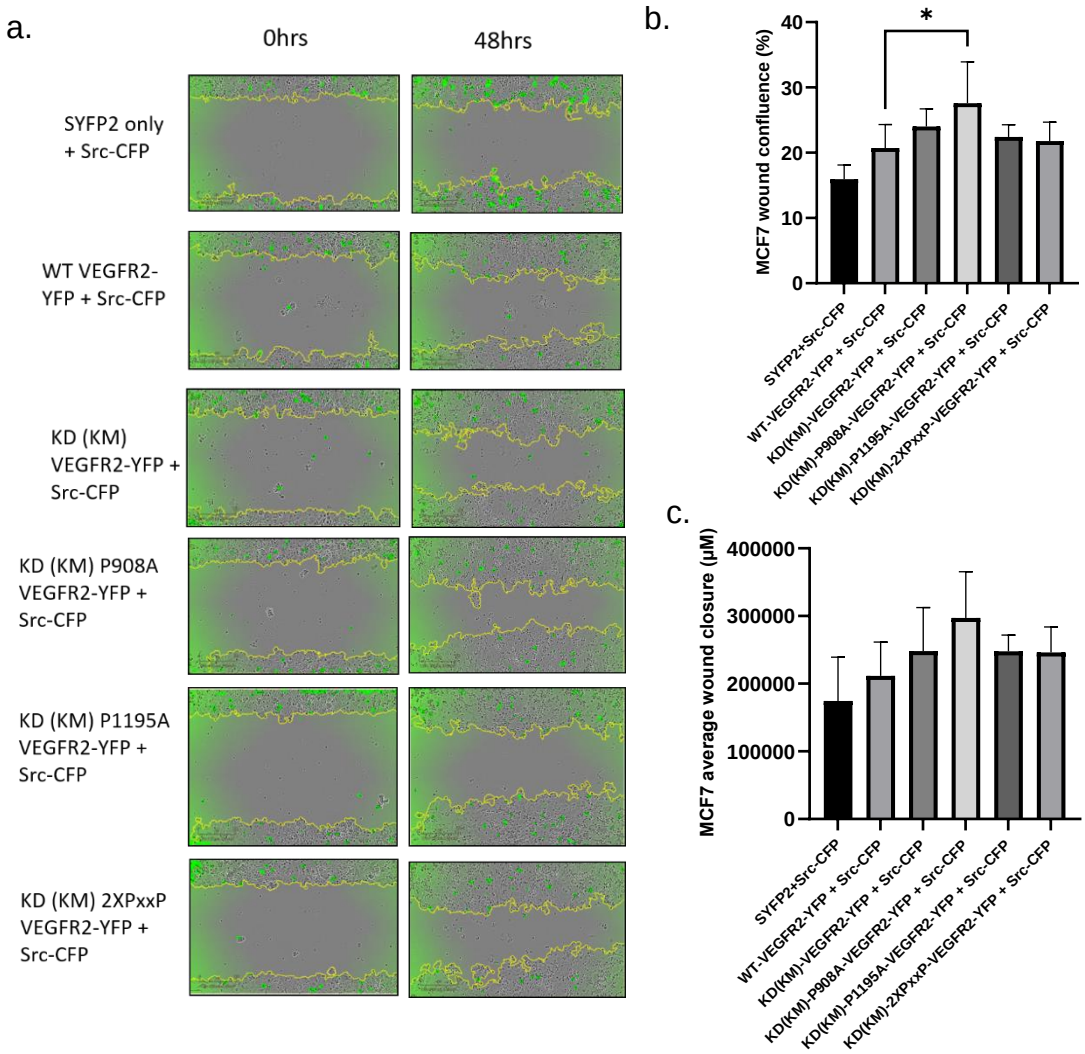

Figure 5.2.3 Cell migration effects of VEGFR2:Src Tier 2 signalling in MCF7 cells, under serum-deprived conditions.

a. Representative images of MCF7 cells grown in a collagen-coated 96 well plate (Essen) under serum-deprived conditions. The cells were transfected with plasmids encoding the expression of VEGFR2-YFP constructs and a YFP only (SYFP2) vehicle-control, alongside a plasmid encoding full-length Src-CFP in each 96-well. A scratch was made to the transfected and confluent cells using a Wound Maker 96 (Essen) and cells were then grown in serum-deprived media. Representative images of the cells were taken at 0hrs and 48hrs after making the scratch. **b.** Average wound confluence (%) of the MCF7 cells normalised to the YFP-only (SYFP2) vehicle-control cells over 48 hours of serum-deprivation. **c.** Average wound closure (µM) of the MCF7 cells normalised to the YFP-only (SYFP2) vehicle-control cells over 48 hours of serum-deprivation.

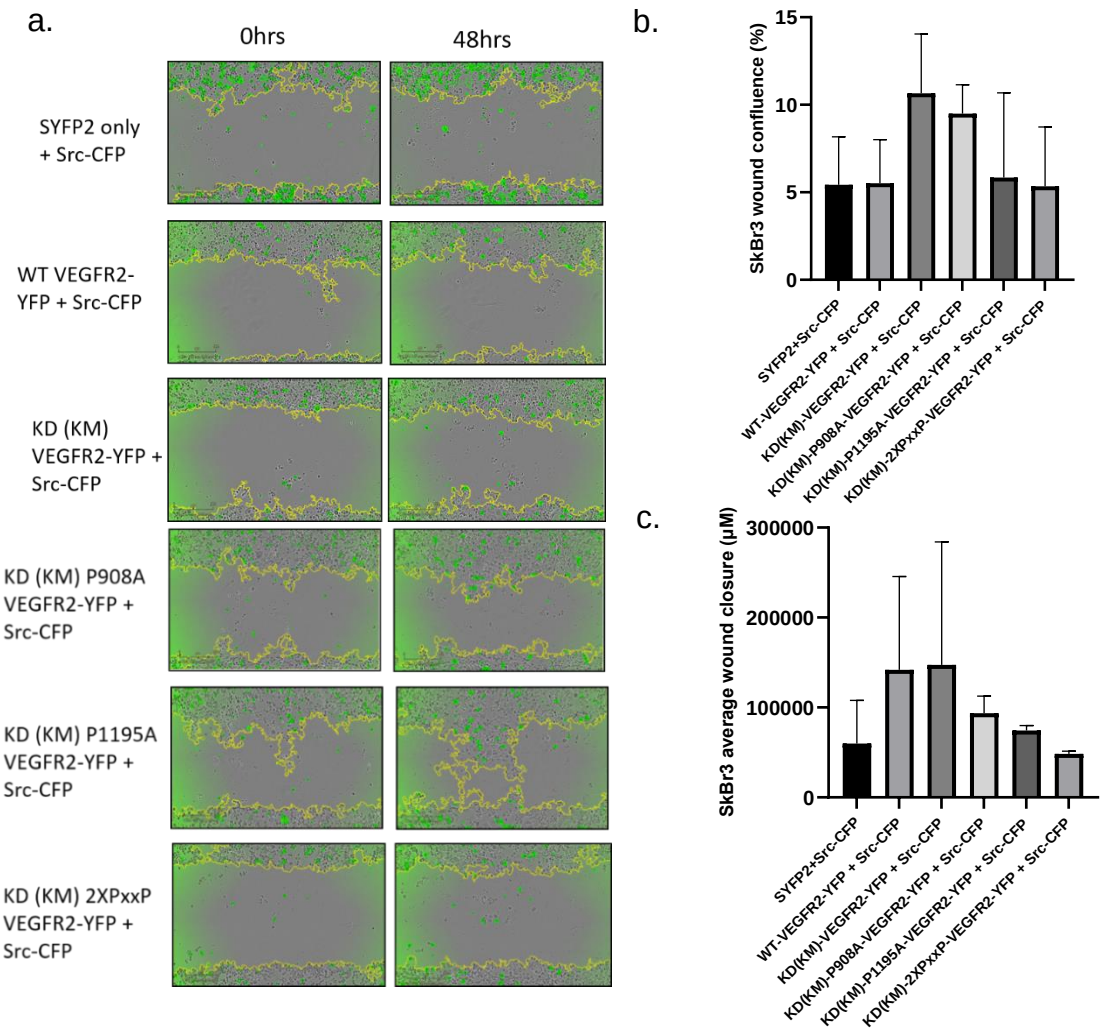

Figure 5.2.4 Cell migration effects of VEGFR2:Src Tier 2 signalling in SkBr3 cells, under serum-deprived conditions

a. Representative images of SkBr3 cells grown in a collagen-coated 96 well plate (Essen) under serum-deprived conditions. The cells were transfected with plasmids encoding the expression of VEGFR2-YFP constructs and a YFP only (SYFP2) vehicle-control, alongside a plasmid encoding full-length Src-CFP in each 96-well. A scratch was made to the transfected and confluent cells using a Wound Maker 96 (Essen) and cells were then grown in serum-deprived media. Representative images of the cells were taken at 0hrs and 48hrs after making the scratch. **b.** Average wound confluence (%) of the SkBr3 cells normalised to the YFP-only (SYFP2) vehicle-control cells over 48 hours of serum-deprivation. **c.** Average wound closure (µM) of the SkBr3 cells normalised to the YFP-only (SYFP2) vehicle-control cells over 48 hours of serum-deprivation.

5.2.3 Independent VEGFR2 and Src expression are associated with a lower OS probability in BC patients

The prognostic value of VEGFR2 (KDR) and Src protein expression levels in BC patients was examined using the Kaplan Meier plotter database. The Kaplan Meier plotter can be used to analyse protein expression and correlate with OS levels using the clinical information from a total of 873 BC patients. OS curves were plotted for all BC patients within the database (n=873) of The Cancer Genome Atlas-reverse phase protein array (TCGA-RPPA) data using UniProt ID: P35968 and ID: P12931 which encodes Human VEGFR2 (KDR) and Human Proto-oncogene tyrosine-protein kinase Src. The plots cover all BC subtypes (ER, PGR and HER2 status, stage, grade, lymph node status, Tumour Node Metastasis stage (TNM)) and all cohorts (race, menopausal status, previous radiation therapy, hormone therapy and chemotherapy).

The Kaplan Meier survival plots obtained showed a lower OS probability in BC patients with a high expression level of VEGFR2, but was not significantly correlated (hazard ratio (HR) = 1.44, 95% confidence interval (95% CI) = 0.97-2.13 and log-rank p value = 0.07) (**Figure 5.2.5a.**). A lower median OS of 97.03 months was calculated in BC patients with high VEGFR2 protein expression compared to a median survival of 148.53 in BC patients with low protein expression of VEGFR2.

A lower OS probability was also found in BC patients with a high expression of Src, but was not significantly correlated (HR = 1.25, 95% CI = 0.87-1.8 and log-rank p value = 0.22) (**Figure 5.2.5b**). A lower median OS of 124.53 months was calculated in BC patients with high Src protein expression compared to a median survival of 142.23 in BC patients with low protein expression of Src.

a.

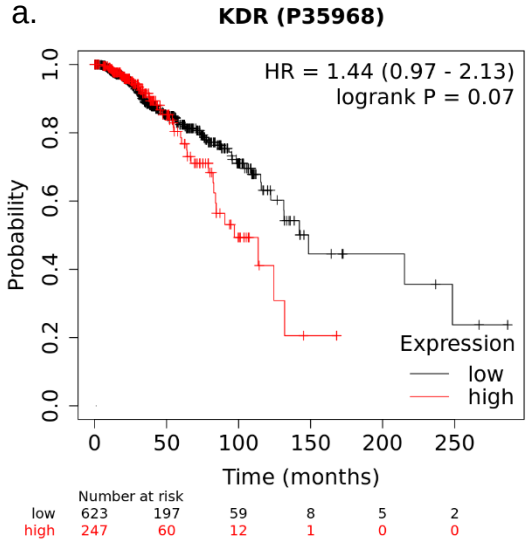

Median overall survival

Low expression cohort (months)	High expression cohort (months)
148.53	97.03

b.

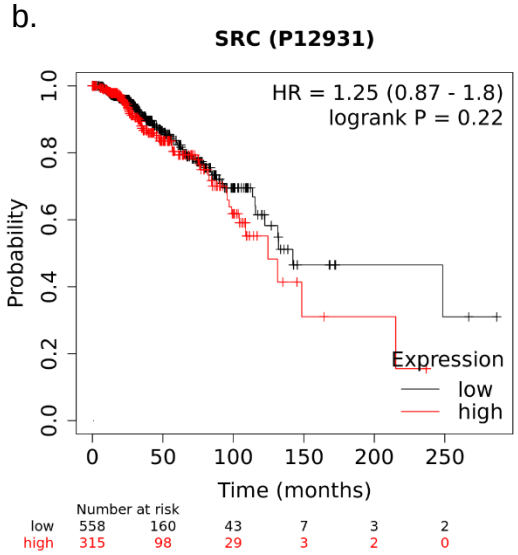

Median overall survival

Low expression cohort (months)	High expression cohort (months)
142.23	124.53

Figure 5.2.5 Independent association of VEGFR2 and Src protein expression levels and overall BC patient survival.

Kaplan Meier OS plots using TCGA-RPPA protein expression BC patient data (n=873 patients). **a.** OS plot of BC patients in respect to VEGFR2 (KDR) low vs. high expression levels and corresponding median OS (months) and **b.** OS plot of BC patients in respect to Src low vs. high expression levels and corresponding median OS (months). Data obtained from http://www.kmplot.com/.

5.3 Discussion

Non-canonical signalling interactions between SH3-domains of intracellular proteins and RTKs, under serum-deprived conditions, has been found to be implicated in upregulating an oncogenic signalling outcome upon changes to relative protein expression levels of the particular proteins involved. When the non-canonical interaction between Plcg1-SH3 domain and FGFR2 C-terminal proline-rich motif occurred at a higher frequency under conditions where Grb2 binding to FGFR2 could be out-competed, Plcg1 non-canonical activation via FGFR2 upregulated the Akt oncogenic signalling pathway via the inhibition of PTEN. This contributed to the excessive proliferation of ovarian cancer cells and towards tumour progression (Timsah et al., 2016b). The prognostic value of the relative protein expression levels of Plcg1, Grb2, and FGFR2 correlated with a higher invasive potential in lung cancer (Timsah et al., 2015). The activation of Akt through non-canonical activation of Plcg1 was found to be a novel signalling mechanism. Therefore, the non-canonical binding and activation of Src-kinase via VEGFR2, under serum-deprived conditions, may activate alternative cell signalling pathways than when canonically activated via ligand-induced VEGFR2 activation in BC cells. Src is known to be implicated in multiple downstream signalling pathways which include the oncogenic signalling pathway Erk/MAPK as well as the PI3K/Akt mechanism. Both signalling cascades upregulate many cellular outcomes including cell survival, angiogenesis, proliferation, cell migration, and invasion (Summy and Gallick, 2006; Finn, 2008). Therefore, the activation of one of these signalling mechanisms may be used to initiate tumorigenesis, progression and chemoresistance under conditions where cancer cells are under nutrient and serum-deprivation stress, via a Tier 2 mechanism of Src activation through VEGFR2.

In this chapter we investigated whether Src-kinase is fully activated via the non-canonical interaction between Src SH3 domain and the P1195P1198 motif of VEGFR2 in BC cells, under serum-deprived conditions. We also examined whether oncogenic signalling mechanisms were upregulated in BC cells when grown under serum-deprived stress conditions, downstream of the Tier 2 non-canonical PPI between Src SH3 domain and the P1195P1198

proline-rich motif of VEGFR2. Additionally, we investigated whether downstream signalling of the Tier 2 non-canonical PPI between Src and VEGFR2 incurs a migratory outcome in BC cells, under serum-deprived conditions. The prognostic significance of both VEGFR2 and Src expression levels in correlation with clinical data of BC patients was also explored. We observed that in both BC cell lines, that Src is phosphorylated at its activating Y416 site in response to binding through its SH3 domain to the intact P1195P1198 proline-rich motif within VEGFR2 C-terminal tail, under serum-deprived conditions. Binding through its SH3 domain is one of the mechanisms of Src activation, but phosphorylation at Y416 gives Src its full catalytic activity (Martin, 2001). The non-canonical PPI between Src SH3 domain and VEGFR2 may render Src to be in its 'open' conformation and thus, leaves the Y416 site free to be phosphorylated by an intracellular kinase. Src can be phosphorylated by the direct binding of FAK and CAS through binding to its SH2-domain within the cytosol (Aleshin and Finn, 2010). FAK is autophosphorylated following the engagement of integrin's at Y397. Y397 is part of a pY-A-E-I motif which binds to Src SH2 domain with a higher affinity than the pY527 site within the C-terminal tail of Src itself, which holds Src in an inactive conformation. Therefore, the binding of activated FAK to Src-SH2 domain displaces the binding of Src via its C-terminal inhibitory phosphosite and leads to the full activation of Src-kinase (Thomas and Brugge, 1997). In turn, Src is known to then fully activate FAK at a number of Y phosphosites to give it full catalytic activity. It has been found that under conditions simulating the breast tumour microenvironment and under anti-angiogenic therapy, BC growth under microenvironmental stress induces c-Met/β1 integrin complex formation which promotes features crucial to overcoming stressors during metastasis or anti-angiogenic therapy (Jahangiri, Arman et al., 2017). The formation of this integrin complex was associated with BC metastases and glioblastoma invasive resistance to bevacizumab. Brain metastases is a common occurrence in BC patients with resistance to bevacizumab (Bergers and Hanahan, 2008; Carbonell et al., 2013; Jahangiri, A. et al., 2013; DeLay et al., 2012; Pàez-Ribes et al., 2009; Kreisl et al., 2009). C-Met/β1 formation was up-regulated in response to growth under hypoxia and under VEGF sequestration, in the presence of bevacizumab. β1 integrin activation is

implicated in mediating metastatic growth of BC cells and leads to the phosphorylation of FAK (Lahlou and Muller, 2011). Therefore, FAK could be activated via this mechanism, mediated by microenvironmental and anti-angiogenic stress in BC cells. We also previously found that FAK phosphorylation levels were high in SkBr3 cells in response to growth under microenvironmental stress conditions. Moreover, the VEGFR2-mediated non-canonical Src activation via Src SH3-domain binding to VEGFR2 C-terminal tail, under serum deprived conditions, appears to be a novel activation mechanism of Src-kinase. Phosphorylated Erk levels were also found to be higher in response to the non-canonical PPI between Src-kinase and VEGFR2, under serum-deprived conditions. Therefore, Erk may be phosphorylated downstream of this VEGFR2-mediated non-canonical PPI. Erk phosphorylation is implicated downstream of Src activation via the phosphorylation of Shc. The phosphorylation of Erk activates multiple downstream signalling pathways and cellular outcomes, including proliferation, angiogenesis and motility, migration and invasion (Summy and Gallick, 2006). In contrast, activated Akt levels in response to overexpression of the VEGFR2 constructs was found to be different for each BC cell line. In MCF7 cells Akt appeared to lose phosphorylation at T308 in response to the dephosphorylation of VEGFR2. On the other hand, SkBr3 cells showed elevated levels of phosphorylated Akt upon dephosphorylation of VEGFR2. However, both of these responses were found to be VEGFR2 P1195P1198 proline-rich motif independent and thus, independent of the non-canonical PPI between Src SH3 domain and VEGFR2 P1195P1198 proline-rich motif within the C-terminal tail. Therefore, Akt is not activated in response to non-canonical activation of Src via VEGFR2. These results were unfortunately only n=1 due to laboratory time restrictions and thus, need to be repeated to obtain statistical validation of these results.

Elevated Src levels have been seen in multiple solid tumours, including BC (Finn, 2008). In models of epithelial cancer, Src activation promotes a more migratory and invasive phenotype, including morphologic and biochemical changes more commonly associated with fibroblasts and cells of mesenchymal origin (Avizienyte and Frame, 2005). Activated Src is associated with the development, progression and metastasis of BCs and a

high expression has been correlated with a low-metastasis-free survival rate in BC patients (Ottenhoff-Kalff et al., 1992). Src activity was also found to be elevated in invasive carcinoma BC patient tissues compared with the neighbouring non-neoplastic tissues (Diaz, N. et al., 2006). Phosphorylated Src has also been found to activate VEGF under hypoxic conditions, to stimulate angiogenesis (Mukhopadhyay et al., 1995), but we found that under serum-deprived conditions, the BC cell lines MCF7 and SkBr3 did not secrete VEGF and therefore our findings under serum-deprived conditions are VEGF independent. Overall, aberrantly high Src activity has been found to be implicated in BC progression, invasion and metastasis. The activation of Erk downstream of non-canonical Src phosphorylation, may also be implicated in a migratory response. Erk activates migration and invasion signalling pathways via regulating cell motility. Erk phosphorylation leads to the activation of MLCK and Myosin. MLCK is implicated in the formation of lamellipodia via the formation of focal adhesions and stress fibres (Vicente-Manzanares et al., 2009). MLCK phosphorylates MLCs which regulate actomyosin contractility at focal adhesions, at the leading edge, which sustains cellular movement (Vicente-Manzanares et al., 2009). Erk also plays a role in focal adhesion turnover at the leading edge of a migrating cell (Drosten et al., 2010; Klein et al., 2008). Here, integrin clustering activates FAK which recruits Src kinase. FAK and Src activate a number of focal adhesion proteins downstream which stimulates actin polymerisation, including Paxillin. Erk is recruited to Paxillin and activated, leading to further phosphorylation of FAK and RAC1 activation (Fincham et al., 2000; Ishibe et al., 2003; Slack-Davis et al., 2003). This promotes actin filament extension and focal adhesion turnover at the leading edge (Ishibe et al., 2004; Woodrow et al., 2003). Erk in turn, phosphorylates FAK at its inhibitory phosphosite, S910 (Zheng et al., 2009). This dual effect of Erk allows for swift turnover of focal adhesions for rapid cell migration.

Here, we investigated the migratory potential of the VEGFR2-mediated non-canonical activation of Src-kinase in BC cells, under serum-deprived conditions and the possible downstream activation of migration signalling pathways. The results from the scratch wound migration assay showed that upregulation of migration of BC cells appeared to be associated with the

VEGFR2-mediated non-canonical activation of Src, when the receptor was dephosphorylated. The migration of the BC cells was upregulated upon dephosphorylation of the VEGFR2 receptor. Upon mutating the second proline-rich motif within VEGFR2 C-terminal tail, and therefore abrogating non-canonical Src activation, the migration levels were found to be lower compared the both the KD VEGFR2 mutant and KD P908AP911A VEGFR2 mutant and of similar levels to that seen with the expression of the WT VEGFR2 receptor. These results indicate that when the VEGFR2 receptor is dephosphorylated and the signalling between VEGFR2 and Src is through SH3 domain:proline-rich VEGFR2 interactions only, a migratory outcome is seen in BC cells. This could be due to this particular interaction occurring more frequently upon dephosphorylation of the receptor, and thus, promotes the binding of Src to occur through its SH3 domain to VEGFR2. Upon mutating the P1195P1198 proline-rich motif within VEGFR2 C-terminal tail, and therefore abrogating non-canonical activation of Src-kinase, the migration is reduced in both BC cell lines compared to the KD receptor and therefore, the upregulation of migration visualised upon dephosphorylation of VEGFR2 occurs via the VEGFR2-mediated non-canonical activation of Src and downstream Tier 2 signalling in BC cells, under serum-deprived conditions. The average wound closure results of the SkBr3 cells were not taken into account in this overall conclusion due to the very large standard error bars for both the WT VEGFR2-YFP + Src-CFP cells and KD VEGFR2-YFP + Src-CFP cells, and thus, the results obtained were not reliable. The standard error bars for the SkBr3 scratch migration assay are in general larger than the MCF7 error bars due to the SkBr3 cells not migrating as much as the MCF7 cells in this experiment. SkBr3 cells did not appear to cope as well with the co-transfection process compared to MCF7 cells, thus a future direction would be to make and utilise VEGFR2 stably expressing BC cell lines of the VEGFR2 mutant constructs and Src, therefore preventing the use of transfection reagents in this experiment.

The patient data obtained from the Kaplan Meier Plotter Database showed an association with independent high levels of VEGFR2 and Src protein expression in BC patients and a lower OS. A significant correlation was not found however, this data indicates a poorer prognosis for BC patients with

higher protein expression levels of VEGFR2 and Src. It would be interesting to see whether dual expression of both VEGFR2 and Src affects BC patient outcome and whether this is correlated with invasive and malignant BC tumours and a worse patient prognosis.

5.3.1 Conclusion

The work presented here shows the utilisation of a novel Tier 2 mechanism in BC cells under serum-deprived stress conditions, via the non-canonical interaction of Src SH3 domain to the P1195P1198 proline-rich motif within VEGFR2 C-terminal tail, which was validated in the previous chapter. The non-canonical activation of Src and Erk was observed in response to the non-canonical PPI between Src and VEGFR2. Non-canonical Src-kinase activation via VEGFR2 was found to play a role in BC cell migration when VEGFR2 was dephosphorylated, and therefore promoting the Src-SH3:VEGFR2-PxxP interaction to occur. Thus, the non-canonical activation of Src may play a role in the phenotypic response of increased cell motility, when BC cells are nutrient and serum-deprived within the middle of a tumour mass and when under anti-angiogenic therapy. Utilisation of this mechanism therefore, has the potential to lead to metastasis in BC cells. Further work needs to be implemented in whether the activation of Erk plays a role in a phenotypic outcome and into the role of non-canonical Src activation and Tier 2 signalling via VEGFR2, in other phenotypic outcomes and chemoresistance. The independent protein expression levels of VEGFR2 and Src were associated with a worse OS in BC patients. Overall, the evidence presented here indicates a role for Tier 2 signalling via VEGFR2-mediated non-canonical activation of Src-kinase, in BC progression and migration and suggests that the relative expression levels of these proteins could provide markers for BC patient metastatic outcome and survival.

Chapter 6 Final discussion

BC has now surpassed lung cancer as the most commonly diagnosed cancer globally and is the leading cause of cancer death among women (Sung, H. et al., 2021). In the UK, around 55,200 new BC cases arise each year, and is the second highest cause of cancer death in women, with around 11,500 deaths a year (CancerResearchUK, 2021). One of the main reasons for the poor prognosis in women is the prevalent rates of BC metastasis (Yan et al., 2015). Despite many advances in treatment, metastatic BC remains essentially incurable (Roy and Perez, 2009). Invasion and metastasis is driven by aberrantly activated cell mechanisms which drive a motile and invasive phenotype (Hanahan and Weinberg, 2011). One way in which BC cells can undergo tumorigenesis and progression is via the aberrant activation of RTKs. RTKs have been found to play a crucial role in tumour progression of BCs. The overexpression of RTKs are implicated in increased BC aggressiveness and disease-free survival (Templeton et al., 2014). The dysregulation of RTK signalling has been implicated in inducing cancer stemness, angiogenesis and metastasis of BCs (Butti et al., 2018). Several RTK inhibitors have been approved for use in BC patient treatment and clinical benefits have been demonstrated in BC patients (Arora and Scholar, 2005). Unfortunately however, BC patients have a high prevalence of *de novo* and/or acquired resistance to RTK-targeted therapy. These tumour recurrences limit the use of anti-RTK therapeutics for treatment of BC and have been explained by the acquisition of certain cellular characteristics at the molecular level that drive a resistant phenotype (Gonzalez-Angulo et al., 2007). Therefore, potential mechanisms that give rise to BC resistance to anti-RTK therapy need to be investigated for successful therapeutic regimens for personalised BC treatment and anti-RTK therapy-resistant BCs.

Our laboratory group discovered a novel signalling mechanism which appears to be initiated in response to perturbation of environmental conditions and cellular stress. This non-classical signal initiation has been termed Tier 2 signalling and is hypothesised to be involved in the maintenance of homeostatic conditions of the cell under periods when there is no external stimulation. Aberrant Tier 2 signalling in response to stress-induced changes in cell protein expression is implicated in tumorigenesis (Timsah et al., 2016a;

Timsah et al., 2015; Lin et al., 2021). Aberrant Tier 2 signalling has been seen to contribute towards oncogenesis and tumour progression in ovarian and lung cancer cells. Non-canonical signalling via FGFR2 RTK and Plcg1 was found to give prognostic significance in ovarian and lung cancer patients. Tier 2 signalling involves the non-canonical activation of intracellular proteins upon binding to proline-rich sites within RTK C-terminal tails via their SH3 domain. There are 58 known RTKs expressed in human cells (Lemmon and Schlessinger, 2010) and around 70% of these receptors express proline-rich sites with the PxxP motif known to be recognised by SH3 domains (Teyra et al., 2017). These sites have the propensity to bind to over 200 intracellular proteins that have over 300 SH3 domains embedded within their structures (Mayer and Gupta, 1998). Proline-rich:SH3 binding events have been found to facilitate specific, moderate to weak interactions that are essential for cell signalling and communication which requires fast, reversible reactions (Bornet et al., 2014). SH3 domains are also highly promiscuous and bind to a wide variety of motifs (Teyra et al., 2017). Therefore, the probability of other proteins binding in such a manner to proline-rich motifs within C-terminal tails of RTKs, under periods of cellular stress is likely. Since Tier 2 signalling does not involve a post-translational modification, as seen via Y phosphorylation in canonical Tier 1 signalling, there is no effective on-off switch for Tier 2 signalling. Tier 2 signalling is thus, dependent solely on the relative intracellular concentrations of SH3 domain-containing proteins and RTKs. Therefore, Tier 2 signalling is able to respond to the changes in protein expression profiles induced by exposing the cell to stress conditions.

This non-canonical signalling between SH3 domain-containing intracellular proteins and RTKs occurs under conditions where there is no external stimulation through binding of extracellular ligands (e.g. GFs). Therefore, this signalling mechanism appears to be physiologically relevant to tumour cells that are under cellular stress of nutrient deprivation through a lack of access to nutrients, GFs and ligands from the tumour vasculature. This can occur within the tumour microenvironment of solid tumours, where a lack of sufficient vasculature leads to a deficiency of nutrients and hypoxia (Anastasiou, 2017). Tumour growth under these conditions can activate signalling pathways which modify tumour behaviour and allow cancer cells to adapt to growth under

stress conditions (Efeyan et al., 2015). These adaptive signalling mechanisms are utilised by advanced tumour cells to enable metastatic-dissemination and growth under anti-angiogenic therapy (White, E. Z. et al., 2020). These adaptive processes have been found to contribute to a more malignant and aggressive cancer phenotype and have been associated with resistance to therapy (Harris, 2002). Consequently, in solid tumour malignancies, including the breast, growth of tumour cells under microenvironmental stress may lead to the aberrant activation of a non-classical Tier 2 signalling mechanism, between RTKs and SH3 domain-containing proteins. Cellular stress can severely alter protein expression levels and thus, give rise to an aberrant signalling outcome when normal homeostatic Tier 2 signalling is out-competed by interactions, whereby the particular proteins involved have elevated expression levels. The activation of oncogenic pathways through non-canonical Tier-2 signalling could aid in cancer progression, survival and drug resistance mechanisms. The role of aberrant RTK expression in BC tumorigenesis and the pathogenesis of BC patients and the high levels of anti-RTK therapy resistance suggest that Tier 2 signalling via RTKs may play a role in BC progression and resistance, under conditions where BC cells are nutrient and serum-deprived. The investigations within this thesis demonstrate the potential of Tier 2 signalling to play a role in BC progression.

Herceptin treatment in BC cells showed batch-to-batch variability concerning Src activation

The initial experiments investigated whether non-canonical activation of Src, via HER2 RTK, could occur under the inhibition of Herceptin in HER2-overexpressing BC cells. The original findings showed promising results, whereby the full catalytic activation of Src occurred under serum-starved conditions, when HER2 was inhibited. The findings here were of particular physiological relevance due to the high levels of Herceptin resistance found in HER2-positive BC patients (Nahta and Esteva, 2006b) and the high levels of relapse and metastasis to the brain after Herceptin therapy (Olson et al., 2013a). HER2 is overexpressed in around 20-25% of invasive breast tumours and has been associated with reduced BC patient survival (Pohlmann et al., 2009). HER2 has previously been validated to bind to a close family member

of Src (Fyn) via HER2 C-terminal proline rich motif to the SH3 domain of Fyn, in a phosphorylation independent manner (Bornet et al., 2014). Src activation was also found to be implicated in Herceptin resistance mechanisms (Zhang, S. et al., 2011) and is known to upregulate cell migration and invasion pathways (Summy and Gallick, 2003). Unfortunately, the original findings were found to be an anomaly which was due to a possible contaminant found in the first batch of drug. After the use of the first batch of drug, the results thereafter showed no activation of Src and thus, our hypothesis was found to be null. Another PhD lab member was investigating the Src-SH3:HER2 proline-rich motif interaction under serum-deprived conditions, in HER2 overexpressing BC cells. The findings concluded that Src could bind via its SH2 and SH3-domain to HER2 under serum-deprived conditions, but no downstream studies were performed on whether these particular interactions gave rise to the activation of an aberrant Tier 2 signalling mechanism via Src SH3 domain and a tumorigenic outcome.

Future work

Further investigation into the activation of downstream oncogenic mechanisms of the Src:HER2 interaction via Src-SH3 domain and HER2 found by another and whether these incur a pathological outcome, could be an important finding for the possibility of the activation of a non-canonical Tier 2 signalling mechanism via HER2 RTK with Src-kinase, under serum-deprived conditions. Thus, a non-canonical Tier 2 mechanism downstream of Src activation in HER2-positive BC cells, under serum-deprived conditions may contribute towards Herceptin resistance and cancer progression when cells are growing under microenvironmental stress. Further study into this possibility needs to be performed.

Non-canonical VEGFR2 interaction with Src-kinase validated in BC cells

VEGFR2 is an RTK which is upregulated in tumour cells in response to growth under conditions which simulate that of the tumour microenvironment within a tumour mass (Olsson et al., 2006; Kranz et al., 1999). Many studies have shed light on the role of VEGFR2 in the initiation of angiogenesis in endothelial cells, but the impact on VEGFR2 expression and signalling in tumour cells has

not been fully elucidated to date (De Palma et al., 2017). The overexpression of VEGFR2 however, has been found in many types of cancer, including the breast and has been linked to the pathogenesis of BC patients (Guo, S. et al., 2010). The upregulation of VEGFR2 mRNA was found earlier in invasive primary and metastatic BCs (Brown et al., 1995). However, how VEGFR2 overexpression and signalling may contribute towards BC tumorigenesis and progression has not been fully examined.

Our findings demonstrated that BC cells change their cellular morphology and proteome in response to growth under conditions simulating the tumour microenvironment of a solid tumour mass. Prominent filopodia and cellular elongation were observed in response to stress-related growth. These characteristics are associated with cells with increased motility and invasion and is implicated with a metastatic phenotype (Machesky, 2008). Results from western blotting profiles of SkBr3 and MCF7 cells confirmed that the relative protein expression levels of VEGFR2 and SH3 domain-containing proteins also changed in response to growth under microenvironmental stress. The proteomic changes were also found to be cell line specific. The two cell lines are of different BC subtypes and thus, the stark differences in response to growth under stress conditions shows the prevalent tumour heterogeneity between BC subtypes, which also contributes towards inconsistencies in therapeutic resistance regimens in BC patients (Aleskandarany et al., 2018). High VEGFR2 expression levels in SkBr3 cells were found in response to growth under hypoxia and serum-deprived conditions and in MCF7 cells under serum-deprived growth only. Overall, an upregulated VEGFR2 expression response was found in both BC cell lines in response to growth under serum-deprived microenvironmental stress. High expression levels of the SH3-domain containing protein, Src, was exhibited in SkBr3 cells in response to growth under serum-deprivation stress conditions and in MCF7 cells, elevated Src levels were observed in response to growth under hypoxia. The elevated expression levels of SH3 domain-containing proteins Plcg1, Src, and Nck1, which are all known to bind to VEGFR2, was observed in response to growth under different microenvironmental stress conditions. Therefore, BC cell growth under microenvironmental stress upregulates the expression levels of both VEGFR2 and SH3 domain-containing proteins. Through immunoblotting

of the relevant media of BC cells grown under the different microenvironmental stress conditions, it was found that under conditions of serum-deprivation that the stark changes in cell morphology and protein expression levels were VEGF independent.

The results from the phospho-kinase array revealed that SkBr3 BC cells exhibited differences in kinase phosphorylation status in response to growth under each microenvironmental stress condition. Serum-deprivation in particular, reduced the number of phosphorylated proteins, which could be an adaptation via the cells 'switching off' certain cellular processes to conserve cellular energy into mechanisms that the cells need to adapt and survive under the harsh growth-conditions. Particular proteins which were phosphorylated in response to serum-deprivation only includes oncoproteins C-Jun, CREB, P70 S6 kinase, Plcg1, and PYK2 which are all implicated in cell survival, proliferation and metastasis (Vleugel, Marije M. et al., 2006; Xiao et al., 2010; Pon et al., 2008; Sala et al., 2008; Al-Juboori et al., 2019). The tumour suppressor proteins p53 and Chk-2 also displayed higher phosphorylation levels in SkBr3 cells grown under serum-deprivation, which are both activated in response to DNA damage and in stress-response (Antoni et al., 2007; Vogelstein et al., 2000). Therefore, the activation of these two proteins may maintain tumour cell survival through DNA-repair. The hyperactivation of kinases was observed in response to growth under hypoxia and in the presence of serum and GFs. This response was hypothesised to be due to the hyperactivation of RTK and GF receptors in adaptation to growth under hypoxic-stress conditions via the binding of available ligands in the FBS serum. Kinases phosphorylated in response to growth under both serum-deprivation and hypoxia included FAK, PRAS40 and CREB which are all implicated in cell proliferation, survival, motility and metastasis (Xiao et al., 2010; Dawson et al., 2021; Lv et al., 2017). The data presented within this thesis revealed the activation of particular kinase in response to growth under microenvironmental stress conditions in BC cells.

Non-canonical PPIs were observed between VEGFR2 and SH3 domain-containing proteins Plcg1, Src, and Nck1 under serum-deprived conditions, via the use of Co-IP and pull-down experiments in BC cells. The Co-IP results from the YFP pull-down, involving the use of VEGFR2-YFP mutant constructs,

confirmed that the mutation of the second proline-rich motif, P1195P1198, within the C-terminal tail of VEGFR2 abrogated the non-canonical PPIs in both BC cell lines. Thus, confirming that the interactions observed between VEGFR2 and the SH3 domain-containing proteins, under serum-deprived conditions, was through binding to the P1195P1198 motif within the C-terminal tail of VEGFR2. Further validation of the interactions occurring through this particular proline-rich motif of VEGFR2, under serum-deprived conditions, was performed via the use of a mutant VEGFR2 C-terminal tail peptide via an MBP pull-down in serum-deprived BC cell lysates. The results from this also concluded that the binding of the SH3 domain-containing proteins was via the P1195P1198 motif. Non-canonical SH3-domain binding of Src to VEGFR2 P1195P1198 proline-rich motif, under serum-deprived conditions in BC cells, was demonstrated through Co-IP and via FRET. Both of these techniques are validated and known methods in detection of PPIs between molecules within cells. These techniques also foster both *in vitro* and *in vivo* methods of PPI detection (Cui et al., 2019). PPIs often require an intact cellular environment, therefore the FRET results validated the Co-IP results obtained from the CFP pull-down experiments.

Future work

Investigations into the proteomic expression profiles of other RTKs and SH3 domain-containing proteins in tumour cells, under microenvironmental-stress growth, may provide further area of study into other possibilities of aberrant Tier 2 signalling mechanisms in various tumour types. Further experiments would need to be performed to elucidate whether Nck1 and Plcg1 also binds via their SH3 domains to the P1195P1198 proline-rich motif within the C-terminal tail of VEGFR2, under serum-deprived conditions in BC cells. The results from the CFP-pull down however, indicated that Plcg1 did not bind via its SH3-domain but via its SH2-domain to VEGFR2 only.

Non-canonical Src interaction via VEGFR2 may activate aberrant Tier 2 oncogenic signalling mechanisms and upregulate a migratory response in BC cells

Immunoblotting results of BC cells with the overexpression of each mutant of VEGFR2 confirmed that Src and Erk were phosphorylated in response to an intact P1195P1198 motif within VEGFR2 C-terminal tail, under serum-deprived conditions. A proposed hypothesis for Src activation at Y416 was through the non-canonical SH3-domain binding to VEGFR2 P1195P1198 proline-rich motif, which changes the conformation of Src to an 'open' state. This open conformation renders Src to be available to phosphorylation at Y416 via intracellular kinases. Src can be phosphorylated and activated via the intracellular kinase, FAK (Aleshin and Finn, 2010). FAK autophosphorylation occurs through integrin's (Thomas and Brugge, 1997). It has previously been reported that the c-Met/β1-integrin is upregulated in response to growth under microenvironmental stress and under the sequestration of VEGF via the anti-angiogenic bevacizumab in BC cells (Jahangiri, Arman et al., 2017). C-Met/β1 formation was associated with the promotion of features important for overcoming these stressors, including increased BC metastases and glioblastoma invasive resistance, a common occurrence after short-lived response to bevacizumab (Bergers and Hanahan, 2008; Carbonell et al., 2013; Jahangiri, A. et al., 2013; DeLay et al., 2012; Pàez-Ribes et al., 2009; Kreisl et al., 2009). β1 integrin activation has been previously found to be implicated in mediating metastatic growth of BC cells and leads to the phosphorylation of FAK (Lahlou and Muller, 2011). Therefore, FAK activation through this mechanism, mediated by microenvironmental and anti-angiogenic stress in BC cells could be a possible mechanism of Src intracellular phosphorylation, via VEGFR2-mediated non-canonical Src conformational activation through SH3-domain binding to VEGFR2. Erk phosphorylation is also implicated downstream of FAK-Src activation, and phosphorylates cytoplasmic proteins MLCK and MLC (Barkan and Chambers, 2011). This signalling is implicated in the formation of lamellipodia via the formation of focal adhesions and stress fibres (Vicente-Manzanares et al., 2009). The activation of Erk is also implicated in upregulating proliferation signalling and thus, further work into the effect of non-canonical Erk activation

with respect to proliferation still needs to be performed. Repeated immunoblotting needs to be accomplished to further validate these findings.

The migration assay results revealed a novel mechanism whereby, the non-canonical activation of Src-kinase via VEGFR2 promoted a migratory phenotype in BC cells, when the VEGFR2 receptor was dephosphorylated. Upon VEGFR2 dephosphorylation, the signalling between VEGFR2 and Src occurs via Src SH3 domain:P1195P1198 VEGFR2 interactions only. Therefore the frequency of Src binding to VEGFR2 in this manner may occur more frequently upon dephosphorylation of the VEGFR2 receptor, and thus, promotes higher levels of non-canonical activation of Src to occur. BC cell migration was reduced upon the mutation of the P1195P1198 motif within VEGFR2 C-terminal tail compared to the expression of the KD VEGFR2 constructs with an intact P1195P1198 proline-rich VEGFR2 motif. Therefore, the migratory response observed in the BC cells upon dephosphorylation of the VEGFR2 receptor appears to be through the non-canonical activation of Src-kinase via the binding through its SH3-domain to VEGFR2 P1195P1198 motif, occurring at a higher frequency. The work presented here supports the utilisation of a novel non-canonical Tier 2 mechanism in BC cells, which is implicated in the activation of cell migration pathways, through the non-canonical activation of Src-kinase. Thus, the aberrant activation of Src and consequent Tier 2 signalling may play a role in the phenotypic response of BC cells, which are under nutrient and serum-deprived microenvironmental stress, for example within a solid tumour mass and under anti-angiogenic therapy. The upregulation of this mechanism, therefore has the potential to lead to BC survival and metastasis when under these microenvironmental stress conditions.

The VEGFR2-YFP-mutant construct pull-down, CFP pull-down and FRET results revealed that a basal phosphorylation of VEGFR2 is maintained under serum-deprived conditions and allows the binding of Src via its SH2 domain to also occur. The migration results indicated that wildtype-VEGFR2 co-expression with Src-kinase showed lower migration levels in BC cells compared to that seen when the receptor was dephosphorylated. The proposed hypothesis here, is that when Src is activated via binding through its SH3 domain only, under serum-deprived microenvironmental stress

conditions, promotes a Tier 2 signalling response and activates downstream migration pathways. The SH2-domain of Src was also observed to bind to wildtype VEGFR2 under serum-deprived conditions in the CFP pull-down and FRET results. When binding of Src can occur via its SH2-domain to basal-phosphorylated wildtype VEGFR2 this appears to maintain a homeostatic signal when cells are under basal conditions and thus, a migratory outcome was not seen with expression of the WT VEGFR2 construct in BC cells. Consequently, the binding of Src to VEGFR2 appears to maintain cellular homeostasis. When binding via its SH3 domain-only prevails, an aberrant Tier 2 mechanism is activated. Therefore, BC utilisation of the non-canonical activation of Src via its SH3 domain may play a role in the activation of BC Tier 2 oncogenic signalling mechanisms, to contribute towards BC cell survival, migration and progression, when under microenvironmental stress growth and under anti-angiogenic therapy. A schematic of the proposed hypothesis of the utilisation of non-canonical Src activation via VEGFR2, to promote BC cell survival and progression via the upregulation of downstream aberrant Tier 2 signalling in BC cells, when under microenvironmental stress conditions is shown in **Figure 6.1**.

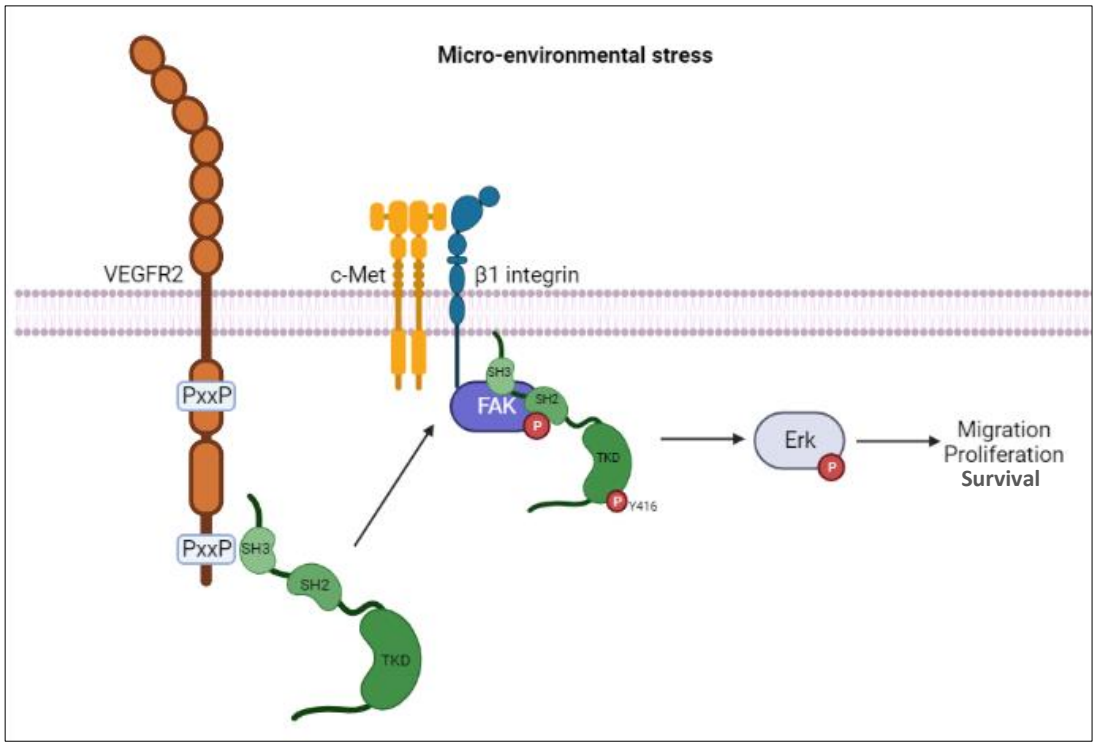

Figure 6.1 The proposed hypothesis of non-canonical Src activation and downstream Tier 2 signalling in BC cells, under microenvironmental stress growth

When the non-canonical binding of Src-kinase occurs via its SH3-domain to VEGFR2 P1195P1198 proline-rich motif, it renders Src to be in an 'open' conformation. FAK, which is activated in response to β1-integrin activation under microenvironmental stress, gives full catalytic activation of Src kinase at Y416. Src activation can phosphorylate Erk downstream of this pathway and therefore activate downstream migration and proliferation pathways in BC cells, under nutrient and serum-deprived microenvironmental stress conditions. These conditions are in response to growth within a tumour mass and when under anti-angiogenic therapy.

Future work

A future direction of the project would be to further investigate into other downstream phenotypic outcomes of Src and Erk signalling, including cellular proliferation as a possible phenotypic outcome of the VEGFR2-mediated non-canonical activation of Src-kinase in BC cells, under serum-deprived conditions. Erk is implicated in the activation of many genes which activate proliferation signalling pathways (Eblen, 2018; Kolch, 2000; Schulze et al., 2001; Deming et al., 2008; O'Neill and Kolch, 2004). Here, a proliferation assay, such as the bromodeoxyuridine (BrdU) incorporation assay which detects DNA synthesis during cell proliferation, could be utilised.

Moreover, further study to validate the particular downstream signalling proteins which are activated by non-canonical Src and Erk activation, their phosphorylation status and other phenotypic outcomes of this non-canonical Tier 2 signalling in BC cells would be an interesting area of study.

Further work into the hypothesised activation mechanism via FAK activation through C1-Met/β1 integrin complex formation in BC cells would need to performed to further validate this hypothesis of FAK activation in response to tumour microenvironmental stress growth conditions. Therefore, the verification of FAK activation playing a role in the full activation of Src via Y416 phosphorylation also needs to be implemented in future study. The activation of kinases seen in the kinase array in response to growth under

microenvironment stress needs to be validated as to whether they are activated downstream of the Tier 2 signalling pathway.

The role of Tier 2 signalling via non-canonical Src activation in drug-resistance mechanisms could also be investigated further, via the treatment of different therapeutic drugs used to treat BC patients and determining whether BC cells with non-canonical activation of Src-kinase show a resistant phenotype compared to control BC cells. This would include investigating the effect of Bevacuzimab treatment which sequesters VEGF-A and the VEGFR2-targeting mAb, Ramucirumab in BC cells and to determine whether Tier 2 signalling through non-canonical Src activation is a possible drug-resistance mechanism in BC.

Final conclusion

The main novel findings here are particularly relevant to BC research. High VEGFR2 expression levels have been correlated with a significantly worse OS in BC patients and is correlated with lymph node metastasis of BC (Yan et al., 2015) and with decreased BC-specific survival (Rydén et al., 2010). The expression of migration markers and proliferation markers have also been correlated with a high level of VEGFR2 expression in BC patient samples (Yan et al., 2015; Nakopoulou et al., 2002). The lower OS of BC patients with high expression levels of VEGFR2 and Src indicates a poorer prognosis for patients with high expression levels of both proteins. Overall, VEGFR2 is overexpressed in BCs and appears to be implicated in tumour metastasis and proliferation. The data presented here suggests a role for Tier 2 signalling via VEGFR2-mediated non-canonical activation of Src-kinase to be implicated in BC progression and migration under microenvironmental stress growth, including tumour growth within a solid tumour mass and when under anti-angiogenic therapy. Therefore, the findings suggest that the relative protein expression levels of VEGFR2 and Src could be used as prognostic factors for BC patient metastatic outcome and survival. Further work needs to be implemented into the possible role of non-canonical Src activation via VEGFR2 and consequential downstream Tier 2 signalling, in other phenotypic outcomes and chemoresistance. Consequently, further insight into this area

of research may contribute towards the development of new therapeutic strategies for personalised BC patient treatment.

In conclusion, the data presented within this thesis supports a novel Tier 2 signalling mechanism in BC cells, which is upregulated in response to growth under nutrient and serum-deprived microenvironmental stress. Here, the non-canonical PPI between VEGFR2 P1195P1198 proline-rich motif and the SH3 domain of Src allows Src kinase to become fully activated via phosphorylation at Y416. This has been hypothesised to occur through the binding of microenvironmental stress-activated FAK intracellular kinase. Further work needs to be carried out to support this theory. Furthermore, the aberrant non-canonical activation of Src-kinase via binding through its SH3 domain to VEGFR2 upregulates BC cell migration. The activation of Erk observed, downstream of non-canonical Src activation via VEGFR2, may play a role in the activation of Tier 2 migration signalling pathways. This novel Tier 2 mechanism of signalling may play an important role in BC survival and progression under growth within the microenvironment of a tumour mass and towards resistance to anti-angiogenic therapies when BC patients are under anti-angiogenic treatment.

List of References

Ahmadiankia, N., Bagheri, M. and Fazli, M. 2019. Nutrient Deprivation Modulates the Metastatic Potential of Breast Cancer Cells. *Rep Biochem Mol Biol.* **8**, 139-146.

Ahmed, Z., Schüller, A.C., Suhling, K., Tregidgo, C. and Ladbury, J.E. 2008. Extracellular point mutations in FGFR2 elicit unexpected changes in intracellular signalling. *Biochem J*. **413**, 37-49.

Ahmed, Z., George, R., Lin, C.C., Suen, K.M., Levitt, J.A., Suhling, K. and Ladbury, J.E. 2010. Direct binding of Grb2 SH3 domain to FGFR2 regulates SHP2 function. *Cell Signal*. **22**, 23-33.

Ahmed, Z., Lin, C.C., Suen, K.M., Melo, F.A., Levitt, J.A., Suhling, K. and Ladbury, J.E. 2013. Grb2 controls phosphorylation of FGFR2 by inhibiting receptor kinase and Shp2 phosphatase activity. *J Cell Biol*. **200**, 493-504.

Ahmed, Z., Timsah, Z., Suen, K.M., Cook, N.P., Lee, G.R., Lin, C.C., Gagea, M., Marti, A.A. and Ladbury, J.E. 2015. Grb2 monomer-dimer equilibrium determines normal versus oncogenic function. *Nat Commun*. **6**, 7354.

Al-Juboori, S.I.K., Vadakekolathu, J., Idri, S., Wagner, S., Zafeiris, D., Pearson, J.R.D., Almshayakhchi, R., Caraglia, M., Desiderio, V., Miles, A.K., Boocock, D.J., Ball, G.R. and Regad, T. 2019. PYK2 promotes HER2-positive breast cancer invasion. *Journal of Experimental & Clinical Cancer Research.* **38**, 210.

Aleshin, A. and Finn, R.S. 2010. SRC: a century of science brought to the clinic. *Neoplasia.* **12**, 599-607.

Aleskandarany, M.A., Vandenberghe, M.E., Marchiò, C., Ellis, I.O., Sapino, A. and Rakha, E.A. 2018. Tumour Heterogeneity of Breast Cancer: From Morphology to Personalised Medicine. *Pathobiology.* **85**, 23-34.

Altomare, D.A. and Testa, J.R. 2005. Perturbations of the AKT signaling pathway in human cancer. *Oncogene.* **24**, 7455-7464.

Anastasiou, D. 2017. Tumour microenvironment factors shaping the cancer metabolism landscape. *Br J Cancer.* **116**, 277-286.

Anders, C.K. and Carey, L.A. 2009. Biology, metastatic patterns, and treatment of patients with triple-negative breast cancer. *Clin Breast Cancer.* **9**, 73-81.

Anjum, R. and Blenis, J. 2008. The RSK family of kinases: emerging roles in cellular signalling. *Nat Rev Mol Cell Biol.* **9**, 747-758.

Antoni, L., Sodha, N., Collins, I. and Garrett, M.D. 2007. CHK2 kinase: cancer susceptibility and cancer therapy – two sides of the same coin? *Nature Reviews Cancer.* **7**, 925-936.

Appert-Collin, A., Hubert, P., Crémel, G. and Bennasroune, A. 2015. Role of ErbB Receptors in Cancer Cell Migration and Invasion. *Front Pharmacol.* **6**, 283.

Arjonen, A., Kaukonen, R. and Ivaska, J. 2011. Filopodia and adhesion in cancer cell motility. *Cell Adh Migr.* **5**, 421-430.

Arora, A. and Scholar, E.M. 2005. Role of tyrosine kinase inhibitors in cancer therapy. *J Pharmacol Exp Ther.* **315**, 971-979.

Aryal, A.C.S., Miyai, K., Izu, Y., Hayata, T., Notomi, T., Noda, M. and Ezura, Y. 2015. Nck influences preosteoblastic/osteoblastic migration and bone mass. *Proc Natl Acad Sci U S A.* **112**, 15432-15437.

Aversa, C., Rossi, V., Geuna, E., Martinello, R., Milani, A., Redana, S., Valabrega, G., Aglietta, M. and Montemurro, F. 2014. Metastatic breast cancer subtypes and central nervous system metastases. *Breast.* **23**, 623-628.

Avizienyte, E. and Frame, M.C. 2005. Src and FAK signalling controls adhesion fate and the epithelial-to-mesenchymal transition. *Current Opinion in Cell Biology.* **17**, 542-547.

Badalian, G., Derecskei, K., Szendroi, A., Szendroi, M. and Tímár, J. 2007. EGFR and VEGFR2 protein expressions in bone metastases of clear cell renal cancer. *Anticancer Res.* **27**, 889-894.

Bang, Y.J., Kwon, J.H., Kang, S.H., Kim, J.W. and Yang, Y.C. 1998. Increased MAPK activity and MKP-1 overexpression in human gastric adenocarcinoma. *Biochem Biophys Res Commun.* **250**, 43-47.

Barkan, D. and Chambers, A.F. 2011. β1-integrin: a potential therapeutic target in the battle against cancer recurrence. *Clin Cancer Res.* **17**, 7219-7223.

Barleon, B., Sozzani, S., Zhou, D., Weich, H.A., Mantovani, A. and Marmé, D. 1996. Migration of human monocytes in response to vascular endothelial growth factor (VEGF) is mediated via the VEGF receptor flt-1. *Blood.* **87**, 3336-3343.

Bartholomeusz, C., Gonzalez-Angulo, A.M., Liu, P., Hayashi, N., Lluch, A., Ferrer-Lozano, J. and Hortobágyi, G.N. 2012. High ERK protein expression levels correlate with shorter survival in triple-negative breast cancer patients. *Oncologist.* **17**, 766-774.

Baselga, J., Albanell, J., Molina, M.A. and Arribas, J. 2001. Mechanism of action of trastuzumab and scientific update. *Semin Oncol.* **28**, 4-11.

Baselga, J. and Swain, S.M. 2009. Novel anticancer targets: revisiting ERBB2 and discovering ERBB3. *Nat Rev Cancer.* **9**, 463-475.

Baselga, J., Tripathy, D., Mendelsohn, J., Baughman, S., Benz, C.C., Dantis, L., Sklarin, N.T., Seidman, A.D., Hudis, C.A., Moore, J., Rosen, P.P., Twaddell, T., Henderson, I.C. and Norton, L. 1996. Phase II study of weekly intravenous recombinant humanized anti-p185HER2 monoclonal antibody in patients with HER2/neu-overexpressing metastatic breast cancer. *J Clin Oncol.* **14**, 737-744.

Bellacosa, A., de Feo, D., Godwin, A.K., Bell, D.W., Cheng, J.Q., Altomare, D.A., Wan, M., Dubeau, L., Scambia, G., Masciullo, V., Ferrandina, G., Benedetti Panici, P., Mancuso, S., Neri, G. and Testa, J.R. 1995. Molecular alterations of the AKT2 oncogene in ovarian and breast carcinomas. *Int J Cancer.* **64**, 280-285.

Bellacosa, A., Kumar, C.C., Di Cristofano, A. and Testa, J.R. 2005. Activation of AKT kinases in cancer: implications for therapeutic targeting. *Adv Cancer Res.* **94**, 29-86.

Belli, S. and Esposito, D. 2020. c-Src and EGFR Inhibition in Molecular Cancer Therapy: What Else Can We Improve? **12**.

Belov, A.A. and Mohammadi, M. 2012. Grb2, a Double-Edged Sword of Receptor Tyrosine Kinase Signaling. *Science Signaling.* **5**, 49.

Bergers, G. and Hanahan, D. 2008. Modes of resistance to anti-angiogenic therapy. *Nature Reviews Cancer.* **8**, 592-603.

Berns, K., Horlings, H.M., Hennessy, B.T., Madiredjo, M., Hijmans, E.M., Beelen, K., Linn, S.C., Gonzalez-Angulo, A.M., Stemke-Hale, K., Hauptmann, M., Beijersbergen, R.L., Mills, G.B., van de Vijver, M.J. and Bernards, R. 2007. A functional genetic approach identifies the PI3K pathway as a major determinant of trastuzumab resistance in breast cancer. *Cancer Cell.* **12**, 395-402.

Bharti, A.C., Vishnoi, K., Singh, S.M. and Aggarwal, B.B. 2018. Chapter 1 - Pathways Linked to Cancer Chemoresistance and Their Targeting by Nutraceuticals. In: Bharti, A.C. and Aggarwal, B.B. eds. *Role of Nutraceuticals in Cancer Chemosensitization.* Academic Press, 1-30.

Bhartiya, D. and Singh, J. 2015. FSH-FSHR3-stem cells in ovary surface epithelium: basis for adult ovarian biology, failure, aging, and cancer. *Reproduction.* **149**, 35-48.

Bladt, F., Aippersbach, E., Gelkop, S., Strasser, G.A., Nash, P., Tafuri, A., Gertler, F.B. and Pawson, T. 2003. The murine Nck SH2/SH3 adaptors are important for the development of mesoderm-derived embryonic structures and for regulating the cellular actin network. *Mol Cell Biol.* **23**, 4586-4597.

Blume-Jensen, P. and Hunter, T. 2001. Oncogenic kinase signalling. *Nature.* **411**, 355-365.

Boggon, T.J. and Eck, M.J. 2004. Structure and regulation of Src family kinases. *Oncogene.* **23**, 7918-7927.

Bornet, O., Nouailler, M., Feracci, M., Sebban-Kreuzer, C., Byrne, D., Halimi, H., Morelli, X., Badache, A. and Guerlesquin, F. 2014. Identification of a Src kinase SH3 binding site in the C-terminal domain of the human ErbB2 receptor tyrosine kinase. *FEBS Lett.* **588**, 2031-2036.

Boulton, T.G., Nye, S.H., Robbins, D.J., Ip, N.Y., Radziejewska, E., Morgenbesser, S.D., DePinho, R.A., Panayotatos, N., Cobb, M.H. and Yancopoulos, G.D. 1991. ERKs: a family of protein-serine/threonine kinases

that are activated and tyrosine phosphorylated in response to insulin and NGF. *Cell.* **65**, 663-675.

Brazil, D.P., Yang, Z.Z. and Hemmings, B.A. 2004. Advances in protein kinase B signalling: AKTion on multiple fronts. *Trends Biochem Sci.* **29**, 233-242.

Bria, E., Cuppone, F., Fornier, M., Nisticò, C., Carlini, P., Milella, M., Sperduti, I., Terzoli, E., Cognetti, F. and Giannarelli, D. 2008. Cardiotoxicity and incidence of brain metastases after adjuvant trastuzumab for early breast cancer: the dark side of the moon? A meta-analysis of the randomized trials. *Breast Cancer Res Treat.* **109**, 231-239.

Brown, L.F., Berse, B., Jackman, R.W., Tognazzi, K., Guidi, A.J., Dvorak, H.F., Senger, D.R., Connolly, J.L. and Schnitt, S.J. 1995. Expression of vascular permeability factor (vascular endothelial growth factor) and its receptors in breast cancer. *Human Pathology.* **26**, 86-91.

Brufsky, A.M., Mayer, M., Rugo, H.S., Kaufman, P.A., Tan-Chiu, E., Tripathy, D., Tudor, I.C., Wang, L.I., Brammer, M.G., Shing, M., Yood, M.U. and Yardley, D.A. 2011. Central nervous system metastases in patients with HER2-positive metastatic breast cancer: incidence, treatment, and survival in patients from registHER. *Clin Cancer Res.* **17**, 4834-4843.

Butti, R., Das, S., Gunasekaran, V.P., Yadav, A.S., Kumar, D. and Kundu, G.C. 2018. Receptor tyrosine kinases (RTKs) in breast cancer: signaling, therapeutic implications and challenges. *Mol Cancer.* **17**, 34.

Cai, S., Sun, P.-H., Resaul, J., Shi, L., Jiang, A., Satherley, L.K., Davies, E.L., Ruge, F., Douglas-Jones, A., Jiang, W.G. and Ye, L. 2017. Expression of phospholipase C isozymes in human breast cancer and their clinical significance. *Oncol Rep.* **37**, 1707-1715.

Carbonell, W.S., DeLay, M., Jahangiri, A., Park, C.C. and Aghi, M.K. 2013. β1 Integrin Targeting Potentiates Antiangiogenic Therapy and Inhibits the Growth of Bevacizumab-Resistant Glioblastoma. *Cancer Research.* **73**, 3145-3154.

Carey, L., Winer, E., Viale, G., Cameron, D. and Gianni, L. 2010. Triple-negative breast cancer: disease entity or title of convenience? *Nat Rev Clin Oncol.* **7**, 683-692.

Carrillo de Santa Pau, E., Arias, F.C., Caso Peláez, E., Muñoz Molina, G.M., Sánchez Hernández, I., Muguruza Trueba, I., Moreno Balsalobre, R., Sacristán López, S., Gómez Pinillos, A. and del Val Toledo Lobo, M. 2009. Prognostic significance of the expression of vascular endothelial growth factors A, B, C, and D and their receptors R1, R2, and R3 in patients with nonsmall cell lung cancer. *Cancer.* **115**, 1701-1712.

Caruso Bavisotto, C., Alberti, G., Vitale, A.M., Paladino, L., Campanella, C., Rappa, F., Gorska, M., Conway de Macario, E., Cappello, F., Macario, A.J.L. and Marino Gammazza, A. 2020. Hsp60 Post-translational Modifications: Functional and Pathological Consequences. *Front Mol Biosci.* **7**, 95.

Castello, A., Gaya, M., Tucholski, J., Oellerich, T., Lu, K.-H., Tafuri, A., Pawson, T., Wienands, J., Engelke, M. and Batista, F.D. 2013. Nck-mediated recruitment of BCAP to the BCR regulates the PI(3)K-Akt pathway in B cells. *Nature Immunology.* **14**, 966-975.

Chaki, S.P., Barhoumi, R., Berginski, M.E., Sreenivasappa, H., Trache, A., Gomez, S.M. and Rivera, G.M. 2013. Nck enables directional cell migration through the coordination of polarized membrane protrusion with adhesion dynamics. *J Cell Sci.* **126**, 1637-1649.

Chaki, S.P., Barhoumi, R. and Rivera, G.M. 2019. Nck adapter proteins promote podosome biogenesis facilitating extracellular matrix degradation and cancer invasion. *Cancer Med.* **8**, 7385-7398.

Chaki, S.P. and Rivera, G.M. 2013. Integration of signaling and cytoskeletal remodeling by Nck in directional cell migration. *Bioarchitecture.* **3**, 57-63.

Chen, H., Ye, D., Xie, X., Chen, B. and Lu, W. 2004. VEGF, VEGFRs expressions and activated STATs in ovarian epithelial carcinoma. *Gynecologic Oncology.* **94**, 630-635.

Christinger, H.W., Fuh, G., de Vos, A.M. and Wiesmann, C. 2004. The crystal structure of placental growth factor in complex with domain 2 of

vascular endothelial growth factor receptor-1. *J Biol Chem.* **279**, 10382-10388.

Cicchetti, P., Mayer, B.J., Thiel, G. and Baltimore, D. 1992. Identification of a protein that binds to the SH3 region of Abl and is similar to Bcr and GAP-rho. *Science.* **257**, 803-806.

Citri, A., Skaria, K.B. and Yarden, Y. 2003. The deaf and the dumb: the biology of ErbB-2 and ErbB-3. *Exp Cell Res.* **284**, 54-65.

Cobleigh, M.A., Vogel, C.L., Tripathy, D., Robert, N.J., Scholl, S., Fehrenbacher, L., Wolter, J.M., Paton, V., Shak, S., Lieberman, G. and Slamon, D.J. 1999. Multinational study of the efficacy and safety of humanized anti-HER2 monoclonal antibody in women who have HER2-overexpressing metastatic breast cancer that has progressed after chemotherapy for metastatic disease. *J Clin Oncol.* **17**, 2639-2648.

Conus, N.M., Hannan, K.M., Cristiano, B.E., Hemmings, B.A. and Pearson, R.B. 2002. Direct identification of tyrosine 474 as a regulatory phosphorylation site for the Akt protein kinase. *J Biol Chem.* **277**, 38021-38028.

Cui, Y., Zhang, X., Yu, M., Zhu, Y., Xing, J. and Lin, J. 2019. Techniques for detecting protein-protein interactions in living cells: principles, limitations, and recent progress. *Sci China Life Sci.* **62**, 619-632.

Dai, X., Cheng, H., Bai, Z. and Li, J. 2017. Breast Cancer Cell Line Classification and Its Relevance with Breast Tumor Subtyping. *J Cancer.* **8**, 3131-3141.

Darlix, A., Louvel, G., Fraisse, J., Jacot, W., Brain, E., Debled, M., Mouret-Reynier, M.A., Goncalves, A., Dalenc, F., Delaloge, S., Campone, M., Augereau, P., Ferrero, J.M., Levy, C., Fumet, J.D., Lecouillard, I., Cottu, P., Petit, T., Uwer, L., Jouannaud, C., Leheurteur, M., Dieras, V., Robain, M., Chevrot, M., Pasquier, D. and Bachelot, T. 2019. Impact of breast cancer molecular subtypes on the incidence, kinetics and prognosis of central nervous system metastases in a large multicentre real-life cohort. *Br J Cancer.* **121**, 991-1000.

Dawson, J.C., Serrels, A., Stupack, D.G., Schlaepfer, D.D. and Frame, M.C. 2021. Targeting FAK in anticancer combination therapies. *Nat Rev Cancer.* **21**, 313-324.

De Palma, M., Biziato, D. and Petrova, T.V. 2017. Microenvironmental regulation of tumour angiogenesis. *Nature Reviews Cancer.* **17**, 457-474.

DeLay, M., Jahangiri, A., Carbonell, W.S., Hu, Y.L., Tsao, S., Tom, M.W., Paquette, J., Tokuyasu, T.A. and Aghi, M.K. 2012. Microarray analysis verifies two distinct phenotypes of glioblastomas resistant to antiangiogenic therapy. *Clin Cancer Res.* **18**, 2930-2942.

Deming, D., Geiger, P., Chen, H., Vaccaro, A., Kunnimalaiyaan, M. and Holen, K. 2008. ZM336372, a Raf-1 activator, causes suppression of proliferation in a human hepatocellular carcinoma cell line. *J Gastrointest Surg.* **12**, 852-857.

Diaz, N., Minton, S., Cox, C., Bowman, T., Gritsko, T., Garcia, R., Eweis, I., Wloch, M., Livingston, S., Seijo, E., Cantor, A., Lee, J.H., Beam, C.A., Sullivan, D., Jove, R. and Muro-Cacho, C.A. 2006. Activation of stat3 in primary tumors from high-risk breast cancer patients is associated with elevated levels of activated SRC and survivin expression. *Clin Cancer Res.* **12**, 20-28.

Diaz, R.J., Ali, S., Qadir, M.G., De La Fuente, M.I., Ivan, M.E. and Komotar, R.J. 2017. The role of bevacizumab in the treatment of glioblastoma. *J Neurooncol.* **133**, 455-467.

Diermeier-Daucher, S., Breindl, S., Buchholz, S., Ortmann, O. and Brockhoff, G. 2011. Modular anti-EGFR and anti-Her2 targeting of SK-BR-3 and BT474 breast cancer cell lines in the presence of ErbB receptor-specific growth factors. *Cytometry A.* **79**, 684-693.

Ditlev, J.A., Michalski, P.J., Huber, G., Rivera, G.M., Mohler, W.A., Loew, L.M. and Mayer, B.J. 2012. Stoichiometry of Nck-dependent actin polymerization in living cells. *J Cell Biol.* **197**, 643-658.

Donnelly, S.K., Weisswange, I., Zettl, M. and Way, M. 2013. WIP provides an essential link between Nck and N-WASP during Arp2/3-dependent actin polymerization. *Curr Biol.* **23**, 999-1006.

Drosten, M., Dhawahir, A., Sum, E.Y., Urosevic, J., Lechuga, C.G., Esteban, L.M., Castellano, E., Guerra, C., Santos, E. and Barbacid, M. 2010. Genetic analysis of Ras signalling pathways in cell proliferation, migration and survival. *Embo j.* **29**, 1091-1104.

Du, Z. and Lovly, C.M. 2018. Mechanisms of receptor tyrosine kinase activation in cancer. *Mol Cancer.* **17**, 58.

Duronio, V. 2008. The life of a cell: apoptosis regulation by the PI3K/PKB pathway. *Biochem J.* **415**, 333-344.

Eblen, S.T. 2018. Extracellular-Regulated Kinases: Signaling From Ras to ERK Substrates to Control Biological Outcomes. *Adv Cancer Res.* **138**, 99-142.

Eccles, S.A. 2005. Targeting key steps in metastatic tumour progression. *Current Opinion in Genetics & Development.* **15**, 77-86.

Eden, S., Rohatgi, R., Podtelejnikov, A.V., Mann, M. and Kirschner, M.W. 2002. Mechanism of regulation of WAVE1-induced actin nucleation by Rac1 and Nck. *Nature.* **418**, 790-793.

Efeyan, A., Comb, W.C. and Sabatini, D.M. 2015. Nutrient-sensing mechanisms and pathways. *Nature.* **517**, 302-310.

Eichler, A.F., Chung, E., Kodack, D.P., Loeffler, J.S., Fukumura, D. and Jain, R.K. 2011. The biology of brain metastases-translation to new therapies. *Nat Rev Clin Oncol.* **8**, 344-356.

Emmanouilidi, A., Lattanzio, R., Sala, G., Piantelli, M. and Falasca, M. 2017. The role of phospholipase Cγ1 in breast cancer and its clinical significance. *Future Oncol.* **13**, 1991-1997.

Eswarakumar, V.P., Lax, I. and Schlessinger, J. 2005. Cellular signaling by fibroblast growth factor receptors. *Cytokine Growth Factor Rev*. **16**, 139-49.

Fearon, A.E. and Grose, R.P. 2014. Grb-ing receptor activation by the tail. *Nat Struct Mol Biol.* **21**, 113-114.

Feng, S., Chen, J.K., Yu, H., Simon, J.A. and Schreiber, S.L. 1994. Two binding orientations for peptides to the Src SH3 domain: development of a general model for SH3-ligand interactions. *Science.* **266**, 1241-1247.

Ferrara, N. and Davis-Smyth, T. 1997. The biology of vascular endothelial growth factor. *Endocr Rev.* **18**, 4-25.

Ferrara, N., Gerber, H.P. and LeCouter, J. 2003. The biology of VEGF and its receptors. *Nat Med.* **9**, 669-676.

Ferrara, N. and Kerbel, R.S. 2005. Angiogenesis as a therapeutic target. *Nature.* **438**, 967-974.

Fincham, V.J., James, M., Frame, M.C. and Winder, S.J. 2000. Active ERK/MAP kinase is targeted to newly forming cell-matrix adhesions by integrin engagement and v-Src. *Embo j.* **19**, 2911-2923.

Finn, R.S. 2008. Targeting Src in breast cancer. *Ann Oncol.* **19**, 1379-1386.

Folkman, J., Merler, E., Abernathy, C. and Williams, G. 1971. Isolation of a tumor factor responsible for angiogenesis. *J Exp Med.* **133**, 275-288.

Forbes, S.A., Tang, G., Bindal, N., Bamford, S., Dawson, E., Cole, C., Kok, C.Y., Jia, M., Ewing, R., Menzies, A., Teague, J.W., Stratton, M.R. and Futreal, P.A. 2010. COSMIC (the Catalogue of Somatic Mutations in Cancer): a resource to investigate acquired mutations in human cancer. *Nucleic Acids Res.* **38**, 652-657.

Fresno Vara, J.A., Casado, E., de Castro, J., Cejas, P., Belda-Iniesta, C. and González-Barón, M. 2004. PI3K/Akt signalling pathway and cancer. *Cancer Treat Rev.* **30**, 193-204.

Fuh, G., Li, B., Crowley, C., Cunningham, B. and Wells, J.A. 1998. Requirements for binding and signaling of the kinase domain receptor for vascular endothelial growth factor. *J Biol Chem.* **273**, 11197-11204.

Geyer, C.E., Forster, J., Lindquist, D., Chan, S., Romieu, C.G., Pienkowski, T., Jagiello-Gruszfeld, A., Crown, J., Chan, A., Kaufman, B., Skarlos, D., Campone, M., Davidson, N., Berger, M., Oliva, C., Rubin, S.D., Stein, S. and Cameron, D. 2006. Lapatinib plus capecitabine for HER2-positive advanced breast cancer. *N Engl J Med.* **355**, 2733-2743.

Gijsen, M., King, P., Perera, T., Parker, P.J., Harris, A.L., Larijani, B. and Kong, A. 2016. Correction: HER2 Phosphorylation Is Maintained by a PKB

Negative Feedback Loop in Response to Anti-HER2 Herceptin in Breast Cancer. *PLoS Biol.* **14**, 1002414.

Gockel, I., Moehler, M., Frerichs, K., Drescher, D., Trinh, T.T., Duenschede, F., Borschitz, T., Schimanski, K., Biesterfeld, S., Herzer, K., Galle, P.R., Lang, H., Junginger, T. and Schimanski, C.C. 2008. Co-expression of receptor tyrosine kinases in esophageal adenocarcinoma and squamous cell cancer. *Oncol Rep.* **20**, 845-850.

Goh, K.I., Cusick, M.E., Valle, D., Childs, B., Vidal, M. and Barabási, A.L. 2007. The human disease network. *Proc Natl Acad Sci U S A.* **104**, 8685-8690.

Gonzalez-Angulo, A.M., Morales-Vasquez, F. and Hortobagyi, G.N. 2007. Overview of resistance to systemic therapy in patients with breast cancer. *Adv Exp Med Biol.* **608**, 1-22.

Gori, S., Rimondini, S., De Angelis, V., Colozza, M., Bisagni, G., Moretti, G., Sidoni, A., Basurto, C., Aristei, C., Anastasi, P. and Crino, L. 2007. Central nervous system metastases in HER-2 positive metastatic breast cancer patients treated with trastuzumab: incidence, survival, and risk factors. *Oncologist.* **12**, 766-773.

Graham, K. and Unger, E. 2018. Overcoming tumor hypoxia as a barrier to radiotherapy, chemotherapy and immunotherapy in cancer treatment. *Int J Nanomedicine.* **13**, 6049-6058.

Gresset, A., Hicks, S.N., Harden, T.K. and Sondek, J. 2010. Mechanism of phosphorylation-induced activation of phospholipase C-gamma isozymes. *J Biol Chem.* **285**, 35836-35847.

Guarino, M. 2010. Src signaling in cancer invasion. *J Cell Physiol.* **223**, 14-26.

Guo, S., Colbert, L.S., Fuller, M., Zhang, Y. and Gonzalez-Perez, R.R. 2010. Vascular endothelial growth factor receptor-2 in breast cancer. *Biochim Biophys Acta.* **1806**, 108-121.

Guo, Y.J., Pan, W.W., Liu, S.B., Shen, Z.F., Xu, Y. and Hu, L.L. 2020. ERK/MAPK signalling pathway and tumorigenesis (Review). *Exp Ther Med.* **19**, 1997-2007.

Gupta, M.K. and Qin, R.Y. 2003. Mechanism and its regulation of tumor-induced angiogenesis. *World J Gastroenterol*. **9**, 1144-1155.

Hadari, YR., Kouhara, H., Lax, I. and Schlessinger, J. 1998. Binding of Shp2 tyrosine phosphatase to FRS2 is essential for fibroblast growth factor-induced PC12 cell differentiation. *Mol Cell Biol*. **18**, 3966-3973.

Haddadi, N., Lin, Y., Travis, G., Simpson, A.M., Nassif, N.T. and McGowan, E.M. 2018. PTEN/PTENP1: 'Regulating the regulator of RTK-dependent PI3K/Akt signalling', new targets for cancer therapy. *Mol Cancer.* **17**, 37.

Hanahan, D. and Weinberg, R.A. 2011. Hallmarks of cancer: the next generation. *Cell.* **144**, 646-674.

Hao, J.J., Liu, Y., Kruhlak, M., Debell, K.E., Rellahan, B.L. and Shaw, S. 2009. Phospholipase C-mediated hydrolysis of PIP2 releases ERM proteins from lymphocyte membrane. *J Cell Biol.* **184**, 451-462.

Harris, A.L. 2002. Hypoxia — a key regulatory factor in tumour growth. *Nature Reviews Cancer.* **2**, 38-47.

Hayes, D.F., Miller, K. and Sledge, G. 2007. Angiogenesis as targeted breast cancer therapy. *The Breast.* **16**, 17-19.

He, M. and Wei, M.J. 2012. Reversing multidrug resistance by tyrosine kinase inhibitors. *Chin J Cancer.* **31**, 126-133.

Hers, I., Vincent, E.E. and Tavaré, J.M. 2011. Akt signalling in health and disease. *Cell Signal.* **23**, 1515-1527.

Holmes, K., Roberts, O.L., Thomas, A.M. and Cross, M.J. 2007. Vascular endothelial growth factor receptor-2: Structure, function, intracellular signalling and therapeutic inhibition. *Cellular Signalling.* **19**, 2003-2012.

Huang, K., Andersson, C., Roomans, G.M., Ito, N. and Claesson-Welsh, L. 2001. Signaling properties of VEGF receptor-1 and -2 homo- and heterodimers. *The International Journal of Biochemistry & Cell Biology.* **33**, 315-324.

Huang, L. and Fu, L. 2015. Mechanisms of resistance to EGFR tyrosine kinase inhibitors. *Acta Pharm Sin B.* **5**, 390-401.

Hubbard, S.R., Mohammadi, M. and Schlessinger, J. 1998. Autoregulatory mechanisms in protein-tyrosine kinases. *J Biol Chem.* **273**, 11987-11990.

Hurvitz, S.A., Martin, M., Symmans, W.F., Jung, K.H., Huang, C.S., Thompson, A.M., Harbeck, N., Valero, V., Stroyakovskiy, D., Wildiers, H., Campone, M., Boileau, J.F., Beckmann, M.W., Afenjar, K., Fresco, R., Helms, H.J., Xu, J., Lin, Y.G., Sparano, J. and Slamon, D. 2018. Neoadjuvant trastuzumab, pertuzumab, and chemotherapy versus trastuzumab emtansine plus pertuzumab in patients with HER2-positive breast cancer (KRISTINE): a randomised, open-label, multicentre, phase 3 trial. *Lancet Oncol.* **19**, 115-126.

Huse, M. and Kuriyan, J. 2002. The conformational plasticity of protein kinases. *Cell.* **109**, 275-282.

Ibrahim, S.A., Gadalla, R., El-Ghonaimy, E.A., Samir, O., Mohamed, H.T., Hassan, H., Greve, B., El-Shinawi, M., Mohamed, M.M. and Götte, M. 2017. Syndecan-1 is a novel molecular marker for triple negative inflammatory breast cancer and modulates the cancer stem cell phenotype via the IL-6/STAT3, Notch and EGFR signaling pathways. *Mol Cancer.* **16**, 57.

Irby, R.B. and Yeatman, T.J. 2000. Role of Src expression and activation in human cancer. *Oncogene.* **19**, 5636-5642.

Ishibe, S., Joly, D., Liu, Z.X. and Cantley, L.G. 2004. Paxillin serves as an ERK-regulated scaffold for coordinating FAK and Rac activation in epithelial morphogenesis. *Mol Cell.* **16**, 257-267.

Ishibe, S., Joly, D., Zhu, X. and Cantley, L.G. 2003. Phosphorylation-dependent paxillin-ERK association mediates hepatocyte growth factor-stimulated epithelial morphogenesis. *Mol Cell.* **12**, 1275-1285.

Itakura, J., Ishiwata, T., Shen, B., Kornmann, M. and Korc, M. 2000. Concomitant over-expression of vascular endothelial growth factor and its receptors in pancreatic cancer. *Int J Cancer.* **85**, 27-34.

Iwata, H., Narabayashi, M., Ito, Y., Saji, S., Fujiwara, Y., Usami, S., Katsura, K. and Sasaki, Y. 2013. A phase II study of lapatinib for brain metastases in patients with HER2-overexpressing breast cancer following trastuzumab

based systemic therapy and cranial radiotherapy: subset analysis of Japanese patients. *Int J Clin Oncol.* **18**, 621-628.

Izuishi, K., Kato, K., Ogura, T., Kinoshita, T. and Esumi, H. 2000. Remarkable tolerance of tumor cells to nutrient deprivation: possible new biochemical target for cancer therapy. *Cancer Res.* **60**, 6201-6207.

Jahangiri, A., De Lay, M., Miller, L.M., Carbonell, W.S., Hu, Y.L., Lu, K., Tom, M.W., Paquette, J., Tokuyasu, T.A., Tsao, S., Marshall, R., Perry, A., Bjorgan, K.M., Chaumeil, M.M., Ronen, S.M., Bergers, G. and Aghi, M.K. 2013. Gene expression profile identifies tyrosine kinase c-Met as a targetable mediator of antiangiogenic therapy resistance. *Clin Cancer Res.* **19**, 1773-1783.

Jahangiri, A., Nguyen, A., Chandra, A., Sidorov, M.K., Yagnik, G., Rick, J., Han, S.W., Chen, W., Flanigan, P.M., Schneidman-Duhovny, D., Mascharak, S., De Lay, M., Imber, B., Park, C.C., Matsumoto, K., Lu, K., Bergers, G., Sali, A., Weiss, W.A. and Aghi, M.K. 2017. Cross-activating c-Met/β1 integrin complex drives metastasis and invasive resistance in cancer. *Proceedings of the National Academy of Sciences.* **114**, 8685-8694.

Jang, K., Kim, M., Gilbert, C.A., Simpkins, F., Ince, T.A. and Slingerland, J.M. 2017. VEGFA activates an epigenetic pathway upregulating ovarian cancer-initiating cells. *EMBO Mol Med.* **9**, 304-318.

Jemal, A., Siegel, R., Xu, J. and Ward, E. 2010. Cancer statistics, 2010. *CA Cancer J Clin.* **60**, 277-300.

Jiang, Z., Wang, L., Liu, X., Chen, C., Wang, B., Wang, W., Hu, C., Yu, K., Qi, Z., Liu, Q., Wang, A., Liu, J., Hong, G., Wang, W. and Liu, Q. 2020. Discovery of a highly selective VEGFR2 kinase inhibitor CHMFL-VEGFR2-002 as a novel anti-angiogenesis agent. *Acta Pharmaceutica Sinica B.* **10**, 488-497.

Jones, R.B., Gordus, A., Krall, J.A. and MacBeath, G. 2006. A quantitative protein interaction network for the ErbB receptors using protein microarrays. *Nature.* **439**, 168-174.

Kaplan, M.A., Ertugrul, H., Firat, U., Kucukoner, M., Inal, A., Urakci, Z., Pekkolay, Z. and Isikdogan, A. 2015. Brain metastases in HER2-positive

metastatic breast cancer patients who received chemotherapy with or without trastuzumab. *Breast Cancer.* **22**, 503-509.

Karkkainen, M.J., Mäkinen, T. and Alitalo, K. 2002. Lymphatic endothelium: a new frontier of metastasis research. *Nat Cell Biol.* **4**, 2-5.

Kay, B.K., Williamson, M.P. and Sudol, M. 2000. The importance of being proline: the interaction of proline-rich motifs in signaling proteins with their cognate domains. *Faseb j.* **14**, 231-241.

Kendall, R.L. and Thomas, K.A. 1993. Inhibition of vascular endothelial cell growth factor activity by an endogenously encoded soluble receptor. *Proc Natl Acad Sci U S A.* **90**, 10705-10709.

Kennecke, H., Yerushalmi, R., Woods, R., Cheang, M.C., Voduc, D., Speers, C.H., Nielsen, T.O. and Gelmon, K. 2010. Metastatic behavior of breast cancer subtypes. *J Clin Oncol.* **28**, 3271-3277.

Kenworthy, A.K. 2001. Imaging protein-protein interactions using fluorescence resonance energy transfer microscopy. *Methods.* **24**, 289-296.

Keshet, Y. and Seger, R. 2010. The MAP kinase signaling cascades: a system of hundreds of components regulates a diverse array of physiological functions. *Methods Mol Biol.* **661**, 3-38.

Kim, R.D., Lazaryan, A., Aucejo, F., Eghtesad, B., Pelley, R., Fung, J., Miller, C. and Yerian, L. 2008. Vascular endothelial growth factor receptor 2 (VEGFr2) expression and recurrence of hepatocellular carcinoma following liver transplantation: The Cleveland Clinic experience. *Journal of Clinical Oncology.* **26**, 4594-4594.

Klein, R.M., Spofford, L.S., Abel, E.V., Ortiz, A. and Aplin, A.E. 2008. B-RAF regulation of Rnd3 participates in actin cytoskeletal and focal adhesion organization. *Mol Biol Cell.* **19**, 498-508.

Koch, S., Tugues, S., Li, X., Gualandi, L. and Claesson-Welsh, L. 2011. Signal transduction by vascular endothelial growth factor receptors. *Biochem J.* **437**, 169-183.

Kodack, D.P., Askoxylakis, V., Ferraro, G.B., Fukumura, D. and Jain, R.K. 2015. Emerging strategies for treating brain metastases from breast cancer. *Cancer Cell.* **27**, 163-175.

Kolch, W. 2000. Meaningful relationships: the regulation of the Ras/Raf/MEK/ERK pathway by protein interactions. *Biochem J.* **351**, 289-305.

Kölsch, V., Charest, P.G. and Firtel, R.A. 2008. The regulation of cell motility and chemotaxis by phospholipid signaling. *J Cell Sci.* **121**, 551-559.

Kranz, A., Mattfeldt, T. and Waltenberger, J. 1999. Molecular mediators of tumor angiogenesis: enhanced expression and activation of vascular endothelial growth factor receptor KDR in primary breast cancer. *Int J Cancer.* **84**, 293-298.

Kreisl, T.N., Kim, L., Moore, K., Duic, P., Royce, C., Stroud, I., Garren, N., Mackey, M., Butman, J.A., Camphausen, K., Park, J., Albert, P.S. and Fine, H.A. 2009. Phase II trial of single-agent bevacizumab followed by bevacizumab plus irinotecan at tumor progression in recurrent glioblastoma. *J Clin Oncol.* **27**, 740-745.

Kroll, J. and Waltenberger, J. 1997. The Vascular Endothelial Growth Factor Receptor KDR Activates Multiple Signal Transduction Pathways in Porcine Aortic Endothelial Cells. *Journal of Biological Chemistry.* **272**, 32521-32527.

Lahlou, H. and Muller, W.J. 2011. β1-integrins signaling and mammary tumor progression in transgenic mouse models: implications for human breast cancer. *Breast Cancer Research.* **13**, 229.

Lamalice, L., Houle, F. and Huot, J. 2006. Phosphorylation of Tyr1214 within VEGFR-2 Triggers the Recruitment of Nck and Activation of Fyn Leading to SAPK2/p38 Activation and Endothelial Cell Migration in Response to VEGF*. *Journal of Biological Chemistry.* **281**, 34009-34020.

Lamalice, L., Houle, F., Jourdan, G. and Huot, J. 2004. Phosphorylation of tyrosine 1214 on VEGFR2 is required for VEGF-induced activation of Cdc42 upstream of SAPK2/p38. *Oncogene.* **23**, 434-445.

Laplante, M. and Sabatini, D.M. 2012. mTOR signaling in growth control and disease. *Cell.* **149**, 274-293.

Lattanzio, R., Iezzi, M., Sala, G., Tinari, N., Falasca, M., Alberti, S., Buglioni, S., Mottolese, M., Perracchio, L., Natali, P.G. and Piantelli, M. 2019. PLC-gamma-1 phosphorylation status is prognostic of metastatic risk in patients with early-stage Luminal-A and -B breast cancer subtypes. *BMC Cancer.* **19**, 747.

Lawrence, M.C., Jivan, A., Shao, C., Duan, L., Goad, D., Zaganjor, E., Osborne, J., McGlynn, K., Stippec, S., Earnest, S., Chen, W. and Cobb, M.H. 2008. The roles of MAPKs in disease. *Cell Res.* **18**, 436-442.

Lemmon, M.A. and Schlessinger, J. 2010. Cell signaling by receptor tyrosine kinases. *Cell.* **141**, 1117-1134.

Lettau, M., Pieper, J. and Janssen, O. 2009. Nck adapter proteins: functional versatility in T cells. *Cell Communication and Signaling.* **7**, 1.

Leyland-Jones, B. 2009. Human epidermal growth factor receptor 2-positive breast cancer and central nervous system metastases. *J Clin Oncol.* **27**, 5278-5286.

cite

Li, N., Batzer, A., Daly, R., Yajnik, V., Skolnik, E., Chardin, P., Bar-Sagi, D., Margolis, B. and Schlessinger, J. 1993. Guanine-nucleotide-releasing factor hSos1 binds to Grb2 and links receptor tyrosine kinases to Ras signalling. *Nature*. **363**, 85-88.

Li, W., Fan, J. and Woodley, D.T. 2001. Nck/Dock: an adapter between cell surface receptors and the actin cytoskeleton. *Oncogene.* **20**, 6403-6417.

Lim, W.A., Richards, F.M. and Fox, R.O. 1994. Structural determinants of peptide-binding orientation and of sequence specificity in SH3 domains. *Nature.* **372**, 375-379.

Lin, C.C., Melo, F.A., Ghosh, R., Suen, K.M., Stagg, L.J., Kirkpatrick, J., Arold, S.T., Ahmed, Z. and Ladbury, J.E. 2012. Inhibition of basal FGF receptor signaling by dimeric Grb2. *Cell.* **149**, 1514-1524.

Lin, C.C., Wieteska, L., Suen, K.M., Kalverda, A.P., Ahmed, Z. and Ladbury, J.E. 2021. Grb2 binding induces phosphorylation-independent activation of Shp2. *Commun Biol.* **4**, 437.

Lin, N.U. and Winer, E.P. 2007. Brain metastases: the HER2 paradigm. *Clin Cancer Res.* **13**, 1648-1655.

Liu, F., Yang, X., Geng, M. and Huang, M. 2018. Targeting ERK, an Achilles' Heel of the MAPK pathway, in cancer therapy. *Acta Pharmaceutica Sinica B.* **8**, 552-562.

Liu, P., Cheng, H., Roberts, T.M. and Zhao, J.J. 2009. Targeting the phosphoinositide 3-kinase pathway in cancer. *Nat Rev Drug Discov.* **8**, 627-644.

Loibl, S., Poortmans, P., Morrow, M., Denkert, C. and Curigliano, G. 2021. Breast cancer. *The Lancet.* **397**, 1750-1769.

Longatto-Filho, A., Pinheiro, C., Martinho, O., Moreira, M.A., Ribeiro, L.F., Queiroz, G.S., Schmitt, F.C., Baltazar, F. and Reis, R.M. 2009. Molecular characterization of EGFR, PDGFRA and VEGFR2 in cervical adenosquamous carcinoma. *BMC Cancer.* **9**, 212.

Lou, L., Yu, Z., Wang, Y., Wang, S. and Zhao, Y. 2018. c-Src inhibitor selectively inhibits triple-negative breast cancer overexpressed Vimentin in vitro and in vivo. **109**, 1648-1659.

Lu-Emerson, C., Duda, D.G., Emblem, K.E., Taylor, J.W., Gerstner, E.R., Loeffler, J.S., Batchelor, T.T. and Jain, R.K. 2015. Lessons from anti-vascular endothelial growth factor and anti-vascular endothelial growth factor receptor trials in patients with glioblastoma. *J Clin Oncol.* **33**, 1197-1213.

Luo, M. and Guan, J.L. 2010. Focal adhesion kinase: a prominent determinant in breast cancer initiation, progression and metastasis. *Cancer Lett*. **289**, 127-139.

Lv, D., Guo, L., Zhang, T. and Huang, L. 2017. PRAS40 signaling in tumor. *Oncotarget.* **8**, 69076-69085.

Machesky, L.M. 2008. Lamellipodia and filopodia in metastasis and invasion. *FEBS Letters.* **582**, 2102-2111.

Mahbub Hasan, A.K., Ijiri, T. and Sato, K. 2012. Involvement of Src in the Adaptation of Cancer Cells under Microenvironmental Stresses. *J Signal Transduct.* **2012**, 483796.

Mahfouz, N., Tahtouh, R., Alaaeddine, N., El Hajj, J., Sarkis, R., Hachem, R., Raad, I. and Hilal, G. 2017. Gastrointestinal cancer cells treatment with bevacizumab activates a VEGF autoregulatory mechanism involving telomerase catalytic subunit hTERT via PI3K-AKT, HIF-1α and VEGF receptors. *PLoS One.* **12**, 0179202.

Maignan, S., Guilloteau, JP., Fromage, N., Arnoux, B., Becquart, J. and Ducruix, A. 1995. Crystal structure of the mammalian Grb2 adaptor. *Science*. **268**, 291-293.

Manning, G., Whyte, D.B., Martinez, R., Hunter, T. and Sudarsanam, S. 2002. The protein kinase complement of the human genome. *Science.* **298**, 1912-1934.

Margolis, B. and Skolnik, EY. 1994. Activation of Ras by receptor tyrosine kinases. *J Am Soc Nephrol*. **5**, 1288-1299.

Marmor, M.D., Skaria, K.B. and Yarden, Y. 2004. Signal transduction and oncogenesis by ErbB/HER receptors. *Int J Radiat Oncol Biol Phys.* **58**, 903-913.

Martin, G.S. 2001. The hunting of the Src. *Nat Rev Mol Cell Biol.* **2**, 467-475.

Matsumoto, T., Bohman, S., Dixelius, J., Berge, T., Dimberg, A., Magnusson, P., Wang, L., Wikner, C., Qi, J.H., Wernstedt, C., Wu, J., Bruheim, S., Mugishima, H., Mukhopadhyay, D., Spurkland, A. and Claesson-Welsh, L. 2005. VEGF receptor-2 Y951 signaling and a role for the adapter molecule TSAd in tumor angiogenesis. *Embo j.* **24**, 2342-2353.

Matsumoto, T. and Claesson-Welsh, L. 2001. VEGF receptor signal transduction. *Sci STKE.* **2001**, 21.

Mattila, P.K. and Lappalainen, P. 2008. Filopodia: molecular architecture and cellular functions. *Nat Rev Mol Cell Biol.* **9**, 446-454.

Mayer, B.J. and Gupta, R. 1998. Functions of SH2 and SH3 domains. *Curr Top Microbiol Immunol.* **228**, 1-22.

Mayer, E.L. and Krop, I.E. 2010. Advances in targeting SRC in the treatment of breast cancer and other solid malignancies. *Clin Cancer Res.* **16**, 3526-3532.

Memmott, R.M. and Dennis, P.A. 2009. Akt-dependent and -independent mechanisms of mTOR regulation in cancer. *Cell Signal.* **21**, 656-664.

Meyer, R.D., Sacks, D.B. and Rahimi, N. 2008. IQGAP1-dependent signaling pathway regulates endothelial cell proliferation and angiogenesis. *PLoS One.* **3**, 3848.

Miricescu, D., Totan, A., Stanescu, S., II, Badoiu, S.C., Stefani, C. and Greabu, M. 2020. PI3K/AKT/mTOR Signaling Pathway in Breast Cancer: From Molecular Landscape to Clinical Aspects. *Int J Mol Sci.* **22,** 173.

Mitchell, M.I. and Engelbrecht, A.M. 2017. Metabolic hijacking: A survival strategy cancer cells exploit? *Crit Rev Oncol Hematol.* **109**, 1-8.

Mitra, S.K. and Schlaepfer, D.D. 2006. Integrin-regulated FAK–Src signaling in normal and cancer cells. *Current Opinion in Cell Biology*. **18**, 516-523,

Mora, A., Komander, D., van Aalten, D.M. and Alessi, D.R. 2004. PDK1, the master regulator of AGC kinase signal transduction. *Semin Cell Dev Biol.* **15**, 161-170.

Morris, D.C., Popp, J.L., Tang, L.K., Gibbs, H.C., Schmitt, E., Chaki, S.P., Bywaters, B.C., Yeh, A.T., Porter, W.W., Burghardt, R.C., Barhoumi, R. and Rivera, G.M. 2017. Nck deficiency is associated with delayed breast carcinoma progression and reduced metastasis. *Mol Biol Cell.* **28**, 3500-3516.

Moscat, J., Richardson, A. and Diaz-Meco, M.T. 2015. Nutrient stress revamps cancer cell metabolism. *Cell Research.* **25**, 537-538.

Mukhopadhyay, D., Tsiokas, L., Zhou, X.M., Foster, D., Brugge, J.S. and Sukhatme, V.P. 1995. Hypoxic induction of human vascular endothelial growth factor expression through c-Src activation. *Nature.* **375**, 577-581.

Myoui, A., Nishimura, R., Williams, P.J., Hiraga, T., Tamura, D., Michigami, T., Mundy, G.R. and Yoneda, T. 2003. C-SRC tyrosine kinase activity is associated with tumor colonization in bone and lung in an animal model of human breast cancer metastasis. *Cancer Res.* **63**, 5028-5033.

Nagata, Y., Lan, K.H., Zhou, X., Tan, M., Esteva, F.J., Sahin, A.A., Klos, K.S., Li, P., Monia, B.P., Nguyen, N.T., Hortobagyi, G.N., Hung, M.C. and

Yu, D. 2004. PTEN activation contributes to tumor inhibition by trastuzumab, and loss of PTEN predicts trastuzumab resistance in patients. *Cancer Cell.* **6**, 117-127.

Nahta, R. 2012. Pharmacological strategies to overcome HER2 cross-talk and Trastuzumab resistance. *Curr Med Chem.* **19**, 1065-1075.

Nahta, R. and Esteva, F.J. 2006a. HER2 therapy: Molecular mechanisms of trastuzumab resistance. *Breast Cancer Res.* **8**, 215.

Nahta, R. and Esteva, F.J. 2006b. Herceptin: mechanisms of action and resistance. *Cancer Lett.* **232**, 123-138.

Nakopoulou, L., Stefanaki, K., Panayotopoulou, E., Giannopoulou, I., Athanassiadou, P., Gakiopoulou-Givalou, H. and Louvrou, A. 2002. Expression of the vascular endothelial growth factor receptor-2/Flk-1 in breast carcinomas: Correlation with proliferation. *Human Pathology.* **33**, 863-870.

Neuzillet, C., Hammel, P., Tijeras-Raballand, A., Couvelard, A. and Raymond, E. 2013. Targeting the Ras-ERK pathway in pancreatic adenocarcinoma. *Cancer Metastasis Rev.* **32**, 147-162.

Newton, A.C. and Trotman, L.C. 2014. Turning off AKT: PHLPP as a drug target. *Annu Rev Pharmacol Toxicol.* **54**, 537-558.

Nishizuka, Y. 1992. Intracellular signaling by hydrolysis of phospholipids and activation of protein kinase C. *Science.* **258**, 607-614.

Nitulescu, G.M., Van De Venter, M., Nitulescu, G., Ungurianu, A., Juzenas, P., Peng, Q., Olaru, O.T., Grădinaru, D., Tsatsakis, A., Tsoukalas, D., Spandidos, D.A. and Margina, D. 2018. The Akt pathway in oncology therapy and beyond (Review). *Int J Oncol.* **53**, 2319-2331.

Nolen, B., Taylor, S. and Ghosh, G. 2004. Regulation of protein kinases; controlling activity through activation segment conformation. *Mol Cell.* **15**, 661-675.

O'Neill, E. and Kolch, W. 2004. Conferring specificity on the ubiquitous Raf/MEK signalling pathway. *Br J Cancer.* **90**, 283-288.

Olayioye, M.A., Neve, R.M., Lane, H.A. and Hynes, N.E. 2000. The ErbB signaling network: receptor heterodimerization in development and cancer. *Embo j.* **19**, 3159-3167.

Olson, E.M., Abdel-Rasoul, M., Maly, J., Wu, C.S., Lin, N.U. and Shapiro, C.L. 2013a. Incidence and risk of central nervous system metastases as site of first recurrence in patients with HER2-positive breast cancer treated with adjuvant trastuzumab. *Annals of Oncology.* **24**, 1526-1533.

Olson, E.M., Najita, J.S., Sohl, J., Arnaout, A., Burstein, H.J., Winer, E.P. and Lin, N.U. 2013b. Clinical outcomes and treatment practice patterns of patients with HER2-positive metastatic breast cancer in the post-trastuzumab era. *Breast.* **22**, 525-531.

Olsson, A.K., Dimberg, A., Kreuger, J. and Claesson-Welsh, L. 2006. VEGF receptor signalling - in control of vascular function. *Nat Rev Mol Cell Biol.* **7**, 359-371.

Oser, M., Dovas, A., Cox, D. and Condeelis, J. 2011. Nck1 and Grb2 localization patterns can distinguish invadopodia from podosomes. *Eur J Cell Biol.* **90**, 181-188.

Ottenhoff-Kalff, A.E., Rijksen, G., van Beurden, E.A., Hennipman, A., Michels, A.A. and Staal, G.E. 1992. Characterization of protein tyrosine kinases from human breast cancer: involvement of the c-src oncogene product. *Cancer Res.* **52**, 4773-4778.

Ouyang, Z.H., Wang, W.J., Yan, Y.G., Wang, B. and Lv, G.H. 2017. The PI3K/Akt pathway: a critical player in intervertebral disc degeneration. *Oncotarget.* **8**, 57870-57881.

Pàez-Ribes, M., Allen, E., Hudock, J., Takeda, T., Okuyama, H., Viñals, F., Inoue, M., Bergers, G., Hanahan, D. and Casanovas, O. 2009. Antiangiogenic therapy elicits malignant progression of tumors to increased local invasion and distant metastasis. *Cancer Cell.* **15**, 220-231.

Palmieri, D., Bronder, J.L., Herring, J.M., Yoneda, T., Weil, R.J., Stark, A.M., Kurek, R., Vega-Valle, E., Feigenbaum, L., Halverson, D., Vortmeyer, A.O., Steinberg, S.M., Aldape, K. and Steeg, P.S. 2007. Her-2 overexpression

increases the metastatic outgrowth of breast cancer cells in the brain. *Cancer Res.* **67**, 4190-4198.

Paplomata, E. and O'Regan, R. 2013. New and emerging treatments for estrogen receptor-positive breast cancer: focus on everolimus. *Ther Clin Risk Manag.* **9**, 27-36.

Park, S., Takeuchi, K. and Wagner, G. 2006. Solution Structure of the First Src Homology 3 Domain of Human Nck2. *Journal of Biomolecular NMR.* **34**, 203-208.

Parsons, S.J. and Parsons, J.T. 2004. Src family kinases, key regulators of signal transduction. *Oncogene.* **23**, 7906-7909.

Pawson, T. 2004. Specificity in signal transduction: from phosphotyrosine-SH2 domain interactions to complex cellular systems. *Cell.* **116**, 191-203.

Pedersen, K., Angelini, P.D., Laos, S., Bach-Faig, A., Cunningham, M.P., Ferrer-Ramón, C., Luque-García, A., García-Castillo, J., Parra-Palau, J.L., Scaltriti, M., Ramón y Cajal, S., Baselga, J. and Arribas, J. 2009. A naturally occurring HER2 carboxy-terminal fragment promotes mammary tumor growth and metastasis. *Mol Cell Biol.* **29**, 3319-3331.

Pengcheng, S., Ziqi, W., Luyao, Y., Xiangwei, Z., Liang, L., Yuwei, L., Lechen, L. and Wanhai, X. 2017. MicroRNA-497 suppresses renal cell carcinoma by targeting VEGFR-2 in ACHN cells. *Bioscience reports.* **37**, 20170270.

Pinto, M.P., Owen, G.I., Retamal, I. and Garrido, M. 2017. Angiogenesis inhibitors in early development for gastric cancer. *Expert Opin Investig Drugs.* **26**, 1007-1017.

Plotnikov, A., Zehorai, E., Procaccia, S. and Seger, R. 2011. The MAPK cascades: signaling components, nuclear roles and mechanisms of nuclear translocation. *Biochim Biophys Acta.* **1813**, 1619-1633.

Pohlmann, P.R., Mayer, I.A. and Mernaugh, R. 2009. Resistance to Trastuzumab in Breast Cancer. *Clin Cancer Res.* **15**, 7479-7491.

Pollok, B.A. and Heim. R. 1999. Using GFP in FRET-based applications. *Trends Cell Biol*. **9**, 57–60.

Pon, Y.L., Zhou, H.Y., Cheung, A.N., Ngan, H.Y. and Wong, A.S. 2008. p70 S6 kinase promotes epithelial to mesenchymal transition through snail induction in ovarian cancer cells. *Cancer Res.* **68**, 6524-6532.

Pugh, C.W. and Ratcliffe, P.J. 2003. Regulation of angiogenesis by hypoxia: role of the HIF system. *Nat Med.* **9**, 677-684.

Puputti, M., Tynninen, O., Sihto, H., Blom, T., Mäenpää, H., Isola, J., Paetau, A., Joensuu, H. and Nupponen, N.N. 2006. Amplification of KIT, PDGFRA, VEGFR2, and EGFR in gliomas. *Mol Cancer Res.* **4**, 927-934.

Rao, A. and Herr, D.R. 2017. G protein-coupled receptor GPR19 regulates E-cadherin expression and invasion of breast cancer cells. *Biochim Biophys Acta Mol Cell Res.* **1864**, 1318-1327.

Rebecchi, M.J. and Pentyala, S.N. 2000. Structure, function, and control of phosphoinositide-specific phospholipase C. *Physiol Rev.* **80**, 1291-1335.

Ren, R., Mayer, B.J., Cicchetti, P. and Baltimore, D. 1993. Identification of a ten-amino acid proline-rich SH3 binding site. *Science.* **259**, 1157-1161.

Rhee, S.G. 2001. Regulation of phosphoinositide-specific phospholipase C. *Annu Rev Biochem.* **70**, 281-312.

Riquelme, E., Suraokar, M., Behrens, C., Lin, H.Y., Girard, L., Nilsson, M.B., Simon, G., Wang, J., Coombes, K.R., Lee, J.J., Hong, W.K., Heymach, J., Minna, J.D. and Wistuba, II. 2014. VEGF/VEGFR-2 upregulates EZH2 expression in lung adenocarcinoma cells and EZH2 depletion enhances the response to platinum-based and VEGFR-2-targeted therapy. *Clin Cancer Res.* **20**, 3849-3861.

Robinson, D.R., Wu, Y.M. and Lin, S.F. 2000. The protein tyrosine kinase family of the human genome. *Oncogene.* **19**, 5548-5557.

Rockberg, J., Schwenk, J.M. and Uhlen, M. 2009. Discovery of epitopes for targeting the human epidermal growth factor receptor 2 (HER2) with antibodies. *Mol Oncol.* **3**, 238-247.

Roskoski, R., Jr. 2005. Src kinase regulation by phosphorylation and dephosphorylation. *Biochem Biophys Res Commun.* **331**, 1-14.

Ross, J.S., Slodkowska, E.A., Symmans, W.F., Pusztai, L., Ravdin, P.M. and Hortobagyi, G.N. 2009. The HER-2 receptor and breast cancer: ten years of targeted anti-HER-2 therapy and personalized medicine. *Oncologist.* **14**, 320-368.

Roy, V. and Perez, E.A. 2009. Biologic therapy of breast cancer: focus on co-inhibition of endocrine and angiogenesis pathways. *Breast Cancer Research and Treatment.* **116**, 31-38.

Rozakis-Adcock, M., Fernley, R., Wade, J., Pawson, T. and Bowtell, D. 1993. The SH2 and SH3 domains of mammalian Grb2 couple the EGF receptor to the Ras activator mSos1. *Nature*. **363**, 83-5.

Rydén, L., Jirström, K., Haglund, M., Stål, O. and Fernö, M. 2010. Epidermal growth factor receptor and vascular endothelial growth factor receptor 2 are specific biomarkers in triple-negative breast cancer. Results from a controlled randomized trial with long-term follow-up. *Breast Cancer Research and Treatment.* **120**, 491-498.

Rydén, L., Linderholm, B., Nielsen, N.H., Emdin, S., Jönsson, P.-E. and Landberg, G. 2003. Tumor Specific VEGF-A and VEGFR2/KDR Protein are Co-expressed in Breast Cancer. *Breast Cancer Research and Treatment.* **82**, 147-154.

Sabio, G. and Davis, R.J. 2014. TNF and MAP kinase signalling pathways. *Semin Immunol.* **26**, 237-245.

Saksela, K. and Permi, P. 2012. SH3 domain ligand binding: What's the consensus and where's the specificity? *FEBS Lett.* **586**, 2609-2614.

Sala, G., Dituri, F., Raimondi, C., Previdi, S., Maffucci, T., Mazzoletti, M., Rossi, C., Iezzi, M., Lattanzio, R., Piantelli, M., Iacobelli, S., Broggini, M. and Falasca, M. 2008. Phospholipase Cgamma1 is required for metastasis development and progression. *Cancer Res.* **68**, 10187-10196.

Salaroglio, I.C., Mungo, E., Gazzano, E., Kopecka, J. and Riganti, C. 2019. ERK is a Pivotal Player of Chemo-Immune-Resistance in Cancer. *Int J Mol Sci.* **20**.

Sato, H. and Takeda, Y. 2009. VEGFR2 expression and relationship between tumor neovascularization and histologic characteristics in oral squamous cell carcinoma. *Journal of Oral Science.* **51**, 551-557.

Scheid, M.P. and Woodgett, J.R. 2003. Unravelling the activation mechanisms of protein kinase B/Akt. *FEBS Lett.* **546**, 108-112.

Schillaci, R., Guzmán, P., Cayrol, F., Beguelin, W., Díaz Flaqué, M.C., Proietti, C.J., Pineda, V., Palazzi, J., Frahm, I., Charreau, E.H., Maronna, E., Roa, J.C. and Elizalde, P.V. 2012. Clinical relevance of ErbB-2/HER2 nuclear expression in breast cancer. *BMC Cancer.* **12**, 74.

Schlessinger, J. 2000. Cell signaling by receptor tyrosine kinases. *Cell.* **103**, 211-225.

Schlessinger, J. and Lemmon, M.A. 2003. SH2 and PTB domains in tyrosine kinase signaling. *Sci STKE.* **2003**, 12.

Schulze, A., Lehmann, K., Jefferies, H.B., McMahon, M. and Downward, J. 2001. Analysis of the transcriptional program induced by Raf in epithelial cells. *Genes Dev.* **15**, 981-994.

Sekar, R.B. and Periasamy, A. 2003. Fluorescence resonance energy transfer (FRET) microscopy imaging of live cell protein localizations. *J Cell Biol*. **160**, 629-33.

Shibuya, M. 2011. Vascular Endothelial Growth Factor (VEGF) and Its Receptor (VEGFR) Signaling in Angiogenesis: A Crucial Target for Anti- and Pro-Angiogenic Therapies. *Genes Cancer.* **2**, 1097-1105.

Shibuya, M. and Claesson-Welsh, L. 2006. Signal transduction by VEGF receptors in regulation of angiogenesis and lymphangiogenesis. *Experimental Cell Research.* **312**, 549-560.

Singer, W.D., Brown, H.A. and Sternweis, P.C. 1997. Regulation of Eukaryotic Phosphatidylinositol-Specific Phopsholipase C and Phospholipase D. *Annual Review of Biochemistry.* **66**, 475-509.

Slack-Davis, J.K., Eblen, S.T., Zecevic, M., Boerner, S.A., Tarcsafalvi, A., Diaz, H.B., Marshall, M.S., Weber, M.J., Parsons, J.T. and Catling, A.D.

2003. PAK1 phosphorylation of MEK1 regulates fibronectin-stimulated MAPK activation. *J Cell Biol.* **162**, 281-291.

Song, G., Ouyang, G. and Bao, S. 2005. The activation of Akt/PKB signaling pathway and cell survival. *J Cell Mol Med.* **9**, 59-71.

Spector, N.L., Xia, W., Burris, H., 3rd, Hurwitz, H., Dees, E.C., Dowlati, A., O'Neil, B., Overmoyer, B., Marcom, P.K., Blackwell, K.L., Smith, D.A., Koch, K.M., Stead, A., Mangum, S., Ellis, M.J., Liu, L., Man, A.K., Bremer, T.M., Harris, J. and Bacus, S. 2005. Study of the biologic effects of lapatinib, a reversible inhibitor of ErbB1 and ErbB2 tyrosine kinases, on tumor growth and survival pathways in patients with advanced malignancies. *J Clin Oncol.* **23**, 2502-2512.

Stadler, W.M., Cao, D., Vogelzang, N.J., Ryan, C.W., Hoving, K., Wright, R., Karrison, T. and Vokes, E.E. 2004. A randomized Phase II trial of the antiangiogenic agent SU5416 in hormone-refractory prostate cancer. *Clin Cancer Res.* **10**, 3365-3370.

Storz, P., Döppler, H., Copland, J.A., Simpson, K.J. and Toker, A. 2009. FOXO3a promotes tumor cell invasion through the induction of matrix metalloproteinases. *Mol Cell Biol.* **29**, 4906-4917.

Straume, O. and Akslen, L.A. 2003. Increased expression of VEGF-receptors (FLT-1, KDR, NRP-1) and thrombospondin-1 is associated with glomeruloid microvascular proliferation, an aggressive angiogenic phenotype, in malignant melanoma. *Angiogenesis.* **6**, 295-301.

Stuttfeld, E. and Ballmer-Hofer, K. 2009. Structure and function of VEGF receptors. *IUBMB Life.* **61**, 915-922.

Suen, K.M., Lin, C.C., George, R., Melo, F.A., Biggs, E.R., Ahmed, Z., Drake, M.N., Arur, S., Arold, S.T. and Ladbury, J.E. 2013. Interaction with Shc prevents aberrant Erk activation in the absence of extracellular stimuli. *Nat Struct Mol Biol.* **20**, 620-627.

Summy, J.M. and Gallick, G.E. 2003. Src family kinases in tumor progression and metastasis. *Cancer Metastasis Rev.* **22**, 337-358.

Summy, J.M. and Gallick, G.E. 2006. Treatment for advanced tumors: SRC reclaims center stage. *Clin Cancer Res.* **12**, 1398-1401.

Sun, C., Yang, F., Zhang, Y., Chu, J., Wang, J., Wang, Y., Zhang, Y., Li, J., Li, Y., Fan, R., Li, W., Huang, X., Wu, H., Fu, Z., Jiang, Z. and Yin, Y. 2018. tRNA-Derived Fragments as Novel Predictive Biomarkers for Trastuzumab-Resistant Breast Cancer. *Cell Physiol Biochem.* **49**, 419-431.

Sung, H., Ferlay, J., Siegel, R.L., Laversanne, M., Soerjomataram, I., Jemal, A. and Bray, F. 2021. Global Cancer Statistics 2020: GLOBOCAN Estimates of Incidence and Mortality Worldwide for 36 Cancers in 185 Countries. *CA Cancer J Clin.* **71**, 209-249.

Takahashi, T. and Shibuya, M. 1997. The 230 kDa mature form of KDR/Flk-1 (VEGF receptor-2) activates the PLC-γ pathway and partially induces mitotic signals in NIH3T3 fibroblasts. *Oncogene.* **14**, 2079-2089.

Takahashi, T., Ueno, H. and Shibuya, M. 1999. VEGF activates protein kinase C-dependent, but Ras-independent Raf-MEK-MAP kinase pathway for DNA synthesis in primary endothelial cells. *Oncogene.* **18**, 2221-2230.

Takahashi, T., Yamaguchi, S., Chida, K. and Shibuya, M. 2001. A single autophosphorylation site on KDR/Flk-1 is essential for VEGF-A-dependent activation of PLC-gamma and DNA synthesis in vascular endothelial cells. *Embo j.* **20**, 2768-2778.

Takahashi, Y., Kitadai, Y., Bucana, C.D., Cleary, K.R. and Ellis, L.M. 1995. Expression of vascular endothelial growth factor and its receptor, KDR, correlates with vascularity, metastasis, and proliferation of human colon cancer. *Cancer Res.* **55**, 3964-3968.

Tang, Q., Wu, J., Zheng, F., Hann, S.S. and Chen, Y. 2017. Emodin Increases Expression of Insulin-Like Growth Factor Binding Protein 1 through Activation of MEK/ERK/AMPKα and Interaction of PPARγ and Sp1 in Lung Cancer. *Cell Physiol Biochem.* **41**, 339-357.

Templeton, A.J., Diez-Gonzalez, L., Ace, O., Vera-Badillo, F., Seruga, B., Jordán, J., Amir, E., Pandiella, A. and Ocaña, A. 2014. Prognostic relevance of receptor tyrosine kinase expression in breast cancer: a meta-analysis. *Cancer Treat Rev.* **40**, 1048-1055.

Teyra, J., Huang, H., Jain, S., Guan, X., Dong, A., Liu, Y., Tempel, W., Min, J., Tong, Y., Kim, P.M., Bader, G.D. and Sidhu, S.S. 2017. Comprehensive

Analysis of the Human SH3 Domain Family Reveals a Wide Variety of Non-canonical Specificities. *Structure.* **25**, 1598-1610.

Thomas, S.M. and Brugge, J.S. 1997. Cellular functions regulated by Src family kinases. *Annu Rev Cell Dev Biol.* **13**, 513-609.

Timsah, Z., Ahmed, Z., Ivan, C., Berrout, J., Gagea, M., Zhou, Y., Pena, G.N., Hu, X., Vallien, C., Kingsley, C.V., Lu, Y., Hancock, J.F., Liu, J., Gladden, A.B., Mills, G.B., Lopez-Berestein, G., Hung, M.C., Sood, A.K., Bogdanov, M. and Ladbury, J.E. 2016. Grb2 depletion under non-stimulated conditions inhibits PTEN, promotes Akt-induced tumor formation and contributes to poor prognosis in ovarian cancer. *Oncogene.* **35**, 2186-2196.

Timsah, Z., Ahmed, Z., Lin, C.C., Melo, F.A., Stagg, L.J., Leonard, P.G., Jeyabal, P., Berrout, J., O'Neil, R.G., Bogdanov, M. and Ladbury, J.E. 2014. Competition between Grb2 and Plcγ1 for FGFR2 regulates basal phospholipase activity and invasion. *Nat Struct Mol Biol.* **21**, 180-188.

Timsah, Z., Berrout, J., Suraokar, M., Behrens, C., Song, J., Lee, J.J., Ivan, C., Gagea, M., Shires, M., Hu, X., Vallien, C., Kingsley, C.V., Wistuba, I. and Ladbury, J.E. 2015. Expression pattern of FGFR2, Grb2 and Plcγ1 acts as a novel prognostic marker of recurrence recurrence-free survival in lung adenocarcinoma. *Am J Cancer Res.* **5**, 3135-3148.

Tomiguchi, M., Yamamoto, Y., Yamamoto-Ibusuki, M., Goto-Yamaguchi, L., Fujiki, Y., Fujiwara, S., Sueta, A., Hayashi, M., Takeshita, T., Inao, T. and Iwase, H. 2016. Fibroblast growth factor receptor-1 protein expression is associated with prognosis in estrogen receptor-positive/human epidermal growth factor receptor-2-negative primary breast cancer. *Cancer Sci.* **107**, 491-498.

Touat, M., Ileana, E., Postel-Vinay, S., André, F. and Soria, J.C. 2015. Targeting FGFR Signaling in Cancer. *Clin Cancer Res.* **21**, 2684-2694.

Tseng, P.H., Wang, Y.C., Weng, S.C., Weng, J.R., Chen, C.S., Brueggemeier, R.W., Shapiro, C.L., Chen, C.Y., Dunn, S.E., Pollak, M. and Chen, C.S. 2006. Overcoming trastuzumab resistance in HER2-overexpressing breast cancer cells by using a novel celecoxib-derived

phosphoinositide-dependent kinase-1 inhibitor. *Mol Pharmacol.* **70**, 1534-1541.

Ullrich, A. and Schlessinger, J. 1990. Signal transduction by receptors with tyrosine kinase activity. *Cell.* **61**, 203-212.

Ulmer, T.S., Werner, J.M. and Campbell, I.D. 2002. SH3-SH2 domain orientation in Src kinases: NMR studies of Fyn. *Structure.* **10**, 901-911.

Valabrega, G., Montemurro, F. and Aglietta, M. 2007. Trastuzumab: mechanism of action, resistance and future perspectives in HER2-overexpressing breast cancer. *Ann Oncol.* **18**, 977-984.

Vestey, S.B., Sen, C., Calder, C.J., Perks, C.M., Pignatelli, M. and Winters, Z.E. 2005. Activated Akt expression in breast cancer: correlation with p53, Hdm2 and patient outcome. *Eur J Cancer.* **41**, 1017-1025.

Vicente-Manzanares, M., Ma, X., Adelstein, R.S. and Horwitz, A.R. 2009. Non-muscle myosin II takes centre stage in cell adhesion and migration. *Nat Rev Mol Cell Biol.* **10**, 778-790.

Vleugel, M.M., Greijer, A.E., Bos, R., van der Wall, E. and van Diest, P.J. 2006. c-Jun activation is associated with proliferation and angiogenesis in invasive breast cancer. *Hum Pathol.* **37**, 668-674.

Vogel, C.L., Cobleigh, M.A., Tripathy, D., Gutheil, J.C., Harris, L.N., Fehrenbacher, L., Slamon, D.J., Murphy, M., Novotny, W.F., Burchmore, M., Shak, S., Stewart, S.J. and Press, M. 2002. Efficacy and safety of trastuzumab as a single agent in first-line treatment of HER2-overexpressing metastatic breast cancer. *J Clin Oncol.* **20**, 719-726.

Vogelstein, B., Lane, D. and Levine, A.J. 2000. Surfing the p53 network. *Nature.* **408**, 307-310.

Vu, T. and Claret, F.X. 2012. Trastuzumab: Updated Mechanisms of Action and Resistance in Breast Cancer. *Front Oncol.* **2**.

Wahl, M. and Carpenter, G. 1991. Selective phospholipase C activation. *Bioessays.* **13**, 107-113.

Waltenberger, J., Claesson-Welsh, L., Siegbahn, A., Shibuya, M. and Heldin, C.H. 1994. Different signal transduction properties of KDR and Flt1,

two receptors for vascular endothelial growth factor. *Journal of Biological Chemistry.* **269**, 26988-26995.

Wang, Z., Glück, S., Zhang, L. and Moran, M.F. 1998. Requirement for phospholipase C-gamma1 enzymatic activity in growth factor-induced mitogenesis. *Mol Cell Biol.* **18**, 590-597.

Warner, A.J., Lopez-Dee, J., Knight, E.L., Feramisco, J.R. and Prigent, S.A. 2000. The Shc-related adaptor protein, Sck, forms a complex with the vascular-endothelial-growth-factor receptor KDR in transfected cells. *Biochem J.* **347**, 501-509.

Webb, D.J., Donais, K., Whitmore, L.A., Thomas, S.M., Turner, C.E., Parsons, J.T. and Horwitz, A.F. 2004. FAK–Src signalling through paxillin, ERK and MLCK regulates adhesion disassembly. *Nature Cell Biology.* **6**, 154-161.

Weigand, M., Hantel, P., Kreienberg, R. and Waltenberger, J. 2005. Autocrine vascular endothelial growth factor signalling in breast cancer. Evidence from cell lines and primary breast cancer cultures in vitro. *Angiogenesis.* **8**, 197-204.

Weiss, A. and Schlessinger, J. 1998. Switching signals on or off by receptor dimerization. *Cell.* **94**, 277-280.

Wells, A. and Grandis, J.R. 2003. Phospholipase C-gamma1 in tumor progression. *Clin Exp Metastasis.* **20**, 285-290.

White, E.Z., Pennant, N.M., Carter, J.R., Hawsawi, O., Odero-Marah, V. and Hinton, C.V. 2020. Serum deprivation initiates adaptation and survival to oxidative stress in prostate cancer cells. *Scientific Reports.* **10**, 12505.

Wise, R. and Zolkiewska, A. 2017. Metalloprotease-dependent activation of EGFR modulates CD44(+)/CD24(-) populations in triple negative breast cancer cells through the MEK/ERK pathway. **166**, 421-433.

Woodrow, M.A., Woods, D., Cherwinski, H.M., Stokoe, D. and McMahon, M. 2003. Ras-induced serine phosphorylation of the focal adhesion protein paxillin is mediated by the Raf-->MEK-->ERK pathway. *Exp Cell Res.* **287**, 325-338.

Xia, G., Kumar, S.R., Hawes, D., Cai, J., Hassanieh, L., Groshen, S., Zhu, S., Masood, R., Quinn, D.I., Broek, D., Stein, J.P. and Gill, P.S. 2006. Expression and Significance of Vascular Endothelial Growth Factor Receptor 2 in Bladder Cancer. *The Journal of Urology.* **175**, 1245-1252.

Xiao, X., Li, B.X., Mitton, B., Ikeda, A. and Sakamoto, K.M. 2010. Targeting CREB for cancer therapy: friend or foe. *Curr Cancer Drug Targets.* **10**, 384-391.

Yakisich, J.S., Venkatadri, R., Azad, N. and Iyer, A.K.V. 2017. Chemoresistance of Lung and Breast Cancer Cells Growing Under Prolonged Periods of Serum Starvation. *J Cell Physiol.* **232**, 2033-2043.

Yamaguchi, H. and Condeelis, J. 2007. Regulation of the actin cytoskeleton in cancer cell migration and invasion. *Biochim Biophys Acta.* **1773**, 642-652.

Yamaoka-Tojo, M., Tojo, T., Kim, H.W., Hilenski, L., Patrushev, N.A., Zhang, L., Fukai, T. and Ushio-Fukai, M. 2006. IQGAP1 mediates VE-cadherin-based cell-cell contacts and VEGF signaling at adherence junctions linked to angiogenesis. *Arterioscler Thromb Vasc Biol.* **26**, 1991-1997.

Yan, J.D., Liu, Y., Zhang, Z.Y., Liu, G.Y., Xu, J.H., Liu, L.Y. and Hu, Y.M. 2015. Expression and prognostic significance of VEGFR-2 in breast cancer. *Pathol Res Pract.* **211**, 539-543.

Yang, Z.-Y., Di, M.-Y., Yuan, J.-Q., Shen, W.-X., Zheng, D.-Y., Chen, J.-Z., Mao, C. and Tang, J.-L. 2015. The prognostic value of phosphorylated Akt in breast cancer: a systematic review. *Scientific Reports.* **5**, 7758.

Yarden, Y. and Pines, G. 2012. The ERBB network: at last, cancer therapy meets systems biology. *Nat Rev Cancer.* **12**, 553-563.

Yarden, Y. and Sliwkowski, M.X. 2001. Untangling the ErbB signalling network. *Nat Rev Mol Cell Biol.* **2**, 127-137.

Yeatman, T.J. 2004. A renaissance for SRC. *Nat Rev Cancer.* **4**, 470-480.

Yu, H., Chen, J.K., Feng, S., Dalgarno, D.C., Brauer, A.W. and Schreiber, S.L. 1994. Structural basis for the binding of proline-rich peptides to SH3 domains. *Cell.* **76**, 933-945.

Zhang, D., Pal, A., Bornmann, W.G., Yamasaki, F., Esteva, F.J., Hortobagyi, G.N., Bartholomeusz, C. and Ueno, N.T. 2008. Activity of lapatinib is independent of EGFR expression level in HER2-overexpressing breast cancer cells. *Mol Cancer Ther.* **7**, 1846-1850.

Zhang, S., Huang, W.C., Li, P., Guo, H., Poh, S.B., Brady, S.W., Xiong, Y., Tseng, L.M., Li, S.H., Ding, Z., Sahin, A.A., Esteva, F.J., Hortobagyi, G.N. and Yu, D. 2011. Combating trastuzumab resistance by targeting SRC, a common node downstream of multiple resistance pathways. *Nat Med.* **17**, 461-469.

Zhang, X.-m., Li, B.-l., Song, M. and Song, J.-y. 2004. Expression and significance of ERK protein in human breast carcinoma. *Chinese Journal of Cancer Research.* **16**, 269-273.

Zhang, X., Tang, N., Hadden, T.J. and Rishi, A.K. 2011. Akt, FoxO and regulation of apoptosis. *Biochim Biophys Acta.* **1813**, 1978-1986.

Zhao, D., Pan, C., Sun, J., Gilbert, C., Drews-Elger, K., Azzam, D.J., Picon-Ruiz, M., Kim, M., Ullmer, W., El-Ashry, D., Creighton, C.J. and Slingerland, J.M. 2015. VEGF drives cancer-initiating stem cells through VEGFR-2/Stat3 signaling to upregulate Myc and Sox2. *Oncogene.* **34**, 3107-3119.

Zhao, G.X., Pan, H., Ouyang, D.Y. and He, X.H. 2015. The critical molecular interconnections in regulating apoptosis and autophagy. *Ann Med.* **47**, 305-315.

Zheng, Y., Xia, Y., Hawke, D., Halle, M., Tremblay, M.L., Gao, X., Zhou, X.Z., Aldape, K., Cobb, M.H., Xie, K., He, J. and Lu, Z. 2009. FAK phosphorylation by ERK primes ras-induced tyrosine dephosphorylation of FAK mediated by PIN1 and PTP-PEST. *Mol Cell.* **35**, 11-25.

Zhong, Z., Huang, M., Lv, M., He, Y., Duan, C., Zhang, L. and Chen, J. 2017. Circular RNA MYLK as a competing endogenous RNA promotes bladder cancer progression through modulating VEGFA/VEGFR2 signaling pathway. *Cancer Letters.* **403**, 305-317.

Zhou, J., Xu, M., Le, K., Ming, J., Guo, H., Ruan, S. and Huang, T. 2020. SRC Promotes Tamoxifen Resistance in Breast Cancer via Up-Regulating SIRT1. *OncoTargets and therapy.* **13**, 4635-4647.

Supplementary

Supplementary 1.1 CFP-domain construct sequencing results

The following results were obtained via sending the cloned CFP plasmid to Genewiz and determining the sequencing via Clustal Omega (EMBL). Each insert is highlighted in yellow. Src domain sequence was checked against the sequence provided via UniProtKB - P12931 (SRC_HUMAN) and the Plcg1 sequence checked against the sequence provided via UniProtKB – P19174 (PLCG1_HUMAN).

1.1.1 Src full length-CFP construct

Forward EGFP-C primer

```
WT_Src_FL                 ---ATGGGTAGCAACAAGAGCAAGCCCAAGGATGCCAGCCAGCGGCGCCGCAGCCTGGAG     57
Src_FL_2-EGFP-C-FOR_E14   TATATGGGTAGCAACAAGAGCAAGCCCAAGGATGCCAGCCAGCGGCGCCGCAGCCTGGAG     120
                             ************************************************************

WT_Src_FL                 CCCGCCGAGAACGTGCACGGCGCTGGCGGGGGCGCTTTCCCCGCCTCGCAGACCCCCAGC     117
Src_FL_2-EGFP-C-FOR_E14   CCCGCCGAGAACGTGCACGGCGCTGGCGGGGGCGCTTTCCCCGCCTCGCAGACCCCCAGC     180
                          ************************************************************

WT_Src_FL                 AAGCCAGCCTCGGCCGACGGCCACCGCGGCCCCAGCGCGGCCTTCGCCCCCGCGGCCGCC     177
Src_FL_2-EGFP-C-FOR_E14   AAGCCAGCCTCGGCCGACGGCCACCGCGGCCCCAGCGCGGCCTTCGCCCCCGCGGCCGCC     240
                          ************************************************************

WT_Src_FL                 GAGCCCAAGCTGTTCGGAGGCTTCAACTCCTCGGACACCGTCACCTCCCCGCAGAGGGCG     237
Src_FL_2-EGFP-C-FOR_E14   GAGCCCAAGCTGTTCGGAGGCTTCAACTCCTCGGACACCGTCACCTCCCCGCAGAGGGCG     300
                          ************************************************************

WT_Src_FL                 GGCCCGCTGGCCGGTGGAGTGACCACCTTTGTGGCCCTCTATGACTATGAGTCTAGGACG     297
Src_FL_2-EGFP-C-FOR_E14   GGCCCGCTGGCCGGTGGAGTGACCACCTTTGTGGCCCTCTATGACTATGAGTCTAGGACG     360
                          ************************************************************

WT_Src_FL                 GAGACAGACCTGTCCTTCAAGAAAGGCGAGCGGCTCCAGATTGTCAACAACACAGAGGGA     357
Src_FL_2-EGFP-C-FOR_E14   GAGACAGACCTGTCCTTCAAGAAAGGCGAGCGGCTCCAGATTGTCAACAACACAGAGGGA     420
                          ************************************************************

WT_Src_FL                 GACTGGTGGCTGGCCCACTCGCTCAGCACAGGACAGACAGGCTACATCCCCAGCAACTAC     417
Src_FL_2-EGFP-C-FOR_E14   GACTGGTGGCTGGCCCACTCGCTCAGCACAGGACAGACAGGCTACATCCCCAGCAACTAC     480
                          ************************************************************

WT_Src_FL                 GTGGCGCCCTCCGACTCCATCCAGGCTGAGGAGTGGTATTTTGGCAAGATCACCAGACGG     477
Src_FL_2-EGFP-C-FOR_E14   GTGGCGCCCTCCGACTCCATCCAGGCTGAGGAGTGGTATTTTGGCAAGATCACCAGACGG     540
                          ************************************************************

WT_Src_FL                 GAGTCAGAGCGGTTACTGCTCAATGCAGAGAACCCGAGAGGGACCTTCCTCGTGCGAGAA     537
Src_FL_2-EGFP-C-FOR_E14   GAGTCAGAGCGGTTACTGCTCAATGCAGAGAACCCGAGAGGGACCTTCCTCGTGCGAGAA     600
                          ************************************************************

WT_Src_FL                 AGTGAGACCACGAAAGGTGCCTACTGCCTCTCAGTGTCTGACTTCGACAACGCCAAGGGC     597
Src_FL_2-EGFP-C-FOR_E14   AGTGAGACCACGAAAGGTGCCTACTGCCTCTCAGTGTCTGACTTCGACAACGCCAAGGGC     660
                          ************************************************************

WT_Src_FL                 CTCAACGTGAAGCACTACAAGATCCGCAAGCTGGACAGCGGCGGCTTCTACATCACCTCC     657
Src_FL_2-EGFP-C-FOR_E14   CTCAACGTGAAGCACTACAAGATCCGCAAGCTGGACAGCGGCGGCTTCTACATCACCTCC     720
                          ************************************************************

WT_Src_FL                 CGCACCCAGTTCAACAGCCTGCAGCAGCTGGTGGCCTACTACTCCAAACACGCCGATGGC     717
Src_FL_2-EGFP-C-FOR_E14   CGCACCCAGTTCAACAGCCTGCAGCAGCTGGTGGCCTACTACTCCAAACACGCCGATGGC     780
                          ************************************************************

WT_Src_FL                 CTGTGCCACCGCCTCACCACCGTGTGCCCCACGTCCAAGCCGCAGACTCAGGGCCTGGCC     777
Src_FL_2-EGFP-C-FOR_E14   CTGTGCCACCGCCTCACCACCGTGTGCCCCACGTCCAAGCCGCAGACTCAGGGCCTGGCC     840
                          ************************************************************

WT_Src_FL                 AAGGATGCCTGGGAGATCCCTCGGGAGTCGCTGCGGCTGGAGGTCAAGCTGGGCCAGGGC     837
Src_FL_2-EGFP-C-FOR_E14   AAGGATGCCTGGGAGATCCCTCGGGAGTCGCTGCGGCTGGAGGTCAAGCTGGGCCAGGGC     900
                          ************************************************************

WT_Src_FL                 TGCTTTGGCGAGGTGTGGATGGGGACCTGGAACGGTACCACCAGGGTGGCCATCAAAACC     897
Src_FL_2-EGFP-C-FOR_E14   TGCTTTGGCGAGGTGTGGATGGGGACCTGGAACGGTACCACCAGGGTGGCCATCAAAACC     960
                          ************************************************************
```

```
WT_Src_FL                 CTGAAGCCTGGCACGATGTCTCCAGAGGCCTTCCTGCAGGAGGCCCAGGTCATGAAGAAG     957
Src_FL_2-EGFP-C-FOR_E14   CTGAAGCCTGGCACGATGTCTCCAGAGGCCTTCCTGCAGGAGGCCCAGGTCATGAAAAAG     1020
                          ************************************************** ***
```

SV40pA-R Reverse primer

```
WT_Src_FL                 TTTGGCGAGGTGTGGATGGGGACCTGGAACGGTACCACCAGGGTGGCCATCAAAACCCTG 900
Src_FL_2-SV40pA-R_G14     TTTGGCGAGGTGTGGATGGGGACCTGGAACGGTACCACCAGGGTGGCCATCAAAACCCTG 331
                          ************************************************************

WT_Src_FL                 AAGCCTGGCACGATGTCTCCAGAGGCCTTCCTGCAGGAGGCCCAGGTCATGAAGAAGCTG 960
Src_FL_2-SV40pA-R_G14     AAGCCTGGCACGATGTCTCCAGAGGCCTTCCTGCAGGAGGCCCAGGTCATGAAGAAGCTG 391
                          ************************************************************

WT_Src_FL                 AGGCATGAGAAGCTGGTGCAGTTGTATGCTGTGGTTTCAGAGGAGCCCATTTACATCGTC 1020
Src_FL_2-SV40pA-R_G14     AGGCATGAGAAGCTGGTGCAGTTGTATGCTGTGGTTTCAGAGGAGCCCATTTACATCGTC 451
                          ************************************************************

WT_Src_FL                 ACGGAGTACATGAGCAAGGGGAGTTTGCTGGACTTTCTCAAGGGGGAGACAGGCAAGTAC 1080
Src_FL_2-SV40pA-R_G14     ACGGAGTACATGAGCAAGGGGAGTTTGCTGGACTTTCTCAAGGGGGAGACAGGCAAGTAC 511
                          ************************************************************

WT_Src_FL                 CTGCGGCTGCCTCAGCTGGTGGACATGGCTGCTCAGATCGCCTCAGGCATGGCGTACGTG 1140
Src_FL_2-SV40pA-R_G14     CTGCGGCTGCCTCAGCTGGTGGACATGGCTGCTCAGATCGCCTCAGGCATGGCGTACGTG 571
                          ************************************************************

WT_Src_FL                 GAGCGGATGAACTACGTCCACCGGGACCTTCGTGCAGCCAACATCCTGGTGGGAGAGAAC 1200
Src_FL_2-SV40pA-R_G14     GAGCGGATGAACTACGTCCACCGGGACCTTCGTGCAGCCAACATCCTGGTGGGAGAGAAC 631
                          ************************************************************

WT_Src_FL                 CTGGTGTGCAAAGTGGCCGACTTTGGGCTGGCTCGGCTCATTGAAGACAATGAGTACACG 1260
Src_FL_2-SV40pA-R_G14     CTGGTGTGCAAAGTGGCCGACTTTGGGCTGGCTCGGCTCATTGAAGACAATGAGTACACG 691
                          ************************************************************

WT_Src_FL                 GCGCGGCAAGGTGCCAAATTCCCCATCAAGTGGACGGCTCCAGAAGCTGCCCTCTATGGC 1320
Src_FL_2-SV40pA-R_G14     GCGCGGCAAGGTGCCAAATTCCCCATCAAGTGGACGGCTCCAGAAGCTGCCCTCTATGGC 751
                          ************************************************************

WT_Src_FL                 CGCTTCACCATCAAGTCGGACGTGTGGTCCTTCGGGATCCTGCTGACTGAGCTCACCACA 1380
Src_FL_2-SV40pA-R_G14     CGCTTCACCATCAAGTCGGACGTGTGGTCCTTCGGGATCCTGCTGACTGAGCTCACCACA 811
                          ************************************************************

WT_Src_FL                 AAGGGACGGGTGCCCTACCCTGGGATGGTGAACCGCGAGGTGCTGGACCAGGTGGAGCGG 1440
Src_FL_2-SV40pA-R_G14     AAGGGACGGGTGCCCTACCCTGGGATGGTGAACCGCGAGGTGCTGGACCAGGTGGAGCGG 871
                          ************************************************************

WT_Src_FL                 GGCTACCGGATGCCCTGCCCGCCGGAGTGTCCCGAGTCCCTGCACGACCTCATGTGCCAG 1500
Src_FL_2-SV40pA-R_G14     GGCTACCGGATGCCCTGCCCGCCGGAGTGTCCCGAGTCCCTGCACGACCTCATGTGCCAG 931
                          ************************************************************

WT_Src_FL                 TGCTGGCGGAAGGAGCCTGAGGAGCGGCCCACCTTCGAGTACCTGCAGGCCTTCCTGGAG 1560
Src_FL_2-SV40pA-R_G14     TGCTGGCGGAAGGAGCCTGAGGAGCGGCCCACCTTCGAGTACCTGCAGGCCTTCCTGGAG 991
                          ************************************************************

WT_Src_FL                 GACTACTTCACGTCCACCGAGCCCCAGTACCAGCCCGGGGAGAACCTCTAG--------- 1611
Src_FL_2-SV40pA-R_G14     GACTACTTCACGTCCACCGAGCCCCAGTACCAGCCCGGGGAGAACCTCTAGATGAATTCT 1051
                          ************************************************
```

1.1.2 Src SH3 domain-CFP construct

Forward EGFP-C primer

```
WT_Src_FL                 CCGCTGGCCGGTGGAGTGACCACCTTTGTGGCCCTCTATGACTATGAGTCTAGGACGGAG      300
Src_SH3-EGFP-C-FOR_E18    CAAGCTTATGGTGGAGTGACCACCTTTGTGGCCCTCTATGACTATGAGTCTAGGACGGAG      113
                          *       **************************************************

WT_Src_FL                 ACAGACCTGTCCTTCAAGAAAGGCGAGCGGCTCCAGATTGTCAACAACACAGAGGGAGAC      360
Src_SH3-EGFP-C-FOR_E18    ACAGACCTGTCCTTCAAGAAAGGCGAGCGGCTCCAGATTGTCAACAACACAGAGGGAGAC      173
                          ************************************************************

WT_Src_FL                 TGGTGGCTGGCCCACTCGCTCAGCACAGGACAGACAGGCTACATCCCCAGCAACTACGTG      420
Src_SH3-EGFP-C-FOR_E18    TGGTGGCTGGCCCACTCGCTCAGCACAGGACAGACAGGCTACATCCCCAGCAACTACGTG      233
                          ************************************************************

WT_Src_FL                 GCGCCCTCCGACTCCATCCAGGCTGAGGAGTGGTATTTTGGCAAGATCACCAGACGGGAG      480
Src_SH3-EGFP-C-FOR_E18    GCGCCCTCCGACTCCATGAATTCTGCAGTCGACGGTACCGCGGGCCCGGGATCCACCGGA      293
                          ****************  *  ***  *       *   *               *
```

1.1.3 Src SH2 domain-CFP construct

Forward EGFP-C primer

```
WT_Src_FL                  GCGCCCTCCGACTCCATCCAGGCTGAGGAGTGGTATTTTGGCAAGATCACCAGACGGGAG   480
Src_SH2_2-EGFP-C-FOR_I14   TCCGGACTCAGATCTCGAGCTCAAGCTTATTGGTATTTTGGCAAGATCACCAGACGGGAG   93
                            *      *   **          *   * ****************************

WT_Src_FL                  TCAGAGCGGTTACTGCTCAATGCAGAGAACCCGAGAGGGACCTTCCTCGTGCGAGAAAGT   540
Src_SH2_2-EGFP-C-FOR_I14   TCAGAGCGGTTACTGCTCAATGCAGAGAACCCGAGAGGGACCTTCCTCGTGCGAGAAAGT   153
                           ************************************************************

WT_Src_FL                  GAGACCACGAAAGGTGCCTACTGCCTCTCAGTGTCTGACTTCGACAACGCCAAGGGCCTC   600
Src_SH2_2-EGFP-C-FOR_I14   GAGACCACGAAAGGTGCCTACTGCCTCTCAGTGTCTGACTTCGACAACGCCAAGGGCCTC   213
                           ************************************************************

WT_Src_FL                  AACGTGAAGCACTACAAGATCCGCAAGCTGGACAGCGGCGGCTTCTACATCACCTCCCGC   660
Src_SH2_2-EGFP-C-FOR_I14   AACGTGAAGCACTACAAGATCCGCAAGCTGGACAGCGGCGGCTTCTACATCACCTCCCGC   273
                           ************************************************************

WT_Src_FL                  ACCCAGTTCAACAGCCTGCAGCAGCTGGTGGCCTACTACTCCAAACACGCCGATGGCCTG   720
Src_SH2_2-EGFP-C-FOR_I14   ACCCAGTTCAACAGCCTGCAGCAGCTGGTGGCCTACTACTCCAAACACGCCGATGGCCTG   333
                           ************************************************************

WT_Src_FL                  TGCCACCGCCTCACCACCGTGTGCCCCACGTCCAAGCCGCAGACTCAGGGCCTGGCCAAG   780
Src_SH2_2-EGFP-C-FOR_I14   TGCCACCGCCTCACCACCGTGTGCATGAATTCTGCAGTCGACGGTACCGCGGGC--CCGG   391
                           **********************   *  **       *   *   *      *  *
```

1.1.4 Plcg1 SH2-N domain-CFP construct

Forward EGFP-C primer

```
WT_PLCY1                   CAGCACAGAGCTGCACTCCAATGAGAAGTGGTTCCATGGGAAGCTAGGGGCAGGGCGTGA  1679
PLCY1_SH2_N-EGFP-C-FOR_I18 CGGACTCAGATCTCGAGCTCAAGCTTATTGGTTCCATGTCAAGCTAGGGGCAGGGCGTGA  76
                           * *          *   *  * *   * ********************************

WT_PLCY1                   CGGGCGTCACATCGCTGAGCGCCTGCTTACTGAGTACTGCATCGAGACCGGAGCCCCTGA  1739
PLCY1_SH2_N-EGFP-C-FOR_I18 CGGGCGTCACATCGCTGAGCGCCTGCTTACTGAGTACTGCATCGAGACCGGAGCCCCTGA  136
                           ************************************************************

WT_PLCY1                   CGGCTCCTTCCTCGTGCGAGAGAGTGAGACCTTCGTGGGCGACTACACGCTCTCTTTCTG  1799
PLCY1_SH2_N-EGFP-C-FOR_I18 CGGCTCCTTCCTCGTGCGAGAGAGTGAGACCTTCGTGGGCGACTACACGCTCTCTTTCTG  196
                           ************************************************************

WT_PLCY1                   GCGGAACGGGAAAGTCCAGCACTGCCGTATCCACTCCCGGCAAGATGCTGGGACCCCCAA  1859
PLCY1_SH2_N-EGFP-C-FOR_I18 GCGGAACGGGAAAGTCCAGCACTGCCGTATCCACTCCCGGCAAGATGCTGGGACCCCCAA  256
                           ************************************************************

WT_PLCY1                   GTTCTTCTTGACAGACAACCTCGTCTTTGACTCCCTCTATGACCTCATCACGCACTACCA  1919
PLCY1_SH2_N-EGFP-C-FOR_I18 GTTCTTCTTGACAGACAACCTCGTCTTTGACTCCCTCTATGACCTCATCACGCACTACCA  316
                           ************************************************************

WT_PLCY1                   GCAGGTGCCCCTGCGCTGTAATGAGTTTGAGATGCGACTTTCAGAGCCTGTCCCACAGAC  1979
PLCY1_SH2_N-EGFP-C-FOR_I18 GCAGGTGCCCCTGCGCTGTAATGAGTTTGAGATGCGACTTTCAGAGCCTGTCATGAATTC  376
                           ************************************************    *  *
```

1.1.5 Plcg1 SH2-C domain-CFP construct

Forward EGFP-C primer

```
WT_PLCY1                   AACGCCCACGAGAGCAAAGAGTGGTACCACGCGAGCCTGACCAGAGCACAGGCTGAGCAC  2040
PLCY1_SH2_C-EGFP-C-FOR_M18 AGATCTCGAGCTCAAGCTTATTGGTACCACGCGAGCCTGACCAGAGCACAGGCTGAGCAC  102
                           *   * *  *         * ****************************************

WT_PLCY1                   ATGCTAATGCGCGTCCCTCGTGATGGGGCCTTCCTGGTGCGGAAGCGGAATGAACCCAAC  2100
PLCY1_SH2_C-EGFP-C-FOR_M18 ATGCTAATGCGCGTCCCTCGTGATGGGGCCTTCCTGGTGCGGAAGCGGAATGAACCCAAC  162
                           ************************************************************

WT_PLCY1                   TCATATGCCATCTCTTTCCGGGCTGAGGGCAAGATCAAGCATTGCCGTGTCCAGCAAGAG  2160
PLCY1_SH2_C-EGFP-C-FOR_M18 TCATATGCCATCTCTTTCCGGGCTGAGGGCAAGATCAAGCATTGCCGTGTCCAGCAAGAG  222
                           ************************************************************

WT_PLCY1                   GGCCAGACAGTGATGCTAGGGAACTCGGAGTTCGACAGCCTTGTTGACCTCATCAGCTAC  2220
PLCY1_SH2_C-EGFP-C-FOR_M18 GGCCAGACAGTGATGCTAGGGAACTCGGAGTTCGACAGCCTTGTTGACCTCATCAGCTAC  282
                           ************************************************************
```

```
WT_PLCY1                    TATGAGAAACACCCGCTATACCGCAAGATGAAGCTGCGCTATCCCATCAACGAGGAGGCA  2280
PLCY1_SH2_C-EGFP-C-FOR_M18  TATGAGAAACACCCGCTATACCGCAAGATGAAGCTGCGCTATCCCATCATGAATTCTGCA  342
                            ************************************************   *    ***
```

1.1.6 Plcg1 SH3-domain-CFP construct

Forward EGFP-C primer

```
WT_PLCY1                    GGCTTCTATGTAGAGGCAAACCCTATGCCAACTTTCAAGTGTGCAGTCAAAGCCCTCTTT  2400
PLCY1_SH3-EGFP-C-FOR_I16    TCCGGACTCAGATCTCGAGCTCAAGCTTATACTTTCAAGTGTGCAGTCAAAGCCCTCTTT  91
                              *        *     *   *        ******************************

WT_PLCY1                    GACTACAAGGCCCAGAGGGAGGACGAGCTGACCTTCATCAAGAGCGCCATCATCCAGAAT  2460
PLCY1_SH3-EGFP-C-FOR_I16    GACTACAAGGCCCAGAGGGAGGACGAGCTGACCTTCATCAAGAGCGCCATCATCCAGAAT  151
                            ************************************************************

WT_PLCY1                    GTGGAGAAGCAAGAGGGAGGCTGGTGGCGAGGGGACTACGGAGGGAAGAAGCAGCTGTGG  2520
PLCY1_SH3-EGFP-C-FOR_I16    GTGGAGAAGCAAGAGGGAGGCTGGTGGCGAGGGGACTACGGAGGGAAGAAGCAGCTGTGG  211
                            ************************************************************

WT_PLCY1                    TTCCCATCAAACTACGTGGAAGAGATGGTCAACCCCGTGGCCCTGGAGCCGGAGAGGGAG  2580
PLCY1_SH3-EGFP-C-FOR_I16    TTCCCATCAAACTACGTGGAAGAGATGGTCAACATGAATTCTGCAGTCGACGGTACCGCG  271
                            *********************************       *    *     *  *  * *
```